Development of a Carborane Framework for Fragment-Based Drug Discovery

Eliash M. Hemzal

A thesis submitted to fulfil the requirements for the degree of
Doctor of Philosophy

School of Chemistry
Faculty of Science
The University of Sydney
2025

Statement of Originality

This is to certify that the content of this thesis is my own work. This thesis has not been submitted for any other degree or purpose.

I certify that the intellectual content of this thesis is the product of my own work. All assistance received in preparing this thesis and all sources have been acknowledged.

Eliash Hemzal

Acknowledgements

To start, I want to thank my amazing supervisor, Professor Lou Rendina. I am immensely grateful for your wealth of knowledge, guidance and support throughout the years. Thank you for sharing my love of carboranes (and putting up with my crazy ideas!), for running hundreds of hours of DFT calculations and for proof-reading three PhD theses in two months with less than 48 hour turnover times for each chapter. Thank you as well for being great banter and fostering an amazing culture in your research group.

Office 318 has felt like a revolving door of amazing and interesting people who I'm all grateful to have spent time with. To my partner in carborane (and *many* other) crimes, Tom, I could not have imagined a better person to work through the long years of a PhD with. Your endless help with chemistry and friendship outside the lab has been an incredible gift and I will cherish that forever. To Xinyi, I don't think there's any better late-night lab shift company than you. I've missed our convos big time ever since you started writing and can't wait to get back to it once we're both free. Poya, thank you for showing me the Rendina way in the lab and beyond. It's probably not too much of an exaggeration to say our office DIY project is the crowning achievement of my time in the Chemistry building. Anita, I will always be grateful for the friendship we built over our time in Chemistry, even though it took you a while to start talking to me! I can also say I've finally come to terms with you being a Man U fan, no one's perfect as they say. Leila, thank you for all your expert advice throughout the years and for keeping my secret after I tried to Shawshank Redemption myself out of the building. Jayden, your time at Uni was one of my favourite periods in the group and I thoroughly enjoyed all our adventures. Nick, thank you for being a calming presence around the group, a great chat and occasionally getting the memo about shirt coordination.

To the Honours students who have come and gone during my time, thank you for bringing a fresh spark to the group with your amazing personalities. Callum, I loved your crazy cooking exploits and can't wait to go fishing again; Nina, your indecisiveness was always entertaining and I promise I'll finally finish watching My Brilliant Friend now I have time; Izzy, your vibrant personality and crazy antics were a highlight of a sometimes tough 2024, keep on mish-moshing; Will, I've never met someone as crazy about carboranes as Tom and me and am certain you will go far in all of your endeavours.

I want to thank the technical staff of the Chemistry building, in particular Dr Denis Cheng who was always insanely helpful with just about any problem I ever had. Thank you to Dr Nick

Proschogo for being helpful beyond reason and the great chats the few times I happened to trek down to mass spec. Thank you as well to Dr Paige Hawkins for all your assistance with NMR and especially catering to our group's odd ^{11}B needs.

I'd also like to thank Professor Shane Thomas for his assistance with the biological side of my project, particularly with procuring the protein. Thank you also to Dr Jacqueline Ku and Dr Elias Glaros for getting me up and running with biological assays. I hope you enjoyed that crazy semi-post-COVID adventure as much as I did.

Finally, and definitely most importantly, thank you to my amazing family. There is absolutely no way I could have managed this PhD without your boundless support over the last few years and beyond. I hope this thesis answers at least some of your questions as to what the hell I was doing all this time! I love you all.

Eliash

This research was supported by an Australian Government Research Training Program (RTP) Scholarship.

Table of Contents

Abstract

Since the first boron-containing drug entered the clinic in the early 2000s, there has been an increased interest in harnessing the unusual properties of this atypical element in drug design. Carboranes, an important class of boron cluster compounds, have garnered particular attention for their use as a novel drug framework due to their hydrophobic nature, resistance to catabolism and ability to form unusual dihydrogen bonds. Despite this interest, however, their use in this field has remained limited in part due to an inability to access certain positions of the icosahedral cage. In this thesis, we attempt to address this significant synthetic barrier in carborane research and, furthermore, report our efforts at utilising these compounds as a structural framework for fragment-based drug discovery (FBDD), the first time such an approach has ever been used for carboranes.

In Chapter Two, we describe the development of new methods for functionalising unusual positions of the carborane cage. In so doing, an iodo protecting group for carborane B-vertices is reported for the first time. Using this protecting group, *closo*-1,2- and *closo*-1,7-carborane brominated at the B(8/10) and B(5/12) positions, respectively, were synthesised and fully characterised for the first time. These novel isomers allow routine access to a range of derivatives functionalised at these unique sites, a significant advancement in carborane chemistry. Progress towards the synthesis of two other novel bromocarboranes functionalised at the B(2/3) and B(4,6,8,11) positions of the *closo*-1,7-carborane cage is also presented.

Chapter Three details the preparation of a small library of low-molecular weight carborane fragments for use in FBDD, where a range of synthetic methods were utilised and further developed. These compounds were subsequently tested for their ability to bind to and inhibit the function of myeloperoxidase (MPO), a haem enzyme that is an emerging target for the treatment of a range of inflammatory disorders but to date has only had limited success in being targeted by small molecules. Surface plasmon resonance (SPR) studies and *in vitro* inhibition assays identified new *closo*-carborane derivatives with μM potency that are promising lead fragments for the development of a novel and potent MPO inhibitor.

Finally, our endeavours towards increasing the potency of one of the lead fragments discovered in Chapter Three are presented in Chapter Four. New synthetic methods were developed which allowed the expansion of this fragment at various structural positions. Several key derivatives were synthesised and fully characterised, with a focus on producing hetero-disubstituted carboranes, which to date have only seen limited application in medicinal chemistry.

List of Abbreviations

APCI	atmospheric pressure chemical ionization
BSH	sodium mercaptoundecahydro-*closo*-dodecaborate
CA	carbonic anhydrase
COSAN	cobalt bis(dicarbollide)
COSY	correlation spectroscopy
DCE	1,2-dichloroethane
DCM	dichloromethane
DFT	density functional theory
DIAD	diisopropyl azodicarboxylate
DME	1,2-dimethoxyethane
DMF	N,N-dimethylformamide
DMPS	diphenylmethylsilyl
DMSO	dimethylsulfoxide
ER	oestrogen receptor
ESI	electrospray ionization
FDA	(U.S.) food and drug administration
HAC	heavy atom count
HFIP	1,1,1,3,3,3-hexafluoro-2-propanol
HPLC	high-performance liquid chromatography
HTS	high-throughput screening
IC_{50}	half-maximal inhibitory concentration
IDO1	indoleamine 2,3-deoxygenase 1
KHMDS	potassium hexamethyldisilizane

LDA	lithium diisopropylamide
LE	ligand efficiency
LED	light-emitting diode
LRMS	low-resolution mass spectrometry
MW	molecular weight
NBS	*N*-bromosuccinimide
NIS	*N*-iodosuccinimide
NMR	nuclear magnetic resonance
RT	room temperature
SAR	structure activity relationship
SEM	standard error of the mean
SET	single-electron transfer
SPR	surface plasmon resonance
TBAB	tetra-*n*-butylammonium bromide
TBAF	tetra-*n*-butylammonium flouride
TBCA	tribromoisocyanuric acid
TEA	triethylamine
THF	tetrahydrofuran
TLC	thin layer chromatography
TMB	3,3′,5,5′-tetramethylbenzidine
TNB	5-thio-2-nitrobenzoic acid
^{t}RNA	transfer ribonucleic acid
USyd	the University of Sydney
UV	ultraviolet

1

Introduction

It is estimated that the number of unique combinations of atoms that produce drug-like molecules (MW < 500) is well above 10^{63}, a figure that is many orders of magnitude greater than the estimated number of stars in the known Universe.[1] Attempting to synthesise even a small fraction of these compounds is untenable, yet it remains the task of medicinal chemists to find those that can influence biological systems in a therapeutically useful manner. Historically, bioactive compounds have been designed using only a small subset of this vast chemical space, working on the assumption that known drugs offered "the most fruitful basis" for new ones.[2] This is reflected in the structures of clinically-approved compounds, with approximately 70% of new drugs consisting solely of ring systems found in pre-existing drugs.[3] It is now accepted, however, that this approach is ineffective in targeting many of the complex underlying mechanisms of certain diseases.[4] In fact, recent data suggests that new molecular entities based on novel structures are almost three times more likely to be designated 'breakthrough therapy' status.[5] As such, it is clear that expanding the chemical diversity of the drug discovery pipeline is a critical target in tackling the continuing challenges facing modern medicine.

The medicinal chemist's 'toolbox' has traditionally consisted of the six elements that are predominant in life: C, H, N, O, S and P. The use of atypical elements is therefore a direct pathway to areas of unexplored chemical space that presents exciting new opportunities in drug discovery. The element boron can play a vital role in this regard, where its incorporation into drug design is a unique avenue to developing new molecular scaffolds and unlocking novel modes of action.

Boron in Medicine

Despite its rich chemistry, boron is comparatively less prominent in the function of living organisms. It is an essential micronutrient for plants, where it helps maintains cell wall

integrity,[6] but its role in human and animal physiology is not completely understood.[7] In fact, the unfamiliarity of boron to biological systems makes its inclusion in bioactive molecules a viable strategy to increase the metabolic stability of drugs and hinder the ability of pathogens to develop resistance.[8] Many simple boron compounds, such as boric acid, are known to be non-toxic and are thus viable candidates for compounds intended for use *in vivo*.[9]

While boric acid has been used for over a century as a mild antiseptic and eye wash, boron derivatives have been largely overlooked in the design of bioactive molecules until recently. A boron-containing compound entered the clinic for the first time in 2003, when the proteasome inhibitor bortezomib (**1**) was approved by the FDA for the treatment of multiple myeloma. The incorporation of a boronic acid group was crucial in transforming early lead compounds in this class into an effective clinical candidate. Notably, the empty *p*-orbital of boron allows it to form a strong but reversible covalent bond with the oxygen lone-pair of the threonine residue at the proteasome active site,[10] leading to a 100-fold increase in inhibitory effect over related aldehyde analogues.[11] In contrast, the interactions between boron and soft nucleophiles such as sulfur are rather weak, a key reason behind the excellent selectivity of **1** for the 20S proteasome over off-target cysteine proteases.[10]

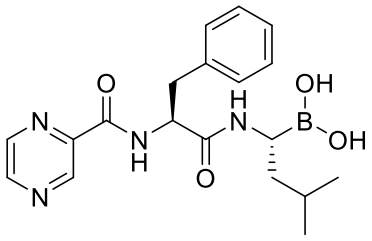

1

Bortezomib (2003)
Multiple myeloma treatment

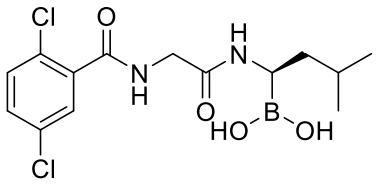

2

Ixazomib (2015)
Multiple myeloma treatment

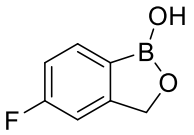

3

Tavaborole (2014)
Anti-fungal medication

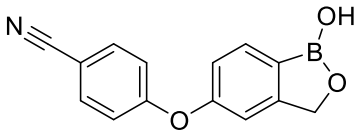

4

Crisaborole (2016)
Dermatitis treatment

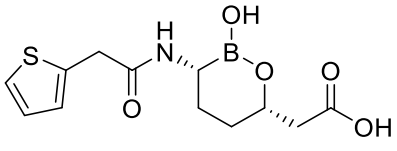

5

Vaborbactam (2017)
β-lactamase inhibitor

Figure 1. FDA-approved boron-containing pharmaceuticals along with their year of approval and intended use.

The clinical success of bortezomib sparked an increased interest in the use of boron in medicine, with several other boron-containing compounds approved for clinical use in the following years. Ixazomib (**2**), another boronic acid-based proteasome inhibitor, achieved FDA approval in 2015 for the treament of multiple myeloma and has overcome many of the limitations of bortezomib, including its dose-limiting toxicity and patient-developed drug resistance.[12] Benzoxaboroles, the cyclic conjugates of phenyl boronic acids, also emerged as valuable pharmacophores with the clinical success of tavaborole (**3**), an anti-fungal medication approved for the treatment of onychomycosis in 2014. This drug relies on the strong affinity of benzoxaboroles for diols,[13] forming a tetrahedral boronate adduct with the terminal adenosine in *t*RNA that prevents protein synthesis and ultimately terminates the fungal infection.[14] Notably, organic analogues and non-cyclised boronic acids derivatives were found to be completely inactive.[15] Crisaborole (**4**) was discovered by the same company following a screen of boron-containing compounds,[16] and is now approved for use as an anti-inflammatory in the treatment of atopic dermatitis.

Vaborbactam (**5**), the most recent FDA-approved boron-containing drug, is another excellent demonstration of the unique abilities of boron in bioactive agents. Vaborbactam is administered as part of a cocktail to treat gram-negative bacterial infections, where it functions as an inhibitor of β-lactamase enzymes that otherwise degrade and, as result, neutralise the antibiotics it is co-administered with.[17] In this case, the cyclisation of the boronic acid was a crucial modification as it locks the hydroxyl groups into a position that is optimal for enzyme complexation.[18] Furthermore, off-target interactions with serine proteases are prevented as these enzymes cannot accommodate the more sterically demanding structure, making the compound exceptionally selective.

The success of these agents has demonstrated the potential of increasing chemical diversity in drug screens and the important role that boron can play in medicinal chemistry. In fact, it has even inspired some companies to repurpose their collections of Suzuki coupling reagents into fragment libraries intended for biological testing.[19] The chemistry of boron, however, extends beyond boronic acids and their derivatives and offers yet more opportunities for the drug discovery pipeline that have, to date, not been fully harnessed.

Carboranes

In certain situations, boron participates in unusual multicentre, multi-electron bonds that underpin the molecular structures of polyhedral (hetero)boranes. These cluster compounds,

ranging in structures composed of 4 vertices to as many as 16,[20] were first studied in the early 1900s and have attracted great interest for their use in catalysis, polymers, energy storage as well as in medicine.[21–24]

One of the most important sub-classes of boron cluster compounds are the carboranes, in which one or more of the boron atoms has been replaced by a carbon. The most well-studied of these, the dicarba-*closo*-dodecaboranes, are icosahedral clusters with two carbon and ten boron atoms. Dicarba-*closo*-dodecaboranes are remarkably stable; they are not susceptible to oxidation and resist degradation under even extremely acidic conditions.[25] Even high temperatures do not degrade these compounds, but rather cause isomerisation between the three possible configurations of a *closo*-$C_2B_{10}H_{12}$ cluster: *closo*-1,2-carborane (1,2-dicarba-*closo*-dodecaborane(12)), where the carbon atoms are located at the adjacent 1 and 2 positions, rearranges to *closo*-1,7-carborane (1,7-dicarba-*closo*-dodecaborane(12)) at 400–500 °C,[26] which finally forms the thermodynamic product, *closo*-1,12-carborane (1,12-dicarba-*closo*-dodecaborane(12)), above 600 °C (**Figure 2**).[27]

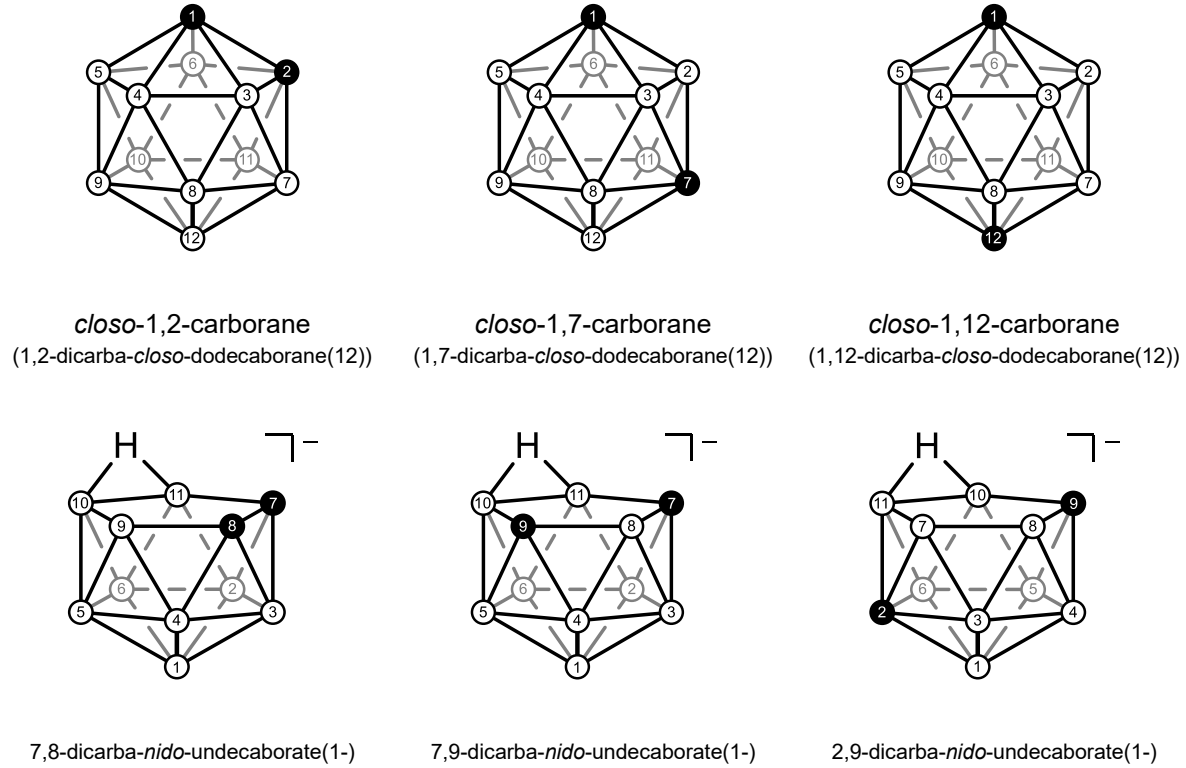

Figure 2. Structures of the three possible dicarba-*closo*-dodecaborane isomers and their respective deboronated, *nido*-compounds. The connecting lines are used to represent atom connectivity within the cluster and are not indicative of an electron pair forming a covalent bond. C–H units are represented in black (●) and B–H units in white (○).

The relative positioning of the carbon atoms in these isomers effects subtle but important changes in their properties. Although carbon is not conventionally regarded as an electron-withdrawing element, it is considerably more electronegative than boron and therefore has an inductive effect on its electropositive neighbours. As a result, a charge dipole is present across the cage of the carbons-adjacent *closo*-1,2-carborane, which is substantially less prominent in *closo*-1,7-carborane and non-existent in the highly symmetric *closo*-1,12-carborane.[28] Another consequence of this inductive effect is that the boron atoms adjacent to both carbons of the cluster are especially electron-poor, rendering them susceptible to attack by certain nucleophiles. This nucleophilic attack results in the regioselective removal of the most electrophilic boron vertex (in a process known as 'deboronation'), producing a negatively charged, open-cage *nido*-carborane which is much more hydrophilic than its *closo*- isomer. The configuration of the carbon atoms in *closo*-1,2-carborane make it particularly prone to this reaction, whereas *closo*-1,7-carborane is much more resistant. The corresponding transformation of *closo*-1,12-carborane has only been achieved under extremely forcing conditions.[29] While deboronation is often considered a nuisance when attempting to synthesise *closo*-carborane derivatives, this transformation is a powerful method of attenuating the properties of carborane compounds (*vide infra*), and *nido*-carboranes have been studied as interesting compounds in their own right.

Carboranes in Medicinal Chemistry

Because of their high boron-content, carboranes (and other boron clusters) first garnered attention in medicine as potential boron neutron capture therapy (BNCT) agents. This treatment involves irradiating a patient with thermal neutrons that are poorly absorbed by endogenous nuclei and takes advantage of the comparatively high neutron capture cross-section of the boron-10 isotope.[30] Provided a boron-rich agent can be selectively delivered to the desired biomolecular target, absorption of the neutrons by the boron-10 nuclei results in localised release of therapeutically-useful radiation, thereby creating a targeted treatment. While several agents, including the related borane sodium mercaptoundecahydro-*closo*-dodecaborate ($Na_2B_{12}H_{11}SH$, BSH), were explored,[31] clinical results were mixed and suffered from difficulties in selectively delivering a clinically relevant concentration of boron-10 nuclei to the target in a non-toxic manner.[30]

More recent research has focused on using carboranes as novel pharmacophores in bioactive molecules. A number of features make them attractive in this regard. The clusters are highly lipophilic due to their non-polar, hydridic B–H bonds, and their 3-dimensional volume (slightly larger than the sweep of a rotated phenyl ring)[32] allows for increased hydrophobic interactions with key protein structures. The nature of the B–H bonds in the clusters also allows the formation of unique 'dihydrogen' bonds involving nearby proton donors of amino acid residues located in protein receptors (e.g. B–H···H–N).[33] Owing to their inorganic nature, they are also naturally inert to many of the mechanisms responsible for drug metabolism and are thus kinetically stable under biological conditions.[34] Finally, the facile and regioselective deboronation reaction provides a powerful late-stage modification method that makes the carborane derivative more water-soluble and allows for more electrostatic interactions. While no carborane derivative has progressed to clinical trials to date, there is a rich literature that demonstrates the utility of these unique properties in designing biologically-active compounds.

An important example of the use of carboranes as hydrophobic bioisosteres is their incorporation into oestrogen receptor (ER) agonists. Oestrogens are hormones that modulate a range of physiological functions by binding to the intracellular oestrogen receptors, ERα and ERβ.[35] While ERβ is known to supress tumour progression,[36] the endogenous ligand 17β-oestradiol (**6**) has been shown to accelerate proliferation of breast cancer cells, an effect linked to ERα activation.[37,38] Because of this, the design of selective ERβ agonists is seen as a promising avenue in breast cancer treatment. The structural similarity of the ERα and ERβ ligand-binding cavities makes this a challenging task, with only two amino acid substitutions differentiating the subtypes.[39]

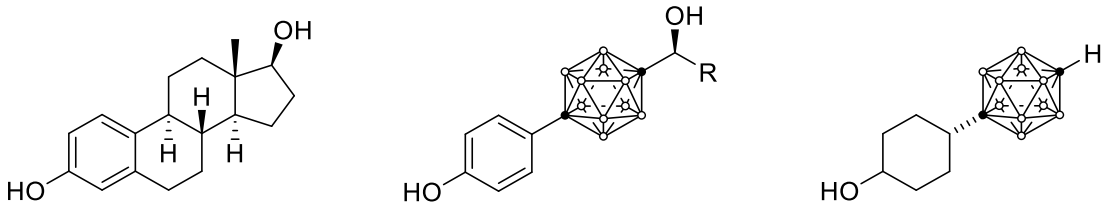

6 **7**: R = H; **8**: R = $(CH_2)_5CH_3$ **9**

Figure 3. Structures of endogenous (**6**) and carborane-containing (**7**, **8** and **9**) oestrogen receptor ligands. ● = C; ○ = B–H.

Noting that the oestrogenic activity of **6** is in part due to hydrophobic interactions of its cyclohexyl rings with the ligand binding domain, Endo *et al.* designed compound **7**, which replaced these rings with a *closo*-1,12-carborane cluster.[40] This compound exhibited 10-fold greater ERα activity than **6**, explained by the enhanced van der Waals interactions of the larger carborane in the hydrophobic pocket of the receptor.[41] Later studies by the same group focused on achieving ERβ selectivity,[42,43] with compound **9** being found to have almost 60 times greater affinity for ERβ over ERα,[44] albeit with reduced overall potency. Recent work by another research team led to the discovery of **8**, which is 200 times more selective for ERβ and has low nanomolar potency,[45] making it a promising pre-clinical drug lead.

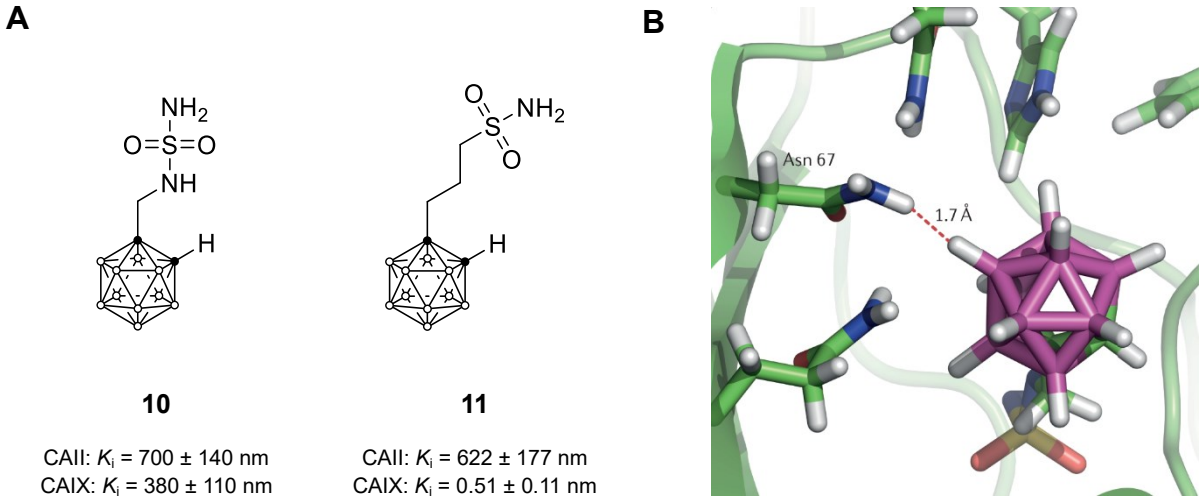

10

CAII: K_i = 700 ± 140 nm
CAIX: K_i = 380 ± 110 nm

11

CAII: K_i = 622 ± 177 nm
CAIX: K_i = 0.51 ± 0.11 nm

Figure 4. Structures of the carborane-containing carbonic anhydrase (CA) inhibitors **10** and **11** along with their inhibitory constants (A) and the binding pose of a *nido*-carborane derivative in the CAIX active site, showing a strong dihydrogen (B–H···H–N) bond between the carborane cage and enzyme (B). Figure adapted from reference 49. ● = C; ○ = B–H.

The utility of carboranes as pharmacophores has been further demonstrated in the development of novel inhibitors of carbonic anhydrases (CA). This family of enzymes has long been a therapeutic target for a range of disorders, but selective inhibition of CAIX is of particular interest as it is overexpressed in many tumour types.[46] Brynda *et al.* designed a series of carborane compounds, such as **10**, containing the sulfamide functional group common to many known CA inhibitors.[47] Many of these compounds were unselective but effective inhibitors, due in part to the van der Waals interactions of the carborane cage with hydrophobic amino acid residues. Importantly, these compounds demonstrated the first confirmed example

of dihydrogen bonding, with analysis of the *nido*-carborane derivative's binding pose revealing a H···H distance of 1.7 Å between the B(6)–H of the cluster and N–H of an asparagine residue (**Figure 4**).[48] Replacement of the lead compound's sulfamide group with an extended propyl sulfonamide structure resulted in a remarkable sub-nanomolar CAIX inhibitor (**11**) that is over 10^3 times less active on the CAII isoform.[49]

One final example of carborane use in bioactive compounds highlights the value of the tuneable properties of these structures. During their design of COX-II selective inhibitors as potential anti-inflammatories, Scholz *et al.* found that replacement of the 4-chlorophenyl ring in indomethacin (**12**) with a carborane group (**13**) increased the inhibitory effect of the compound.[50] Unfortunately, the electron-withdrawing effects of the C-substituted carborane cage destabilised the amide bond leading to hydrolysis and decomposition of the compound.[51] In this case, a facile deboronation reaction gave the *nido*-derivative **14**, which not only stabilised the amide but produced a more water-soluble compound, creating a highly selective COX-II inhibitor. We note that in such a case, reconfiguring the compound to its B-substituted congener would be an alternative strategy, as the carborane would then be electron-*donating*, stabilising the amide.

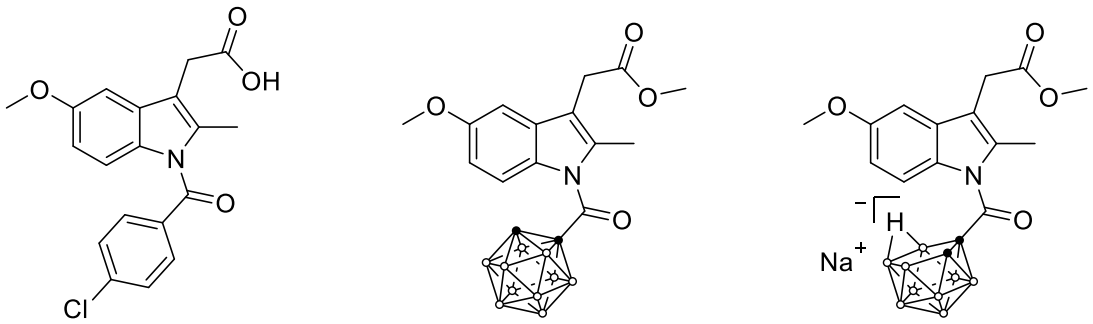

12 **13** **14**

Figure 5. Structure of the COX inhibitor indomethacin (**12**) and its *closo*- (**13**) and *nido*-carborane (**14**) analogues. ● = C–H (or C if substituted); ○ = B–H.

Despite many successful applications, carboranes have struggled to gain wide-spread adoption, and their usage remains, in many ways, limited. While most examples of their use in the literature focus on incorporating them into pre-established drugs, it is clear that many drug discovery projects would benefit from using carborane compounds earlier in the lead discovery

process. Fragment based drug discovery (FBDD), which has been used in recent years by pharmaceutical companies to design drugs with specific properties or scaffolds, is an ideal strategy to realise this.

Fragment-Based Drug Discovery

The predominant method of identifying lead compounds in the pharmaceutical industry is by means of high-throughput screening (HTS). As part of this approach, libraries containing hundreds of thousands of 'drug-like' compounds are tested in an assay for the desired target and the most active compounds are subsequently modified to optimise activity and pharmacokinetic properties. Advances in automation technologies have made HTS a powerful method, accelerating the lead discovery phase of the drug discovery pipeline. There are, however, several limitations associated with screening 'drug-like' compounds. The number of possible structures increases exponentially with the number of atoms in a molecule, meaning that vast numbers of compounds must be synthesised to effectively sample chemical space. Furthermore, hit rates for HTS screens are often low, a consequence of the greater likelihood of ligand-target mismatches when testing more complex molecules.[52] Ultimately, the leads that are discovered from HTS still require pharmacokinetic optimisation, a process that is complicated with larger compounds and frequently results in a loss of potency.[53]

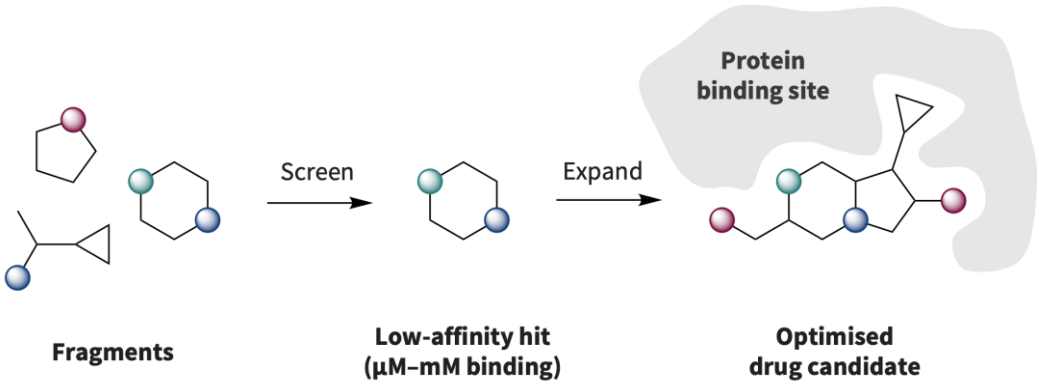

Figure 6. Schematic overview of the fragment-based drug discovery (FBDD) process.

FBDD is designed to address these shortcomings. In this approach, the compounds screened are low molecular weight (<300 Da) 'fragments' which are prioritised based on how

efficiently they interact with the target. This is typically quantified using a metric called ligand efficiency (LE),[54] which is defined as:

$$\mathrm{LE} = -\frac{\Delta G}{\mathrm{HAC}} = -\frac{RT\ln(K_d)}{\mathrm{HAC}} \approx -\frac{RT\ln(\mathrm{IC}_{50})}{\mathrm{HAC}}$$

where *HAC* is the number of constituent heavy atoms. In this way, only structures that interact strongly with the target are selected, and rational expansion or linking of fragment hits ultimately leads to a highly potent drug candidate.[55] In addition, because the range of molecular complexity is smaller at these molecular weights, FBDD can more effectively sample chemical space and has as a result become a powerful tool for generating leads for difficult targets.[56]

FBDD continues to become increasingly popular in the pharmaceutical industry, with numerous examples of its successful use. The G12C KRAS mutation, a notorious cancer drug target previously thought 'undruggable', now has an inhibitor in the market (sotorasib) developed through a fragment-guided program.[57] Five other drugs used in the clinic have fragment origins, and many others are in clinical trials.[58] The development of one of these, erdafitinib (**18**), provides an excellent example of the FBDD process (**Figure 7**).

In a collaboration seeking to develop an FGFR inhibitor with low off-target activity for the similar kinase VEGFR2, Astex and Janssen Pharmaceuticals initiated a fragment screen which identified quinoxaline **15** as a potent hit with a high ligand efficiency.[59] A related fragment (**16**) displayed higher inhibition of both kinases, and expansion of this fragment using the amino vector found in **15** gave a compound (**17**) with greatly enhanced potency and selectivity for FGFR3. Comparison of the protein-bound crystal structure of **17** and another FGFR3 inhibitor developed previously indicated that further elaboration at the amine site could give increased binding interactions. Exploration and optimisation of such derivatives ultimately resulted in the selection of **18** (erdafitinib) as a clinical candidate, which is now a first-in-class medication used for the treatment of bladder cancer.

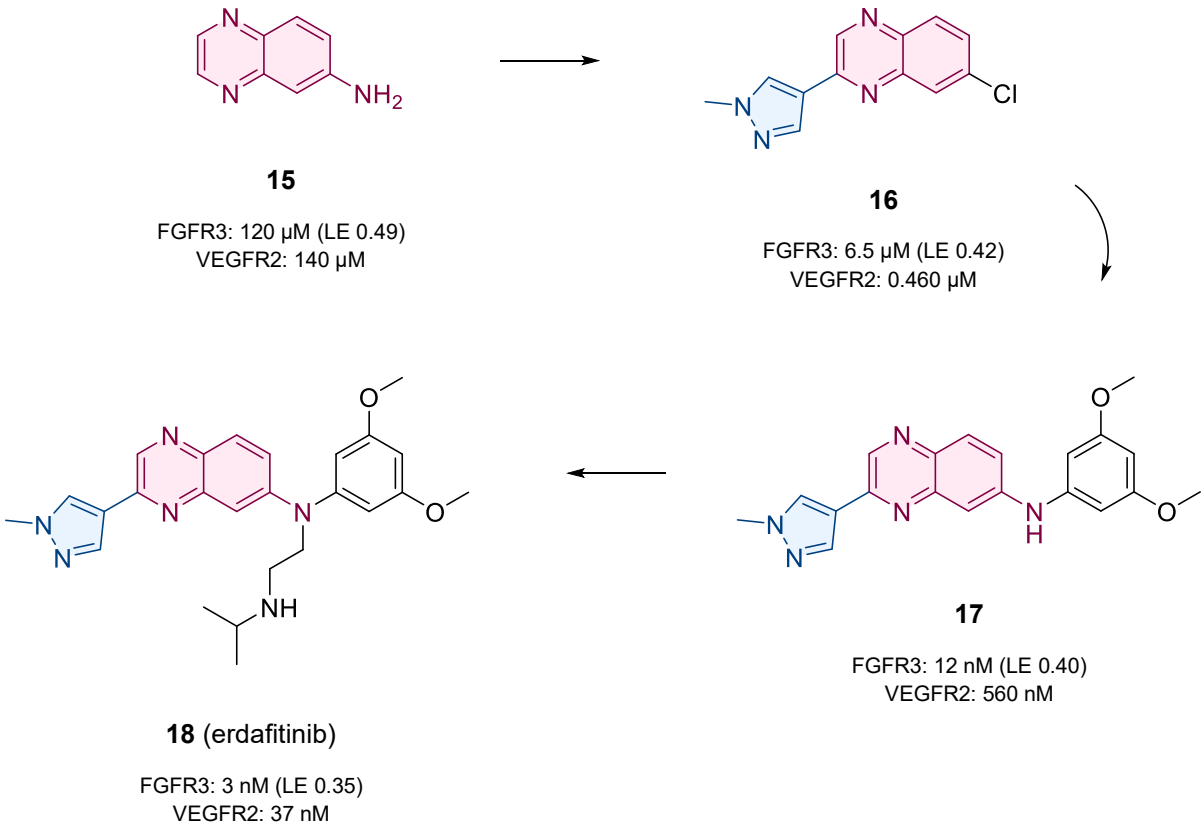

Figure 7. Overview of the fragment expansion and optimisation process involved in the development of FDA-approved erdafitinib (**18**), highlighting the conserved structures from the initial fragment hit. Figure adapted from reference 60.

The Present Study

The Rendina group recently began development of the world's first boron-based fragment library intended to help design novel bioactive compounds. This library provides an excellent means of exploring the under-utilised areas of chemical space that boron-containing compounds occupy. There is a strong interest in harnessing the unique properties of carboranes through an FBDD program, with which we have already seen promising results in other projects.

During the expansion and diversification of this library, several difficulties were encountered when using carboranes in this context. Part of the strength of an FBDD project lies in the range and diversity of the fragments screened, which can be bolstered by purchasing commercially-available compounds and applying well-established synthetic methods to diversify them. While tremendous progress has been made in synthetic carborane chemistry in

the past two decades, many of the transformations that are crucial to medicinal chemistry remain difficult to apply to carboranes. This is particularly an issue with *closo*-1,2-carborane, which has a propensity to deboronate under certain reaction conditions. The use of *closo*-1,7-carborane, while attractive due to its greater stability, is limited due to the lack of methods to functionalise certain vertices selectively. This thesis details our efforts to solve these issues and, in so doing, show that carboranes can indeed be an effective basis for a fruitful FBDD project.

In Chapter Two, we report our attempts to functionalise the previously inaccessible 4- and 5-positions of *closo*-1,7-carborane, including the development of a first-of-its-kind protecting group for carborane B-vertices. Using this protecting group, novel halogenated carboranes are synthesised and fully characterised for the first time.

Chapter Three details an initial screen of a small library of carboranes against myeloperoxidase (MPO), a promising new target for the treatment of a range of inflammatory disorders. The synthesis of a range of low molecular-weight carboranes is presented with the goal of expanding the chemical diversity of our fragment library. The Chapter ends with the results of an assessment of the inhibitory abilities of these novel fragments.

In Chapter Four, a ‘hit’ fragment identified in the previous chapter is expanded upon. We apply a range of cutting-edge carborane synthetic methods to create a suite of follow-up fragments that have the potential to be further expanded into a new class of MPO inhibitors.

2

Accessing Unusual Carborane Vertices

One of the cornerstones of a successful medicinal chemistry project is having useful synthetic tools to modify and expand a lead compound's structure. In this way, a range of analogues can be easily generated that allow investigation of structure activity relationships (SARs) and, as a result, optimisation of the lead's properties. Two criteria need to be met in order to achieve this: (a) the ability to selectively functionalise different sites of the scaffold of interest, and (b) to further install a variety of functional groups at these positions. These factors are of particular importance for niche scaffolds such as carboranes, where the lack of such synthetic methods is a barrier to their more widespread adoption.

The reactivity of carboranes can be broadly categorised into reactions that functionalise the slightly Brønsted acidic C–H vertices and those that modify the more hydridic B–H vertices.

Functionalising Carboranes at Carbon Vertices

As mentioned previously, the C–H bonds of carboranes are slightly acidic (pK_a 23.3, 27.9 and 30.0 for *closo*-1,2-, *closo*-1,7- and *closo*-1,12-carborane, respectively)[60] and one or both can be readily deprotonated using strong bases such as *n*-butyllithium or fluoride sources such as tetrabutylammonium fluoride (TBAF).[61] The resulting carbanion species can react with a range of electrophiles to afford C-substituted carboranes. Using this strategy carboranyl carboxylic acids,[62] alcohols,[63] amines[64] and aldehydes[65] are all accessible and serve as important building blocks to introduce carboranes into larger structures. While the degree of substitution is mediated by the amount of base used, an equilibrium exists between the parent carborane and its mono- and di-anionic forms when one equivalent of base is used (**Scheme 1**).[66] As expected, the more hydridic B–H groups in the carborane cage remain unchanged. Careful tuning of

reaction conditions generally provides sufficient control to ensure mono- or di-substitution as desired, however this effect is highly substrate dependent.[67] In cases where this proves difficult, silyl groups can be installed onto one of the C-vertices which act as protecting groups that block electrophilic addition to the second cage carbon atom.[68,69] These groups can then be readily removed using a fluoride source or mildly basic conditions to furnish the desired mono-substituted carborane.

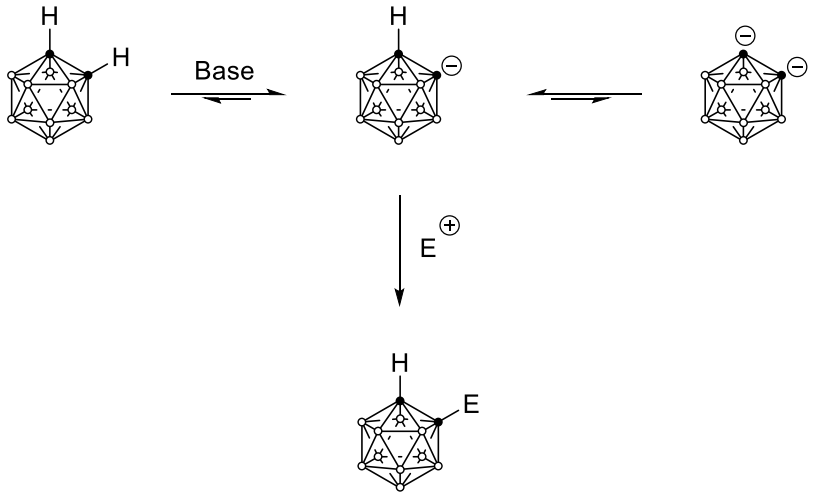

Scheme 1. C-functionalisation of *closo*-1,2-carborane through substitution of its mono-anion with an electrophile E^+. The mono-anion disproportionates to a small degree in solution, forming the di-anion and re-protonated *closo*-1,2-carborane. ● = C; ○ = B–H.

For *closo*-1,2-carborane, two other strategies are available to introduce C-substituents. Deprotonation of *closo*-1,2-carboranes substituted with a good leaving group (halogen, triflate or diazo group) and subsequent heating produces the metastable carboryne, which can be considered as an inorganic equivalent of benzyne. The Xie group has pioneered use of this species which opens the door to interesting structures through Diels-Alder type reactions and other useful organic transformations.[70] Alternatively, C-substituted *closo*-1,2-carboranes can be prepared through insertion of a substituted alkyne into the *nido*-decaborane(14) cage (*nido*-$B_{10}H_{14}$). Lewis bases such as acetonitrile or dimethyl sulfide are used as activators in these reactions, however the yields of these alkyne condensation reactions are often poor, especially when using electron-rich alkynes.[71] Furthermore, many substituted alkynes can degrade the decaborane cage, further limiting the utility of this reaction.

Functionalising Carboranes at Boron Vertices

The B–H bonds in carboranes are entirely unaffected by the strong bases used to deprotonate the carbon vertices and must be functionalised using different chemical means. While the D_{5d} symmetry of *closo*-1,12-carborane renders all its boron vertices chemically equivalent, *closo*-1,2- and *closo*-1,7-carborane each have four unique boron environments that require different methods to access (**Figure 8**). The positioning of these vertices relative to the carbon atoms in the cluster influences their properties, which can be exploited to functionalise certain sites selectively.

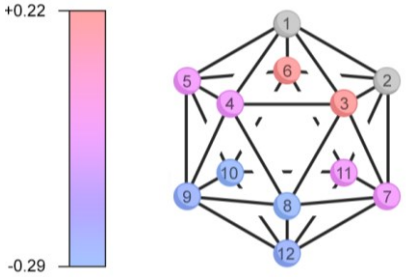

closo-1,2-		*closo*-1,7-	
Site	Charge	Site	Charge
3,6	0.22	2,3	0.13
4,5,7,11	-0.02	4,6,8,11	-0.03
9,12	-0.27	5,12	-0.06
8,10	-0.29	9,10	-0.25

Figure 8. Graphical (left) and tabular (right) representation of the computationally calculated ground-state charges for the boron vertices of *closo*-1,2- and *closo*-1,7-carborane.[72]

The boron atoms furthest away from the carbon vertices, i.e. B(9/12) for *closo*-1,2-carborane and B(9/10) for *closo*-1,7-carborane, are least effected by the electron-withdrawing effects of the carbons and are therefore the most electron-rich. This means that they are the first to be attacked in electrophilic substitution reactions, where the use of a Lewis acid catalyst such as $AlCl_3$ allows selective functionalisation at these sites (**Scheme 2**). Alkyl,[73] benzyl[74] and amino[75] groups can all be introduced in this manner. Halogenation, however, remains the most useful reaction of this class as the resulting halogenated carboranes provide access to a range of B-functionalised derivatives through transition metal catalysed cross-coupling reactions. The addition of electron-poor transition metals such as palladium(II) also occurs selectively at these vertices, which has recently been used to activate these sites and directly install certain types of functional groups.[76–78]

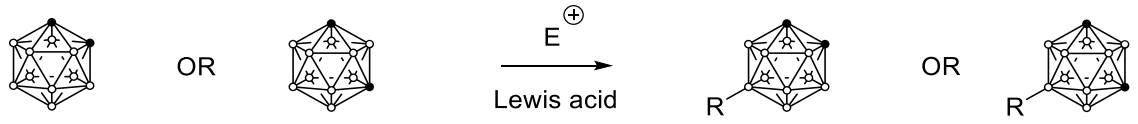

Scheme 2. Functionalistion of *closo*-1,2-carborane at the B(9/12) positions and *closo*-1,7-carborane at the B(9/10) positions through electrophilic substitution. ● = C–H; ○ = B–H (or B if substituted).

In contrast, the B-vertices adjacent to both carbons are exceptionally electron-poor and can be targeted through two different methods (**Scheme 3**). Oxidative addition of electron-rich transition metals is most favourable at B(3/6) for *closo*-1,2-carborane and B(2/3) for *closo*-1,7-carborane due to their low electron-density, and the resultant activated boron vertex is amenable to arylation,[79] amination,[80] alkenylation[81] and borylation.[82] These reactions often have issues with over-substitution and the range of functional groups that can be introduced is currently limited. An alternative method to functionalise these sites involves using a strong base or fluoride source to 'deboronate' the carborane cage, which removes the most electron-deficient B–H unit (formally as BH^{2+}). Subsequent abstraction of the bridging hydrogen with a strong base gives the dicarbollide dianion, which can be recapped with a dihaloborane compound to give B(3/6)- and B(2/3)-substituted *closo*-1,2- and *closo*-1,7-carboranes, respectively.[83–86]

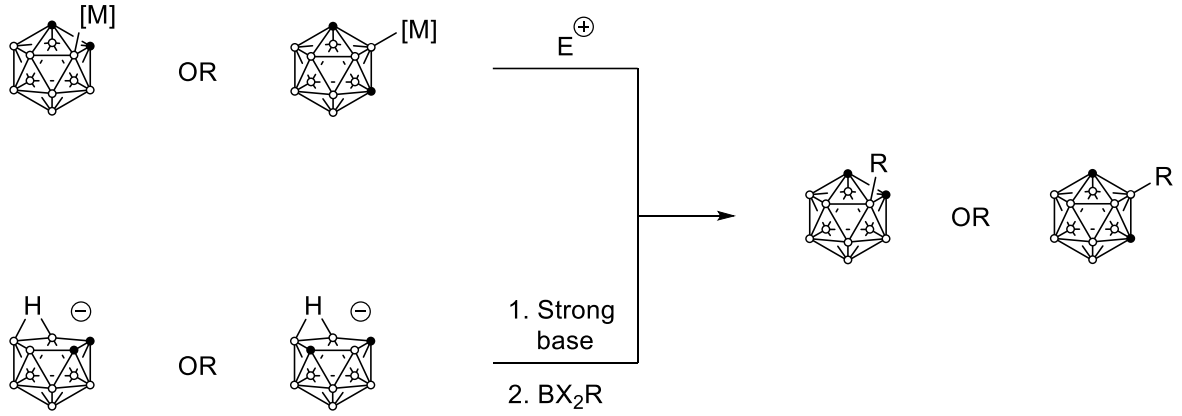

Scheme 3. Functionalisation of *closo*-1,2-carborane at the B(3/6) positions and *closo*-1,7-carborane at the B(2/3) positions following oxidative addition of a transition metal centre [M] (top) and through re-capping of the corresponding *nido*- species (bottom). ● = C–H; ○ = B–H (or B if substituted by an exopolyhedral bond).

The remaining six boron atoms in the carborane cage are the most challenging to functionalise in a regioselective manner. As they possess intermediate electronic properties, they are difficult to differentiate solely through their electronics. In unsubsituted carboranes, sterics play little or no role in functionalisation of B–H (or C–H) groups and this attribute cannot be exploited either. For *closo*-1,2-carborane, selected examples exist where pre-functionalisation of its *nido*- derivative or of *nido*-decaborane(14) result in B(4/5/7/11)- and B(8/10)-halogenated *closo*-1,2-carboranes following cage reconstruction (**Scheme 4A and B**).[87,88] A more powerful method, however, is to use directing groups installed on other vertices to guide the insertion of transition metals into these sites.[89] Oxidative addition of an appropriate agent into this complex and subsequent reductive elimination typically gives the desired substituted carborane. This strategy has been particularly useful for functionalising *closo*-1,2-carborane; for example, Xie and coworkers have pioneered the use of a C-carboxy directing group to activate B(4/5/7/11) vertices which can be removed post-functionalisation or *in situ* (**Scheme 4C**).[90–104] Once again, installation of halogen atoms provides the most synthetic possibilities, however various structures can be installed directly. B(8/10)-functionalised *closo*-1,2-carboranes have also been prepared using this method,[105] however the process is less convenient as multiple synthetic steps are needed to install the directing group at the required position.

Alternatively, B(5/12) and B(4/6/8/11) derivatives of *closo*-1,7-carborane have seen little mention in the literature. Reports exist of their formation through temperature-induced isomerisation of *closo*-1,2-carborane species or through transition-metal catalysed 'cage-walking',[106–111] however these methods are synthetically impractical due to the poor yields and lack of control over which particular isomer is produced. The difficulty in functionalising these two sites can be attributed to their similar electronic properties; there is very little difference in the electron density of the two B–H environments, making selectivity based on electronics highly inefficient. Moreover, a directing group strategy is complicated by the presence of three different B–H environments adjacent to the C-position.

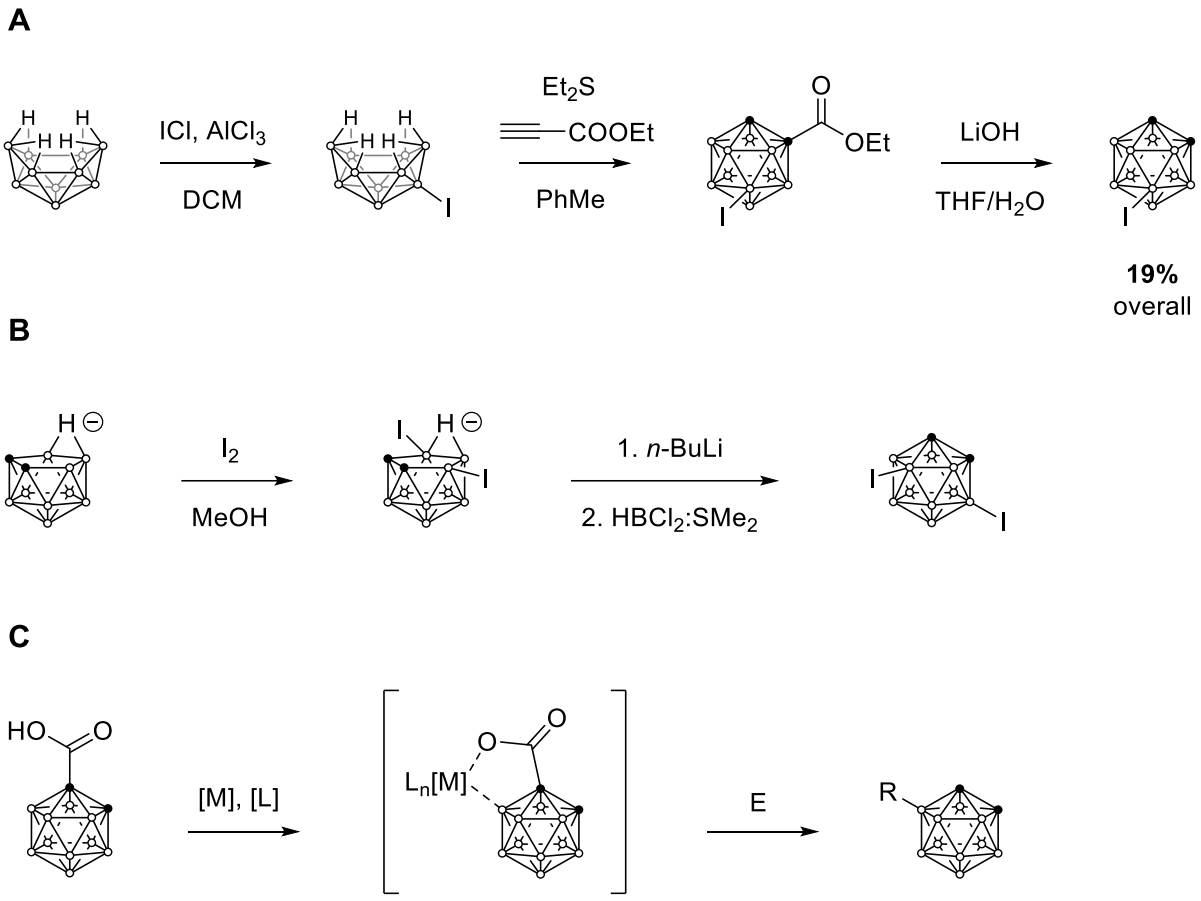

Scheme 4. Literature methods used to functionalise: the B(8/10) position of *closo*-1,2-carborane starting from *nido*-decaborane(14) (A); the B(4) and B(7) positions starting from 7,8-dicarba-*nido*-undecaborate (B); and the B(4/5/7/11) position using a carboxy directing group (C). ● = C–H (or C if substituted); ○ = B–H (or B if substituted by an exopolyhedral bond).

Nonetheless, access to these positions is highly desirable as they provide substitution patterns that are otherwise unattainable for *closo*-1,7-carborane. This, in combination with its greater resistance to deboronation reactions, would make *closo*-1,7-carborane an extremely useful scaffold for a variety of research projects utilising boron clusters. Most importantly, derivatisation of the C(12) position of a 5-functionalised *closo*-1,7-carborane would create a carborane substituted at antipodal vertices ('*para*-type' substitution). This highly desirable geometry is only otherwise accessible by functionalising both carbon atoms of *closo*-1,12-carborane, where its exorbitant cost, commercial unavailability, and low synthetic yield often precludes the use of this rare carborane isomer.

Chapter Aims

In our efforts to develop new bioactive carborane compounds, we have repeatedly encountered the issue of the *closo*-1,2-carborane cage inadvertently degrading into the *nido*- species during a number of chemical transformations. The avoidance of this facile decomposition pathway precludes the use of many base and solvent combinations, especially at elevated temperatures, which limits synthetic possibilities. This made us reconsider the use of *closo*-1,2-carborane and turn to *closo*-1,7-carborane, which is much more stable and therefore amenable to a broader range of transformations. Unfortunately, the lack of access to certain cage vertices limits its utility as a scaffold in medicinal chemistry, and the development of methods to functionalise the B(5/12) and B(4/6/8/11) sites of *closo*-1,7-carborane is of great importance. This Chapter details our pioneering efforts on this front.

Use of a (Transient) Directing Group

Inspired by the recent surge of publications using directing groups to functionalise *closo*-1,2-carboranes at unusual boron vertices, we sought to apply the same strategy to functionalise *closo*-1,7-carborane. While these methods have been used to append a variety of functional groups to the *closo*-1,2-carborane cage, the respective transformations on a *closo*-1,7-carborane framework have been scarcely mentioned in the literature. This is likely due to the electronic differences in boron environments that are in proximity to the carbon atoms in each of the isomers. While *closo*-1,2-carborane has two unique boron sites directly adjacent to the two carbons (B(3/6) and B(4/5/7/11)), *closo*-1,7-carborane has three: B(2/3), B(5/12) and B(4/6/8/11). Furthermore, the adjacent positioning of the carbon atoms in *closo*-1,2-carborane leads to the B(3/6) atoms experiencing a strong inductive effect, electronically differentiating them from the B(4/5/7/11) environments. This effect is not as pronounced in the *closo*-1,7-isomer, which is highlighted by comparing the calculated partial charges for these sites in the respective cages (**Figure 8**). Crucially, the B(5/12) and B(4/6/8/11) sites have very similar calculated charges. These factors make developing a regioselective methodology for *closo*-1,7-carborane significantly more challenging.

Nevertheless, it was hoped that by a judicious choice of reaction conditions, informed by results previously reported in the literature, we would be able to overcome these difficulties and develop a method to functionalise the B(5/12) and B(4/6/8/11) sites of *closo*-1,7-carborane *selectively*. Our goal, at first, was to install halogen atoms onto these vertices, as these can

participate in a range of transition-metal catalysed reactions and could thus act as a springboard to a vast array of novel, functionalised *closo*-1,7-carborane compounds.

Initial attempts at functionalising these vertices involved use of a carboxylic acid as the directing group after attachment to the 1-position. This group is easily introduced through deprotonation/lithiation of *closo*-1,7-carborane followed by nucleophilic addition of this species to carbon dioxide.[62] The Xie group were able to install halogen atoms onto the B(4/6/8/11) sites of *closo*-1,2-carborane using this directing group and *N*-halosuccinimides as the halogen source.[97] In their methodology, $[IrCl_2Cp^*]_2$ was used as the catalyst with silver salts used as an additive to facilitate *in situ* decarboxylation to prevent over-substitution.

When we applied these same conditions to 1-carboxy-*closo*-1,7-carborane (**19**) with NBS as the halogen source (**Scheme 5**), we found that bromination occurred as in the *closo*-1,2- case, however a mixture of products was observed. What appeared to be three distinct products were attributed to *closo*-1,7-carborane brominated at the three different sites adjacent to each carbon vertex, i.e. 5-bromo-*closo*-1,7-carborane (**20**), 4-bromo-*closo*-1,7-carborane (**21**) and 2-bromo-*closo*-1,7-carborane (**22**). Comparisons of ^1H and $^{11}B\{^1H\}$ NMR resonances with an authentic sample of 5-bromo-*closo*-1,7-carborane (*vide infra*) confirmed that this compound was indeed formed in the reaction. Unfortunately, separation of these positional isomers using flash chromatography on silica proved intractable due to their similar elution times, irrespective of which eluent was used. Moreover, if a single isomer is desired for further manipulations, these conditions would be unacceptable due to the formation of two unwanted isomers in a similar proportion.

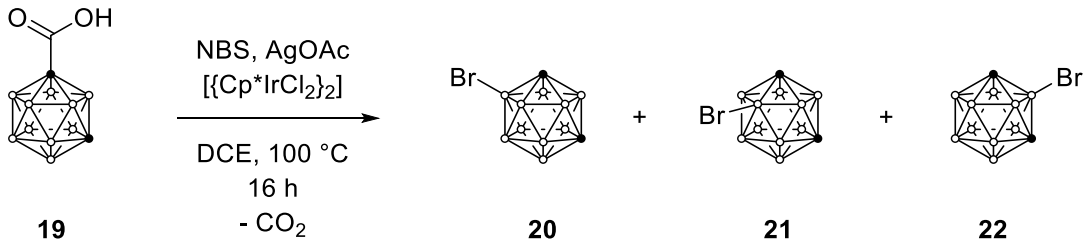

Scheme 5. Bromination of *closo*-1,7-carborane using a carboxy directing group leading to a mixture of isomers. ● = C–H (or C if substituted); ○ = B–H (or B if substituted).

Literature reports have shown that the choice of catalyst, solvent and additive can have significant effects on the selectivity of these directing group-based reactions.[97,112,113] In a notable example, Cao and coworkers found that switching between silver triflate and silver acetate additives allowed direct arylation at either electron-rich or electron-poor carborane B-vertices, respectively.[114] We tested a range of modifications to the reaction conditions such as using different silver salts, halogen sources and metal catalysts as well as changing the solvent and temperature of the reaction. Unfortunately, none of these modifications were successful in achieving the desired transformation effectively. A combination of issues was encountered during our attempts, including poor conversion of the starting material, disubstitution reactions, incomplete decarboxylation during the reaction, along with continued difficulties in achieving selectivity at a single boron site. The result of these reactions was usually a complex mixture of products that resisted separation and made analysis of the constituents difficult. Ultimately, it became clear that a different approach was required to achieve good selectivity.

It has been documented that substituents on the second C-position of the cage can assist in driving the selectivity of these directing group reactions to more distant sites through steric effects.[115,116] While the second carbon in *closo*-1,7-carborane lies further away than in *closo*-1,2-carborane, a sufficiently bulky group at this position should, in principle, hinder access to the nearby B(3/6) sites. This, in turn, would promote substitution at the more distant B(5/12) and B(4/6/8/11) positions, increasing the selectivity of the reaction. As mentioned previously, silyl groups have been used as carborane C-site protecting groups due to their convenient installation and ease of removal.[68,69] A silyl group with bulky substituents such as phenyl or *tert*-butyl groups would therefore serve our needs well, as it can be readily removed post halogenation.

A triphenylsilyl group was selected as the blocking group, which was installed onto *closo*-1,7-carborane through a nucleophilic substitution reaction of commercially-available triphenylsilylchloride and lithio-*closo*-1,7-carborane (**Scheme 6**). Installation of the carboxylic acid directing group was achieved in the same manner as previously, this time using THF to aid solubility, giving the desired product **25** in 51% overall yield. A single crystal X-ray structure of compound **24** (**Figure 9**) was collected and solved by Dr Hunter Windsor (USyd). The molecular structure of this compound shows partial eclipsing of the B(2/3) sites by one of the phenyl groups of the silyl substituent.

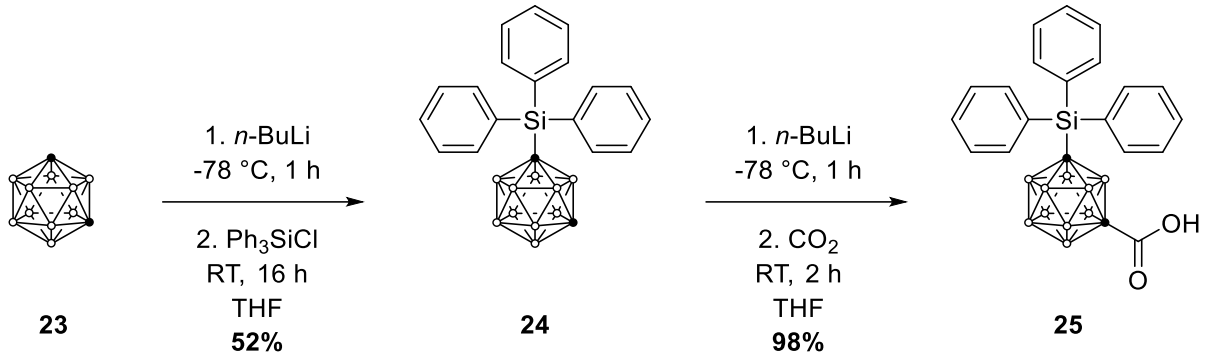

Scheme 6. Synthesis of compound **25** containing a sterically-bulky triphenylsilyl group attached to one of the cage carbon atoms. ● = C–H (or C if substituted); ○ = B–H.

Unfortunately, when compound **25** was subjected to the directing-group assisted halogenation conditions above, a complex reaction mixture was again produced. As before, partial decarboxylation and conversion to the product made analysis of the crude reaction mixture difficult, and attempts at separation were similarly unsuccessful. To investigate whether this silyl blocking group was an effective strategy, an alternative approach was devised. Yan and coworkers reported a directing group method where a substituted formyl-*closo*-1,2-carborane converted into an imine *in situ* can effect palladium-mediated B–H activation.[116] Notably, the palladium(II)-boron bonded complexes that are intermediates in these reactions were isolable and could be fully characterised. With no potential issues of decarboxylation or need to optimise conversion to the halogenated products, synthesis of a palladacycle of triphenylsilyl carborane **24** was attempted to determine whether site selectivity could be achieved.

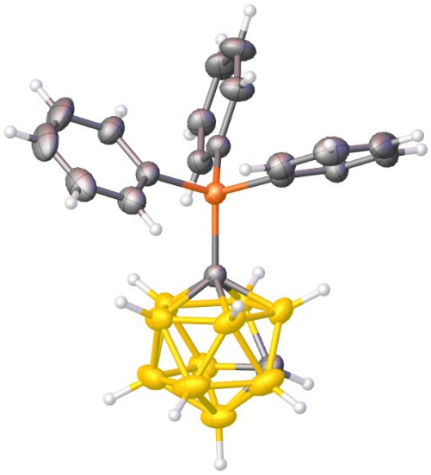

Figure 9. The molecular structure of compound **24** determined using single-crystal X-ray crystallography showing the steric crowding of some boron sites and the unobstructed B12 site.

Synthesis of the di-substituted carborane **26** was achieved using a nucleophilic addition reaction with methyl formate, followed by acid hydrolysis (**Scheme 7**). Subsequently, the 2-aminophenol imine of this compound was readily formed at reflux in toluene with 3Å molecular sieves. Finally, addition of an equimolar quantity of palladium acetate to a toluene solution of this imine resulted in complete consumption of the starting material within 12 hours (**Scheme 7**). The TLC of the crude product showed the formation of two major carborane products, and following chromatographic separation, two carborane palladacycles were isolated. Both products displayed the expected aromatic peaks in their ^{1}H NMR spectra but differed more significantly in their ^{11}B{^{1}H} spectra. Notably, the first of these showed 6 distinct peaks, which suggests a palladacycle bonded through a boron vertex that lies on the symmetry plane of the cage. Only a B(5/12) bonded compound would satisfy this requirement and this product is therefore assigned as compound **28**. The other major product showed 10 peaks in its ^{11}B{^{1}H} spectrum, which would be expected of both a B(4/6/8/11) or a B(2/3) bound palladacycle. While we were unable to grow suitable crystals for X-ray analysis and insufficient material was available to characterise this compound using 2D COSY (^{11}B{^{1}H}–^{11}B{^{1}H}) NMR spectroscopy, this compound is tentatively assigned as the B4-substituted palladacycle **29** due to the expected steric hindrance making Pd–B(2/3) bond formation unfavourable.

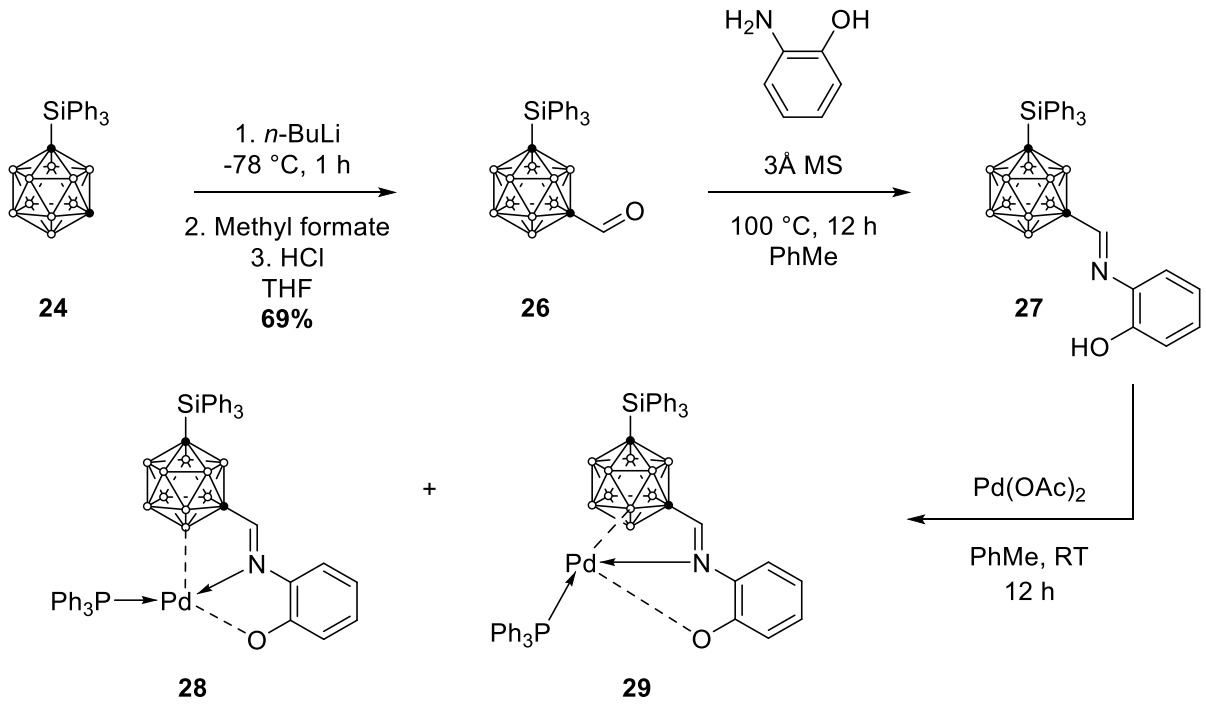

Scheme 7. Synthesis of the sterically-bulky formyl-*closo*-1,7-carborane **26** and the isolable imine palladacycle complexes **28** and **29**. The reaction produced two major products that could not be fully characterized but are assigned to the above isomers. ● = C–H (or C if substituted); ○ = B–H (or B if substituted).

Although these compounds demonstrate that the triphenylsilyl group can influence which B–H site of *closo*-1,7-carborane is activated by a transition metal centre, it does not completely resolve selectivity issues. An optimisation of reaction conditions including changing the amine and phosphine ligand used might improve results, but complete regioselectivity and access to both isomers through orthogonal conditions seemed unlikely. Ultimately, it was decided that a new approach was needed to effectively functionalise these positions.

A Novel Protecting Group for Carborane B-Vertices

During our attempts to develop new methods for the functionalisation of carboranes at C-vertices, we were seeking to attach amines directly to the cage using carboranes bearing C–X bonds as the electrophiles in cross-coupling reactions (**Scheme 8**). Using palladium or copper catalysts in these reactions, it was found that instead of isolating the desired cross-coupling product, these reaction conditions resulted in cleavage of the C–X bond and provided only the parent, unsubstituted carborane. These results provided us with an inspiration for another application: considering the ease of halogenation of the B(9/10) positions of *closo*-1,7-carborane, a method of removing them would allow the exciting possibility of using halogens as protecting groups for the boron vertices of carboranes. In this way, the most electron-rich sites of the cage would be blocked, allowing electrophilic substitution at the 'intermediate' boron atoms as the next-most electron-rich vertices. Subsequent removal of the protecting groups would provide *closo*-1,7-carborane substituted only at these difficult to access sites. To our knowledge, no protecting groups exist for carborane boron vertices and this approach would constitute the first such example.

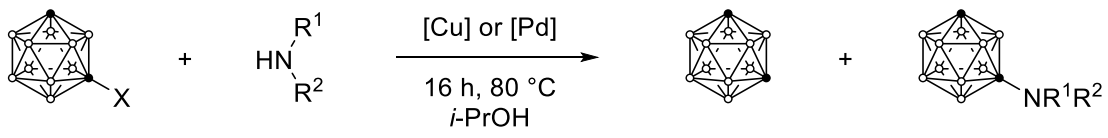

Scheme 8. Attempted cross-coupling of C-halo-carboranes with amine nucleophiles leading to cleavage of the C–X bond. ● = C–H (or C if substituted); ○ = B–H.

Naturally, carborane B–X bonds are chemically very different to their carbon bonded counterparts, experiencing an electron-donating effect from the cage rather than an electron-withdrawing one. When the same conditions shown in Scheme 8 were applied to 9-iodo-*closo*-1,2-carborane as a test substrate, the starting material was recovered unchanged. This is unsurprising, as the B–I bond in carboranes is unusually stable when compared to that in an aryl iodide. Notably, many researchers have tried (and failed) to isolate or characterise oxidative addition complexes of halocarboranes with palladium,[117–120] likely because the formation of these complexes is reversible and thermodynamically disfavoured. This explains the often-sluggish reactivity of halocarboranes in transition metal catalysed cross-coupling reactions, where carefully tuned conditions are required to achieve satisfactory yields. While some literature reports on palladium-catalysed cross-coupling reactions with carboranyl halides do note dehalogenated carboranes as side-products, the conversions are generally low and thus this would not serve as an effective deprotection method. Alkali metals are also known to cause cleavage of carborane B(3)–X bonds,[118] however dehalogenation of the less reactive 9-halo-carboranes is only known to occur with sodium in liquid ammonia,[121] conditions that are likely intolerant of other functional groups installed on the cage. In their paper investigating B–I bond activation, Viñas *et al.* reported a handful of conditions where nickel and palladium complexes in stoichiometric quantities removed an iodine atom from the 3-position of *closo*-1,2-carborane.[118] When we applied these conditions to 9-iodo-*closo*-1,2-carborane however, we found that no dehalogenation reaction had occurred. Again, this example demonstrates the decreased reactivity of B–X bonds connected to more electron-rich boron vertices of the cage. In further research, we screened a range of conditions that are used to dehalogenate organic aromatic compounds but were met with a similar lack of success.

Finally, we noticed a series of papers published by the Xie group which showed activation of B–I bonds using palladium or nickel catalysts with concomitant photoirradiation (**Scheme 9**).[122–124] In these reactions, the transition metal catalyst serves to form a photo-active carborane complex (**A**) that generates a B-centred carboranyl radical (**B**) following photoexcitation in a single-electron transfer (SET) process. Addition of this radical into the C=C bond of a (hetero)aryl compound gives radical **C**, which upon oxidation by Pd(I) species through another SET and deprotonation of the resultant carbocation **D** gives the (hetero)aryl-coupled carborane (**E**). While the authors make no mention of deiodinated side products in these papers, we hypothesised that hydrodehalogenation could occur if carboranyl radical **C** were to be reduced through the abstraction of a hydrogen atom from an appropriate source.

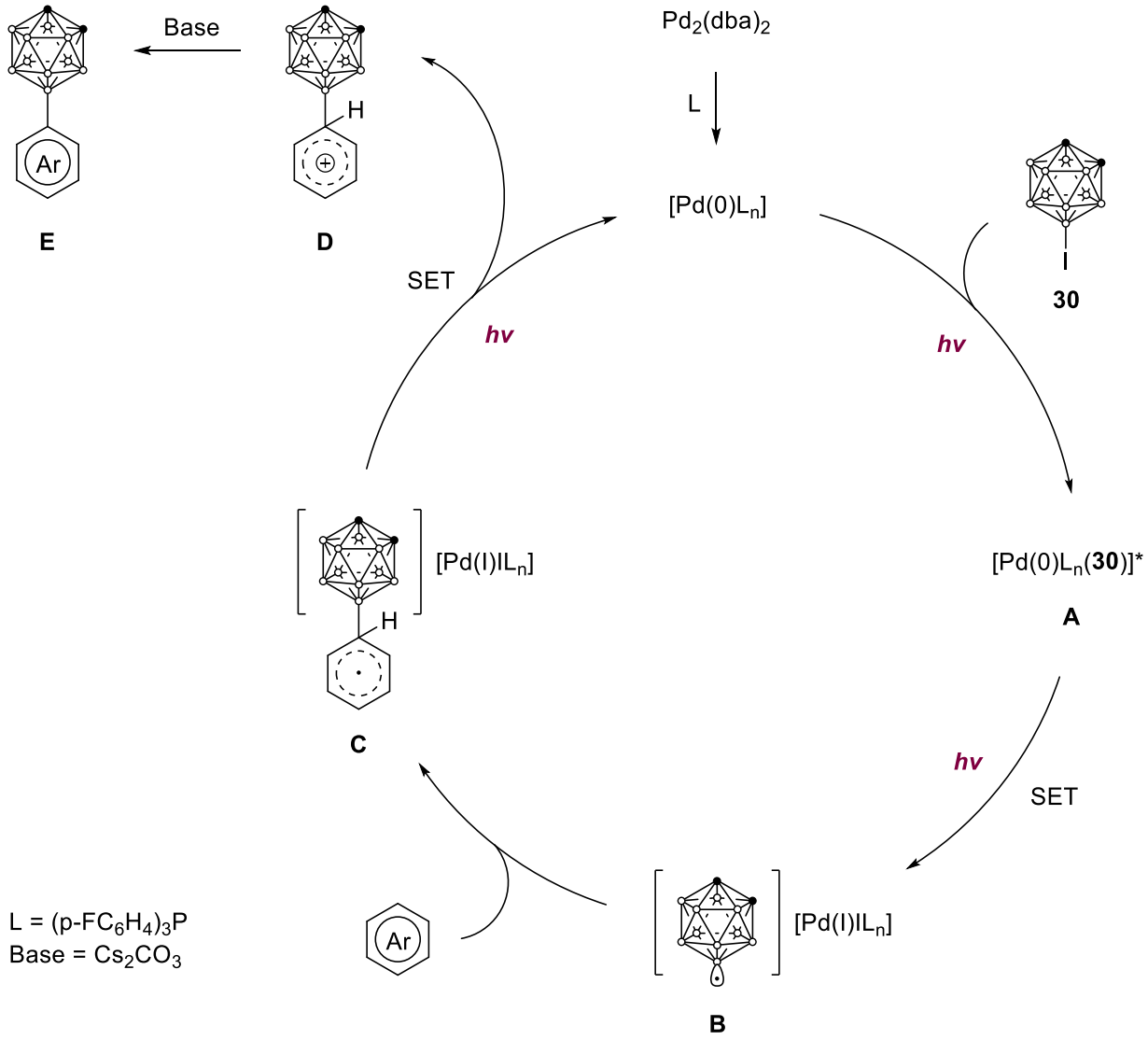

Scheme 9. Proposed catalytic cycle of the palladium catalysed photoinduced coupling of aryl compounds with iodocarboranes developed by Xie and co-workers. Compound **B** is proposed as an intermediate to de-iodination in our deprotection conditions. ● = C–H; ○ = B–H (or B if substituted).

We thus applied similar conditions to 9-iodo-*closo*-1,2-carborane (**30**) *without* a (hetero)aryl coupling partner, using a UV (λ = 365 nm) LED as light source and the more readily available triphenylphosphine as ligand. Under these conditions, mostly starting material was recovered but a small amount of deiodinated product was observed in the $^{11}B\{^{1}H\}$ NMR spectrum of the crude reaction mixture. Encouraged by these results, we changed the solvent from acetonitrile to THF, which is a more effective hydrogen atom source due to its lower bond dissociation energy.[125] To our delight, complete conversion of the starting material was observed after 24 h allowing almost quantitative recovery of 'deprotected' *closo*-1,2-carborane.

Nickel was also found to be an effective catalyst in this reaction, and $[NiCl_2(PPh_3)_2]$ was selected as the active complex in our optimised conditions (**Scheme 10**) due to its low cost and ease of synthesis. Preliminary control experiments found that no conversion occurred when the reaction was repeated at reflux without UV irradiation, indicating that this reaction likely follows a similar radical-based mechanism to that previously reported by Xie and coworkers.[122] Starting material was also recovered in the absence of a metal catalyst, confirming that a complex such as **A** (**Scheme 9**) is the photoactive species rather than 9-iodo-*closo*-1,2-carborane itself. While one cannot definitively confirm that THF is the hydrogen atom source in this reaction, it seems likely given the increased conversion following the change in solvent from acetonitrile. Repeating this reaction in deuterated THF would allow confirmation of this by assessing the degree of deuterium incorporation into the carborane cage in the $^{11}B\{^1H\}$ NMR spectrum of the product.

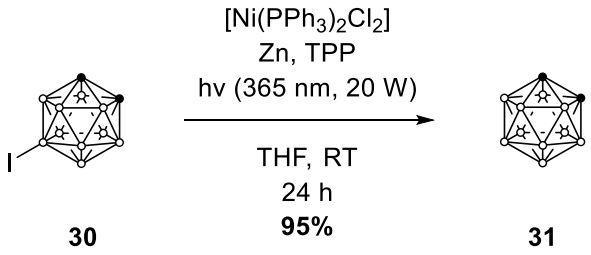

Scheme 10. Optimised conditions for the deiodoniation of 9-iodo-*closo*-1,2-carborane. ● = C–H; ○ = B–H (or B if substituted).

Intriguingly, Xie and coworkers note in one of their papers that bromo- and chlorocarboranes were found to be inactive under these photo-mediated coupling conditions.[123] This may reflect the weaker covalent bonds that iodine forms compared to bromine and chlorine, which in turn makes C–I bonds more reactive in many transition-metal mediated reactions. Despite this, modern catalyst and ligand systems have made organobromides (and chlorides) viable and competent electrophiles in cross-coupling reactions. In fact, work in the Spokoyny group has demonstrated that B-bromocarboranes can participate in these reactions and even outperform their iodo- counterparts when electron-rich, biarylphosphine ligands are used.[110,111,126–128] This makes bromocarboranes effective precursors to a diverse range of carboranes substituted at cage B-sites. We wished to harness the difference in reactivity of B–I and B–Br bonds in these photo-mediated reactions to access carboranes brominated at unusual

boron vertices. Pleasingly, when 9-bromo-*closo*-1,2-carborane was subjected to the optimised deiodination conditions, the starting material remained unchanged even after prolonged reaction times. With a suitable boron-vertex protecting group now in hand and the orthogonality of B–Br bonds under these conditions demonstrated, we turned toward synthesising a range of novel bromocarborane isomers.

Synthesis of Previously Unknown Carborane Isomers Using a Blocking Strategy

While many of the positional isomers of bromo- *closo*-1,2-, *closo*-1,7- and *closo*-1,12-carborane have been synthesised, four others have remained elusive to date. The first of these, 8-bromo-*closo*-1,2-carborane, has never been reported despite the synthesis of the closely related 8-iodo-*closo*-1,2-carborane by Hawthorne and coworkers in 2012.[88] This route, which spans four steps, is somewhat tedious, uses highly toxic *nido*-decaborane(14) as a starting material and affords the product in only 19% overall yield. An alternate pathway to accessing this vertex would therefore be highly desirable. A similar situation exists for the second unknown isomer, where the publication of a route to 2-iodo-*closo*-1,7-carborane over a decade ago has not been followed by a synthesis of the brominated analogue.[129]

The other two unknown isomers, 4-bromo-*closo*-1,7-carborane and 5-bromo-*closo*-1,7-carborane, have only been reported as products in the thermal isomerisation of 9-bromo-*closo*-1,2-carborane or palladium-catalysed 'cage-walking' isomerisation of the same compound.[106,111] Importantly, their separation or characterisation was not reported, and even if successful would provide these isomers in very low yields. To the best of our knowledge, installation of halogens or any other functional groups at these sites in a carborane cage in a *selective* manner has never been reported. A regioselective synthesis of these isomers would therefore not only constitute their first isolation but would also provide unprecedented access to *closo*-1,7-carboranes functionalised at these sites for application in drug design and materials science.

Synthesis of 8-Bromo-*closo*-1,2-Carborane

Of these unknown isomers, 8-bromo-*closo*-1,2-carborane (**32**) was chosen as the first target. Our vision for its synthesis consisted of a three-step procedure: protection of the most electrophilic sites of the *closo*-1,2-carborane cage (positions 9 and 12) with iodine followed by bromination of the 8-vertex as the next most electrophilic site, and finally removal of the iodine protecting groups (**Scheme 11**).

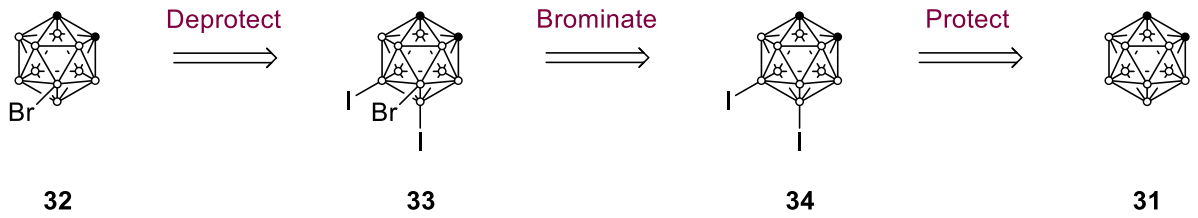

Scheme 11. Proposed retrosynthetic strategy for 8-bromo-*closo*-1,2-carborane (**32**) through iodine-protected *closo*-1,2-carborane intermediates. ● = C–H; ○ = B–H (or B if substituted).

Iodination of the most electrophilic boron vertices of carboranes is generally a straight-forward procedure, with well-established literature methods using molecular iodine and either a strong Lewis acid such as aluminium trichloride or a strongly oxidising mixture of acetic, nitric and sulfuric acids to effect the transformation.[130,131] These produce the desired product in excellent yield and selectivity. In the case of *closo*-1,2-carborane however, the B(9/12) and B(8/11) positions have somewhat similar electron densities, and while mono-iodination produces mainly the 9-isomer with only small amounts of the 8-isomer, di-iodination is known to produce a mixture of 8,9- (**35**) and 9,12-substituted (**34**) products.[132] In our hands, the 9,12-substituted product constituted around 87% of the crude product mixture regardless of the conditions used (**Scheme 12**). Separation of the isomers proved futile and would therefore, following bromination, provide a mixture of 8-bromo- and 9-bromo-*closo*-1,2-carborane. These isomers have very similar properties and fail to separate using common preparative purification techniques. Further development of the protection procedure was thus required.

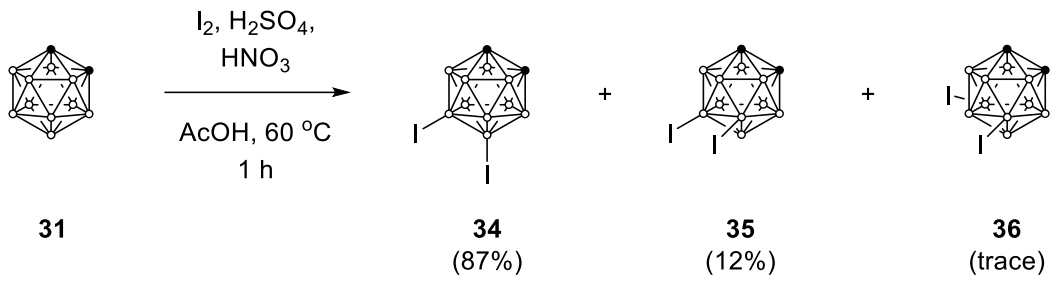

Scheme 12. Initial attempted synthesis of 9,12-protected *closo*-1,2-carborane (**34**) using conventional iodination conditions producing an inseparable mixture containing 8,9-diiodo-*closo*-1,2-carborane (**35**) and 8,10-diiodo-*closo*-1,2-carborane (**36**). ● = C–H; ○ = B–H (or B if substituted).

Initial attempts at solving this issue involved protecting an additional boron vertex to create a tri-iodinated carborane. This, in principle, would convert the three isomers produced in the di-iodination reaction to only two unique isomers: 8,9,10-triodo-*closo*-1,2-carborane (**38**) and 8,9,12-triiodo-*closo*-1,2-carborane (**37**) (**Scheme 13**). The first of these, produced from the 8,10-diiodo derivative, should only form as a minor impurity, as its parent forms only a trace amount of the starting reaction mix. The major product after bromination would therefore be expected to be 8-bromo-9,10,12-iodo-*closo*-1,2-carborane. Unfortunately, when iodination of the isomeric mixture of diiodo-*closo*-1,2-carborane was attempted with one equivalent of iodine a new issue was unexpectedly encountered: formation of the trisubstituted species was always accompanied by significant amounts of the tetra-substituted 8,9,10,12-tetraiodo-*closo*-1,2-carborane as well as unreacted diiodo-*closo*-1,2-carborane. This resulted in the subsequent bromination step yielding a complex mixture of products which proved to be intractable.

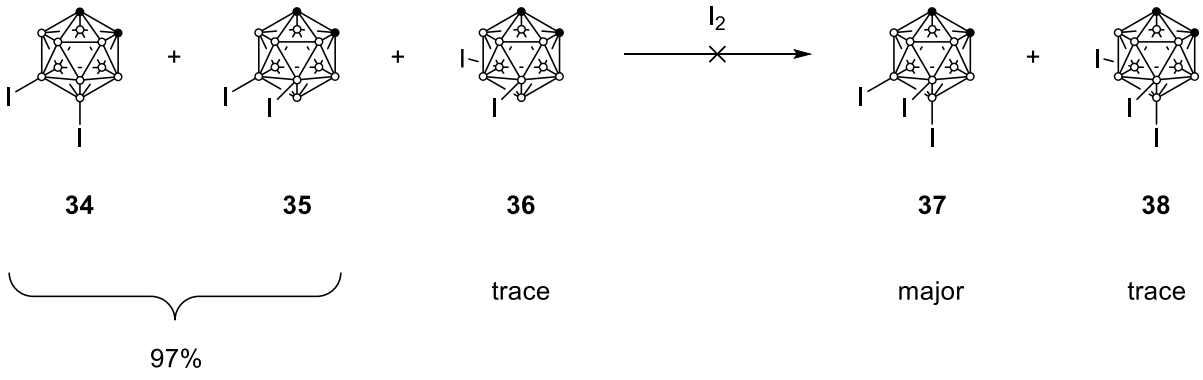

Scheme 13. Expected isomer distribution resulting from the iodination of an isomeric mixture of diiodo-*closo*-1,2-carborane. The reaction instead produces a mixture of di-, tri- and tetra-iodinated *closo*-1,2-carboranes. ● = C–H; ○ = B–H (or B if substituted).

Following these attempts, we became aware of recent publications by Chen and co-workers reporting convenient methods of carborane halogenation using *N*-halosuccinimides in 1,1,1,3,3,3-hexaflouro-2-propanol (HFIP) with triflic acid as a catalyst.[133,134] Notably, the authors reported excellent isomer selectivity for a range of mono- and dihalogenated carboranes using these conditions. When we implemented these conditions, the desired 9,12-diiodo-*closo*-1,2-carborane (**34**) formed in 93% yield (**Scheme 14**) with no evidence of 8-substituted isomers in the NMR spectra of the reaction product. This method is operationally simple and gives a product of sufficient purity following a simple work-up procedure.

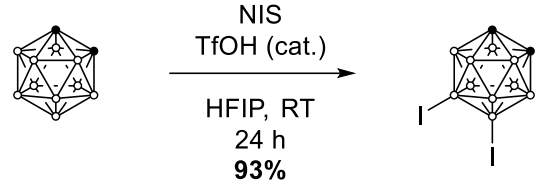

31 **34**

Scheme 14. Regioselective synthesis of 9,12-protected *closo*-1,2-carborane using literature conditions.[134] ● = C–H; ○ = B–H (or B if substituted).

With an effective method to protect the 9,12-positions in place, we moved onto brominating the next most electrophilic site. In this case, bromination of other boron vertices is not a concern, as the B(4/5/7/11) and B(3/6) sites are substantially less electrophilic than the B(8/10) vertices. Using NBS as the brominating reagent in HFIP with triflic acid as catalyst furnished compound **33** in 63% yield (**Scheme 15**). While this is a relatively low yield for reactions of this type, the rest of the reaction mass consists of unreacted starting material that can be recovered easily. Moreover, no attempts were made to optimise these conditions; an increased loading of triflic acid or higher reaction temperatures would likely drive this reaction to completion.

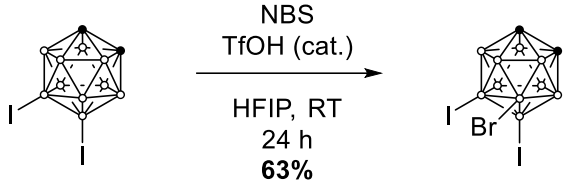

34 **33**

Scheme 15. Synthesis of 8-bromo-9,12-diiodo-*closo*-1,2-carborane. ● = C–H; ○ = B–H or B if substituted.

Finally, completion of the overall synthetic route was achieved by removing the iodine atoms using the optimised deprotection conditions described earlier (**Scheme 16**). To our delight, the iodine atoms were completely removed with no evidence of concomitant removal of the bromine substituent, giving the deprotected product 8-bromo-*closo*-1,2-carborane (**32**) in near quantitative yield. The ^{1}H NMR spectrum of the product showed a single cage C–H resonance at 3.62 ppm as expected for a symmetrically substituted product. The ^{11}B{^{1}H} NMR spectrum consisted of 7 peaks corresponding to the 7 boron environments, with the ^{1}H-coupled ^{11}B NMR spectrum showing a lone singlet at -5.4 ppm which is assigned to the bromine substituted 8-position. Using this fact along with the relative integrals and a 2D ^{11}B–^{11}B COSY NMR spectrum (**Figure 10**) allowed complete, unambiguous assignment of each boron peak and confirmed the identity of the product.

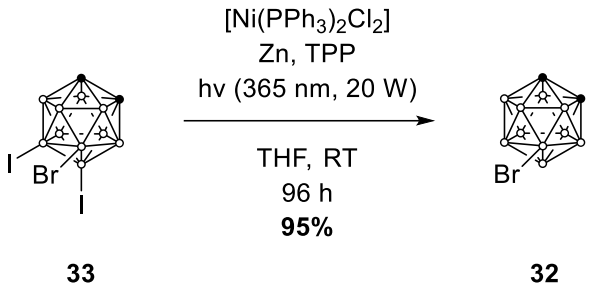

Scheme 16. Deprotection of compound **33** using our previously-tested conditions. ● = C–H; ○ = B–H (or B if substituted).

This three-step process is straight-forward and produces the desired isomer in 57% overall yield, which is a significant improvement on Hawthorne's method of synthesising the related 8-iodo-*closo*-1,2-carborane. As a result, 8-substituted derivatives of *closo*-1,2-carborane can now be conveniently and effectively prepared. In their report on the synthesis of 8-iodo-*closo*-1,2-carborane, Hawthorne and co-workers showed that deboronation of this compound proceeds selectively and solely at the 3-position (which, in this case, is non-equivalent to the 6-position). We have found that the deboronation reaction is similarly selective in the case of 8-bromo-*closo*-1,2-carborane (**Scheme 17**). Recapping of this deboronated species with, for example, boron tribromide would provide access to '*para*-type' substitution on *closo*-1,2-carborane (compound **40**). Similarly, a cobalt bis-dicarbollide complex (COSAN) formed from this brominated *nido*-carborane (**41**) would be substituted at

opposite ends of the complex – an unusual substitution pattern – which could open up interesting new avenues for functional molecules utilising COSAN frameworks.[135]

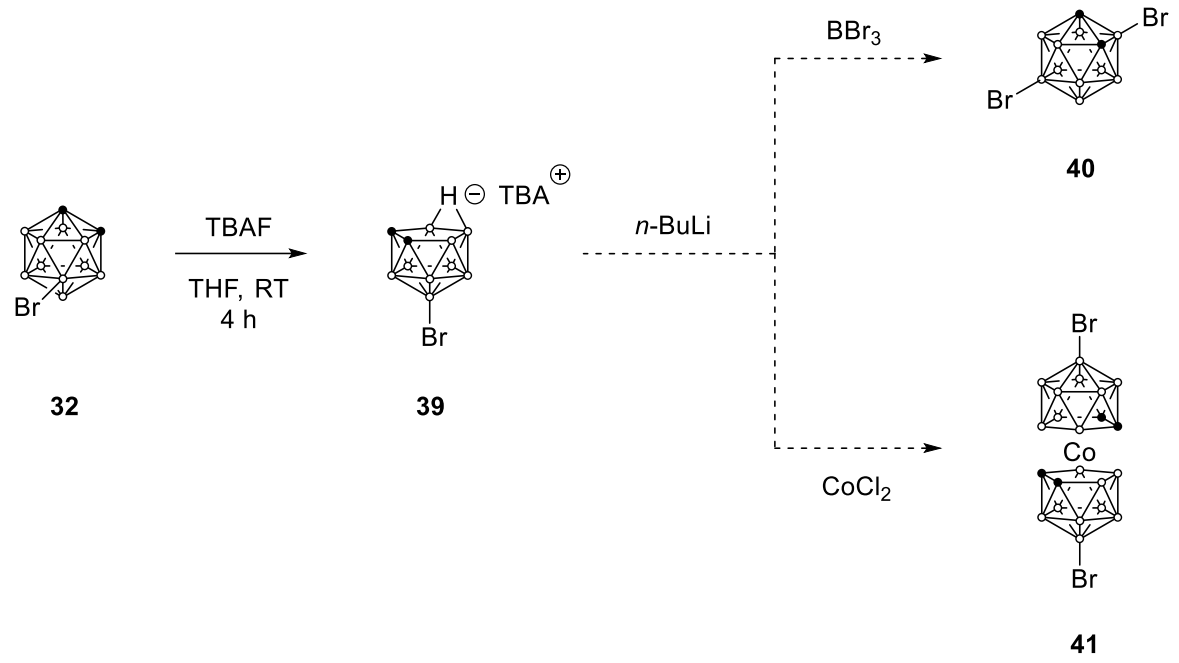

32 39 40 41

Scheme 17. Deboronation of 8-bromo-*closo*-1,2-carborane and potential synthetic operations to transform the resulting *nido*-carborane (**39**) into interesting carborane-based frameworks. ● = C–H; ○ = B–H (or B if substituted by an exopolyhedral bond).

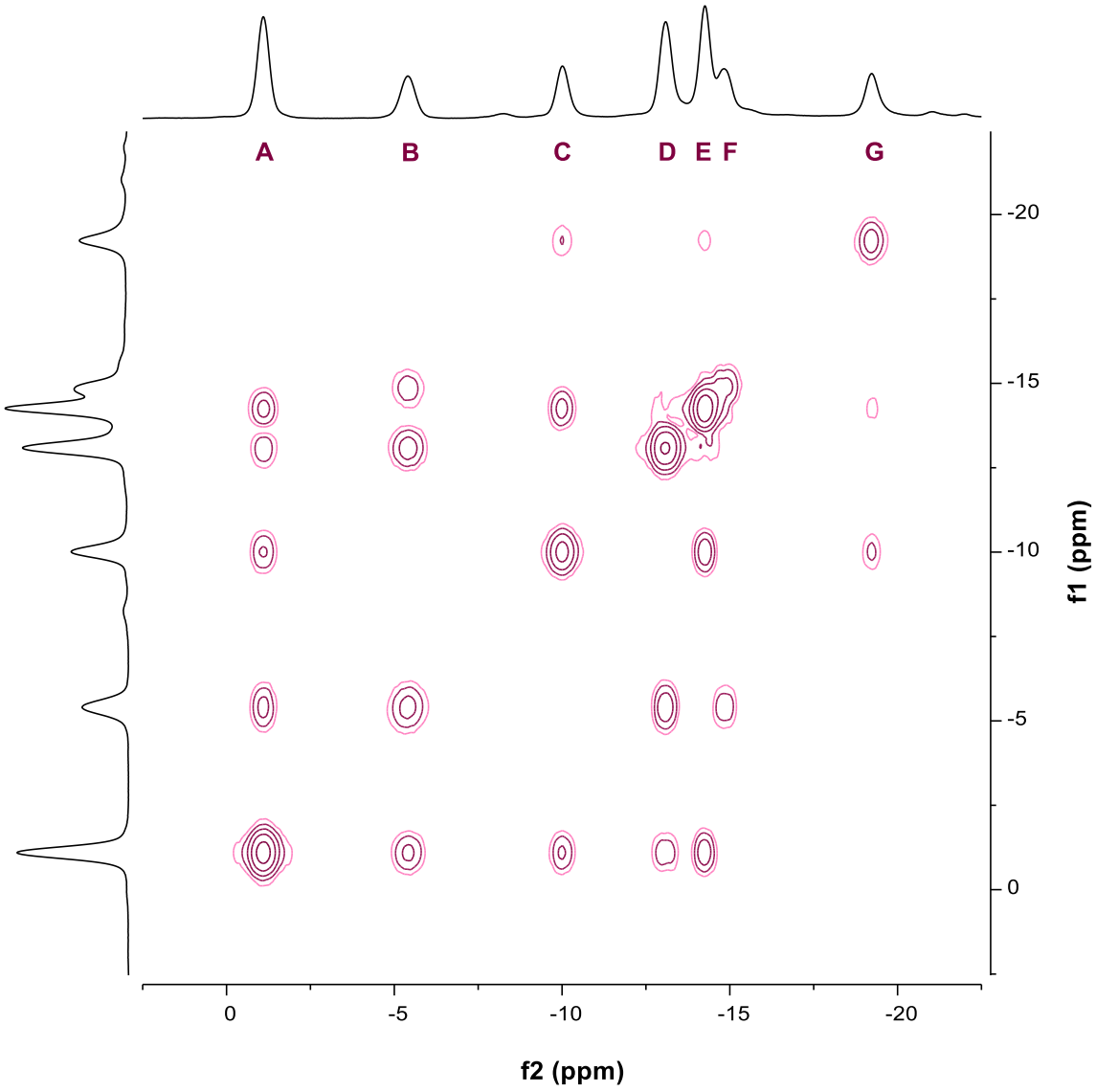

Peak	Integral	Mult.	Cross-peaks	Assignment
A	2	d	B, C, D, E	B(9/12)
B	1	s	A, D, F	B8
C	1	d	A, E, G	B10
D	2	d	A, B, E, F	B(4/7)
E	2	d	A, C, D, G	B(5/11)
F	1	d	B, D	B3
G	1	d	C, E	B6

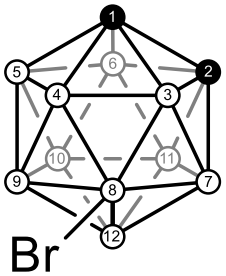

32

Figure 10. The 2D $^{11}B\{^{1}H\}$–$^{11}B\{^{1}H\}$ COSY NMR spectrum of 8-bromo-*closo*-1,2-carborane (**32**) and its peak assignments. The cross-peaks between peaks D and F are difficult to see due to the presence of nearby signals. ● = C–H; ○ = B–H (or B if substituted).

Synthesis of 5-Bromo-*closo*-1,7-Carborane

Our next target was the elusive 5-bromo-*closo*-1,7-carborane (**20**) isomer. The most electrophilic positions on *closo*-1,7-carborane are the B(9/10) sites, with published computational data generally showing similar charge densities for the B(5/12) and B(4/6/8/11) sites.[72] Although there is some disagreement in the literature on which site is substituted after the B(9/10) positions are occupied, more recent papers indicate that the B(5/12) position is preferentially functionalised by halogens.[136] Our own preliminary DFT calculations on 9,12-diiodo-*closo*-1,7-carborane showed that the B(5/12) positions have slightly more partial negative charges than the B(4/6/8/11) sites and would thus be the expected site of attack in a bromination reaction. We therefore envisaged a process to make 5-bromo-*closo*-1,7-carborane (**20**) similar to that which we used to synthesise 8-bromo-*closo*-1,2-carborane (**Scheme 18**).

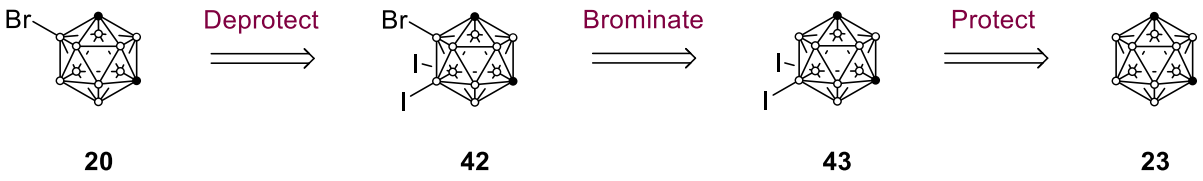

Scheme 18. Proposed retrosynthetic strategy for 5-bromo-*closo*-1,7-carborane (**20**) through iodine-protected *closo*-1,7-carborane intermediates. ● = C–H; ○ = B–H (or B if substituted).

Installation of two protecting iodine groups is straightforward for *closo*-1,7-carborane. Because the B(9/12) positions are substantially more electron-rich than any of the other boron sites, iodination is completely selective under electrophilic halogenation conditions. Thus, when *closo*-1,7-carborane was heated with two reactive equivalents of iodine in a mixture of acetic, nitric and sulfuric acids, 9,10-diiodo-*closo*-1,7-carborane (**43**) was rapidly obtained as the sole product in almost quantitative yield (**Scheme 19**).

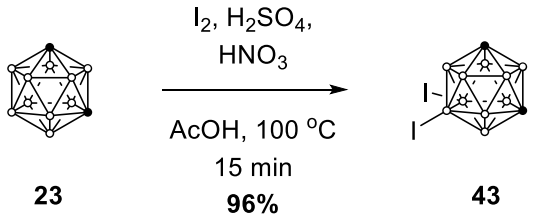

Scheme 19. Synthesis of 9,10-protected *closo*-1,7-carborane using conventional iodination conditions. ● = C–H; ○ = B–H (or B if substituted).

The next stage of the process, bromination of 9,10-diiodo-*closo*-1,7-carborane, proved substantially more troublesome. Over the course of the project, almost 50 different conditions were tested, a subset of which are shown in Table 1. Conditions commonly used to brominate carboranes, using molecular bromine and aluminium trichloride as a Lewis acid in DCM, resulted in complete recovery of the starting material (Entry 1). Other Lewis acids tested also showed no effect, even in equimolar quantities or when heated for prolonged periods in a higher boiling solvent (Entries 2–4). When we tried using bromine in the acid mixture used to iodinate the cluster in the previous step (Entry 5), we were pleased to find that most of the starting material was consumed. However, a portion of the carborane material decomposed under these conditions. While carboranes are known to be sensitive to bases and certain nucleophiles, undergoing deboronation and potentially further oxidative degradation, they generally display excellent stability in acidic environments, even under rather harsh conditions. In these reactions, formation of molecular iodine was observed along with C–H resonances corresponding to 9-iodo-*closo*-1,7-carborane in the ^{1}H NMR spectrum of the crude product, indicating that dehalogenation of the starting material had occurred to some extent. Moreover, we observed a significant upfield shift of some resonances in the boron NMR of the crude product, indicative of the formation of B–O or B–N bonds. These species were only observed when nitric acid was used in the reaction (Entries 6 and 7), which has been previously used under highly acidic conditions to synthesise B-hydroxy carboranes.[137–139] On this basis, we propose that the mechanism in Scheme 20 may account for the formation of hydroxylated carboranes under these conditions. Further investigations into this side-reaction may prove interesting but were deemed beyond the scope of this project due to time constraints. Adjustments to temperature, reaction time and relative acid concentrations proved somewhat effective in limiting the amount of decomposition, but no product conversion was observed under these conditions (Entry 8).

Table 1. Optimization of reaction conditions for the synthesis of compound **42**. ● = C–H; ○ = B–H (or B if substituted).

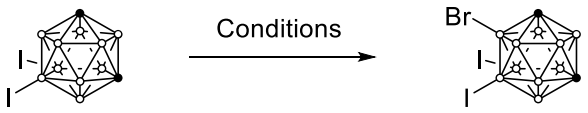

43 **42**

Entry	Br^+ source[a]	Solvent[b]	Additive	Temp. (°C)	Time (h)	Ratio **42**:**43**[c]
1	Br_2	DCM	$AlCl_3$	40	16	NC
2	Br_2	DCE	$AlCl_3$	100	16	NC
3	Br_2	DCE	$FeCl_3$	100	16	NC
4	Br_2	DCE	$HgCl_2$	100	16	NC
5	Br_2	AcOH	H_2SO_4/HNO_3 (50% *v/v*)	120	8	*
6	NBS	H_2SO_4	HNO_3 (50% *v/v*)	100	8	*
7	Br_2	H_2SO_4	–	100	8	NC
8	Br_2	AcOH	H_2SO_4/HNO_3 (33% *v/v*)	80	16	NC
9	NBS	H_2SO_4	–	RT	24	0.9†
10	NBS	H_2SO_4	–	60	16	1.7†
11	NBS	H_2SO_4	–	100	16	3.1†
12	NBS (3 eq.)	H_2SO_4	–	100	16	5.1†
13	NBS (3 eq.)	H_2SO_4	TBAB	100	16	4.6†
14	NBS (3 eq.)	H_2SO_4	TfOH (cat.)	100	16	6.1†
15	TBCA	H_2SO_4	–	60	16	0.9†
16	NBS	HFIP	TfOH (cat.)	RT	16	NC
17	NBS	HFIP	TfOH (cat.)	60	16	0.6
18	NBS	TfOH	–	RT	120	0.9
19	NBS	TfOH	–	60	4	2.0

[a] Used in one molar equivalent unless otherwise specified.
[b] DCE = 1,2-dichloroethane; HFIP = hexafluoroisopropanol; TfOH = triflic acid.
[c] Determined by ^1H NMR. NC: no conversion; *: Deiodinated starting material and other side products observed.
†: 4-bromo isomer also observed.

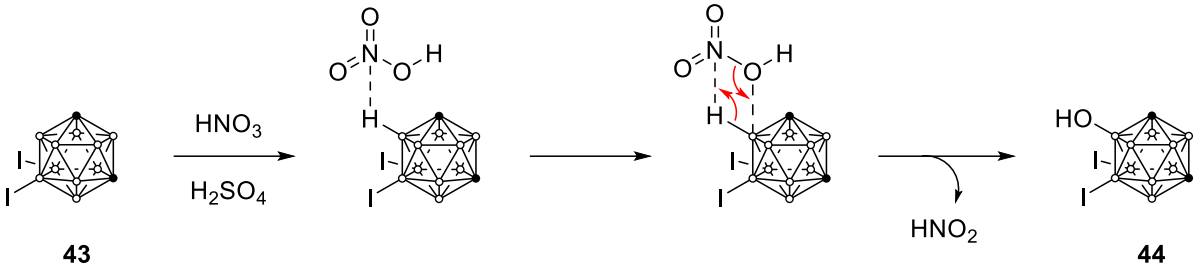

Scheme 20. Proposed mechanism for the formation of hydroxylated carborane side-products in the acid-mediated bromination of compound **43**. ● = C–H; ○ = B–H (or B if substituted).

Ultimately, we decided to explore alternative bromination conditions. The electron-poor nature of the *closo*-1,7-carborane cage coupled with the electronically deactivating and sterically demanding iodine substituents necessitated the use of extremely forcing conditions. A report in the literature on the effective bromination of highly deactivated aromatic substrates using NBS in concentrated sulfuric acid seemed a promising starting point.[140] When these conditions were applied to 9,10-diiodo-*closo*-1,7-carborane (Entry 10), a significant portion of the material was converted to the desired product. Importantly, there was no evidence of decomposition or side product formation that had plagued our previous attempts. Unfortunately, small amounts of what is likely to be the 4-isomer were also evident in the $^{11}B\{^{1}H\}$ NMR spectrum of the crude product, with two other cage C–H resonances evident in the ^{1}H NMR spectrum. Using an excess of NBS and increasing the temperature improved the conversion (Entries 11 and 12), but separation of the isomers proved troublesome. Addition of the phase transfer agent tetrabutylammonium bromide (TBAB) seemed to improve selectivity slightly but reduced the conversion of the reaction (Entry 13). The addition of triflic acid improved conversion but also resulted in increased formation of the 4-isomer (Entry 14), whereas using tribromoisocyanuric acid (TBCA) as the brominating reagent had the opposite effect (Entry 15).

Using the bromination conditions reported by Chen and coworkers[134] for less substituted carboranes proved ineffective for this substrate with only starting material recovered after 24 hours (Entry 16). Increasing the reaction temperature to 60 °C, however, resulted in conversion to the product in approximately 35% yield by NMR (Entry 17). Crucially, no evidence for the formation of other isomers was found, with the only other carborane resonances evident in the ^{1}H and $^{11}B\{^{1}H\}$ NMR spectra arising from unreacted starting material. Running the reaction in neat triflic acid gave minimal product at room

temperature even after several days (Entry 18), but heating at 60 °C improved the conversion to almost 70% without compromising selectivity (Entry 19).

Ultimately, we were unable to increase the conversion of the reaction beyond 70%. Interestingly, working-up the reaction and applying the same conditions to the partially converted product resulted in further reaction and increased the yield of the desired product. Decomposition of NBS under these conditions evidently occurs before bromination of the substrate is complete. Unfortunately, the same effect could not be achieved when additional NBS was added to the reaction mixture after the initial reaction period.

Although purification of compound **42** is achievable, due to the similar polarities of product and starting material, we often found it more convenient to isolate the crude product and proceed to the deprotection without further purification. In this way, any non-brominated carborane is converted to the parent *closo*-1,7-carborane, which was easily separable from the deprotected 5-bromo-*closo*-1,7-carborane. When the trisubstituted carborane **42** was purified before proceeding, deprotection of this compound gave, following purification by flash chromatography on silica, 5-bromo-*closo*-1,7-carborane (**20**) in nearly quantitative yield (**Scheme 21**).

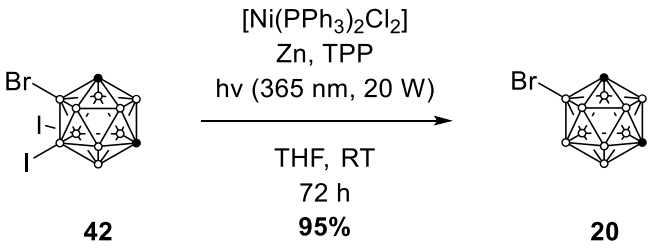

Scheme 21. Deprotection of compound **42** using our previously optimised de-iodination conditions giving 5-bromo-*closo*-1,7-carborane (**20**). ● = C–H; ○ = B–H (or B if substituted).

The ^{1}H NMR spectrum of **20** showed two distinct cage C–H resonances at 3.31 ppm and 2.95 ppm, reflecting the loss of equivalency of these vertices. Although these peaks could not be spectroscopically assigned to their respective positions, the downfield resonance is likely that of the C–H adjacent to the bromine (C1 position) which experiences a strong electron-withdrawing effect due to the adjacent electronegative bromine atom. The ^{11}B{^{1}H} NMR spectrum showed 6 distinct peaks as expected of this structure, where the bromine substituent

lies on a plane of symmetry bisecting the C1, B5, B12 and C7 positions. Notably, the peak at -4.8 ppm is assigned to the B–Br boron as it presents as a singlet in the non-decoupled boron spectrum of the compound. The other $^{11}B\{^{1}H\}$ NMR resonance with a relative integral of one can therefore be assigned to the B(12) position. Using this knowledge, the remaining boron peaks were assigned based on their cross-peaks in the 2D $^{11}B\{^{1}H\}$–$^{11}B\{^{1}H\}$ COSY spectrum (**Figure 11**) of the compound, which completely agrees with the connectivity expected for the desired isomer.

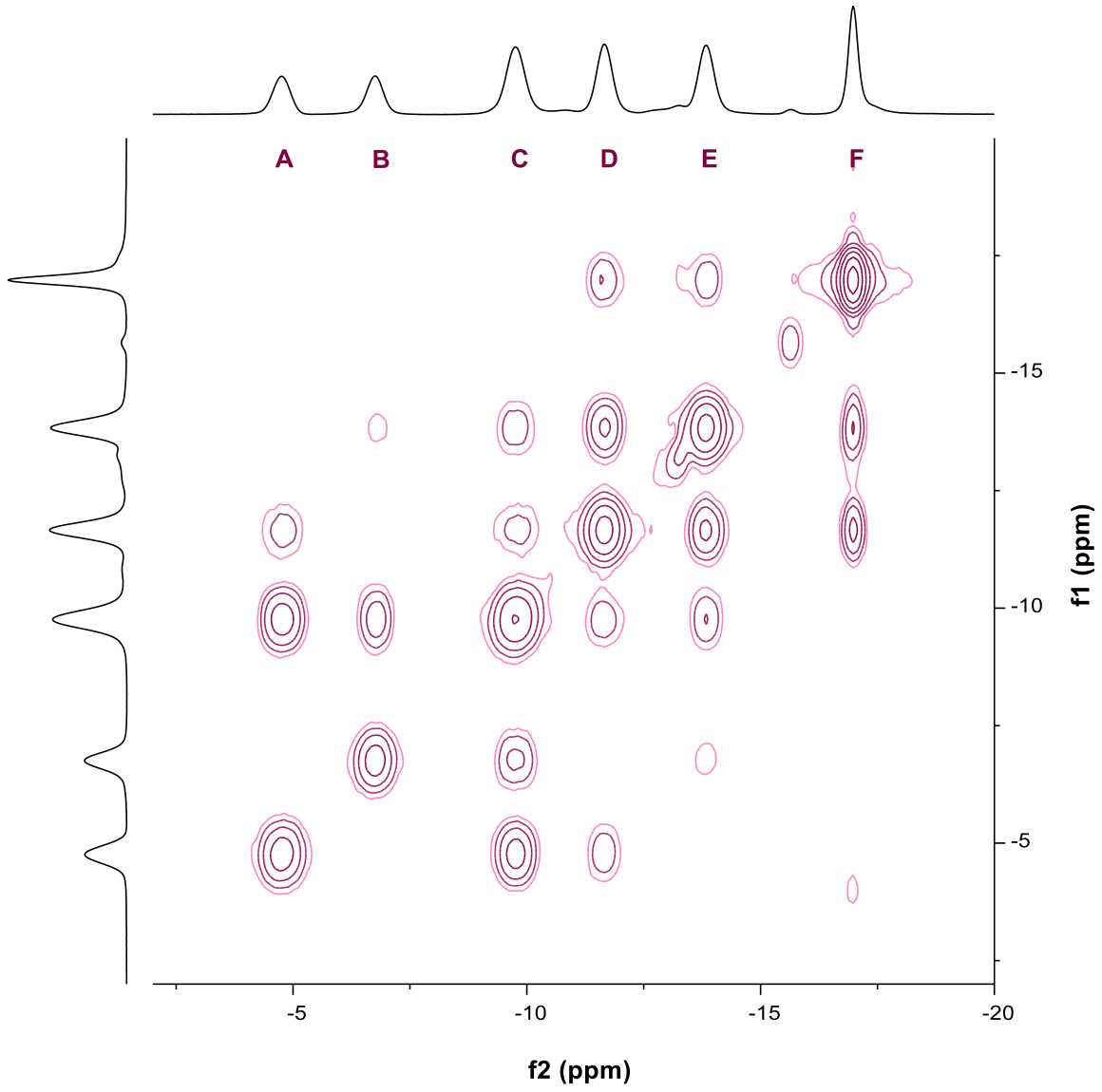

Peak	Integral	Mult.	Cross-peaks	Assignment
A	1	s	C, D	B5
B	1	d	C, E	B12
C	2	d	A, B, D, E	B(9/10)
D	2	d	A, C, E, F	B(4/6)
E	2	d	B, C, D, F	B(8/11)
F	2	d	D, E	B(2/3)

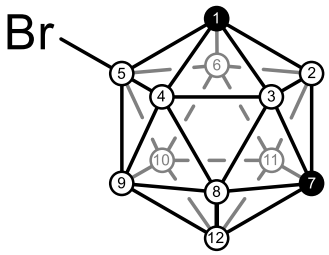

20

Figure 11. The $^{11}B\{^{1}H\}$–$^{11}B\{^{1}H\}$ COSY NMR spectrum of 5-bromo-*closo*-1,7-carborane (**20**) and its peak assignments. The circled cross-peaks are of low intensity and have been overlayed from a zoomed-in view of the spectrum. ● = C–H; ○ = B–H (or B if substituted).

Towards the Synthesis of 4-Bromo-*closo*-1,7-Carborane

The synthesis of the third unknown carborane isomer, 4-bromo-*closo*-1,7-carborane (**21**), proved to be the most challenging. Initially, we used a similar approach to that used in the previous two cases. While the previous synthesis involved selective bromination of the 5-position of *closo*-1,7-carborane following protection of the B(9/10) positions, in this case we sought instead to further protect this site along with the identical 12-position. In this manner, the next site of substitution should be one of the four identical B(4/6/8/11) vertices, which are substantially more electronegative than the last remaining B(2/3) site (**Scheme 22**). Thus, *closo*-1,7-carborane was reacted with four equivalents of iodine under the same halogenation conditions as described previously. In this case, heating the reaction at 120 °C in a sealed system for several hours was required to achieve the complete consumption of iodine. Unfortunately, the presence of four sterically demanding and electron-withdrawing iodine groups makes the tetra-iodinated *closo*-1,7-carborane (**46**) an extremely poor substrate for electrophilic reactions. The cage is so deactivated and sterically crowded that despite using extremely harsh conditions, no evidence of bromine incorporation at all was seen in numerous attempts. Ultimately, it became clear that this strategy was futile, and an alternative approach was required.

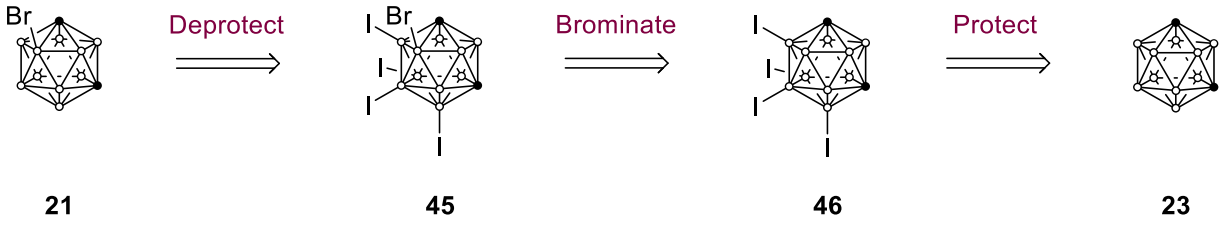

Scheme 22. Initially proposed retrosynthetic approach to 4-bromo-*closo*-1,7-carborane through doubly-protected *closo*-1,7-carborane intermediates. ● = C–H; ○ = B–H (or B if substituted).

A promising strategy is altering the nature of the cage itself – thereby changing the electronic properties of each vertex – before reverting to the original *closo*-1,7-carborane cage. The most obvious and straightforward example of this is the deboronation of the cluster into 7,9-dicarba-*nido*-undecaborate before eventual recapping to reform the *closo*- cage. In 2014, Hawthorne and coworkers showed that following deboronation of *closo*-1,7-carborane, iodination of the resulting 7,9-dicarba-*nido*-undecaborate under electrophilic substitution

conditions gave the 8-iodo isomer selectively in nearly quantitative yield.[129] Following recapping with dichloroborane-dioxane complex, the authors were able to isolate 2-iodo-*closo*-1,7-carborane. This work demonstrated that selective removal of a boron vertex modifies the electronics of the cage to the point where a greater amount of electron density is located at the open face, making it available for electrophilic substitution reactions. Indeed, following deboronation of *closo*-1,2-carborane, the first two sites of the resulting *nido*-carborane cage to be substituted in halogenation reactions are the boron atoms located at the open face of the cage.[141,142] By analogy, we expected that the other two boron atoms making up the open face of 7,9-dicarba-*nido*-undecaborate would be the next most nucleophilic. Following cage recapping, these equivalent sites would make up two of the four B(4/6/8/11) positions, and could therefore provide regioselective access to mono- or di-substituted *closo*-1,7-carborane at these positions (**Scheme 23**).

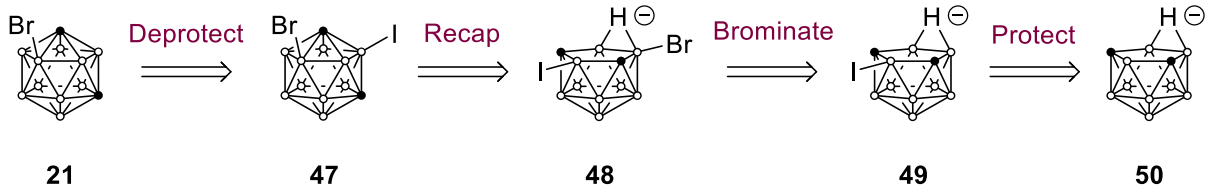

Scheme 23. Alternative retrosynthetic approach to 4-bromo-*closo*-1,7-carborane (**21**) through *nido*-carborane intermediates. ● = C–H; ○ = B–H (or B if substituted by an exopolyhedral bond).

The required precursor, 7,9-dicarba-*nido*-undecaborate (**50**), was thus generated through deboronation of *closo*-1,7-carborane using TBAF as the fluoride source (**Scheme 24**). These well-established conditions furnished the desired *nido*-carborane as the tetrabutylammonium salt,[143] which is conveniently soluble in many organic solvents. While this compound and its derivatives slowly oxidise under ambient conditions, storage under vacuum or at lower temperatures (-20 °C) allows them to be kept for at least a week with only minimal decomposition. Protection of the 8-position of **50** by installation of an iodine at this vertex was attempted using the literature procedure of Hawthorne *et al.* previously mentioned.[129] In our hands, aluminium trichloride proved to be a poor Lewis acid for this transformation, with yields rarely exceeding 50% even with higher catalyst loadings or extended reaction times. Following a small Lewis acid screen, we found that iron(III) chloride and mercury(II) chloride were most effective in this transformation. Iron(III) chloride was

selected as the Lewis acid of choice due to its lower toxicity and the greater ease of purification of the resultant product, which could be isolated in 96% yield (**Scheme 24**).

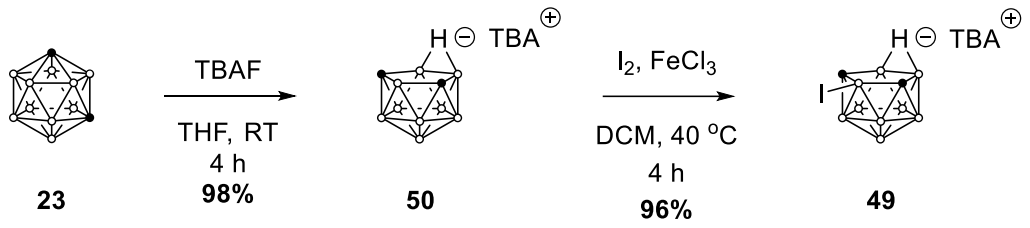

Scheme 24. Synthesis of 8-protected 7,9-dicarba-*nido*-undecaborate (**49**). ● = C–H; ○ = B–H (or B if substituted by an exopolyhedral bond).

With the protected *nido*- species in hand, we turned to installing the desired bromine onto the cage. Initially, conditions similar to those used for iodination were used, however these proved too forcing and resulted in a mixture of products containing di-brominated species (identified by ESI-LRMS), reflecting the greater electrophilicity of bromonium ions. Lowering the reaction temperature and slow addition of bromine prevented di-substitution (**Scheme 25**), however the $^{11}B\{^{1}H\}$ NMR spectrum of the crude reaction mix showed minor impurities indicating the formation of other isomers. Surprisingly, the major product of this reaction showed only 6 resonances in its decoupled boron NMR spectrum, indicating bromination had occurred elsewhere to the open face. If substitution had occurred at one of the desired B(10/11) sites, the loss of cage symmetry would result in 9 distinct boron environments. Moreover, a doublet of doublets of integration two was observed in the non-decoupled ^{11}B NMR spectrum of this compound, a coupling pattern characteristic of boron atoms connected to both an endo- and exopolyhedral proton, confirming that the B(10/11) sites remained unsubstituted in the major product of this reaction. The only isomers that could account for the symmetry displayed in the boron NMR spectra of this compound are 1-bromo-8-iodo-7,9-dicarbo-*nido*-undecaborate and 6-bromo-8-iodo-7,9-dicarbo-*nido*-undecaborate, with 2D $^{11}B\{^{1}H\}$-$^{11}B\{^{1}H\}$ COSY NMR experiments confirming that the 6-isomer (**51**) was in fact the major product. Following recapping and deprotection, this isomer would give *closo*-1,7-carborane brominated at the 9-position. As this isomer is easily accessible through other methods, no further attempts were made to purify this compound or optimise its synthesis.

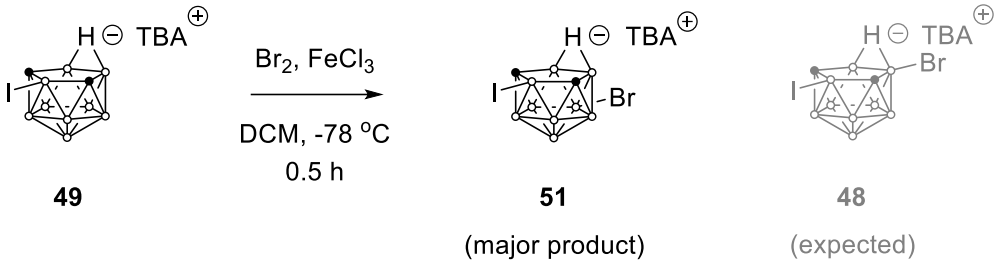

Scheme 25. The major product 6-bromo-8-iodo-7,9-dicarbo-*nido*-undecaborate (**51**) of the bromination of *nido*-carborane **49** along with the expected 10-isomer (grey, **48**). ● = C–H; ○ = B–H (or B if substituted by an exopolyhedral bond).

We next tried to further modify the electronics of the cage so as to encourage bromination at the desired site. When treated with a strong base, *nido*-carboranes lose their bridging proton and form doubly negatively-charged dicarbollide ions. Most salts of these compounds are unstable when exposed to air and moisture, however they can react with electrophiles *in situ* to form substituted monoanionic *nido*-carboranes. Importantly, it has been shown that 7,9-dicarba-*nido*-undecaborate can be sequentially deprotonated and substituted with methyl iodide, ultimately forming a *nido*-carborane that is permethylated only at the boron atoms of the open face.[144] It was anticipated that generation of the dicarbollide of compound **49** would result in a species that favoured incorporation of electrophilic Br^+ at its open face.

When a THF solution of **49** was treated with two equivalents of *n*-butyllithium (**Scheme 26**), monitoring of the reaction mixture with NMR spectroscopy revealed complete consumption of the starting material and formation of a new set of boron resonances. While complete assignment of these peaks could not be achieved due to the overlap of many of the signals, the $^{11}B\{^1H\}$ spectrum shows a significant upfield shift of one of the boron resonances that is characteristic of a dicarbollide anion. Furthermore, comparison of this spectrum with that of the dilithio salt of the parent dicarba-7,9-*nido*-undecaborate dicarbollide (**53**) reported in the literature showed clear differences,[145] indicating that transmetalation of the iodine had not occurred and the desired dicarbollide (**52**) was formed (**Figure 12**). When the dicarbollide solution was quenched with bromine (**Scheme 26**), the reaction rapidly decolourised and NMR indicated complete consumption of the dicarbollide. However, the $^{11}B\{^1H\}$ NMR spectrum of the crude product showed formation of the previously formed 6-bromo isomer **51** as the main product. Evidently, delocalisation of the negative charge throughout the cluster is sufficient to retain the 6-position as the most electron-rich site, yet it is interesting that other electrophiles substitute at different positions when added to similar dicarbollides. Proposed mechanisms for

these reactions involve insertion of the alkyl group into the bridging position, followed by rearrangement (**Scheme 27**), and it is likely that bromine reacts in a different manner. Reaction of dicarborallide **52** with alkyl halides would provide further insight into this reaction and its mechanism but this was beyond the scope of this project.

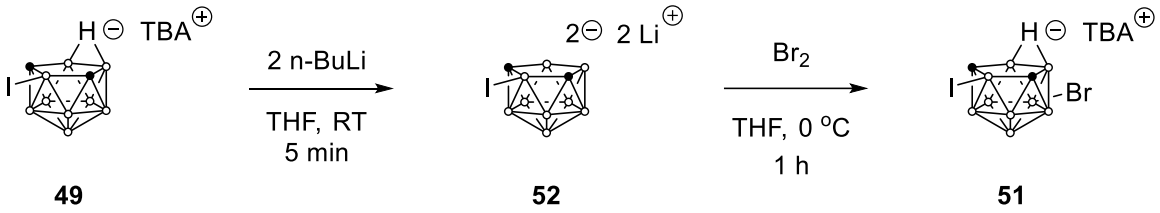

Scheme 26. Synthesis of the lithium dicarbollide of 8-iodo-7,9-dicarbo-nido-undecaborate (**52**) and its subsequent bromination. ● = C–H; ○ = B–H (or B if substituted by an exopolyhedral bond).

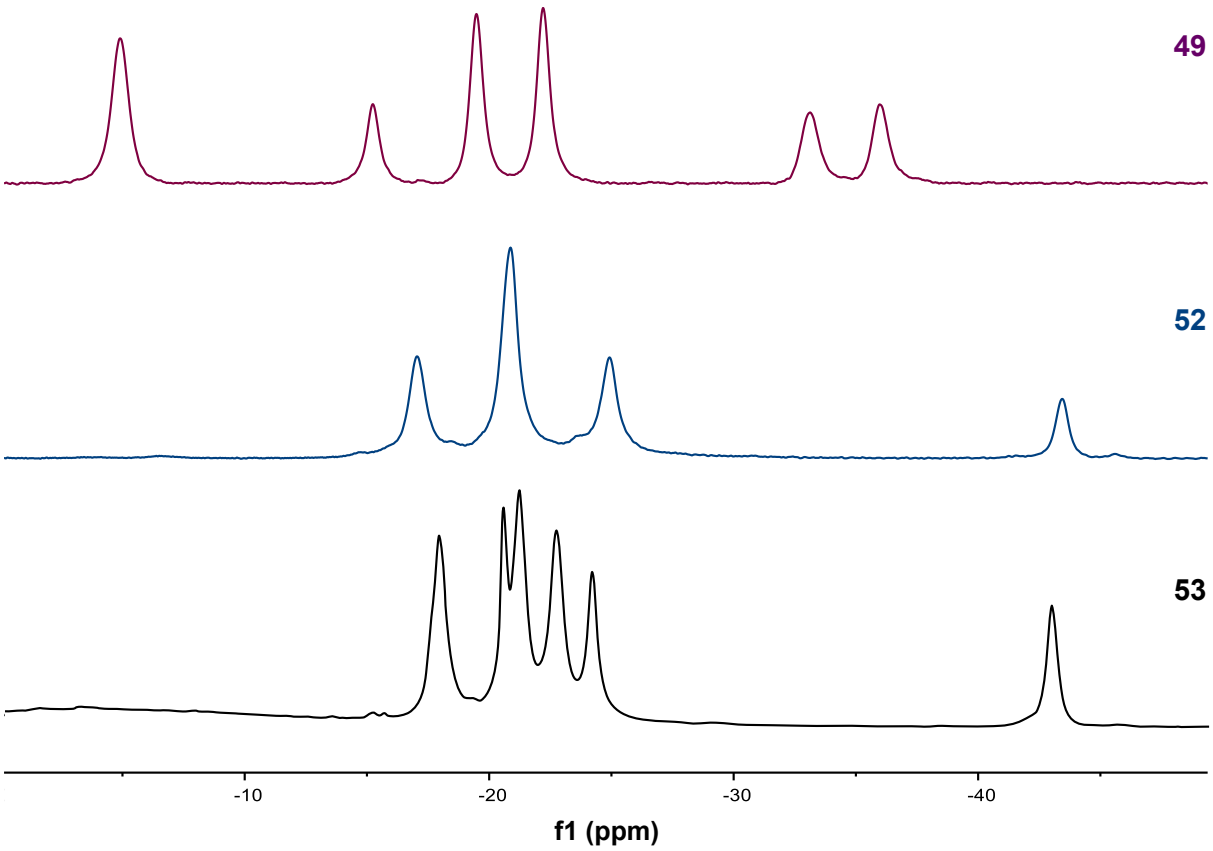

Figure 12. Comparison of the $^{11}B\{^{1}H\}$ NMR spectra of 8-iodo-7,9-dicarba-*nido*-undecaborate (**49**, —) and the two dicarbollides $Li_2(8\text{-I-}7,9\text{-}C_2B_9H_{10})$ (**52**, —) and $Li_2(7,9\text{-}C_2B_9H_{11})$ (**53**, —). The spectrum of **53** was adapted from a literature report.[145]

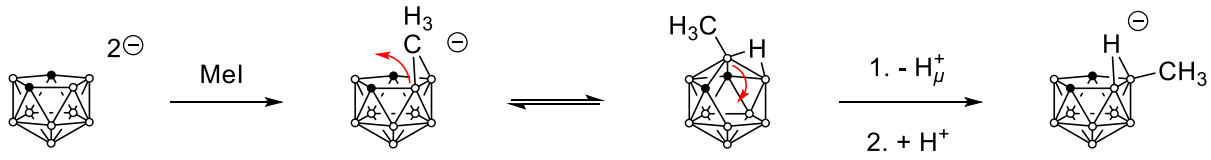

Scheme 27. Proposed literature mechanism for the alkylation of 7,9-dicarbabollides.[144] The alkyl group first inserts into the bridging position of the open face forming a three-centre two-electron bond with two boron vertices. Rearrangement of one of the boron atoms followed by abstraction of the newly formed bridging proton with a base forms the B(10)-substituted 7,9-dicarba-*nido*-undecaborate after reprotonation. ● = C–H; ○ = B–H (or B if substituted by an exopolyhedral bond).

As the second most electrophilic vertex in 7,9-dicarba-*nido*-undecaborate is evidently the 6-position, efforts turned to installing a second protecting iodine group at this position to see whether further substitution would provide access to the desired B(10/11) sites of the *nido*-framework. Because iodination of boron vertices is more straightforward and selective for *closo*-1,7-carboranes, we initially hoped to access the doubly protected compound through deboronation and subsequent iodination of 9-iodo-*closo*-1,7-carborane (**54**). This procedure, however, produces two isomers in approximately equal proportion as the B3 and B6 vertices are no longer equivalent (**Scheme 28**). Despite repeated attempts, we were unable to separate these isomers using preparative chromatographic methods, and a mixture of these would make future synthetic steps intractable. Instead, we opted to use the diiodo species **43**, which upon deboronation gives quantitatively a single isomer **57** that has two undesirable substitution sites protected (**Scheme 29**).

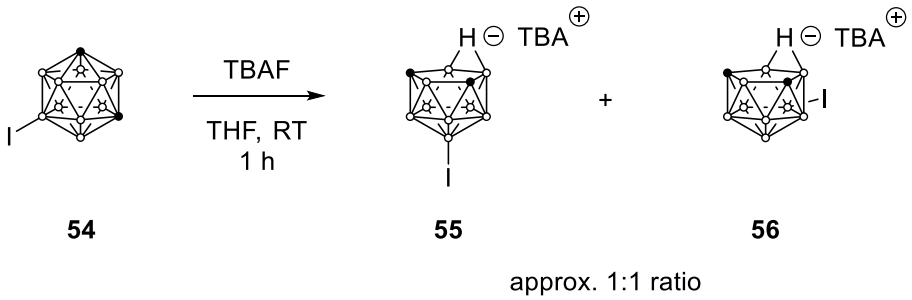

Scheme 28. Deboronation of compound **54** which produces an approximately equal ratio of the 1-iodo isomer (**55**) and 6-iodo isomer (**56**). ● = C–H; ○ = B–H (or B if substituted by an exopolyhedral bond).

The next step was to further protect the 8-position that would presumably be the most electrophilic position of the *nido*- cluster. Naturally, the addition of two electronegative iodine atoms makes the cage less susceptible to electrophilic substitution, and the conditions used to iodinate the parent *nido*-carborane (iodine with $AlCl_3$ or $FeCl_3$ catalyst) returned mostly starting material. Heating for extended periods in a higher boiling solvent (1,2-dichloroethane) and using the more electrophilic iodine monochloride improved conversion but resulted in increased by-product formation. We ultimately found that mercury(II) chloride was the most effective Lewis acid used in this reaction, with almost complete conversion of starting material achieved when **57** was heated at reflux in DCM with molecular iodine (**Scheme 29**). The main product of this reaction showed 6 peaks in its $^{11}B\{^1H\}$ NMR spectrum, indicative of a compound with a symmetry plane that can only result from iodination at the 8-position. Unfortunately, the $^{11}B\{^1H\}$ NMR spectrum also showed evidence of the formation of another isomer in small amounts, which co-eluted with the main product in all chromatographic conditions tested. While it may be possible to further optimize these reaction conditions to minimize formation of the minor isomer, this route was abandoned due to concerns over the likely difficulties in brominating such an electron-poor cluster in the subsequent step.

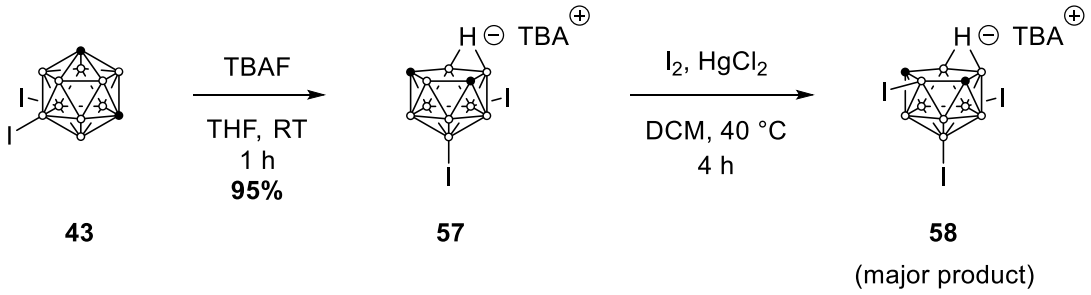

Scheme 29. Synthesis of triply-protected **58** following regioselective deboronation of compound **43**. The formation of **58** was accompanied by small amounts of an uncharacterized regioisomer. ● = C–H; ○ = B–H (or B if substituted by an exopolyhedral bond).

Protection of the B6 position of the *nido*- cluster was therefore achieved by iodination of compound **49**. Similar to our attempts at bromination, this reaction was not completely regioselective and preparative separation of the resultant isomers was unachievable. As a result, a range of conditions were screened in an attempt to drive the selectivity of the substitution. Acid-mediated or oxidative conditions, such as those used for iodination of *closo*-carboranes, could not be used as they result in cage closure to $C_2B_9H_{13}$ species and degradation of the

cluster,[146] respectively. Because of this, we continued with the Lewis acid catalysed approach used previously, varying the solvent, Lewis acid, iodine source and temperature. The range of choice in solvent for this reaction is limited by the tendency of *nido*-carboranes to form stable adducts with Lewis basic compounds such as acetonitrile and THF under these conditions.[147,148] We found, however, that solvent has little effect on this reaction and that the choice of Lewis acid was again the most important factor. Iron(III) chloride proved to be the most effective, with iodination being almost completely selective at the 6-position when it was used in conjunction with molecular iodine in DCM at reflux (**Scheme 30**). The $^{11}B\{^{1}H\}$ NMR spectrum of this compound showed the 6 resonances expected of compound **59**, which has a plane of symmetry bisecting the two vertices substituted by iodine. The non-decoupled boron NMR spectrum shows singlets at -14.4 ppm and -40.4 ppm, identifying these peaks as the two B–I environments. It also shows a doublet of doublets at -19.2 ppm indicative of unsubstituted boron atoms connected to a bridging proton. The 2D $^{11}B\{^{1}H\}$-$^{11}B\{^{1}H\}$ COSY NMR spectrum (**Figure 13**) displays all the cross-peaks expected of compound **59** and allows complete assignment of the boron resonances.

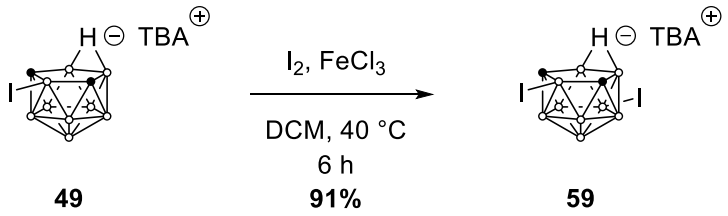

49 **59**

Scheme 30. Iodination of compound **49** giving the doubly protected *nido*-carborane **59**. ● = C–H; ○ = B–H (or B if substituted by an exopolyhedral bond).

With compound **59** in hand, focus shifted to identifying the most electron-rich vertex that would be the site of further halogenation. Although there was insufficient time to trial bromination of this substrate and characterise the resulting product, a test iodination reaction of this compound was performed (**Scheme 31**). With spectra of tri-iodinated compound **58** collected from an orthogonal synthesis, the $^{11}B\{^{1}H\}$ NMR peaks could be compared to determine whether substitution at the B1 position had occurred. Pleasingly, no peaks corresponding to compound **58** were observed in the $^{11}B\{^{1}H\}$ NMR of the iodination reaction, indicating that substitution occurred at one of the other three boron environment pairs. Two of these environments (B(10/11) and B(3/4)), following recapping and deprotection, would give

the desired 4-substituted *closo*-1,7-carborane, while the remaining environment (B(2/5)) would yield *closo*-1,7-carborane substituted at the 5-position, which was synthesised previously. All of these isomers would show 9 peaks in their $^{11}B\{^{1}H\}$ NMR spectra due to a loss of symmetry, and thus no information could be gleaned from this. A lack of material of sufficient purity precluded analysis of the non-decoupled spectrum or by two-dimensional methods. While further work is needed on this front, this appears to be a viable route to synthesising 4-bromo-*closo*-1,7-carborane.

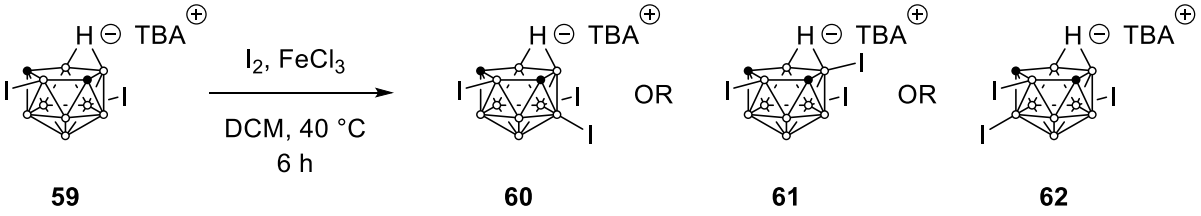

Scheme 31. Test iodination of **59** showing the 3 possible isomers that match the peak pattern shown in the $^{11}B\{^{1}H\}$ NMR spectrum of the crude product. Peaks corresponding to the 1-substituted isomer (**58**) were not visible. ● = C–H; ○ = B–H (or B if substituted by an exopolyhedral bond).

While a new synthesis of 4-bromo-*closo*-1,7-carborane could not be demonstrated in this work, it should be noted that the substitution pattern of **59** makes it an interesting precursor to other compounds. Recapping this compound with dichloroborane-dioxane complex would lead to the disubstituted 2,9-diiodo-*closo*-1,7-carborane (**Scheme 32**), where the two iodine atoms are on opposite vertices of the cage. This compound would be a useful precursor to '*para*-type' substituted compounds using a *closo*-1,7-carborane framework, and is a continuing subject of research in the Rendina group.

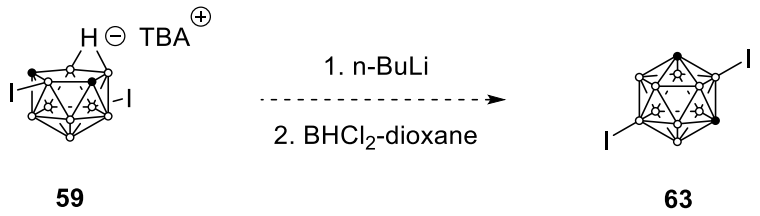

Scheme 32. Proposed synthesis of 2,9-diiodo-*closo*-1,7-carborane (**63**) through the recapping of compound **59**. ● = C–H; ○ = B–H (or B if substituted by an exopolyhedral bond).

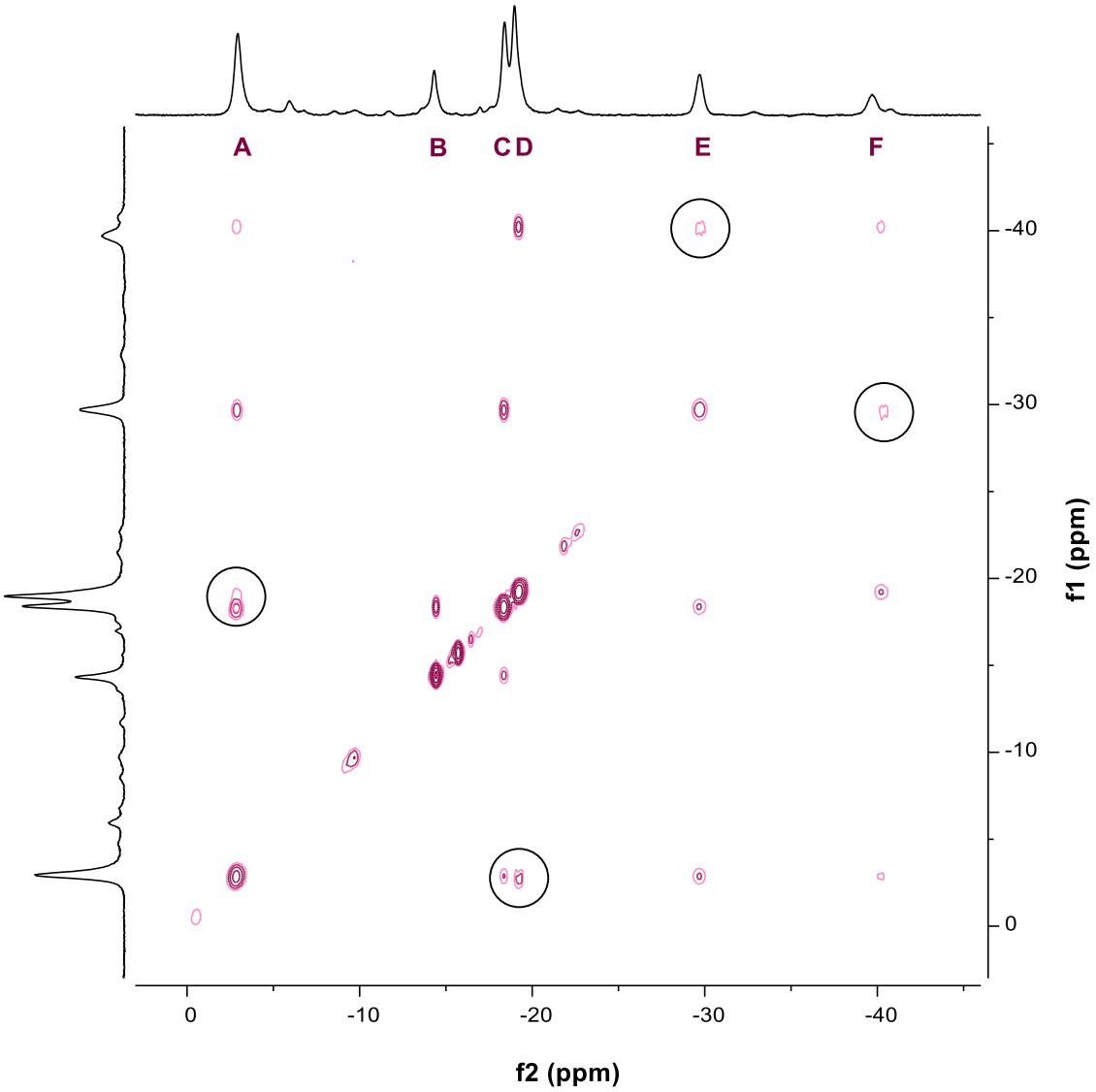

Peak	Integral	Mult.	Cross-peaks	Assignment
A	2	d	C, D, E, F	B(2/5)
B	1	s	C	B8
C	2	d	A, B, D	B(3/4)
D	2	dd	A, F	B(10/11)
E	1	d	A, C, F	B1
F	1	s	A, D, E	B6

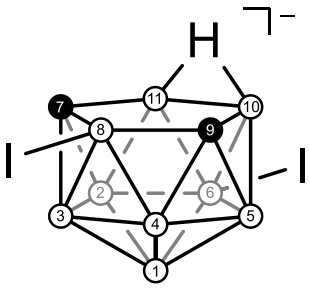

59

Figure 13. The $^{11}B\{^{1}H\}$–$^{11}B\{^{1}H\}$ COSY NMR spectrum of 6,8-diiodo-7,9-dicarba-*nido*-undecaborate(1-) (**59**) and its peak assignments. The circled cross-peaks are of low intensity and have been overlayed from a zoomed-in view of the spectrum for clarity. ● = C–H; ○ = B–H (or B if substituted by an exopolyhedral bond).

Towards the Synthesis of 2-Bromo-*closo*-1,7-Carborane

While functionalisation of the B(2/3) position of *closo*-1,7-carboranes does not require the use of a protecting group, 2-bromo-*closo*-1,7-carborane has never been reported. A synthesis of the related 2-iodo-*closo*-1,7-carborane was recently published,[129] however no attempt at obtaining the bromo- derivative was mentioned in this report or, to the best of our knowledge, any other report. Because of the utility of B-bromocarboranes in cross-coupling reactions, a synthesis of this compound was also attempted.

The published route to 2-iodo-*closo*-1,7-carborane involves initial iodination of 7,9-dicarba-*nido*-undecaborate (**50**) before recapping of the product with dichloroborane-dioxane complex. Using this approach as a template, we first attempted to synthesise the brominated *nido*-carborane **64** under similar conditions. In contrast to the iodination reaction, bromination of the cage was complete within minutes, producing a mixture of products. Reducing the reaction temperature and switching from aluminium(III) chloride to iron(III) chloride improved selectivity, but side-products remained. Further investigations found that this reaction could proceed without a Lewis acid catalyst, which increased selectivity further. Ultimately, we found that using NBS as the brominating reagent in acetonitrile provided mild enough conditions that the desired 8-bromo isomer was formed cleanly in almost quantitative yield (**Scheme 33**).

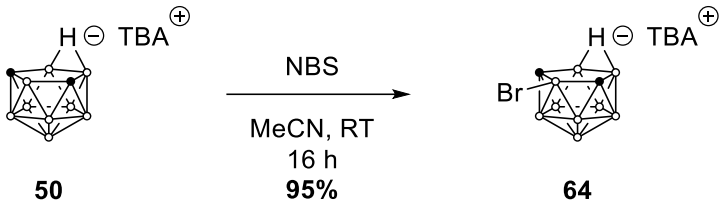

50 **64**

Scheme 33. Optimised conditions for the bromination of compound **50**. ● = C–H; ○ = B–H (or B if substituted by an exopolyhedral bond).

This compound displayed the expected 6 peaks in its $^{11}B\{^{1}H\}$ NMR spectrum with a singlet in the non-decoupled spectrum at -2.6 ppm corresponding to the B–Br vertex. Every other resonance is split by its connected proton, including a doublet of doublets at -22.4 ppm that confirms the open face of the cage remains unsubstituted. The position of substitution was confirmed by 2D $^{11}B\{^{1}H\}$-$^{11}B\{^{1}H\}$ COSY NMR spectroscopy as well as a single crystal X-ray

structure. Due to time constraints, we were unable to complete the recapping of this compound (**Scheme 34**), however work on completing this step continues in the Rendina group.

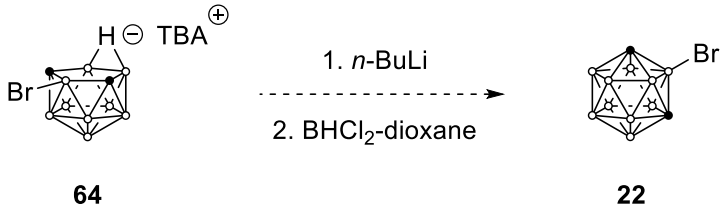

Scheme 34. Proposed synthesis of 2-bromo-*closo*-1,7-carborane (**22**) through the recapping of compound **64**. ● = C–H; ○ = B–H (or B if substituted by an exopolyhedral bond).

Summary and Outlook

This chapter has demonstrated for the first time how iodine atoms can act as protecting groups for carborane boron vertices, and in so doing allow the synthesis of carboranes brominated at previously inaccessible sites. The previously unknown compounds 8-bromo-*closo*-1,2-carborane (**32**) and 5-bromo-*closo*-1,7-carborane (**20**) were synthesised using this protecting group strategy and significant progress was made in the synthesis of the similarly novel 4-bromo-*closo*-1,7-carborane (**21**) and 2-bromo-*closo*-1,7-carborane isomers (**22**). This work represents an important step in expanding the synthetic possibilities of carboranes, a key factor in increasing their adoption as structural frameworks for a variety of applications. The next chapters focus on the use of carboranes within a fragment-based drug discovery project, illustrating their utility in this context.

3

Targeting a Haem Enzyme with a Unique Carborane Fragment Library

Previous research in the Rendina group has found that incorporating carboranes into the structures of known inhibitors of the haem enzyme indoleamine 2,3-deoxygenase 1 (IDO1), which plays a number of key roles in cancer immunity, can enhance their potency.[149] More recently, a small and unique library of low molecular weight carboranes were screened for their ability to inhibit IDO1.[150] A large proportion of these compounds displayed a strong affinity for the enzyme, especially when compared to organic compounds of comparable MW. Encouraged by these results, we sought to extend our assessment of this boron fragment library to other biological targets, focusing on another haem enzyme known as myeloperoxidase (MPO).

Myeloperoxidase

Myeloperoxidase is a mammalian haem enzyme that catalyses the production of hypohalous acids and a range of organic free radicals. When neutrophils ingest pathogens as part of immune response, MPO is released into the resultant phagosome where the products of its catalytic cycle serve as potent microbicidal agents.[151] If MPO escapes into the extracellular environment, however, its highly oxidising products cause damage to host tissues.[152,153] The products of this damage have been detected in a vast range of disorders characterised by inflammation, including atherosclerosis,[154] Alzheimer's disease,[155] rheumatoid arthritis[156] and cancer.[157] There is particularly compelling evidence implicating MPO in cardiovascular disease.[158–160] Inhibition of this enzyme's activity would decrease oxidative stress associated with these conditions and may ultimately allow for their treatment.

The majority of the reactive species released by MPO are produced through two catalytic cycles (**Figure 14**). In its 'native' form, the iron centre of MPO exists in a +3 oxidation state, which is oxidised by hydrogen peroxide to form the highly reactive ferryl-oxo haem species, Compound I.[161] When chloride or other (pseudo)halides such as thiocyanate are abundant, MPO reverts to its resting state through the halogenation cycle, oxidising these halides to their respective hypohalous acid.[162] The 'native' enzyme can also be regenerated through the peroxidase cycle, in which small organic substrates are converted to free radicals in a single-electron oxidation.[163] The resulting iron(IV) species, Compound II, is less reactive but can oxidise many physiological compounds such as tyrosine and hence reform the resting, ferric MPO.[164]

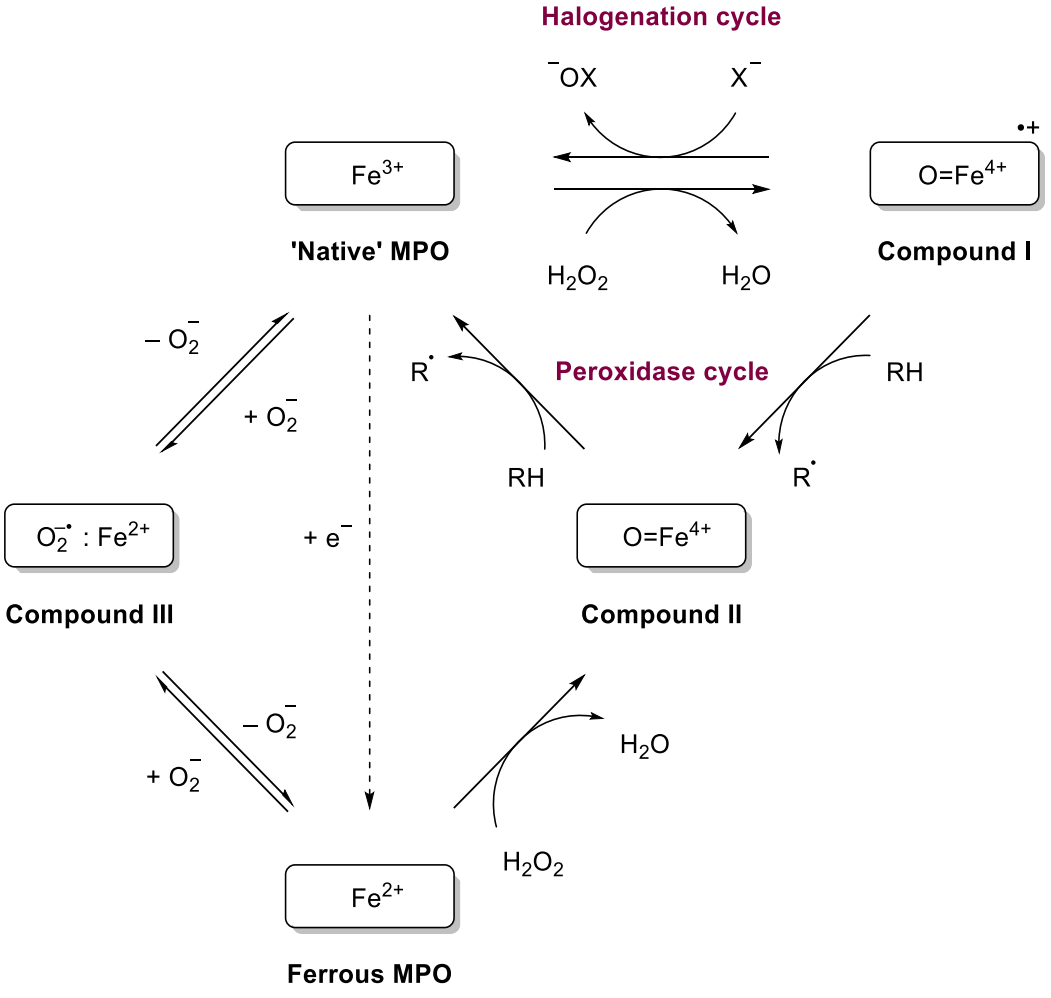

Figure 14. The catalytic cycles of myeloperoxidase. The major route involves initial oxidation of native MPO by H_2O_2 to Compound I. Hypohalous acid production occurs through the halogenation cycle, where a (pseudo)halide (X^-) is oxidised, resulting in the regeneration of resting MPO. Alternatively, the enzyme may proceed through the *per*oxidation cycle, which involves single electron oxidation of an organic substrate (RH) or another small molecule to form Compound II. This form can recycle to native MPO through another oxidation reaction. Superoxide ($O_2^{-\cdot}$) and other radicals mediate cycling through other states.

Attenuation of MPO's activity may be achieved through a few mechanisms.[165] Some anti-inflammatory drugs such as mefenamic acid inhibit this enzyme because they outcompete physiological compounds for oxidation but react poorly with Compound II, effectively forcing the enzyme into an inactive state.[166] These 'Compound II trappers' are ultimately ineffective inhibitors as many physiological substances can reduce the enzyme, regenerating its active form. 'Compound III pushers', which reduce MPO to its ferrous state following oxidation, are similarly ineffective as the active enzyme is regenerated through various pathways. Inhibitors of greater physiological relevance include suicide substrates and tight binding reversible inhibitors.

The first of these agents are the only class of MPO inhibitors to have progressed into clinical trials, all of which are based on a 2-thiouracil core (**Figure 15**). These compounds function as irreversible inhibitors of the protein, forming a covalent thioether bond with one of the pyrrole rings of the MPO haem group following oxidation by the enzyme (**Figure 16**).[167,168] This modification of the enzyme renders it permanently inactive. For the most part, clinical evaluation of these agents has seen only minimal success, largely due to a lack of patient outcomes or unexpected drug-drug interactions.[169,170] Most recently, mitiperstat (**68**) has been investigated in clinical trials for the treatment of heart failure,[171] chronic obstructive pulmonary disease[172] and non-alcoholic fatty liver disease.[173]

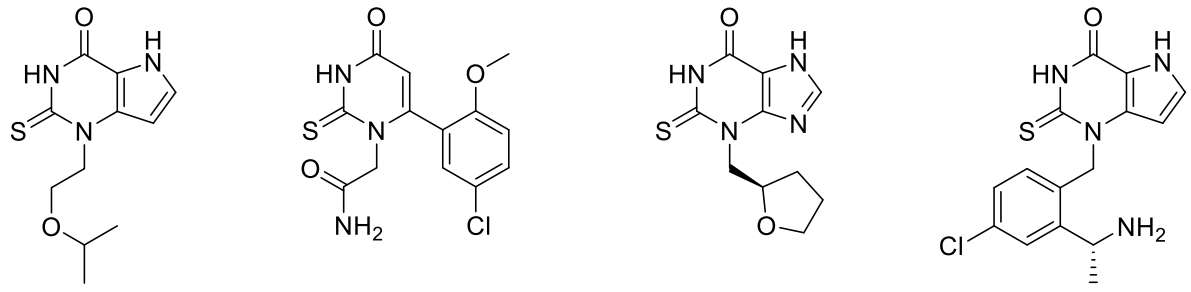

65 Verdiperstat | **66** PF-06282999 | **67** AZD5904 | **68** Mitiperstat

Figure 15. Irreversible MPO inhibitors that have progressed through human clinical trials.

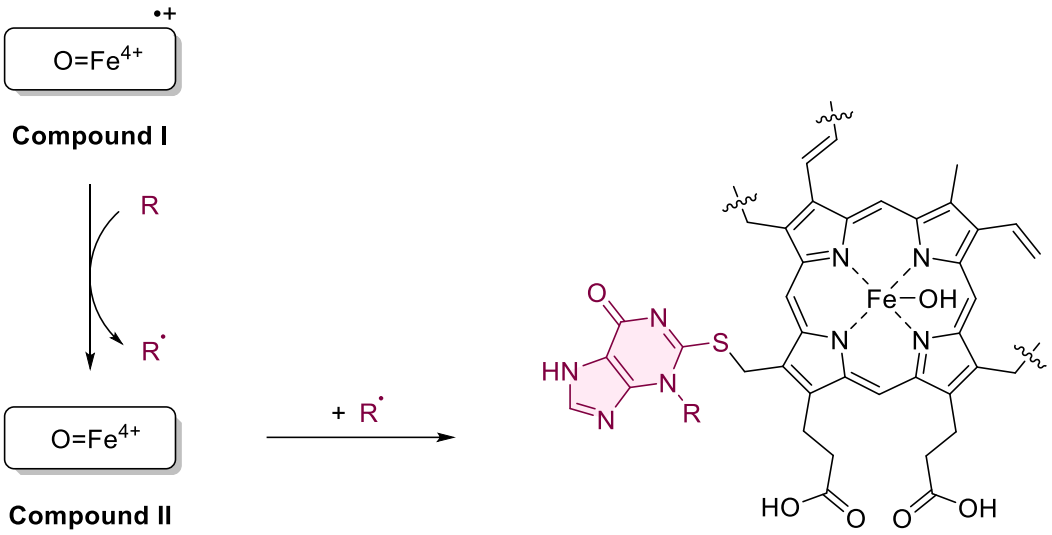

Figure 16. Mode of action of 2-thiouracil irreversible inhibitors (R) involving modification of the MPO haem group following oxidation by Compound I.

Tight binding reversible inhibitors, on the other hand, form strong, non-covalent interactions with the protein without being oxidized. The high affinity of these compounds for the enzyme allows them to outcompete physiological MPO substrates and inhibit enzyme activity by blocking the active site. A key example of this class is the hydroxamate HX1 (**69**),[174] which is the most potent MPO inhibitor reported to date, with a measured IC_{50} of 5 nM. The clinical potential of this inhibitor, however, is limited due to the instability of its hydroxamic acid functional group under biological conditions.[165] Another example of a potent reversible inhibitor reported in the literature is shown in Figure 17.

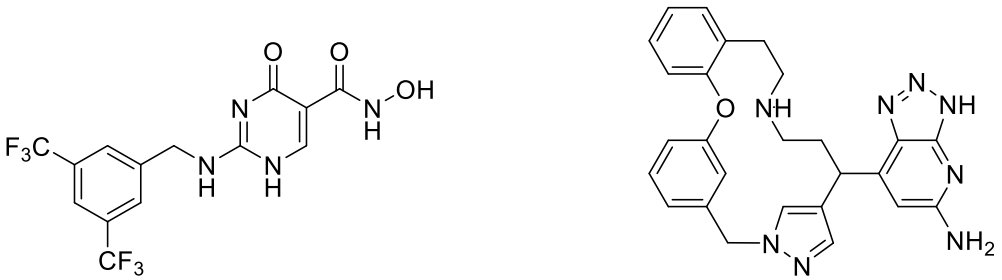

69

IC_{50} = 5 nM

70

IC_{50} = 14 nM

Figure 17. Two potent (nM) and reversible MPO inhibitors reported in the literature.[174,175]

Structurally, MPO is a large protein (*ca*. 150 kDa) consisting of two identical protomers linked by a disulfide bridge. The haem active site is located within a deep cavity that is surrounded at its entrance by a hydrophobic pocket consisting of the Phe99, Phe366 and Phe407 residues, as well as the chain carbons of Arg239. Hydrophobic structures, such as the bis(trifluoromethyl)phenyl group of **69**, are known to bind to this region and restrict substrate access to the catalytic haem group. Because of their hydrophobic nature and size, *closo*-carboranes are ideal candidates to target this pocket and serve as a new class of structural frameworks in the design of novel MPO inhibitors.

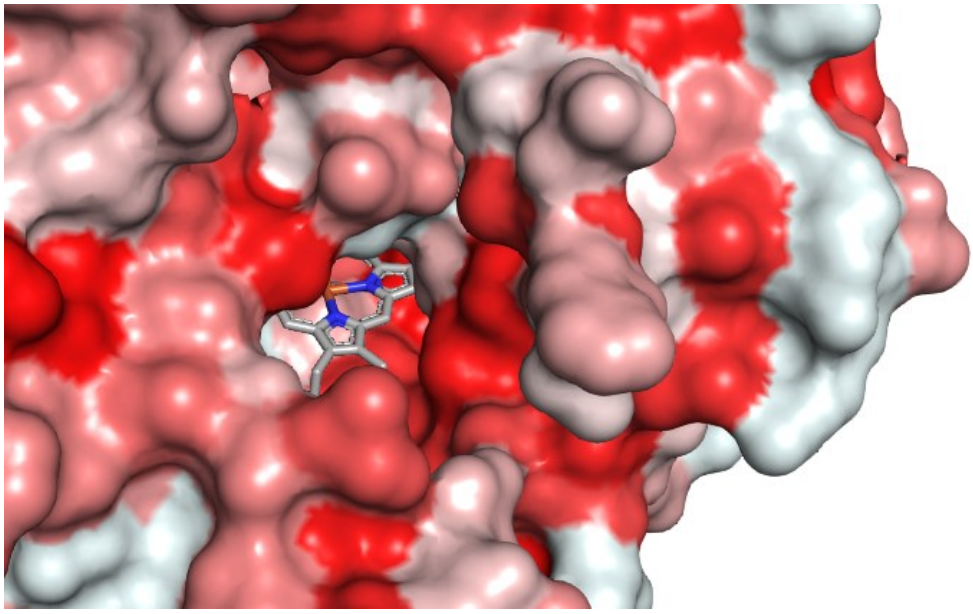

Figure 18. Close-up view of the active-site entrance of MPO. Residues are coloured based on their hydrophobicity (red is hydrophobic, white is hydrophilic). Image rendered in PyMol.

Chapter Aims

Given MPO's implication in the oxidative damage associated with a range of disorders, designing effective inhibitors of this enzyme is critical to further understanding and treating these inflammatory conditions. Unfortunately, all inhibitors reported thus far have failed to meet therapeutic needs. With the promise that carborane derivatives have shown in our previous work with IDO1, we assessed our library of carborane fragments against MPO with the goal of developing novel inhibitors through a fragment-based approach. In this Chapter, the results of a preliminary screen of a set of low molecular weight carborane fragments are reported, as well as initial efforts to expand and diversify this library. Further, a robust,

physiologically relevant bioassay was adapted for use with fragment-like compounds and was used to determine the inhibitory activity of the expanded set of fragments.

Synthesis

C-Substituted Carboranes

While a selection of low molecular weight carboranes were available in our unique boron-based fragment library, additional syntheses were required to broaden the range of structures and hence increase the breadth of chemical space explored. As such, initial syntheses in this project focused on making small batches of chemically distinct carboranes using known methods. Further to this, efforts were directed at expanding the scope of these reactions and we endeavoured, where possible, to extend the range of viable substrates for these transformations. The initial goal was to derive most of these fragments from *closo*-1,2-carborane, as it is the most affordable and readily-available isomer.

As mentioned in Chapter Two, deprotonation of carborane C-vertices followed by nucleophilic addition with an appropriate electrophile is a well-established method of synthesising C-substituted carborane derivatives. This approach served as a cornerstone for our library, with a set of diverse derivatives synthesised using literature procedures and adaptions thereof (**Table 2**). Here, the focus was on installing chemically distinct functional groups that can bind to protein residues in different manners. For some of these derivatives, both the *closo*-1,2- and *closo*-1,7- isomers were synthesised to determine whether cage isomerism affected biological activity. All of the compounds in Table 2 showed the expected increase in peaks in their $^{11}B\{^{1}H\}$ NMR spectra relative to the parent carborane, a result of the partial loss in symmetry of the cage. The presence of a single cage C–H resonance of integration equal to one in each ^{1}H NMR spectrum confirmed mono-substitution.

In a similar set of reactions, a collection of carborane secondary alcohols were synthesised through a facile nucleophilic addition to the corresponding aldehyde with carborane monoanion. In the case of *closo*-1,2-carborane and select aldehydes, this transformation can be effected using excess TBAF in a simple one-pot operation (**Scheme 35**).[61] No disubstitution occurs under these conditions, and a short reaction time precludes significant amounts of cage deboronation. The compounds were isolated as racemic mixtures in all cases, and no attempts were made to resolve the enantiomers at the screening stage.

Table 2. C-substituted carboranes prepared by nucleophilic substitution reaction with a deprotonated carborane.[61–64,176,177] ● = C–H (or C if substituted); ○ = B–H.

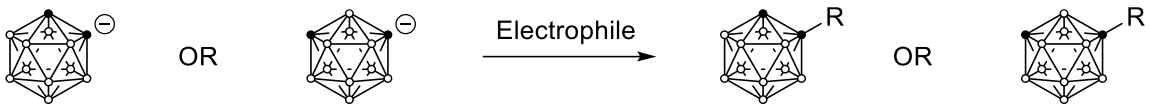

Electrophile	Fragment structure[a]	
	closo-1,2- isomer	*closo*-1,7- isomer
Carbon dioxide	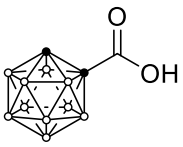 **71** (96%)	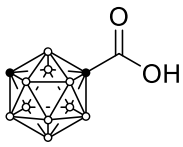 **19** (97%)
Methyl formate (followed by acid hydrolysis)	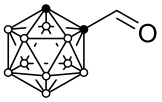 **72** (92%)	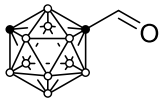 **73** (89%)
Paraformaldehyde	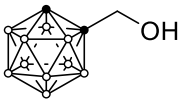 **74** (84%)	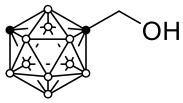 **75** (60%)
Trimethyl borate (followed by oxidation)	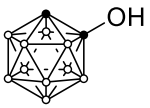 **76** (69%)	–
Elemental sulfur	 **77** (88%)	–
Tosyl azide (followed by reduction)	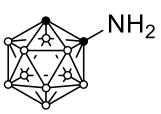 **78** (74%)	–

[a] Isolated yields given in parentheses.

Interestingly, these compounds showed more than 6 peaks in their $^{11}B\{^{1}H\}$ NMR spectra, indicative of a complete loss of symmetry in the cage. This matches the data reported in the literature for compounds of this type,[178] although no explanation is given for this unexpected result. The reasons for this are presently unclear, although it is possible that an intramolecular dihydrogen bonding interaction between the hydroxyl group and one of the B(3,6)–H atoms of the cage is causing the loss in symmetry.

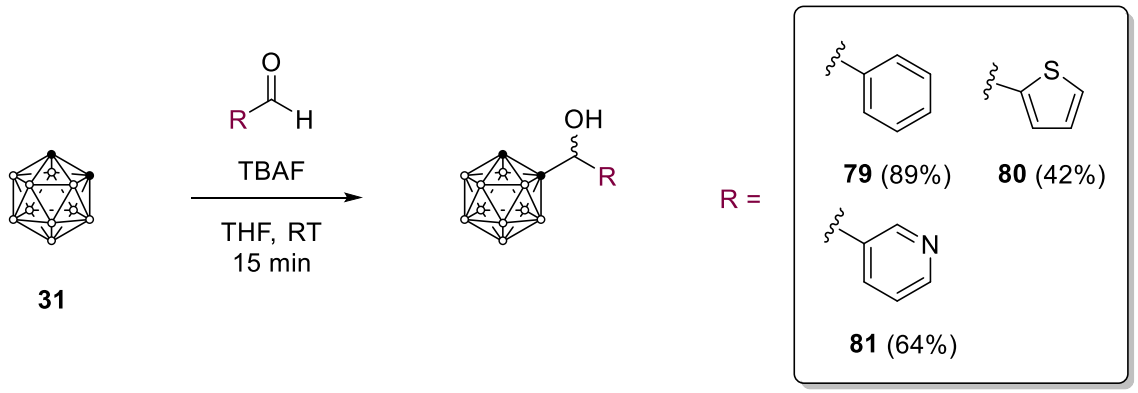

Scheme 35. Synthesis of carborane secondary alcohols from the respective aldehydes. ● = C–H (or C if substituted); ○ = B–H.

Aminomethyl carborane **85** is a useful synthon and desirable fragment. While a number of routes to this compound are feasible, the most straightforward is its synthesis from *nido*-decaborane (**82**) and propargyl phthalimide (**83**) using a Gabriel reaction (**Scheme 36**). In this reaction, the amine group is installed in its phthalimide protected form since free amines are known to cause decomposition of the *nido*-decaborane cage. Silver(I) salts have been found to be useful catalysts in these types of condensation reactions, coordinating to the alkyne and slowing their degradation due to hydroboration,[179] hence improving yields. In this case, the addition of silver nitrate to the reaction was found to have little effect. Regardless, the insertion of this particular alkyne into *nido*-decaborane is rather high yielding, and compound **84** was isolated in 63% yield. Acetonitrile is used in this reaction as a Lewis base to form the more reactive bis(acetonitrile) decaborane adduct *in situ*. Phthalimides are traditionally deprotected to the desired amine using hydrazine in an alcoholic solvent, however there is disagreement in the literature as to whether these conditions cause deboronation when applied to compound **84**.[180] In our hands, an excess of hydrazine hydrate in ethanol at room temperature indeed

caused conversion of most of the product to the respective *nido*-carborane derivative. Instead, Soloway *et al.* reported a milder method of deprotection involving initial reduction of the phthalimide followed by acid hydrolysis of the resulting amide.[181] Applying these conditions without first isolating the reduced intermediate allowed collection of the desired amine **85** as its hydrochloride salt in excellent yield.

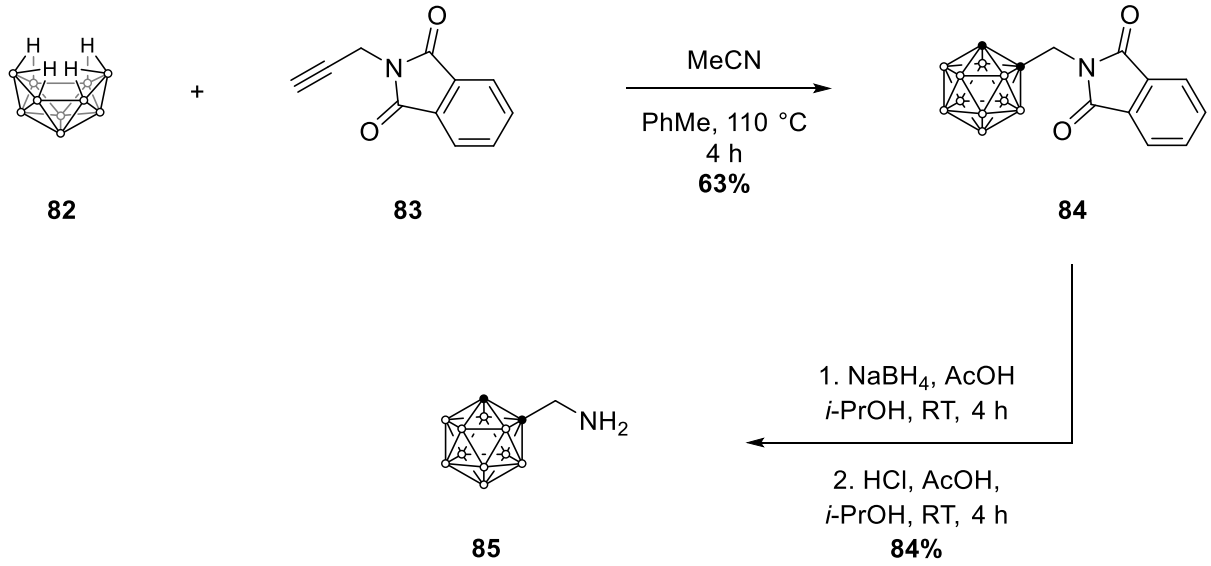

82 **83** **84** **85**

Scheme 36. Synthesis of aminomethyl carborane **85** from *nido*-decaborane. ● = C–H (or C if substituted); ○ = B–H (or B if substituted by an exopolyhedral bond).

B-Substituted Carboranes

We also sought to synthesise B-substituted carborane derivatives, both as a means of generating more fragments for the boron library and to further develop new synthetic methods for *closo*-1,2-carborane in particular.

Palladium catalysed cross-coupling reactions are powerful methods of synthesising biaryl compounds, however the equivalent transformations using carborane electrophiles are much less developed. The Suzuki reaction, for example, is ubiquitous in organic chemistry but has had limited application in carborane chemistry. Select aryl groups have been attached to *closo*-1,7- and *closo*-1,12-carborane,[182,183] but only one report exists of a *closo*-1,2-carborane Suzuki coupling.[184] Even so, the scope of the reaction was limited and functionalisation was only possible at the most electron poor B(3/6) vertex. To the best of our knowledge, a B(9/12)

coupled product has never been realised. In our attempts at achieving this, we experienced similar failures even when using a variety of state-of-the-art Pd catalyst systems.

The use of more nucleophilic coupling partners has emerged as a viable alternative to achieving these sorts of transformations. For example, Negishi coupling of iodocarboranes with aryl zinc reagents has recently been reported as a convenient method of generating B-aryl carboranes.[185] Coupling of heteroaromatic zinc reagents, however, was not attempted in this report. Previous efforts in the literature demonstrate some success with such substrates,[186] however, the reaction was never attempted with *closo*-1,2-carborane and yields for the *closo*-1,7-carborane derivatives were often low. Using the newly reported method, we synthesised 9-phenyl-*closo*-1,2-carborane (**86**) in excellent yield as described in the literature (**Scheme 37**). When the same conditions were used with 3-bromo-pyridine as the organozinc precursor, the coupling product **87** was also obtained, albeit in a slightly reduced yield. Using the even more electron poor 2-chloro-pyrimidine returned mostly starting material under these conditions with only trace amounts of the product detected by NMR spectroscopy. Clearly, heteroarylzinc reagents can be competent nucleophiles in these reactions, but further optimisation is needed to achieve broader substrate scope.

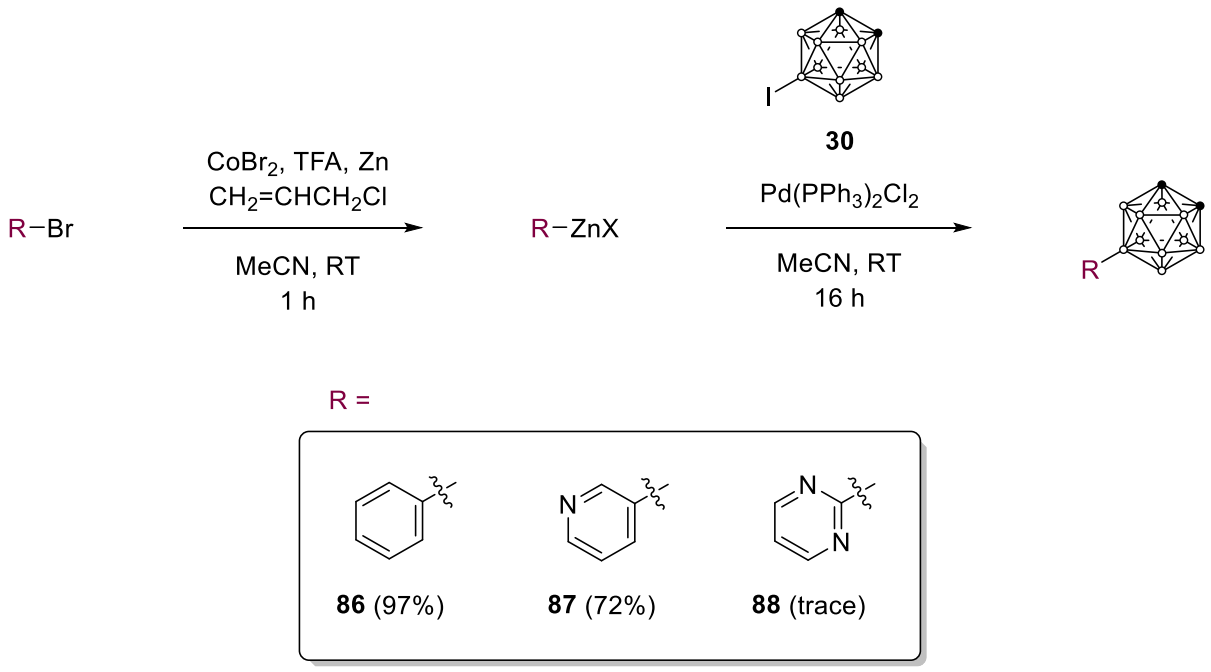

Scheme 37. Pd-catalysed Negishi coupling of 9-iodo-*closo*-1,2-carborane (**30**) with *in situ* generated (hetero)aryl zinc reagents. X = Br or Cl; ● = C–H; ○ = B–H (or B if substituted).

Although installation of benzyl groups onto the B-positions of carboranes can be achieved through Kumada and Negishi coupling of B-iodocarboranes with benzylic Grignard and organozinc reagents,[187,188] a more direct method is the electrophilic substitution of B–H vertices with benzyl bromides. Using equimolar amounts of aluminium trichloride, benzyl groups with electron-withdrawing substituents can be readily installed.[74] Other alkyl halides have also been introduced using this method,[73,189] leading us to attempt the substitution of *closo*-1,2-carborane with *N*-(bromomethyl)phthalimide (**89**) as a method of accessing B-aminomethyl carboranes. Unfortunately, using the same conditions as before returned only starting materials. More forcing conditions (e.g. reflux in 1,2-dichloroethane) gave a complex mixture of carborane species, attributed to various poly-chlorinated *closo*-1,2-carboranes based on the upfield shift of the C_{cage}–H peaks and the absence of a new methylene resonance.

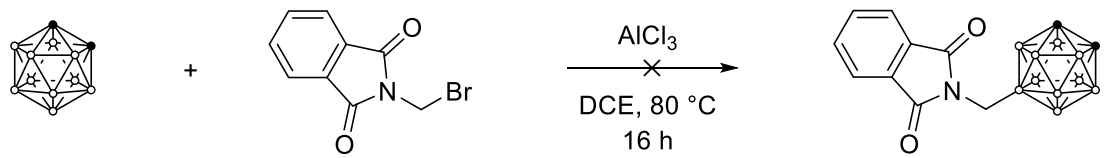

31 **89** **90**

Scheme 38. Attempted synthesis of B-phthalimidomethyl *closo*-1,2-carborane **90** through electrophilic substitution. ● = C–H; ○ = B–H (or B if substituted).

The Buchwald-Hartwig reaction has become a mainstay in organic and medicinal chemistry as a robust and versatile method of generating C–N bonds. The first example of this reaction involving carboranes was reported in 2010,[190] when Hawthorne and coworkers demonstrated the coupling of B-iodocarboranes with select amide nucleophiles using a biaryl phosphine ligand. The Spokoyny group expanded upon this work in a series of papers,[110,126,127] showing improved coupling performance when B-bromocarboranes were utilised as the electrophile. More recently, Mu and coworkers reported a method with extended substrate scope,[128] focusing on disubstituted derivatives. In some of these papers, however, coupling with *closo*-1,2-carboranes was either not reported or performed poorly. In particular, examples of substitution at the electron-rich sites of *closo*-1,2-carborane, i.e. B(9/12), is lacking. Optimising these reactions is difficult due to the steric demands of the carborane cage and slower oxidative addition of a palladium centre into an electron-rich B–X bond. Furthermore, the strong bases and higher temperatures that are often used to drive sluggish couplings can be

detrimental as they promote the facile deboronation reaction of *closo*-1,2-carboranes. The coupling of various *N*-nucleophiles was of particular interest to us as they are common motifs in medicinal chemistry. As such, we attempted to optimise the B–N coupling of 9-bromo-*closo*-1,2-carborane with aniline as a model substrate (**Table 3**).

Table 3. Attempted optimization of the Pd-catalysed coupling of 9-bromo-*closo*-1,2-carborane with aniline. ● = C–H; ○ = B–H (or B if substituted by an exopolyhedral bond).

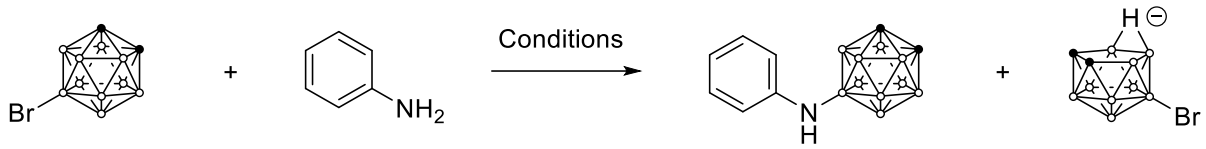

91 **92** **93** **94**

Entry	Pd Source/ligand[b]	Solvent[c]	Temp. (°C)	Time (h)	Product ratio (**91** / **93** / **94**)[d]
1	SPhos-Pd-G3/SPhos (5/5)	Dioxane	70	3	76 / 7 / 17
2	SPhos-Pd-G3/SPhos (5/5)	DME	80	4	90 / 5 / 5
3	$Pd(OAc)_2$/**95** (10/20)	Dioxane	70	8	100 / 0 / 0
4	$Pd(OAc)_2$/**95** (10/20)	Dioxane	100	16	100 / 0 / 0
5	$Pd(OAc)_2$/**95** (10/20)	DME	100	16	0 / 46 / 54
6	$Pd(OAc)_2$/**95** (10/20)	DME	80	8	80 / 20 / 20

[a] All reactions were run using 4 eq. of K_3PO_4 under an atmosphere of dry nitrogen in a sealed tube.
[b] Loading of catalyst and ligand are given in brackets as mol%. **95** = $(2\text{-OMe-}C_6H_4)_3)P$.
[c] DME = 1,2-dimethoxyethane; dioxane = 1,4-dioxane.
[d] Determined using $^{11}B\{^1H\}$ NMR.

We initially trialled the conditions detailed by Spokoyny *et al.*,[126] using SPhos-Pd-G3 as the palladium precatalyst and 1,4-dioxane as solvent (Entry 1). Under these conditions, approximately 10% conversion of the starting material to the desired product was observed by $^{11}B\{^1H\}$ NMR spectroscopy, along with formation of a significant amount of a *nido*-carborane species. Changing the solvent to DME (Entry 2) lowered the conversion slightly but reduced the amount of deboronation by over one-half. We next attempted the conditions used by Mu and coworkers to synthesise disubstituted B–N bonded carboranes,[128] with tris(2-methoxyphenyl)phosphine and palladium acetate as the ligand and palladium source in DME (Entry 5). In this case, complete consumption of the starting material was observed, with a

downfield shifted singlet at -2.5 ppm in the ^{11}B NMR representing the newly formed B–N bond. Unfortunately, the decomposed *nido*-carborane was found in approximately equal proportion to the product. Lowering the temperature and reaction time (Entry 6) led to reduced decomposition but an equal reduction in conversion. Changing the solvent to 1,4-dioxane (Entries 3 and 4) resulted in complete stalling of the reaction with only starting material present in the crude NMR spectrum. When we applied the best conditions (Entry 5) to a reaction with morpholine as the nucleophile (**Scheme 39**), only the deboronated decomposition product was obtained, reflecting the greater basicity of this substrate. Notably, the $^{11}B\{^{1}H\}$ NMR resonances of the *nido*- species were consistent between the reactions of the two different substrates, revealing that the decomposition product results solely from the starting material and that the coupling product is more stable to deboronation. Using the weakly basic pyrazole as the coupling partner gave the desired product, albeit at a lower yield compared to aniline. While these results show that these reactions are possible with electron-rich bromo-*closo*-1,2-carboranes, further optimisation is required. In particular, a ligand and catalyst combination that is active at lower temperatures is needed, especially when using more basic coupling partners.

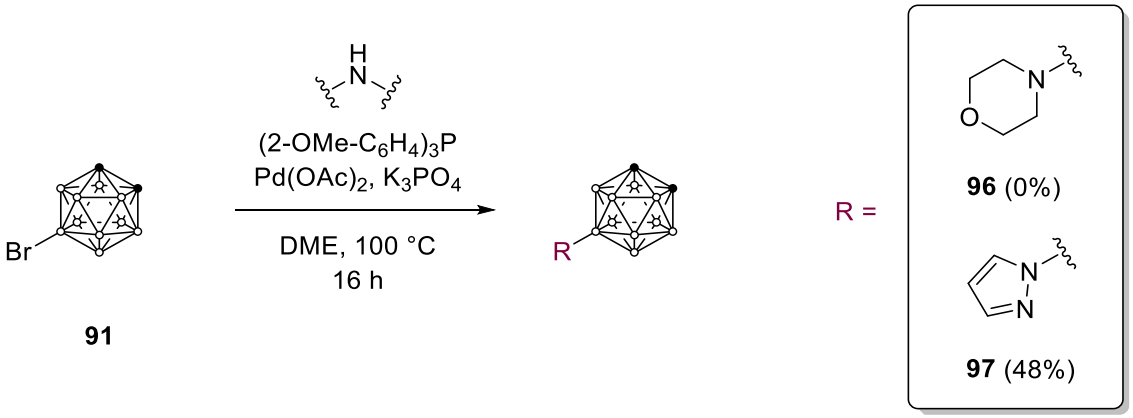

Scheme 39. Optimised conditions for the Buchwald-Hartwig coupling of 9-bromo-*closo*-1,2-carborane (**91**) with amine nucleophiles. ● = C–H; ○ = B–H (or B if substituted).

Amide and Ester Derivatives

Because of the high binding affinity of carborane carboxylic acids and esters (*vide infra*), a small set of esters and amides were synthesised as expansions of these fragments. To make these compounds, we initially trialled conditions using peptide coupling reagents, however these provided the desired products in unsatisfactory yields. Eventually, we turned to

using the carborane acyl chloride **98** as the activated precursor. This was conveniently prepared *in situ* using oxalyl chloride and a catalytic amount of DMF, which we found to be a superior chlorinating agent to thionyl chloride and phosphorus trichloride. The resulting acyl chloride could be substituted with various alcohols and amines to give the desired amides and esters (**Scheme 40**). Originally, 1-carboxy-*closo*-1,2-carborane was used as the starting material in these reactions, but deboronation of the cage under these basic conditions reduced yields and led us to use *closo*-1,7-carborane instead. In the case of ester **99**, it was found that the more nucleophilic sodium phenoxide was required to obtain the phenyl ester in sufficient yield. When diamines were used as the nucleophiles, a mixture of mono- and disubstituted products were obtained even in the presence of large excesses of amine. Disubstituted amines are common side product of these reactions,[191] and in this case served as a convenient method of synthesising additional derivatives. No attempts were made to optimise a route to monosubstituted amines, however Boc-protection of one of the amino groups followed by eventual acid deprotection is a well-established method in achieving mono-acylated diamines.

Other carborane derivatives used in this Chapter were synthesised and provided by Thomas Carraro (USyd).

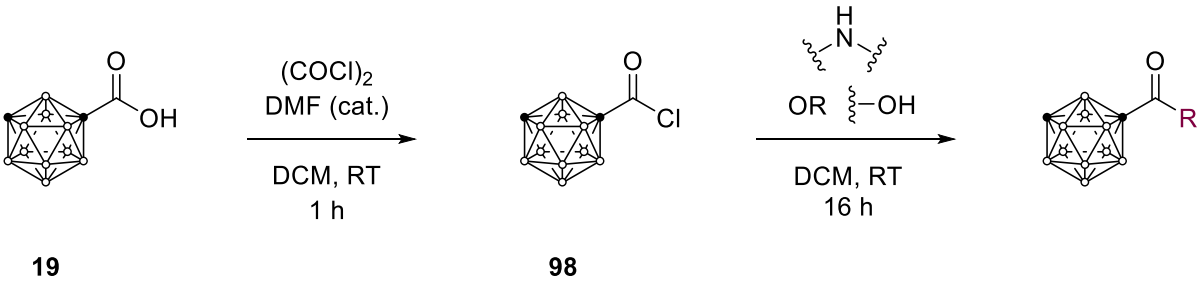

19 **98**

R =

99 (48%) **100** (75%) **101** (63%) **102** (91%)

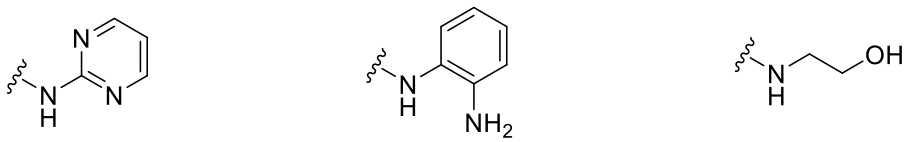

103 (10%) **104** (62%) **105** (71%)

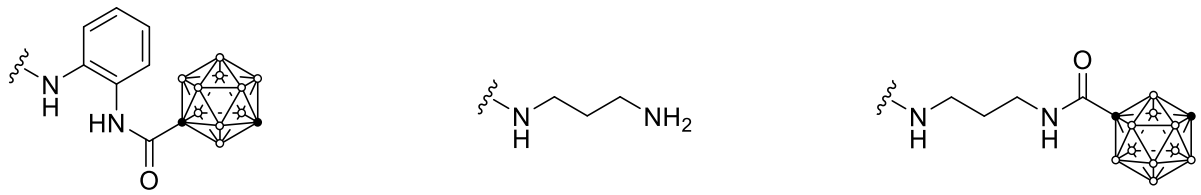

106 (25%) **107** (24%)[a] **108** (68%)

Scheme 40. Synthesis of carborane amides and ester derivatives. [a] Crude yield. ● = C–H (or C if substituted); ○ = B–H.

Biological Evaluation of Fragments

Preliminary Surface Plasmon Resonance Screen

Surface plasmon resonance (SPR) is a technique that is widely-used in FBDD programs to determine the binding affinity of compounds to a biological target. Briefly, the protein of interest is immobilised onto the surface of a sensor chip, onto which polarised light is directed. The angle of this reflected light is dependent on the refractive index of the surface, which in turn is influenced by interactions at the metal-protein interface. When a solution of the analyte (e.g. a fragment) is allowed to flow across the detector surface, binding events with the protein cause a change in refractive index. Measuring the intensity of reflected light therefore allows determination of the analyte's affinity to the protein in the form of a binding constant (K_D).

The SPR measurements for this project were performed by Dr Lorna Wilkinson-White (USyd). A small sample of carboranes was screened to provide initial direction for syntheses, the results of which are presented in Table 4. Compounds were screened in a buffer containing either 1% *v/v* or 5% *v/v* DMSO to aid their dissolution. The K_D values obtained from these two datasets were mostly comparable, with select compounds showing improved affinity at 5% *v/v* DMSO due to their increased solubility. In many cases, K_D values could not be determined due to poor surface behaviour at higher concentrations. In these situations, the response measured is due, at least in part, to non-specific interactions of the ligand with either the protein or sensor surface, and a binding constant determined from the sensorgram would not be a true reflection of the compound's ability to bind to the protein.

Many of the carbonyl compounds showed strong binding to MPO in this screen. Notably, the carboxylic acid derivatives (**19** and **71**) and the formyl derivative **72** all had calculated K_D values much higher than expected for compounds of such low molecular weight. In these cases, it is likely that the compound is binding to the protein at multiple sites, leading to a K_D value that is not reflective of a single molecule's binding affinity. Expansion of such a fragment, even in an optimal manner, would not result in the expected associated increase in K_D, as the additional binding modes would lose viability. Despite this, ester derivatives **118**, **119** and **120**, which can be considered expansions of the carboxylic acid fragments, all showed reasonable binding affinity, indicating that functionalisation at this site is well tolerated. A carboxylic acid at the beta position of the cage (**121**) showed reduced binding affinity, but the corresponding methyl ester (**122**) was a more potent binder relative to the alpha-cage ester. Rearrangement of the compound to a B-substituted carboxylic acid (**113**) also reduced binding

ability, perhaps a result of diminished dihydrogen bonding capabilities in the B-substituted derivative. The di-substituted carborane **123** showed a binding response, but a K_D could not be determined. This implies that substitution *ortho*- to the carboxylic acid is well tolerated but also gives credence to the theory that **71** and related derivatives are promiscuous binders. The two carboxamides (**114** and **115**) were rather strong ligands independent of whether the site of substitution was a carbon or boron vertex and expansion of this fragment into a hydroxamic acid (**117**) had little effect on affinity. Finally, the B-acetyl carborane **116** did not bind to the protein, emphasising the importance of a hydrogen bond donor.

From the other simple carborane derivatives, neither 9-nitrile-*closo*-1,7-carborane (**110**) or 9-amino-*closo*-1,7-carborane (**109**) bound to the protein. 1-Hydroxy-*closo*-1,2-carborane (**76**) showed strong binding, with the 9-hydroxy derivative (**111**) having an even lower K_D value. A binding constant for the methyl ether of this derivative (**112**), on the other hand, could not be determined.

Many of the aromatic derivatives tested were poor binders of MPO, with carboranes bonded directly to phenyl (**125**), tolyl (**126**) or nitrophenyl (**134**) groups showing very weak or no binding at all. The remaining aryl carboranes (**124**, **127**, **128**, **129**, **131**, **132** and **133**) gave sensorgrams from which binding constants could not be determined. One exception was the anisole derivative **130** with an impressive K_D of 98 ± 18 μM, although a large discrepancy in this value was observed when tested at 1% *v/v* DMSO. The C-benzyl carborane **135** did not bind, whereas the related nitrobenzyl fragment **136** was a potent binder. Finally, of the heteroaromatic substituted carboranes, the 2-pyridyl (**137**) and triazole (**140**) fragments showed poor surface behaviour and the pyrazine fragment **138** did not bind. Pyrimidine **139**, however, was a rather strong binder, showing that highly specific heteroatom positioning is required to make a good ligand.

Table 4. Experimentally-determined binding constants of carborane fragments using SPR.

Compound	Structure	K_D (μM)	
		1% DMSO	5% DMSO
109	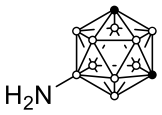	No binding	
110	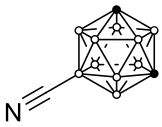	No binding	
76	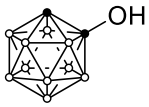	421 ± 60	216 ± 22
111	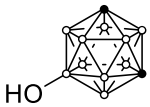	119 ± 6	–
112	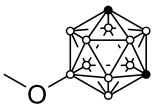	ND*	–
19	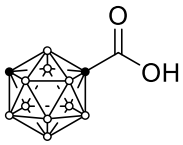	60†	35 ± 6†
71	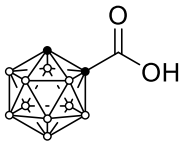	†	
113	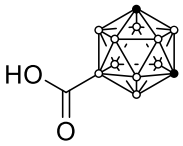	260 ± 31	–

* Poor surface behaviour at higher concentrations.
† K_D is stronger than expected for a compound of this size; it is likely binding to the protein multiple times.
ND: K_D could not be determined.

Table 4. (continued)

Compound	Structure	K_D (μM)	
		1% DMSO	5% DMSO
72	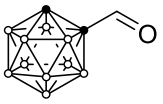	†	
114	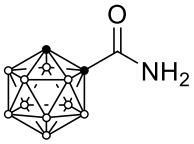	194 ± 13	164 ± 13
115	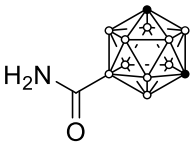	204 ± 47	–
116	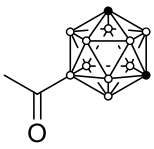	No binding	
117	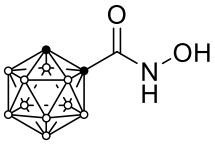	206 ± 13	ND*
118	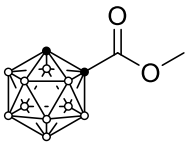	333 ± 45	326 ± 62
119	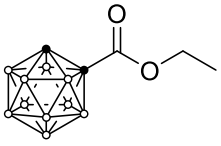	169 ± 16	–

* Poor surface behaviour at higher concentrations.
† K_D is stronger than expected for a compound of this size; it is likely binding to the protein multiple times.
ND: K_D could not be determined.

Table 4. (continued)

Compound	Structure	K_D (μM)	
		1% DMSO	5% DMSO
120	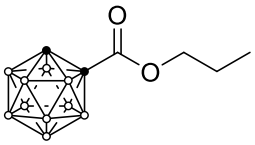	–	153 ± 20
121	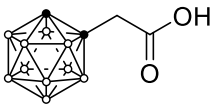	580 ± 50	147 ± 21
122	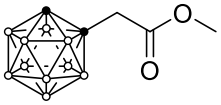	288 ± 36	–
123	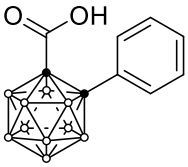	Binding observed*	
124	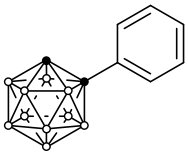	ND*	
125	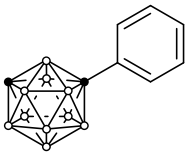	No binding	
126	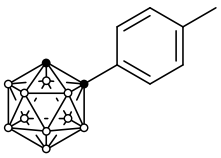	No binding	Weak binding

* Poor surface behaviour at higher concentrations.
† K_D is stronger than expected for a compound of this size; it is likely binding to the protein multiple times.
ND: K_D could not be determined.

Table 4. (continued)

Compound	Structure	K_D (μM)	
		1% DMSO	5% DMSO
127	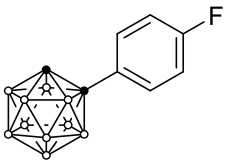		ND*
128	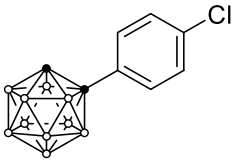		ND*
129	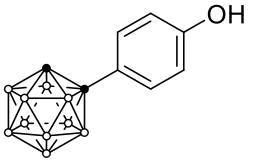		ND*
130	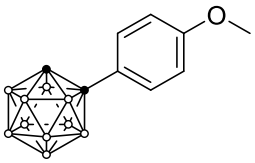	752 ± 87*	98 ± 18
131	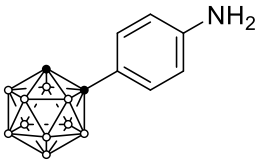		ND*
132	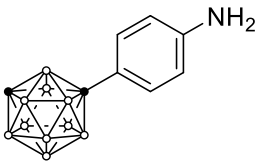		ND*
133	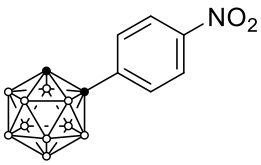		ND*

* Poor surface behaviour at higher concentrations.
† K_D is stronger than expected for a compound of this size; it is likely binding to the protein multiple times.
ND: K_D could not be determined.

Table 4. (continued)

Compound	Structure	K_D (μM)	
		1% DMSO	5% DMSO
134	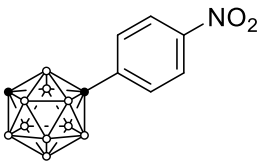	No binding	
135	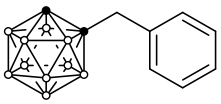	No binding	–
136	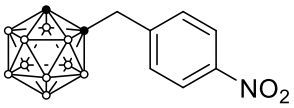	123 ± 6*	–
137	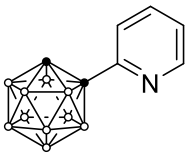	ND*	
138	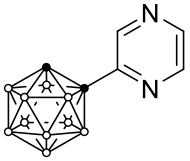	No binding	
139	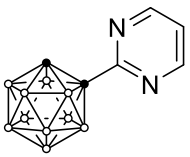	410 ± 35	–
140	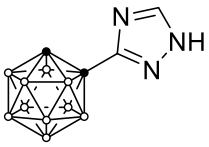	ND*	

* Poor surface behaviour at higher concentrations.
† K_D is stronger than expected for a compound of this size; it is likely binding to the protein multiple times.
ND: K_D could not be determined.

In vitro Inhibition Assays

While SPR provides information on whether a fragment binds to a certain protein, this does not necessarily correlate to its ability to affect the function of this protein. In the case of enzymes, for instance, a compound may bind to a region where its effect on the enzyme's ability to catalyse reactions is limited or even non-existent. These compounds are not useless; linking these structures to fragments that do effect enzyme function can be a powerful method of expanding hits and generating potent structures. On the other hand, binding affinity is not a prerequisite for a potent inhibitor. In the case of MPO, many inhibitors exert their mode of action following oxidation by the enzyme (*vide supra*), a mechanism which would not be captured under the conditions of SPR as hydrogen peroxide is not present in the assay solution. As such, identifying which compounds inhibit the enzyme was an important objective in this project. To this end, we assessed our initial fragment library, along with some additionally synthesised compounds informed by the SPR results, in two *in vitro* assays that assess a compound's effect on MPO's ability to produce oxidants.

One of the most common methods used to test MPO's activity is the taurine chloramine assay,[192] in which HOCl produced by the enzyme is captured as taurine chloramine. This compound oxidises iodide to hypoiodous acid which in turn is able to oxidise the chromophore, TMB (3,3′,5,5′-tetramethylbenzidine), to its light-absorbing diimine (**Scheme 41**). Thus, determining the absorbance of this species provides a measure of the enzyme's catalytic activity and, as a result, the inhibitory effect of the tested carborane fragment.

This assay is indiscriminate in identifying inhibitors; Compound II trappers or Compound III pushers will register as hits even though they would have limited effect *in vivo*. A multi-substrate assay has recently been proposed as a more robust method of detecting physiologically relevant inhibitors.[165] This assay determines enzymatic activity by measuring the rate at which TNB (5-thio-2-nitrobenzoic acid) is bleached to its colourless dimer by the oxidants produced by MPO. Importantly, urate and tyrosine are included in the buffer to mimic the conditions of extracellular environments. Both compounds effectively reduce Compound II to native ferric MPO,[164,193] thereby negating the effects of Compound II trappers. Urate is also an effective reductant of free radicals,[194] preventing their reduction of MPO to its ferrous form and therefore accumulation of Compound III (*vide supra*; **Figure 14**).

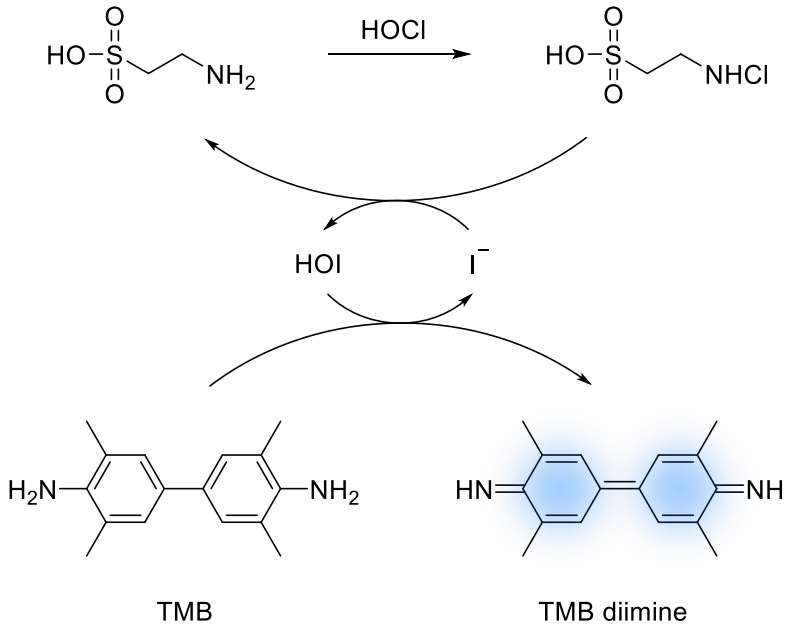

Scheme 41. Capture of HOCl by taurine and its resultant detection by oxidation of iodide and TMB to a blue product.

For this project, the multi-substrate assay was used as the primary method to test inhibition of most fragments. Some compounds were also tested under the taurine chloramine assay to help interpret the results of the SPR screen.

Although the methods reported for these assays are effective for drug-like molecules, screening fragment libraries requires adjustments to these conditions. Of primary concern is the solubility of the small fragments; because of their low potency, they must be tested at concentrations approaching 1 mM, at which point the water solubility of many small molecules is limited. This is particularly important for mono-substituted *closo*-carboranes, where the cage is inherently hydrophobic. A common method of increasing the solubility of hydrophobic compounds is addition of DMSO to the assay medium, with concentrations between 5–10% *v/v* used as the upper limit to preserve protein integrity. For many of the carborane fragments assessed in this thesis, even 10% *v/v* DMSO proved insufficient in dissolving them at a concentration of 500 μM. Addition of 0.01% *v/v* of the non-ionic surfactant Polysorbate 20 resolved this issue, allowing dissolution of most fragments up to a concentration of 1 mM in the assay medium supplemented with 5% *v/v* DMSO. While Polysorbate 20 has been shown to stimulate MPO activity,[195] its effect at this concentration is minimal. Furthermore, each fragment was tested against a negative control with inhibition being measured relative to the activity of MPO in an inhibitor-free medium. Finally, the inhibitory effect of a literature

inhibitor HX1 (**5**) and some selected water-soluble fragments were comparable when tested in the presence and absence of Polysorbate 20, confirming the validity of the measurements.

The results of these assays are presented in Table 4. Fragments were initially screened at a concentration of 500 μM and the percent inhibition relative to the uninhibited enzyme was determined. Some fragments were screened at lower concentrations due to their poor solubility or at higher concentrations if their inhibition at 500 μM was found to be low.

C-substituted carboxylic acid **71**, which was a strong binder in the SPR assays, was also found to be a potent inhibitor, inhibiting more than 50% of enzyme function at a concentration of 500 μM. Expansion of this structure into esters and amides, however, generally resulted in decreased performance. Methyl, ethyl and phenyl esters **118**, **119** and **99** did not inhibit the enzyme at all in the multi-substrate assay. Similarly, the propyl, nitrophenyl and benzyl esters **120**, **100** and **101** as well as the beta-cage carboxylic acid **121** had only minor effects on the enzyme. Some of these fragments were, however, potent inhibitors in the taurine chloramine assay, indicating that these derivatives can act as Compound II pushers or Compound III trappers. Of the amides synthesised, most performed poorly, with **103** showing low inhibition and **105** having no effect on the enzyme. Conversely, the *ortho*-phenylenediamine amide **104** showed comparable activity to the parent carboxylic acid (66%) at half the concentration. The almost complete reduction of potency of **123** compared to **71** shows that large substituents are not tolerated when installed adjacent to the carboxylic acid. Positioning of the carboxy group on the cage also had a profound effect, with B-substituted carboxylic acid **113** being completely inactive. This again may be due to a reduced ability to form dihydrogen bonds, but given the stark difference in activity electronic effects may also be in play.

Many of the phenyl carboranes, as in the SPR screen, performed poorly in the inhibition assays. Most derivatives showed no or very low inhibition in the multi-substrate assay (**126**, **127**, **128**, **129**, **130**, **133** and **124**), even despite strong binding affinity in the SPR screen in the case of **130**. An exception to this trend is fragment **131**, containing an aromatic primary amine, which significantly slowed HOCl production at this concentration (48% inhibition). The pyrimidine fragment **139** showed promise in the taurine chloramine assay, but along with heteroaromatic derivatives **138** and **137** did not inhibit MPO in the multi-substrate assay. Similarly, the benzyl carboranes **135** and **136** were both inactive, however the extended chain derivative **142** was a reasonable inhibitor.

Of the other fragments, C-hydroxy carborane **76** appeared to be a Compound II pusher/Compound III trapper, acting as a strong inhibitor in the taurine chloramine assay but, along with its methyl ether **112**, showed no activity in the multi-substrate assay. Compound **81** was similarly inactive. Cage-substituted amines **109** and **78** had comparably low inhibition, while nitrile **141** was somewhat more active. The related aminomethyl carborane **85** was a very potent inhibitor, with a percent inhibition of 54% at 500 μM.

Out of the compounds assessed in this work, **104**, **131** and **85** were the best performing and full dose-response curves were generated using the multi-substrate assay (**Figure 19**). **85** has a calculated IC_{50} of 133 ± 14 μM, and its curve shows good dose behaviour, reaching almost complete inhibition of the enzyme at a concentration of 1 mM. Fragment **131** has a similar IC_{50} of 124 ± 14 μM, however its effect approaches a limit at just above 60% inhibition. This behaviour reflects that of the related compound 4-bromo-aniline and is likely a result of an inability to completely restrict substrate access.[165] The dose-response curve of compound **104** ($IC_{50} \approx 75$ μM) also has a plateau above a concentration of 125 μM, however the limit is reached more abruptly. In this case, this is attributed to the poor solubility of the compound at higher concentrations. An important metric when comparing hit fragments is their ligand efficiency (LE), which quantifies their potency relative to heavy atom count. Of these fragments, **85** has the highest LE of 0.39, highlighting its impressive inhibition despite its low structural complexity. Although **104** has a lower IC_{50}, its LE (0.26) is not as high revealing a less efficient use of increased molecular size. Fragment **131** has a similar LE of 0.29, and while not as promising as **85**, should also be considered as a useful starting point for the design of an MPO inhibitor.

Table 5. Experimentally-determined IC_{50} values of carborane fragments from two different MPO inhibition assays.

Compound	Structure	% Inhibition at 500 μM	
		Taurine chloramine	Multi-substrate
109	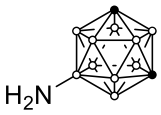	–	14%
76	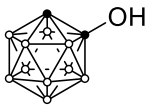	91%	No inhibition
112	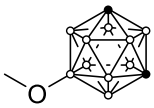	–	No inhibition
71	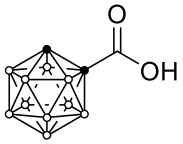	–	55%
113	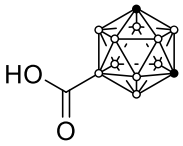	–	No inhibition
118	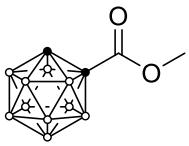	–	No inhibition
119	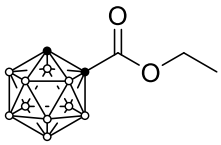	–	No inhibition
120	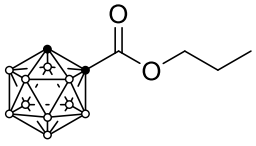	98%	10%*

* Percent inhibition at 1000 μM.
† Percent inhibition at 250 μM.

Table 5. (continued)

Compound	Structure	% Inhibition at 500 μM	
		Taurine chloramine	Multi-substrate
121	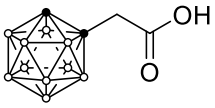	86%	13%*
123	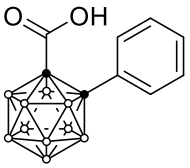	9%	–
124	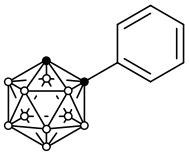	9%†	–
126	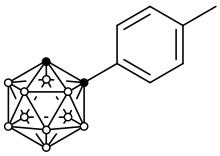	–	No inhibition
127	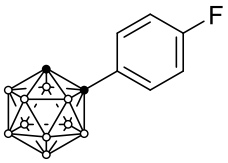	–	No inhibition
128	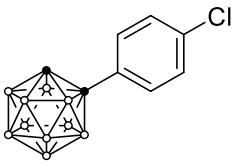	–	No inhibition
129	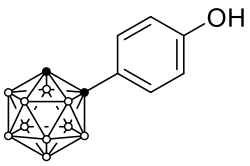	–	No inhibition

* Percent inhibition at 1000 μM.
† Percent inhibition at 250 μM.

Table 5. (continued)

Compound	Structure	% Inhibition at 500 μM	
		Taurine chloramine	Multi-substrate
130	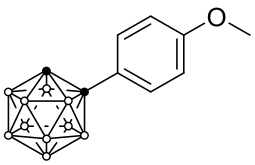	No inhibition	–
131	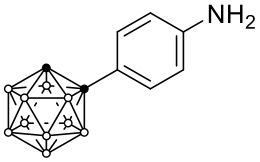	94%†	48%
133	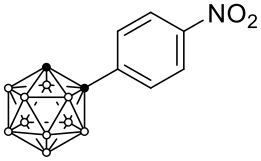	26%†	No inhibition
135	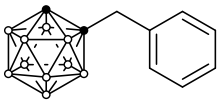	–	No inhibition
136	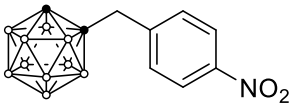	No inhibition	–
137	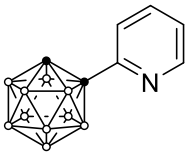	No inhibition	–
138	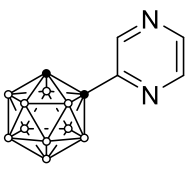	20%	No inhibition

* Percent inhibition at 1000 μM.
† Percent inhibition at 250 μM.

Table 5. (continued)

Compound	Structure	% Inhibition at 500 μM	
		Taurine chloramine	Multi-substrate
139	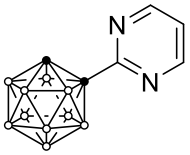	85%	No inhibition
85	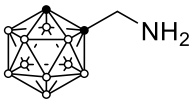	–	54%
104	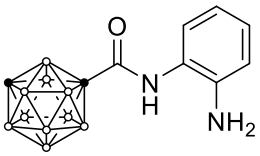	–	66%†
141	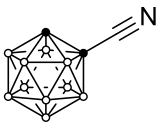	–	29%
78	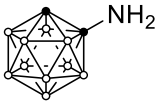	–	13%
142	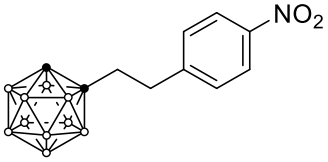	–	25%
101	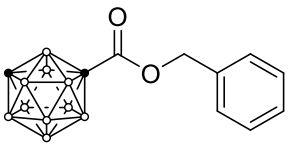	52%	16%

* Percent inhibition at 1000 μM.
† Percent inhibition at 250 μM.

Table 5. (continued)

Compound	Structure	% Inhibition at 500 μM	
		Taurine chloramine	Multi-substrate
99	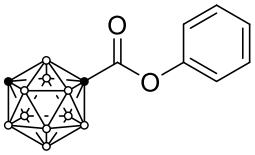	58%	No inhibition
100	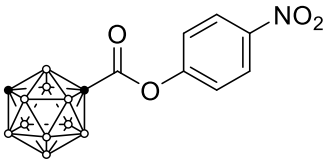	–	22%
81	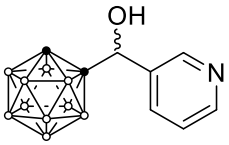	No inhibition	–
105	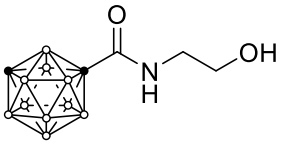	No inhibition	–
103	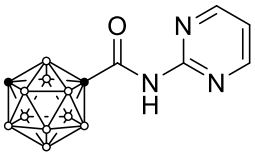	38%	–

* Percent inhibition at 1000 μM.
† Percent inhibition at 250 μM.

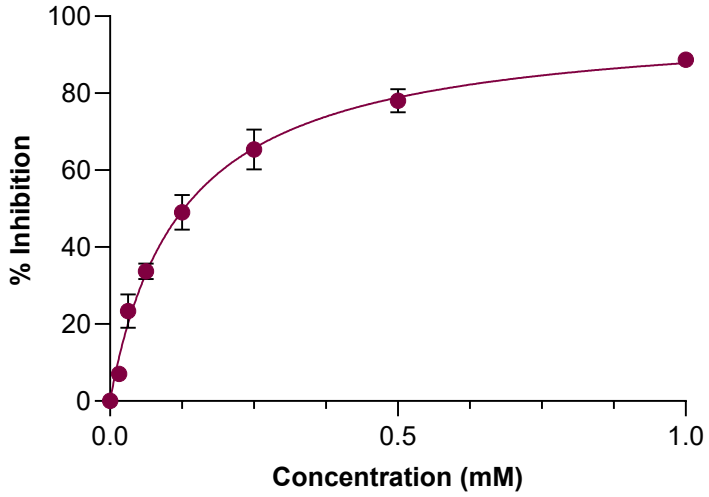

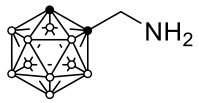

85
IC_{50} = 133 ± 14 µM
LE = 0.39

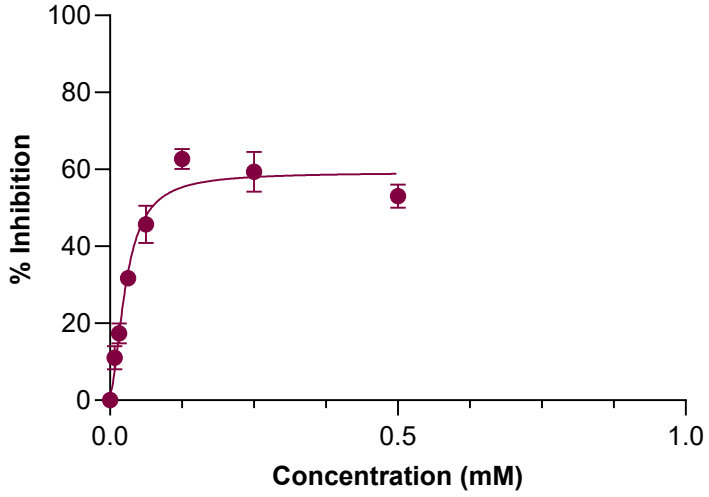

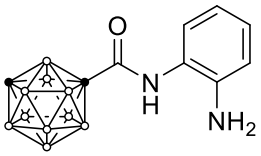

104
IC_{50} = 75 µM
LE = 0.26

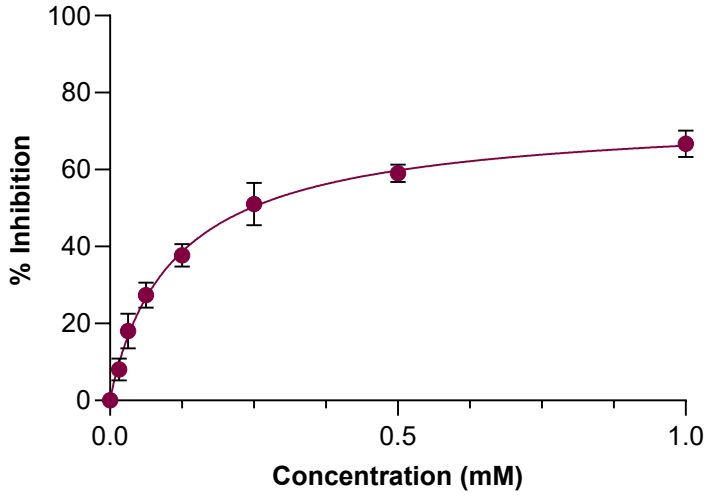

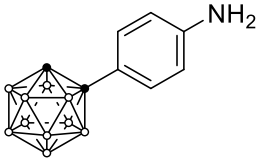

131
IC_{50} = 124 ± 14 µM
LE = 0.29

Figure 19. Dose-response curves and calculated IC_{50} values of hit fragments **85**, **104** and **131** measured using the multi-substrate assay. Data points represent the mean of 3 measurements; errors and error bars are SEMs.

Summary and Outlook

This Chapter detailed the synthesis of a set of low molecular weight carboranes and subsequent studies on their ability to bind and inhibit MPO. Even with a small library, three hit compounds (**85**, **104** and **131**) were identified, demonstrating that carboranes are a promising structural framework for designing 'first-in-class' MPO inhibitors. All of these fragments would serve as suitable leads for an expanded FBDD project, with **85** being particularly promising. In the next Chapter, this preliminary work will be built upon as we attempt to optimise this structure into a more potent MPO inhibitor.

4

Optimisation and Expansion of a Lead Fragment

In the previous chapter, we identified three carborane fragments that were relatively potent (μM) MPO inhibitors. Of these compounds, **85** is particularly promising due to its high ligand efficiency, reasonable water solubility and convenient two-step synthesis from *nido*-decaborane(14). For these reasons, it was chosen as the lead fragment to be expanded upon in this project.

As this is a novel lead, no experimental data on the binding mode of this or related compounds is available in the literature. Some insights can, however, be inferred from the results of Chapter Three. Given that the other fragments that performed well in the inhibition assay also contain primary amines, it is likely that this functional group facilitates strong interactions with amino acid residues near MPO's active site. The cage-substituted amine fragments showed a reduction in potency compared to **85**, indicating that the steric bulk of the carborane cage is not well tolerated close to the binding site and that some degree of conformational freedom is required. The increased distance of the cluster from the active site may also allow it to better interact with the hydrophobic region located at the entrance of the active-site cavity. Enzyme-inhibitor complexes reported in the literature show similar binding modes, where hydrophilic functional groups bind to the haem propionate arms and adjacent hydrophilic residues while more lipophilic sections of the inhibitor are oriented towards the surface of the protein.[174,196]

In order to investigate these aspects, efforts were directed towards synthesising a small library of compounds that could provide important structure activity relationships (SARs). Compound **85** contains three vectors for synthetic elaboration (**Figure 20**):

1. The amino group, which can be modified through a vast range of transformations, most readily through direct substitution of the nitrogen atom;
2. The methylene C–H groups, while not directly accessible from the parent fragment, can be functionalised through modifications in the preceding synthesis;
3. The other vertices of the carborane cage, which are open to functionalisation through either electrophilic (B-vertices) or nucleophilic (C-vertex) reactions. While there are in principle 6 unique boron environments and an additional carbon atom where substitution can occur, if only one substituent is added onto the cage there are three unique geometrical arrangements that can be formed (i.e. *ortho*-, *meta*- and *para*- to the carbon atom functionalised with the aminomethyl group).

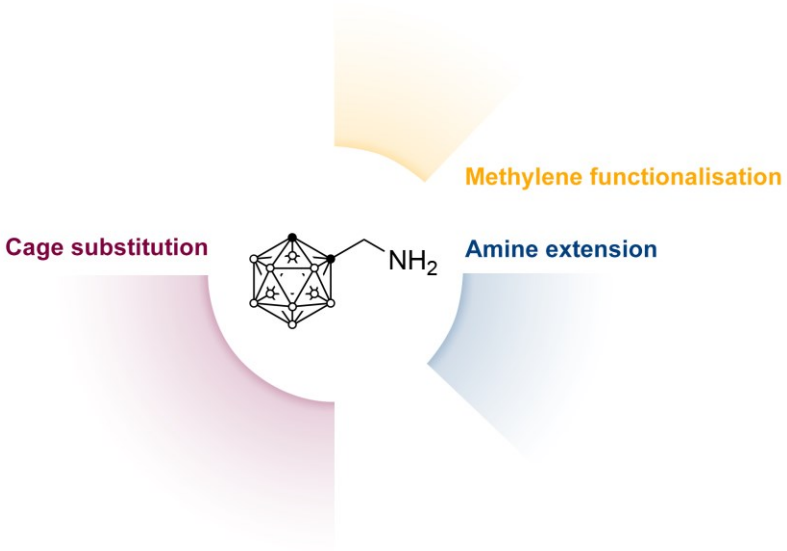

Figure 20. The three possible extension vectors of fragment **85**. ● = C–H (or C if substituted); ○ = B–H.

Because of the lack of information on how compound **85** binds to MPO, attempts were made to expand the lead fragment at all of these three sites, with a focus on developing the synthetic methodology used to access these positions. In this way, a deeper understanding of what structures are tolerated at certain positions can be established, which can potentially lead to a useful pharmacophore model for an MPO inhibitor. Moreover, these methods will provide a template for future synthetic efforts aimed at improving the function and potency of this fragment.

Functionalisation at the Carborane Cage

Substitution at the Free C–H Position

Given the importance of the primary amine functionality for the inhibition of MPO, extension of compound **85** further away from this site (i.e. at another vertex of the cluster) may provide access to new ligand-protein interactions without compromising binding of the $–NH_2$ group. As mentioned previously, three geometric arrangements are possible for disubstituted carboranes. The most straightforward route to accessing all of these is to functionalise the second C-vertex of the respective *closo*-1,2-, 1,7- and 1,12-carborane isomers of the lead fragment. Although this will introduce slight differences in polarity due to the altered arrangement of carbon vertices, only minor differences in activity were observed between isomers in our previous work.

Substitution at carborane C-vertices involves their initial deprotonation with a strong base. The amine protons of fragment **85** are also somewhat acidic and therefore require protection to avoid potential cross-reactivity issues. The precursor to this fragment is the phthalimide **84**, which conveniently provides a protected form of the lead fragment without additional synthetic efforts. The carbonyl groups of this protecting group, however, are susceptible to addition by nucleophilic bases such as *n*-butyllithium. Deprotonation of the cage C–H group in compound **84** must therefore be achieved using an alternative base, for which the bulky, non-nucleophilic lithium diisopropylamide (LDA) was chosen.

Using this base, hydroxylation of the second C-position (usually a high-yielding reaction) was attempted to test the viability of this method (**Scheme 42**). Under these conditions, a mixture of products was produced. The first of these was identified as compound **144**, which is formed as a result of intramolecular attack of the carborane anion into one of the phthalimide carbonyl groups (**Scheme 43**). This assignment was made based on the disappearance of the cage C–H resonance in the ^1H NMR spectrum of the compound, along with a loss in symmetry of the aromatic region. Furthermore, the transformation of the methylene peak into an AX doublet of doublets is indicative of diastereotopic protons at this site. This type of reaction has been observed with similar carborane phthalimide derivatives and is a result of the proximity of the adjacent C-site.[180] A second product from this reaction was also isolated which could not be identified. The alkyl resonance of this compound is split into a doublet, indicating addition of a hydroxyl group at this site. A loss in symmetry in the aromatic region, however, is not consistent with this product. For all of the reaction products,

no substitution of the phthalimide ring was observed, with the ^{1}H NMR spectra of all reactions displaying four protons in the aromatic region.

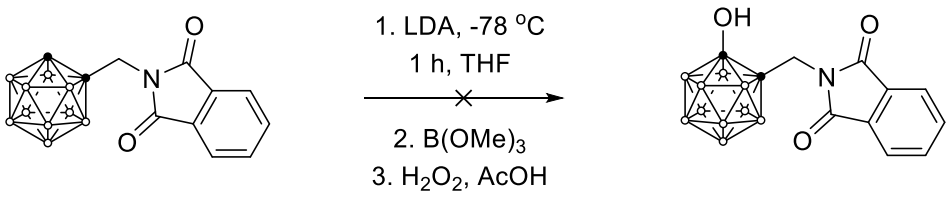

84 **143**

Scheme 42. Attempted hydroxylation of **84** at the free carborane C–H vertex. ● = C–H (or C if substituted); ○ = B–H.

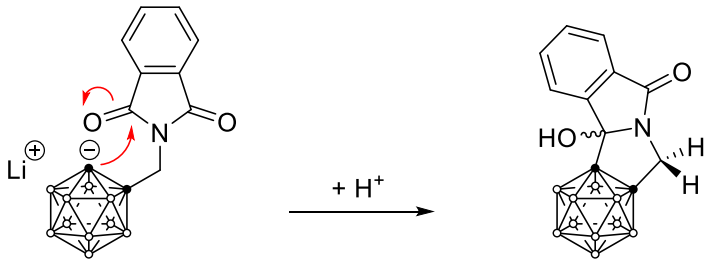

144

Scheme 43. Proposed mechanism for the formation of side-product **144** following deprotonation of **84** and an acidic workup. ● = C–H (or C if substituted); ○ = B–H.

Following the synthesis of the *closo*-1,7-carborane isomer of the starting phthalimide (**154**, *vide infra*), the same transformation was attempted on this substrate. In this case, intramolecular attack of the phthalimide was not observed and a small amount of the desired product was produced. Efforts at improving the yield by using other bases such as sodium hydride and potassium hexamethyldisilizane (KHMDS), however, proved to be ineffective. The use of other protecting groups was briefly considered, but this route was ultimately abandoned in favour of another strategy.

Substitution at Carborane B-Sites

In fragment **85**, the B–H vertices are also available for functionalisation with a second substituent. These are most readily and diversely functionalised through Pd-catalysed cross-coupling reactions following installation of a bromine or iodine atom at the desired site. Depending on the position of the halogen, different geometries relative to the amine chain can be achieved. A divergent synthesis is the most convenient method of generating a range of substituted derivatives, and so protection of the primary amine is also required in this case to prevent side reactions under cross-coupling conditions. The phthalimide group again served as a convenient solution for this strategy.

Initially, *closo*-1,2-carborane was chosen as the boron framework from which expanded fragments would be derived. Substitution adjacent to the phthalimide chain can be achieved by halogenation of the B(3/6) sites through a deboronation/recapping process, whereas *meta*- and *para*-type substitution is accessible through the B9 and B12 sites (**Figure 21**). Because one of the C-sites is substituted, electrophilic halogenation provides a mixture of the latter two, which would require separation to achieve the desired geometries in a pure form.

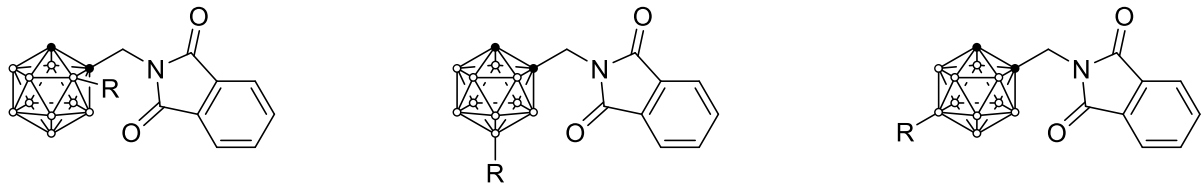

Figure 21. The three possible geometries of a disubstituted carborane achieved through 1,3-substitution (left), 1,9-substitution (centre) and 1,12-substitution (right) of *closo*-1,2-carborane. ● = C–H (or C if substituted); ○ = B–H (or B if substituted).

Initial efforts focused on synthesising the *meta*- and *para*-substituted synthons. Installation of iodine and bromine atoms was achieved using two different methods (**Scheme 44**). The phthalimide group of compound **84** is remarkably stable to strongly acidic conditions and the iodinated derivatives were obtained using conditions previously used in Chapter Two. Substitution occurred preferentially at the carborane cage rather than the phenyl ring, with the B9- (**145a**) and B12-substituted (**145b**) isomers being generated in approximately equal proportion by ^{1}H NMR spectroscopy. Bromination was effected using an alternative method involving NBS and a catalytic amount of triflic acid in HFIP which generated a similar mixture

of isomers (**146a** and **146b**). Unfortunately, separation of the isomers could not be achieved using flash column chromatography in either case. This is consistent with literature reports of similar disubstituted *closo*-1,2-carboranes,[197] where the ability to separate these positional isomers is dependent on the nature of the functional groups at these sites. It was anticipated that replacement of the halogen atoms with other structures in the following steps would allow for resolution of the constituent isomers.

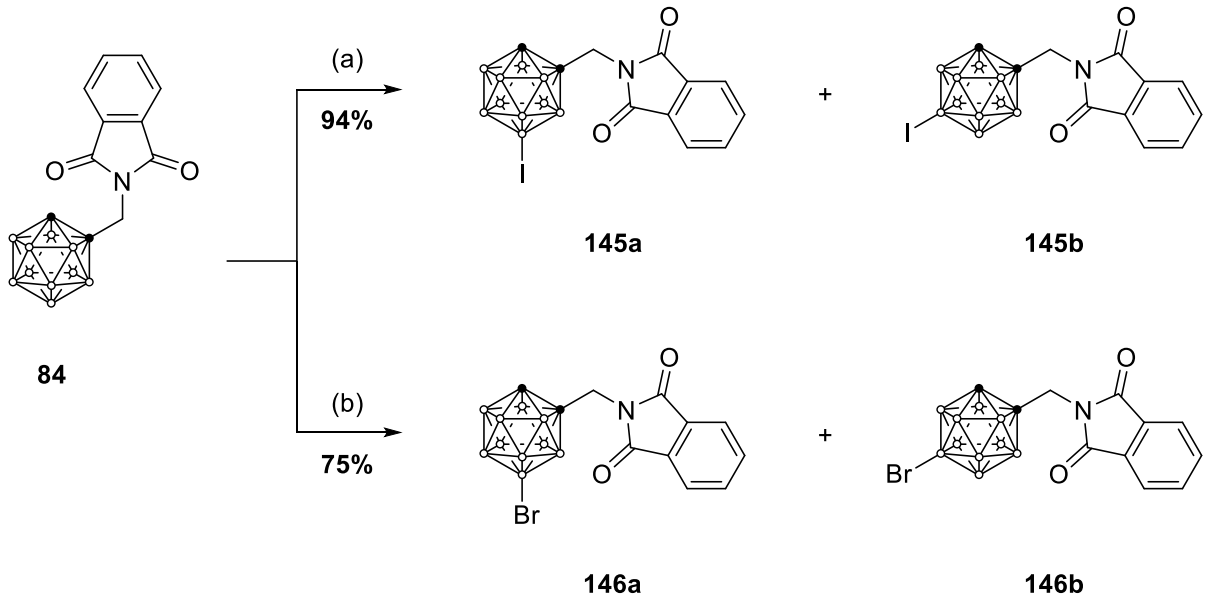

Scheme 44. Bromination (top) and iodination (bottom) of compound **84**, producing approximately equal proportions of B9- and B12-substituted carborane derivatives. (a) I_2, HNO_3/H_2SO_4, AcOH, 60 °C, 3 h; (b) NBS, TfOH (cat.), HFIP, RT, 24 h. ● = C–H (or C if substituted); ○ = B–H (or B if substituted).

As such, cross-coupling of these compounds was performed without further purification. Substrate selection for these reactions was aimed at maximising the structural diversity of the compounds produced. Generation of aryl, alkyl and benzyl derivatives was envisioned through Negishi couplings with the iodinated derivatives **145a** and **145b**, a transformation which is effective for the parent 9-iodo-*closo*-1,2-carborane.[185] Kumada couplings, which have also been used to functionalise carborane B-vertices,[198] are not suitable in this case due to the ability of Grignard reagents to react with the phthalimide carbonyl groups. Alternatively, the bromocarborane mixture **5** was intended as a precursor to B-heteroatom substituted compounds, which are also accessible through Pd-catalysed cross-coupling reactions. As a test reaction, Negishi coupling of phenylzinc bromide using conditions

described in Chapter Three was attempted.[185] While this reaction is robust and high-yielding when 9-iodo-*closo*-1,2-carborane is employed as the electrophile, only starting material was recovered when the isomeric mixture **145** was used as the coupling partner (**Scheme 45**). Similar results were observed with other aryl halides or when a benzyl zinc reagent was used. Difficulties were also encountered when B–N and B–O bond formation was attempted with the bromo-substituted synthons. In these cases, deboronation of the base-sensitive *closo*-1,2-carborane cage was the primary issue, although conversion to the desired product was also largely unsuccessful. Sodium azide was the only effective substrate in these reactions, with incorporation of the functional group being achieved in 78% yield with remarkably little accompanying decomposition to the *nido*- species (**Scheme 46**).

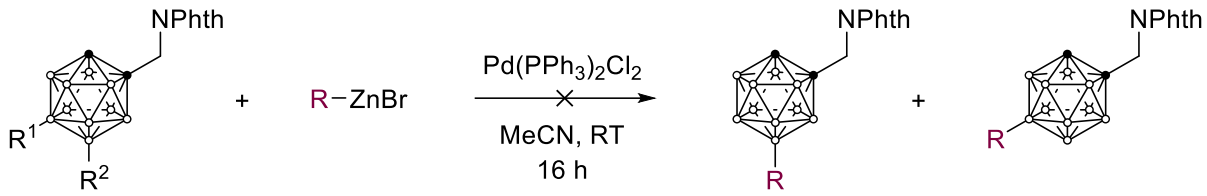

Scheme 45. Attempted Negishi coupling of aryl and benzyl zinc reagents with mixrture **145**. ● = C–H (or C if substituted); ○ = B–H (or B if substituted). NPhth = phthalimide.

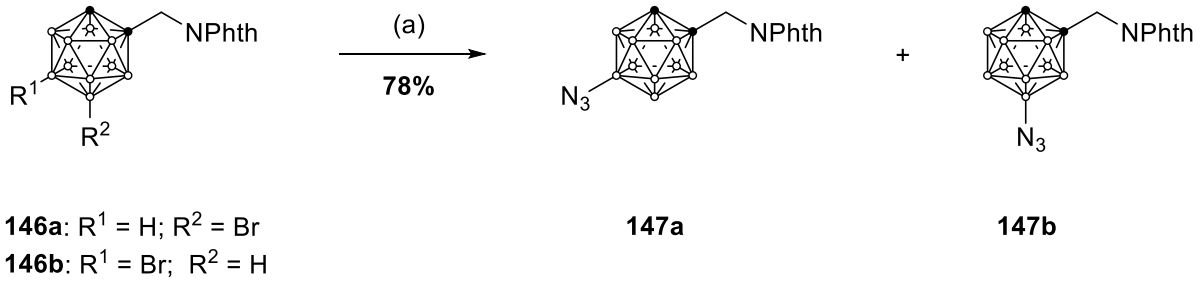

Scheme 46. Pd-catalysed cross coupling of mixture **146** with sodium azide. (a) NaN_3 (2 eq.), SPhos-Pd-G3 (5 mol%), SPhos (5 mol%), K_3PO_4 (2 eq.), DME, 80 °C, 3 h. ● = C–H (or C if substituted); ○ = B–H (or B if substituted). NPhth = phthalimide.

Because of the low reactivity of the halogenated synthons in these reactions, direct B–H functionalisation of compound **84** was explored as an alternative strategy for modifying the B(9/12) sites. Hydroxyl groups have been installed at these positions using nitric acid as the

OH source in HFIP.[139] Compound **84** is somewhat deactivated compared to unfunctionalized *closo*-1,2-carborane, with these conditions resulting in minimal conversion to the desired product. Repeating this reaction in neat triflic acid, however, gave compounds **148a** and **148b** in 87% yield (**Scheme 47**). No deprotection of the phthalimide group was observed, although a small amount of a nitrated phthalimide side-products (**148c** and **148d**) were detected. Separation of this compound was not necessary as it was removed along with the phthalimide group in the following deprotection step.

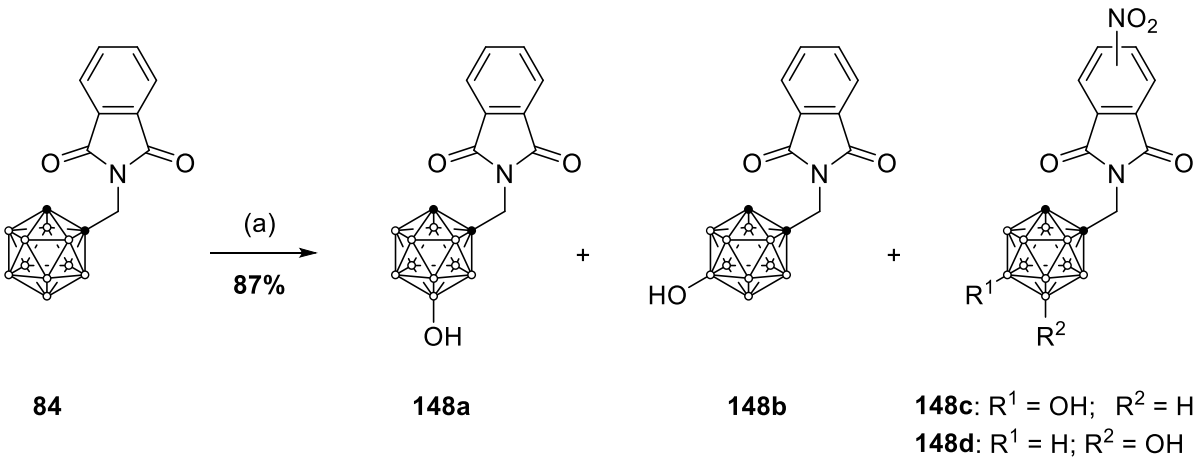

84 **148a** **148b** **148c**: R^1 = OH; R^2 = H **148d**: R^1 = H; R^2 = OH

Scheme 47. Direct hydroxylation of compound **84** giving a mixture of B9- and B12-hydroxy carboranes along with phthalimide-nitrated side products. (a) HNO_3 (1.2 eq.), TfOH, RT, 16 h. ● = C–H (or C if substituted); ○ = B–H (or B if substituted).

Incorporation of amine nucleophiles was achieved using a Pd-mediated electrophilic substitution reaction (**Scheme 48**). Mildly-acidic compounds such as sulfonamides react directly in these reactions, whereas more basic nucleophiles such as morpholine require pre-activation through generation of their *N*-benzoyloxy derivatives.[78] In accordance with their reactivity, benzenesulfonamide and methanesulfonamide were incorporated into the carborane cage of compound **84** in good yields. Conversely, benzophenone imine (**152**, an ammonia equivalent) and *N*-benzoyloxy morpholine (**151**) did not react under these conditions, again reflecting the deactivating effect of the phthalimide group on the cluster. Issues with site-selectivity were also apparent for the successful substrates, with small amounts of B8-substituted product being obtained along with the expected B9- and B12-functionalised compounds. This was evident in the ^{1}H and $^{11}B\{^{1}H\}$ NMR spectra of the purified product which showed three CH_2 and three B–OH resonances, respectively. Separation of these regioisomers using flash chromatography proved to be unsuccessful, and further issues were encountered when deprotection of the phthalimide was attempted. The standard method involving reduction

with sodium borohydride followed by acid hydrolysis resulted in almost complete deboronation of the carborane cage compounds. While decomposition could be minimised by using ethylenediamine in isopropanol as an alternative deprotection method, significant losses of the product to the respective *nido*- compound could never be completely avoided. Taken together, these issues made the use of a *closo*-1,2-carborane framework intractable, and any further work in this direction was abandoned.

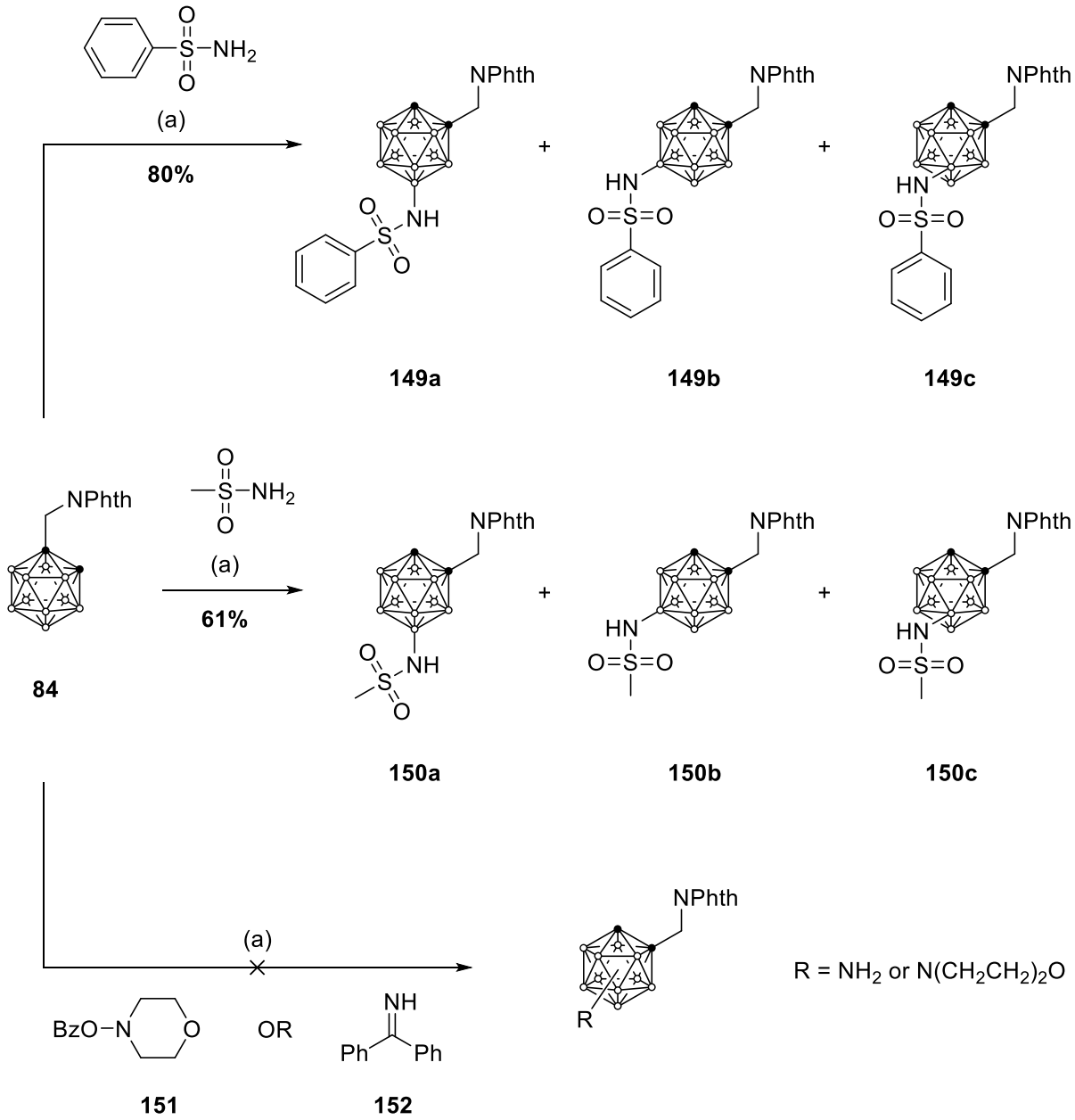

Scheme 48. Pd-catalysed direct B–H functionalisation of compound **84** with various nucleophiles, producing mixtures of B8-, B9- and B12- substituted products. (a) $Pd(OAc)_2$ (10 mol%), AgOAc (2.5 eq.), HFIP, 70 °C, 48 h. ● = C–H (or C if substituted); ○ = B–H (or B if substituted). NPhth = phthalimide.

As a result of our successful synthesis of the unprecedented 5-bromo-*closo*-1,7-carborane (Chapter Two), the preparation of antipodally-functionalised *closo*-1,7-carborane compounds became possible. Following lithiation of 5-bromo-*closo*-1,7-carborane and subsequent nucleophilic addition to methyl formate, two regioisomers (1-formyl-5-bromo-*closo*-1,7-carborane and 1-formyl-12-bromo-*closo*-1,7-carborane) were produced which were separated by means of flash chromatography. Using this approach, a route to *ortho*- and *para*-substituted phthalimidomethyl *closo*-1,7-carboranes can be envisioned (**Figure 22**). Additionally, a *meta*-substituted species is easily accessible through functionalisation of both the C1 and B(9/10) positions. The use of a *closo*-1,7-carborane framework has several advantages over the isomeric *closo*-1,2-carborane in this context:

1. The cluster is far more resistant to cage deboronation;
2. Halogenated *closo*-1,7-carboranes are better substrates in cross-coupling reactions and;
3. The difficulties in separating the very similar B9- and B12-substituted *closo*-1,2-carboranes are avoided.

The use of this carborane isomer in generating difunctionalised follow-up fragments was therefore investigated. Because the *nido*-decaborane-alkyne condensation reaction cannot deliver the *closo*-1,7-carborane isomer of fragment **85**, an alternative synthetic strategy had to be devised for its synthesis.

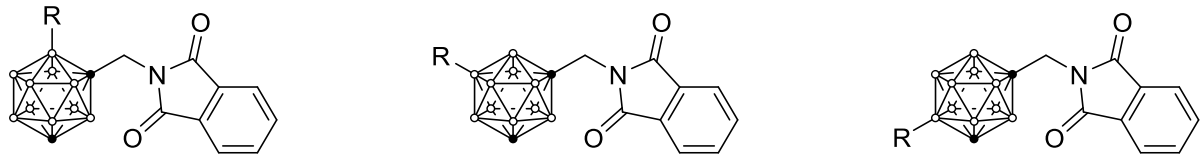

Figure 22. The three possible geometries of a disubstituted carborane achieved through 1,5-substitution (left), 1,9-substitution (centre) and 1,12-substitution (right) of *closo*-1,7-carborane. ● = C–H (or C if substituted); ○ = B–H (or B if substituted).

Utilising a *closo*-1,7-Carborane Framework

Our initial strategy was to produce the phthalimide-protected compound **154** from *N*-bromomethylphthalimide (**153**) and monolithiated *closo*-1,7-carborane in a facile S_N2 reaction

(**Scheme 49**). However, this method provided the desired mono-substituted product in only 20% yield, along with a similar amount of the disubstituted product.

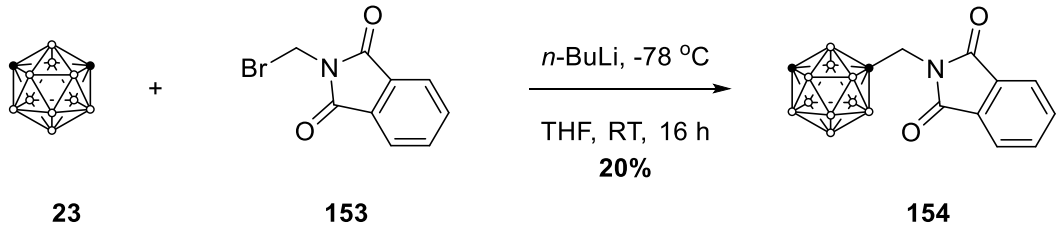

Scheme 49. Synthesis of **154** through a nucleophilic substitution of *N*-bromomethylphthalimide with *closo*-1,7-carborane. ● = C–H (or C if substituted); ○ = B–H.

As a result, a change in approach was devised involving synthesis of phthalimide **154** using the known compound 1-hydroxymethyl-*closo*-1,7-carborane (**75**, **Scheme 50**). This compound has been previously synthesised in an approximately 2:1 ratio with the doubly substituted carborane through reaction of lithio-*closo*-1,7-carborane with paraformaldehyde.[199] In order to avoid formation of the undesired disubstituted by-product, an optimised method was developed wherein 1-formyl-*closo*-1,7-carborane (**73**) was first generated (**Scheme 50**), a reaction which is known to be highly selective for mono-substitution.[65] The resulting crude product could then be directly reduced with sodium borohydride to afford the desired alcohol **75** in 87% yield.

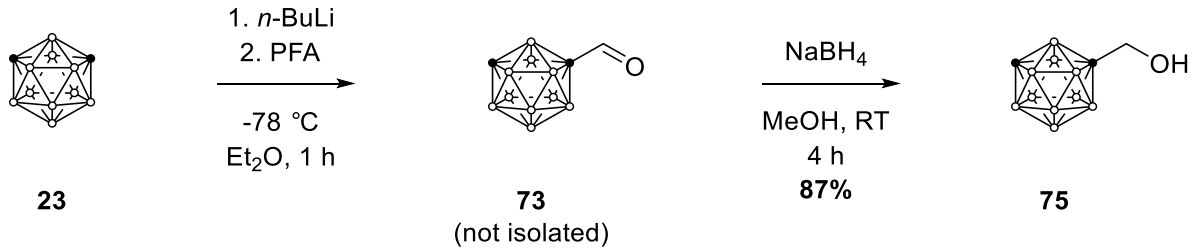

Scheme 50. Synthesis of compound **75** through a (pseudo) one-pot formylation and reduction procedure. ● = C–H (or C if substituted); ○ = B–H.

Initial attempts to convert this species into compound **154** involved a reaction with phthalimide under Mitsunobu conditions (**Scheme 51**), however this method gave very low yields of the product. As a result, efforts turned towards converting the alcohol into a better leaving group that could participate in an S_N2 reaction with phthalimide. Thus, 1-bromomethyl-

closo-1,7-carborane (**156**) was synthesised through a modification of a literature method using triphenylphosphine dibromide as the brominating reagent,[200] with chlorobenzene being used as a substitute for the carcinogenic benzene solvent (**Scheme 52**).

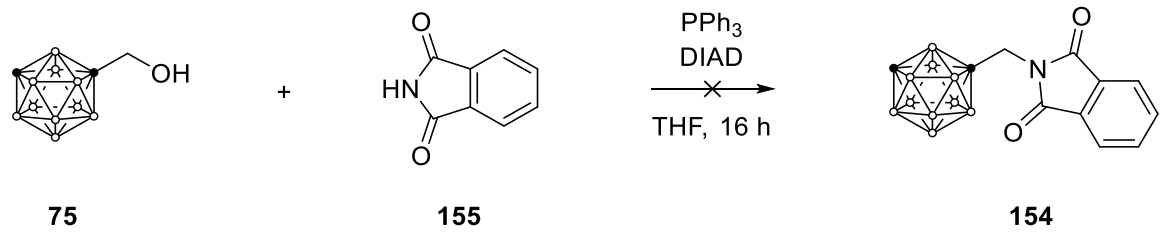

75 **155** **154**

Scheme 51. Attempted synthesis of compound **154** through a Mitsunobu-type reaction with hydroxymethyl-*closo*-1,7-carborane (**75**). ● = C–H (or C if substituted); ○ = B–H.

Unfortunately, this species proved rather unreactive in the alkylation of phthalimide (**Scheme 52**). Reactions performed in THF or acetonitrile at reflux with potassium carbonate as a base returned only starting material, even after extended periods (24–48 h). Using 18-crown-6 as a phase-transfer catalyst in toluene at reflux resulted in consumption of the starting material, however the product formed was the respective *nido*- species, consistent with the documented ability of crown ethers to facilitate cage deboronation.[201] Clearly, a more reactive electrophile was required for this transformation, with the corresponding triflate ester identified as a promising candidate due to the exceptional stability of the triflate anion.

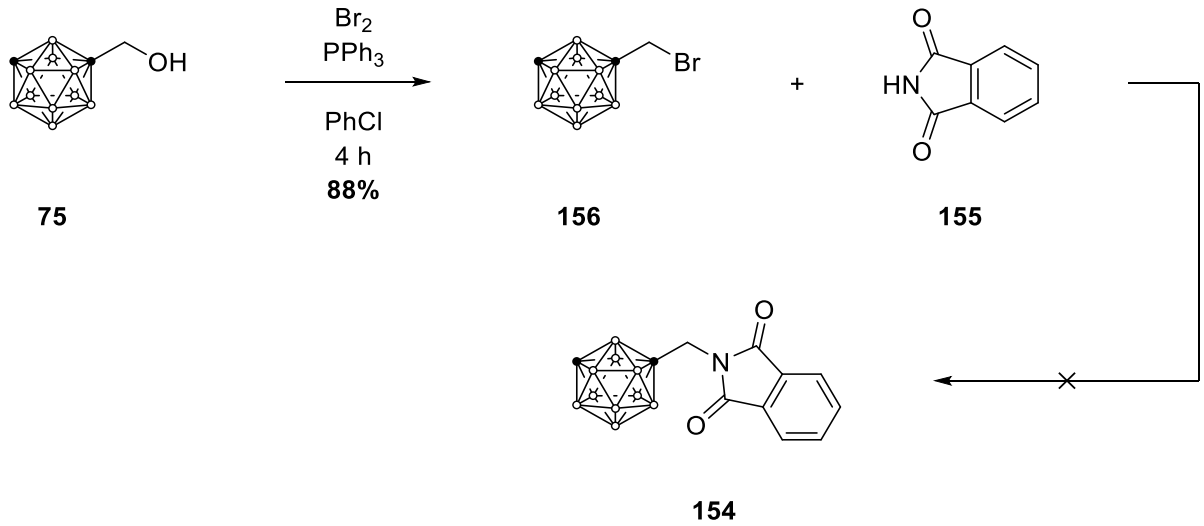

75 **156** **155**

154

Scheme 52. Attempted synthesis of compound **154** through alkylation of phthalimide with 1-bromomethyl-*closo*-1,7-carborane (**156**). Several conditions for the alkylation reaction were tested but none were successful. ● = C–H (or C if substituted); ○ = B–H.

The triflate ester (**157**) was synthesised in excellent yield using a known procedure by treating **75** with triflic anhydride and pyridine (**Scheme 53**).[202] The *closo*-1,2-carborane isomer of this compound has been shown to react with phthalimide and potassium carbonate in THF to produce the alkylation product in 50% yield after 30 hours.[203] In our hands, the *closo*-1,7-carborane derivative was obtained in substantially lower yields under similar conditions, while heating at 100 ºC in diglyme formed the undesired *nido*- species. Using the polar aprotic solvent acetonitrile resulted in improved conversion, but the best results were achieved when the alkylation was performed using potassium phthalimide in DMF. These conditions furnished the desired product without concomitant decomposition, allowing the synthesis of compound **154** in excellent yield and purity with minimal purification (**Scheme 53**).

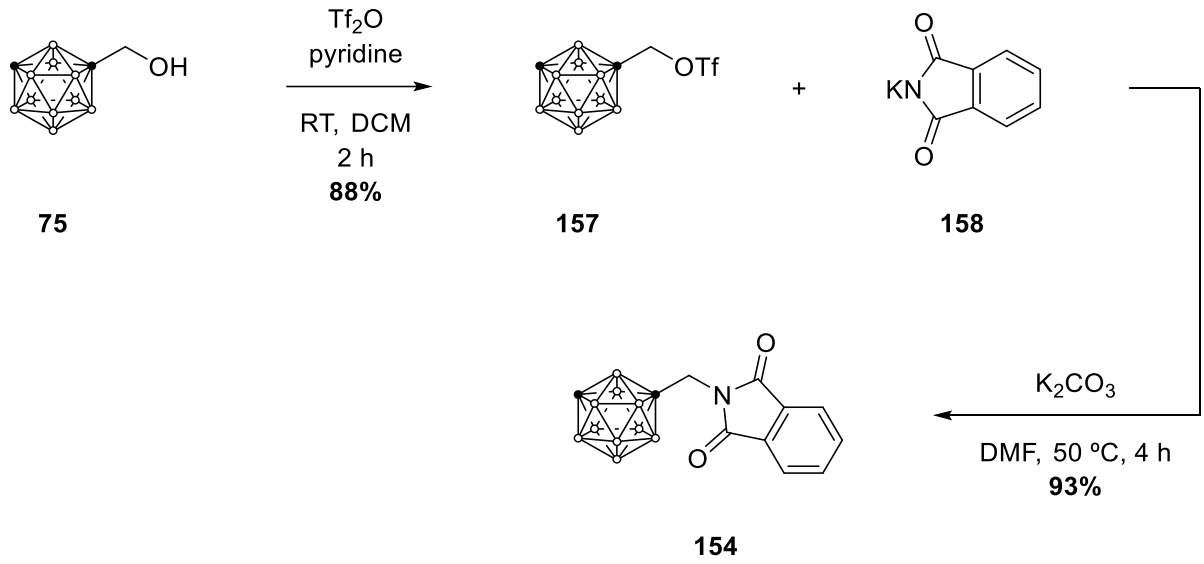

Scheme 53. Preparation of *closo*-1,7-carborane phthalimide **154** using the triflate ester **157**. ● = C–H (or C if substituted); ○ = B–H.

Subsequent bromination of phthalimide **154** under electrophilic conditions in HFIP readily provided the 1,9-disubstituted synthon **159** (**Scheme 54**). The $^{11}B\{^{1}H\}$ NMR of this compound (**Figure 23**) displays ten peaks, reflecting the complete loss of cage symmetry following bromine incorporation. An alternative route to this compound involving the same synthetic steps as above but using 9-bromo-*closo*-1,7-carborane as starting material was also validated. This method afforded the product in similar overall yield but would also be suitable for the synthesis of the 1,5- and 1,12-disubstituted isomers of compound **159** if 5-bromo-*closo*-1,7-carborane were used as the precursor.

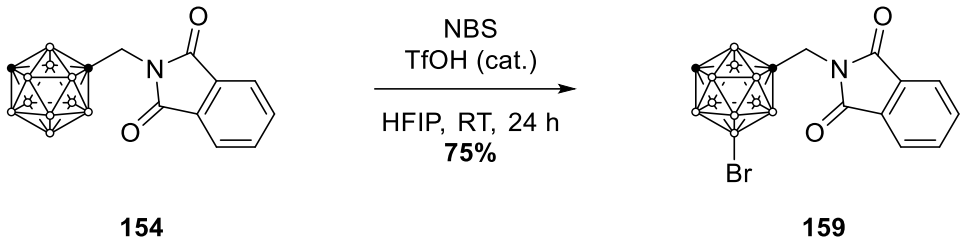

154 **159**

Scheme 54. Bromination of compound **154** to produce the 1,9-disubstituted *closo*-1,7-carborane synthon **159**. ● = C–H (or C if substituted); ○ = B–H (or B if substituted).

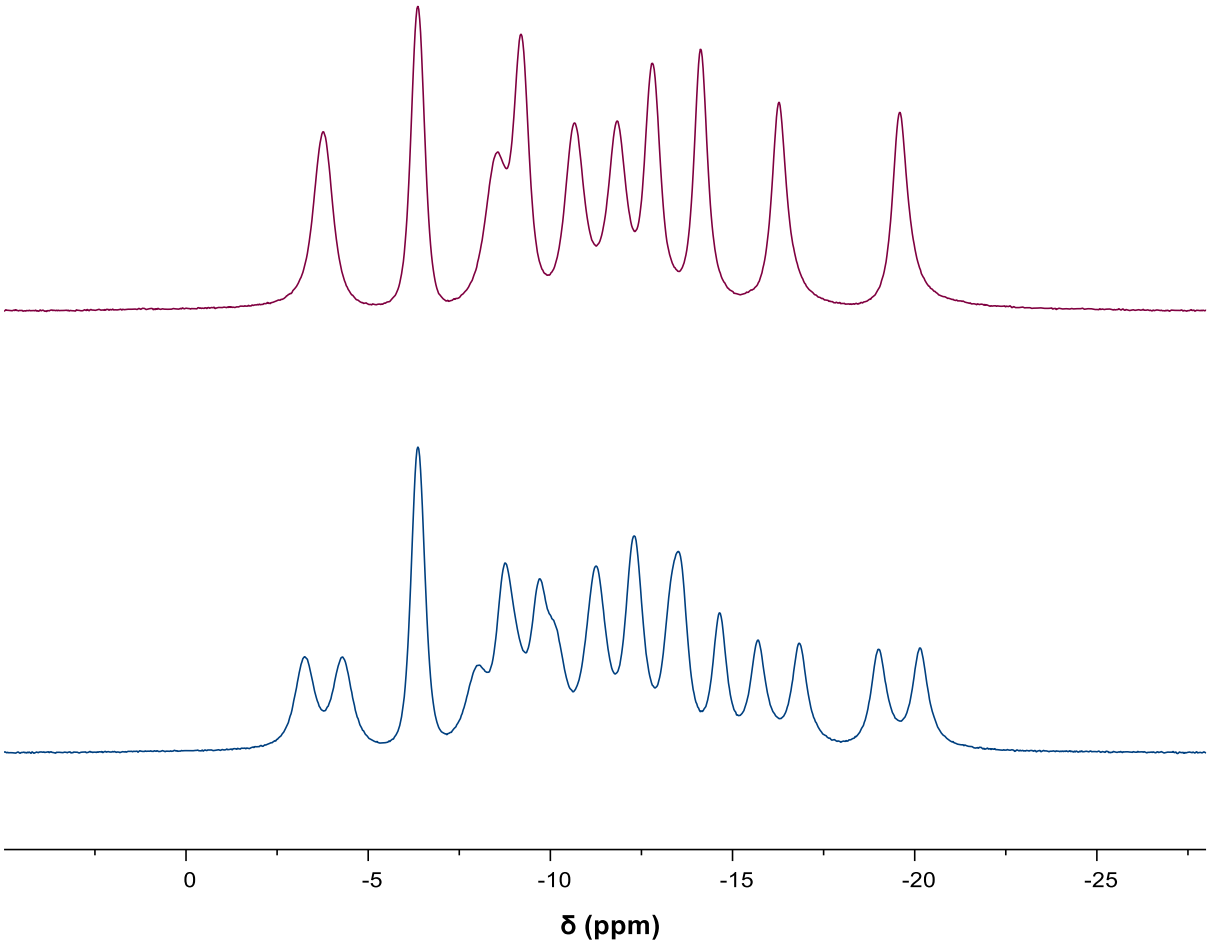

Figure 23. The $^{11}B\{^{1}H\}$ (top) and ^{11}B (bottom) NMR spectra of disubstituted carborane **159**. The singlet at -6.4 ppm is representative of the B–Br vertex.

The *closo*-1,7-carborane synthon **159** was subsequently used as a precursor to synthesise a set of 1,9-disubstituted derivatives (**Scheme 55**). Surprisingly, this compound was somewhat susceptible to cage deboronation under the conditions used to achieve B–N and B–O coupling of 9-bromo-*closo*-1,7-carborane.[126,127] Reactions involving sodium *tert*-butoxide or basic substrates such as morpholine or imidazole were particularly vulnerable to decomposition. Even the synthesis of the 9-hydroxy derivative, which utilises a mixture of weakly basic aqueous potassium phosphate and dioxane as the solvent, resulted in the formation of significant amounts of *nido*-carborane compounds. Less basic substrates such as sulfonamide and aniline derivatives as well as sodium azide were less problematic in this sense and their syntheses were optimised without any associated cage deboronation being observed.

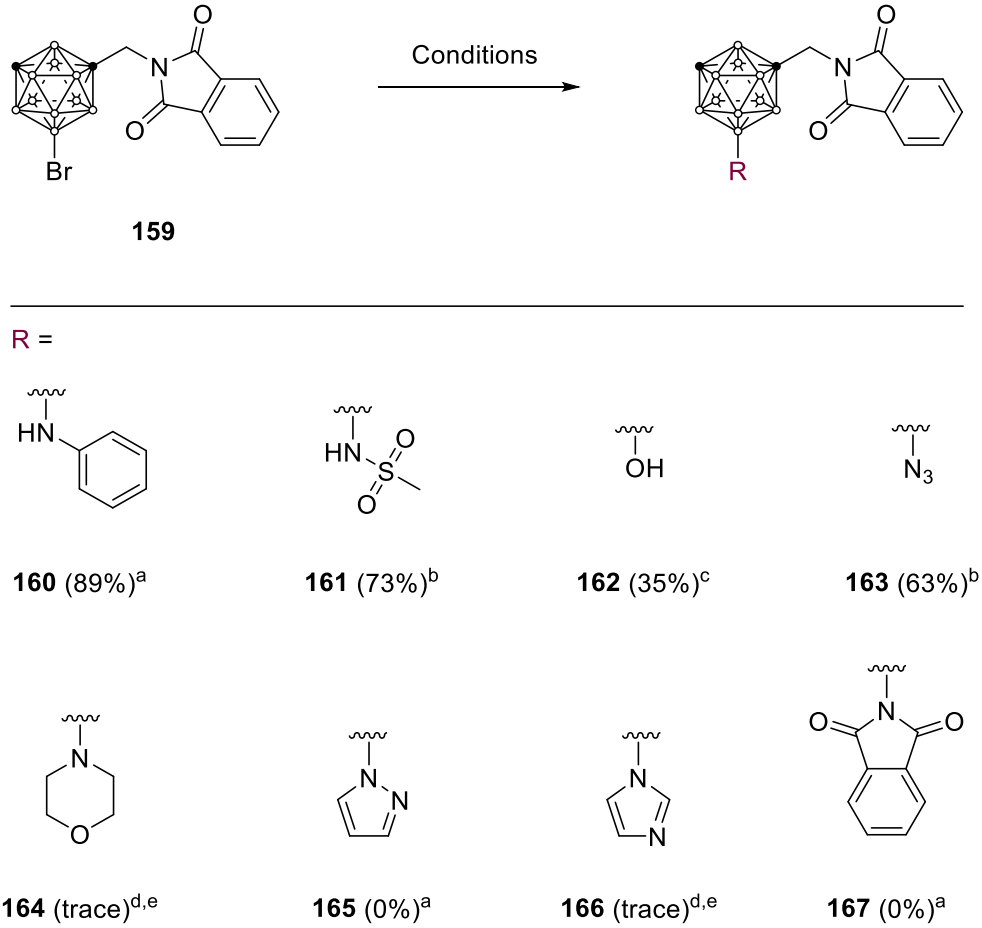

Scheme 55. Pd-catalysed cross coupling of **159** with various nucleophiles. [a] Nucleophile (1.5 eq.), $Pd(OAc)_2$ (10 mol%), $(2\text{-OMe-}C_6H_4)_3P$ (10 mol%), K_3PO_4 (3 eq.), DME, 100 °C, 20 h; [b] Nucleophile (1.5 eq.), SPhos-Pd-G3 (5 mol%), SPhos (5 mol%), K_3PO_4 (2 eq.), DME, 100 °C, 16 h; [c] SPhos-Pd-G3 (5 mol%), SPhos (5 mol%), 1,4-dioxane/1 M $K_3PO_{4\,(aq.)}$, 80 °C, 1 h; [d] Nucleophile (2 eq.), SPhos-Pd-G3 (5 mol%), SPhos (5 mol%), K_3PO_4 (2 eq.), 1,4-dioxane, 80 °C, 4 h; [e] *nido*-Carboranes constituted the bulk of the reaction mixture. ● = C–H (or C if substituted); ○ = B–H (or B if substituted).

The work presented in this chapter clearly demonstrates that the phthalimide group has a deactivating effect on the cluster in these reactions and sensitises it to cage deboronation. Although the reasons for this are unclear, the use of a different protecting group may alleviate some of these problems. An alternative synthon, the benzophenone imine-protected **169**, was therefore synthesised (**Scheme 56**) and assessed. While this compound displayed greater resistance to cage deboronation than the respective phthalimide, NMR conversions to the coupling products were not substantially different. Due to the low yielding synthesis of this compound and its difficult purification, further optimisation of its use in these reactions could not be achieved within the timeframe of this project.

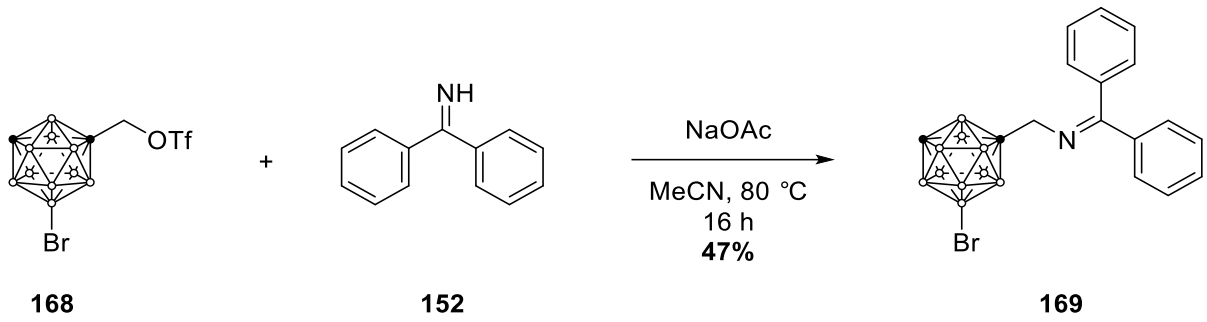

Scheme 56. Synthesis of another 1,9-disubstituted *closo*-1,7-carborane synthon (**169**) containing an alternative protecting group. ● = C–H (or C if substituted); ○ = B–H (or B if substituted).

Expansion and Optimisation of the Amine Warhead

Given the stark difference in activity of fragment **85** and the 'on-cage' amine **78**, the synthesis of longer chain derivatives was carried out to further investigate the effects of chain length on inhibitory activity. In contrast to the methyl linked derivative **84**, the ethyl and propyl phthalimides have been synthesised from *closo*-1,2-carborane in reasonable yields.[204] Thus, nucleophilic substitution of lithio-*closo*-1,2-carborane with the respective *N*-bromoalkylphthalimide in DME gave the desired protected amines **172** and **173** in 34% and 62% yield, respectively (**Scheme 57**).

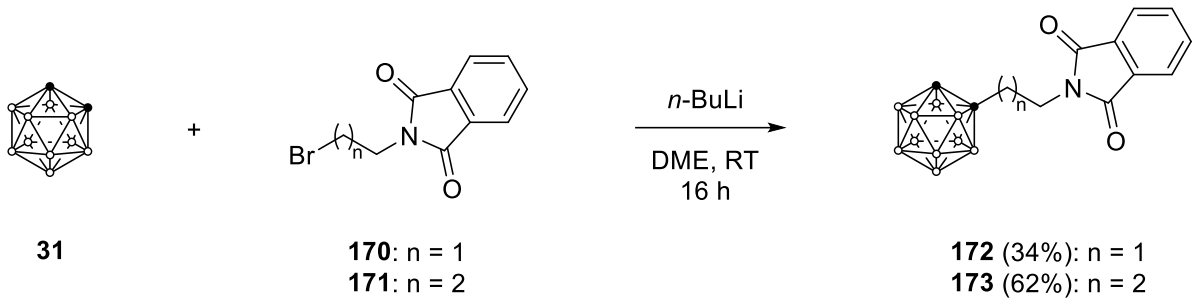

31 **170**: n = 1 **171**: n = 2 **172** (34%): n = 1 **173** (62%): n = 2

Scheme 57. Synthesis of extended chain amines from *closo*-1,2-carborane and the respective *N*-bromoalkylphthalimide. ● = C–H (or C if substituted); ○ = B–H.

Modifications to the amine end group were also briefly investigated. The hit fragment **104** can be seen as an example of such a modification of fragment **85** resulting from substitution at the amino group and addition of a carbonyl group at the methylene position. The improved IC_{50} but lower LE of this compound led us to probe the necessity of the carbonyl group through the synthesis of compound **175** (**Scheme 58**). This was achieved by treating triflate **174** with an excess of *ortho*-phenylenediamine in acetonitrile. The yield of this reaction is low in part due to deboronation of the cage, which would be mitigated if the respective *closo*-1,7-carborane triflate (**157**) was used. In a similar manner, protected O-substituted hydroxylamine **176** was synthesised (**Scheme 59**), of which the deprotected compound would constitute both an extension and modification of the linker.

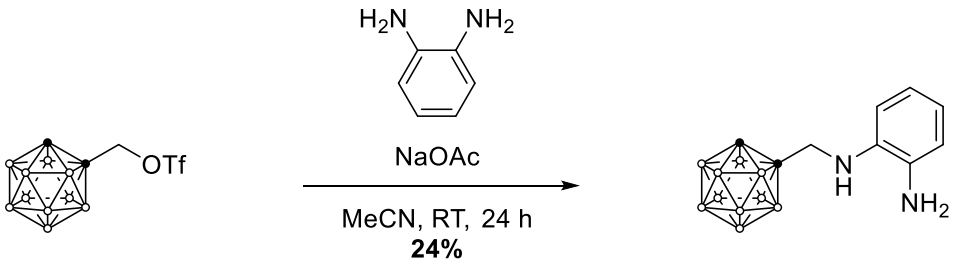

174 **175**

Scheme 58. Synthesis of expanded amine fragment **175** from carborane triflate **174**. ● = C–H (or C if substituted); ○ = B–H.

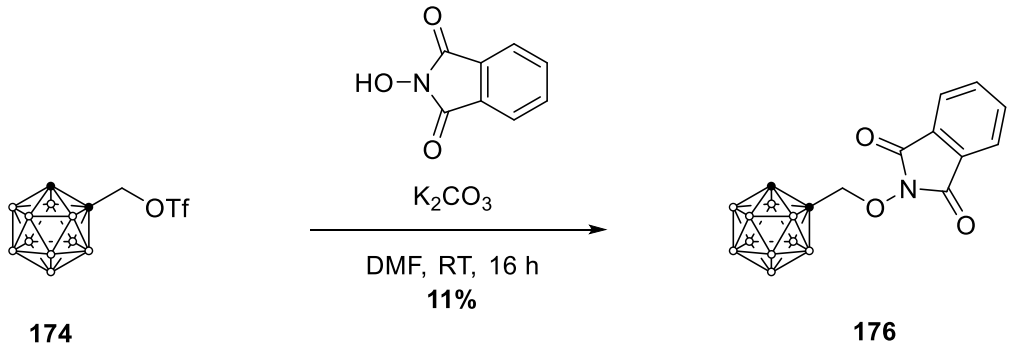

174 176

Scheme 59. Synthesis of expanded amine fragment **176** from carborane triflate **174**. ● = C–H (or C if substituted); ○ = B–H.

As a follow-up to the synthesis of diamine **175**, benzimidazole **178** was also prepared (**Scheme 60**). This was achieved through a one-pot process involving imine condensation of 1-formyl-*closo*-1,2-carborane (**72**) and *ortho*-phenylenediamine (**177**), followed by $FeCl_3$ catalysed cyclisation and oxidation.[205] The secondary amine is conserved in this structure, however, cyclisation of the other amine locks it into a specific configuration. Such conformational restrictions can reduce the entropic penalty of enzyme binding if the resultant conformer resembles the bioactive one, thereby increasing the fragment's potency. Inhibition data for this compound will therefore provide further insights into the binding mode of these compounds.

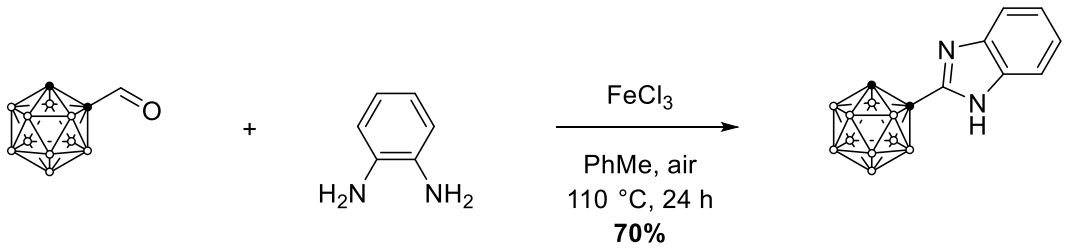

72 177 178

Scheme 60. Synthesis of the benzimidazole-substituted carborane **178** through a tandem condensation and oxidative cyclisation reaction between formyl *closo*-1,2-carborane **72** and *ortho*-phenylenediamine. ● = C–H (or C if substituted); ○ = B–H.

Expansion at the Methylene Position

Because of their ease of synthesis (see Chapter Three), hydroxymethyl carboranes were chosen as precursors to derivatives of compound **85** functionalised at the methylene position. The

hydroxyl group in these compounds can readily be converted into good leaving groups, which can further alkylate *N*-nucleophiles. Using the 3-pyridyl derivative **81** as a prototype, reaction with thionyl chloride or triflic anhydride afforded the chloro and triflate derivatives, respectively, in excellent yields (**Scheme 61**). Triflate **179** was chosen as the intermediate for further transformations due to its greater reactivity and lessened need for harsh reaction conditions. Nucleophilic substitution of this compound with aqueous ammonia in DMF furnished the desired amine in 76% yield. In contrast to alcohol **81**, the methine C–H resonance in the ^{1}H NMR spectrum of compound **180** presented as a singlet, reflecting a lack of spin-spin coupling with the fast-exchanging, adjacent amine protons. The presence of the amine group was further confirmed by a broad singlet at 6.0 ppm that disappeared following addition of D_2O due to deuterium exchange of the protons.

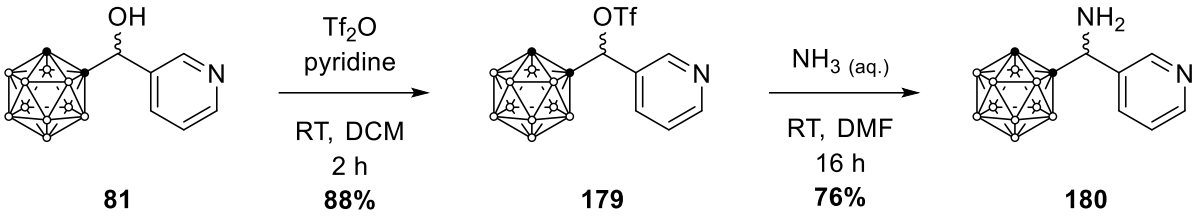

81 **179** **180**

Scheme 61. Synthesis of 1-aminomethyl(pyridin-3-yl)-*closo*-1,2-carborane **180** from the triflate ester of alcohol **81**. ● = C–H (or C if substituted); ○ = B–H.

Although there was insufficient time to produce other representatives of this class of compounds, the synthesis of compound **180** demonstrates that this is an effective approach to expansion of the lead fragment at this site.

Summary and Outlook

In this chapter, preliminary expansion and optimisation of lead fragment **85** was performed. To this end, methods for the synthetic elaboration of this structure at three different vectors were developed, which will serve as guides for future syntheses of derivatives for this project. A set of diverse follow-up fragments were generated using these methods, however, time constraints precluded the deprotection and subsequent biological assessment of these compounds. These assays will be performed in due course, the results of which will provide critical insights into structure activity relationships and facilitate the evolution of fragment **85** into a potent MPO inhibitor.

5

Conclusions and Future Work

At the start of this thesis, a lack of structural diversity was identified as a key potential pitfall in the development of novel bioactive agents. In our view, carboranes present an exciting solution to this problem, offering a range of opportunities in medicinal chemistry that are unattainable with traditional organic structures. Their use in this context, however, has been hindered by the difficulty in regioselective functionalisation of certain positions of the cage. The principal goal of this work was to address this limitation and to further demonstrate that carboranes can be used as effective structural frameworks for future fragment-based drug discovery projects.

Chapter Two detailed our attempts at functionalising unusual boron sites of *closo*-1,2 and *closo*-1,7-carborane. As part of this work, a first-of-its-kind protecting group for carborane B-vertices was developed and its use fully validated. The iodine protecting group is easily installed and can be removed in a mild and highly selective manner. As a result of this pioneering work, two completely novel brominated carborane isomers were synthesised and characterised for the first time (**Figure 24**), and substantial progress was made towards the synthesis of two additional and, until now, never before synthesised isomers.

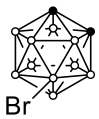

32
8-bromo-*closo*-1,2-carborane

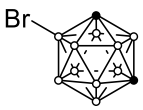

20
5-bromo-*closo*-1,7-carborane

Figure 24. Two novel bromo-carborane isomers synthesised in Chapter Two. ● = C–H; ○ = B–H (or B if substituted).

Our novel protecting group strategy can provide further opportunities in the field of carborane synthetic chemistry. It may be used, for example, as a blocking group to alter the substitution site of directing group-based carborane syntheses, thus further expanding the scope of these methodologies. Moreover, while the electron-withdrawing iodine atoms deactivate the cage towards further electrophilic substitution, nucleophilic substitution at the other boron vertices should, in principle, be facilitated. The Xie group have previously reported nucleophilic substitution of electron-deficient carborane B–H units with Grignard reagents and other nucleophiles,[206–208] with the steric profile of substituents at the C-positions dictating site selectivity. In such reactions, the use of the iodine protecting group could provide a powerful method to further control the final site(s) of substitution (**Scheme 62**).

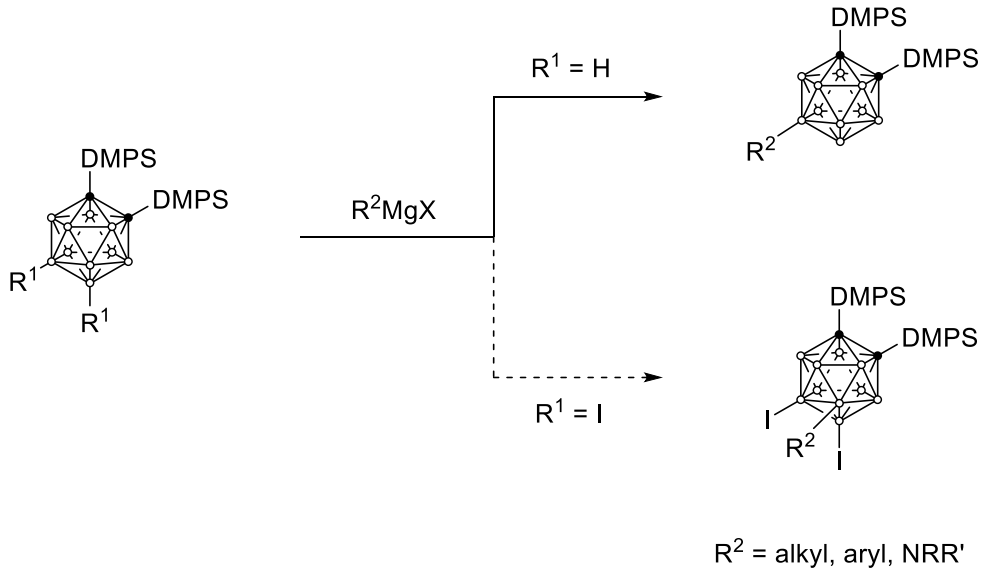

Scheme 62. The direct nucleophilic substitution of carborane B–H bonds developed by Xie and coworkers. The dimethylphenylsilyl (DMPS) groups attached to the C-vertices of the cage block the adjacent boron sites and direct substitution at the B(9/12) positions (top). Protecting these positions with iodine groups could alter the site of substitution (bottom). ● = C–H (or C if substituted); ○ = B–H (or B if substituted).

In Chapter Three, the synthesis of a set of carborane-based fragments was undertaken with a focus on expanding the scope of some of the underlying synthetic chemistry. Subsequent biological testing using SPR and *in vitro* inhibition assays revealed that several of these compounds bind to and inhibit MPO, the most potent of which are shown in Figure 25. These fragments are exceedingly potent for their size and complexity, with potencies in the μM range (cf. organic fragments which are typically mM binders). Additionally, they have inhibitory

activities under physiologically relevant conditions and would make for promising lead structures in the development of novel MPO inhibitors in the future.

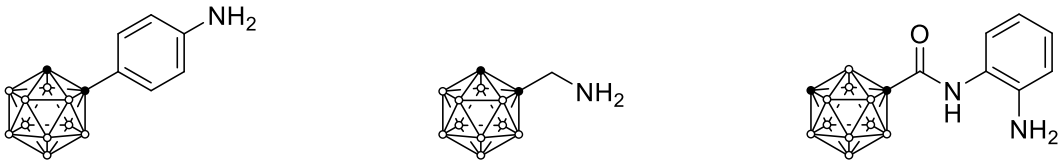

131
IC_{50} = 124 ± 14 μM
LE = 0.29

85
IC_{50} = 133 ± 14 μM
LE = 0.39

104
IC_{50} ≈ 75 μM
LE = 0.26

Figure 25. Fragment hits identified in Chapter Two and their corresponding IC_{50} values and ligand efficiencies. ● = C–H (or C if substituted); ○ = B–H.

The synthetic elaboration of one of these fragments (**85**) was detailed in Chapter Four. Methods for accessing all three possible expansion vectors of this compound were developed, leading to the synthesis of a small library of expanded compounds. Biological testing of the completed follow-up fragments will be reported in due course and will inform further efforts at expanding fragment **85**.

Future work should be directed towards determining whether these compounds act as tight-binders or irreversible inhibitors, which can be achieved through a two-step form of the assay used in this work. In this case, the protein is immobilised and washed following the initial assay and its inhibitory activity is reassessed. Only substrates which permanently modify the haem group of the enzyme will continue to inhibit its function. Co-crystallisation of fragment **85** and its derivatives with MPO would provide further insights into their binding mode by means of X-ray protein crystallography, allowing rational expansion of these compounds into highly potent inhibitors.

With the newfound ability to substitute previously-inaccessible sites of the carborane cage and recent advances in their functionalisation, the potential applications of carboranes in medicinal chemistry are vast. This thesis has demonstrated only a fraction of this potential; it is our hope that continued progress in carborane chemistry will drive mainstream adoption of these fascinating frameworks in drug design, where they can undoubtedly serve as an invaluable tool in tackling the increasingly complex challenges faced by modern medicine and chemical biology.

6

Experimental

General Considerations

All reactions requiring an inert atmosphere are indicated and were performed according to conventional Schlenk techniques using dry nitrogen or argon, as specified. All other reactions were performed in air without precautions to exclude atmospheric moisture or oxygen. Room temperature (RT) was 23–24 °C, unless otherwise stated.

Materials

Solvents used for moisture-sensitive reactions (DCM, toluene, acetonitrile, DCE, THF, diethyl ether) were of HPLC grade, or equivalent, and dried by standing over activated 4Å molecular sieves for 24 h. DMF was dried by performing this procedure and decanting the solvent onto a fresh batch of activated molecular sieves. Sieves were activated at 300 °C for 24 h and allowed to cool to RT under dynamic vacuum before use. All other solvents were of technical grade or above and used without further treatment. Petroleum benzine used in all procedures consisted of hydrocarbons boiling between 40–60 °C at standard pressure. All precursor chemicals were available commercially and used without purification unless otherwise stated. *nido*-Decaborane(14), *closo*-1,2-carborane and *closo*-1,7-carborane were purchased from KatChem (Czechia) or Boron Specialities (US). Cobalt(II) bromide, tribasic potassium phosphate and sodium acetate were dried at 150 °C under dynamic vacuum for 1 h before use. Triphenylsilylchloride was recrystallised from *n*-hexane at -78 °C before use. SPhos-Pd-G3 was prepared as described in the literature.[209] MPO was obtained from Merck or Planta (Vienna, Austria).

Analytical thin layer chromatography (TLC) was performed using Merck silica gel 60 F_{254} aluminium plates. Carborane-containing compounds were visualized by spraying with an acidified $PdCl_2$ stain (~1% *w/v* in 1 M HCl) and heating until black spots appeared.

Instrumentation

All NMR spectra were recorded at 300 K on either a Bruker AVANCE 300 (^{1}H at 300 MHz, ^{11}B at 96 MHz and ^{13}C at 75 MHz), Bruker AVANCE III 400 (^{1}H at 400 MHz, ^{11}B at 128 MHz), Bruker AVANCE III 500 or Bruker NEO 500 (^{1}H at 500 MHz, ^{11}B at 160 MHz and ^{13}C at 125 MHz). Signals (δ) are reported in ppm. ^{1}H and ^{13}C NMR spectra were referenced to the residual solvent peaks. ^{11}B{^{1}H} and ^{11}B spectra were referenced automatically by the spectrometer software according to the unified chemical shift scale by means of the lock frequency of the solvent. Peak multiplicities have been abbreviated as: s (singlet), d (doublet), dd (doublet of doublets), ddd (doublet of doublets of doublets), t (triplet), tt (triplet of triplets), dt (doublet of triplets), td (triplet of doublets), q (quartet), sx (sextet), m (multiplet) and br (broad).

Low-resolution mass spectra (LRMS) were recorded using atmospheric pressure chemical ionisation (APCI) on an AmaZon SL equipped with a Finnigan LCQ ion trap.

Synthesis

1-Triphenylsilyl-1,7-dicarba-*closo*-dodecaborane(12) (**24**)

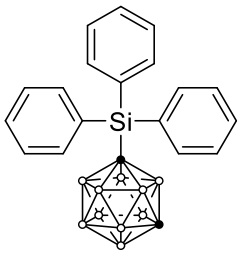

closo-1,7-Carborane (98.9 mg, 686 μmol) was added to an oven-dried, two-neck flask and the flask was evacuated and back-filled with nitrogen three times. The solids were dissolved in anhydrous THF (2 mL) and the resultant solution was cooled to -78 °C, to which *n*-butyllithium (1.6 M in hexanes, 0.47 mL, 0.75 mmol) was added dropwise. The solution was stirred at the same temperature for 15 min before being warmed to 0 °C, at which point a solution of triphenylchlorosilane (206.1 mg, 699 μmol) in THF (2 mL) was added. The solution was stirred at RT for 16 h, during which it turned pale yellow. The solvent was removed *in vacuo* and petroleum benzine (5 mL) was added to the residue. The precipitate was removed by filtration, washed with petroleum benzine (5 mL) and the combined filtrates were reduced *in vacuo*. The crude product was loaded onto Celite filter-aid and purified by means of flash chromatography on silica (100% petroleum benzine to 15% DCM in petroleum benzine) to afford *closo*-1,7-carborane (37% recovery) and give **24** (144 mg, 52%) as colourless prisms. **^{1}H NMR** (300 MHz, $CDCl_3$): δ 7.64 (d, J = 7.4 Hz, 6H, Ar–H), 7.48 (t, J = 7.4 Hz, 3H, Ar–H), 7.39 (t, J = 7.4 Hz, 6H, Ar–H), 3.36–1.08 (br m, 10H, B–H), 2.94 (s, 1H, C_{cage}–H); **^{11}B{^{1}H} NMR** (96 MHz, $CDCl_3$): δ -3.9 (2B), -8.9 (2B), -10.6 (2B), -11.7 (2B), -14.8 (2B).

1-Carboxy-7-triphenylsilyl-1,7-dicarba-*closo*-dodecaborane(12) (**25**)

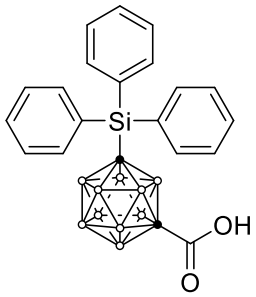

Compound **24** (106 mg, 263 μmol) was added to an oven-dried, two-neck flask and the flask was evacuated and back-filled with nitrogen three times. The solids were dissolved in anhydrous THF (2.5 mL) and the resultant solution was cooled to -78 °C, to which *n*-butyllithium (1.5 M in hexanes, 450 μL, 675 μmol) was added dropwise. The solution was stirred at the same temperature for 15 min before carbon dioxide gas was bubbled into the reaction mixture. The solution was stirred vigorously -78 °C for 1 h and then for a further 30 min after warming to RT. Upon completion, the solvent was removed *in vacuo* and water (10 mL) was added to the residue. The aqueous layer was extracted with petroleum benzine (2 × 5 mL) and the extracts combined to recover any unreacted starting material. The aqueous layer was acidified (pH 1–2) with 3 M HCl to precipitate the product, which was extracted with ether (3 × 5 mL). The combined organic extracts were dried over sodium sulfate, filtered, and reduced *in vacuo.* The residue was redissolved in toluene (1 mL), reduced *in vacuo* and the solids dried over P_2O_5 to give **25** (115 mg, 98%) as colourless needles. **^{1}H NMR** (500 MHz, $CDCl_3$): δ 7.64 (d, *J* = 7.4 Hz, 6H, Ar–H), 7.48 (t, *J* = 7.4 Hz, 3H, Ar–H), 7.40 (t, *J* = 7.4 Hz, 6H, Ar–H), 5.97 (br s, 1H, COOH), 3.51–1.52 (br m, 10H, B–H); **^{11}B{^{1}H} NMR** (160 MHz, $CDCl_3$): δ -2.1 (1B), -4.0 (1B), -9.1 (4B), -10.5 (2B), -13.4 (2B); **^{13}C{^{1}H} NMR** (125 MHz, $CDCl_3$): δ 166.9, 137.4, 130.7 (two overlapping signals), 127.9, 73.5, 64.0; **LRMS (APCI)**: *m*/*z* 446.43 $[M - H]^-$ (calcd for $C_{21}H_{26}B_{10}O_2Si$ 446.26).

1-Formyl-7-triphenylsilyl-1,7-dicarba-*closo*-dodecaborane(12) (**26**)

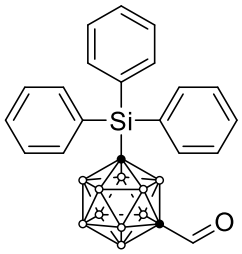

Compound **24** (79.9 mg, 198 μmol) was added to an oven-dried, two-neck flask and the flask was evacuated and back-filled with nitrogen three times. The solids were dissolved in anhydrous diethyl ether (5 mL) and the resultant solution was cooled to -78 °C, to which *n*-butyllithium (1.6 M in hexanes, 150 μL, 240 μmol) was added dropwise. The solution was stirred at the same temperature for 15 min before methyl formate (50 μL, 0.81 mmol) was added to the reaction mixture in one portion. Stirring was continued for 1 h at -78 °C before the reaction was quenched slowly with 1 M HCl (1 mL) and allowed to warm to RT. The ether was removed *in vacuo* and water (4 mL) was added to the residue. The aqueous layer was extracted with petroleum benzine (4 × 5 mL) and the combined extracts were dried over sodium sulfate, filtered and reduced *in vacuo*. The crude product was loaded onto Celite filter-aid and purified by means of flash chromatography on silica (100% petroleum benzine to 20% DCM in petroleum benzine) to give **26** (58.9 mg, 69%) as a colourless oil which solidified on standing into a waxy, colourless solid. **^{1}H NMR** (500 MHz, $CDCl_3$): δ 8.98 (s, 1H, C<u>H</u>O), 7.64 (d, *J* = 7.4 Hz, 6H, Ar–<u>H</u>), 7.49 (t, *J* = 7.4 Hz, 3H, Ar–<u>H</u>), 7.41 (t, *J* = 7.4 Hz, 6H, Ar–<u>H</u>), 3.42–1.62 (br m, 10H, B–<u>H</u>); **^{11}B{^{1}H} NMR** (160 MHz, $CDCl_3$): δ -3.4 (2B), -8.7 (2B), -10.1 (2B), -10.5 (2B), -14.3 (2B); **^{13}C{^{1}H} NMR** (125 MHz, $CDCl_3$): δ 186.1, 137.4, 130.7, 130.6, 128.0, 80.2, 64.9; **LRMS (APCI)**: *m*/*z* 430.42 $[M - H]^-$ (calcd for $C_{21}H_{26}B_{10}OSi$ 430.27).

1-((2-Hydroxyphenyl)imino)methyl-7-triphenylsilyl-1,7-dicarba-*closo*-dodecaborane(12) (**27**)

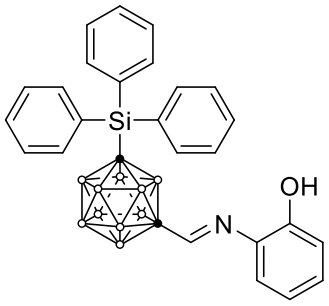

Compound **26** (24.8 mg, 57.6 μmol), 2-aminophenol (6.3 mg, 58 μmol) and 3Å molecular sieves (50 mg) was added to an oven-dried, Schlenk tube and the tube was evacuated and back-filled with nitrogen three times. The solids were suspended in anhydrous toluene (1 mL) and the reaction was stirred at 100 °C for 12 h. The yellow solution was allowed to cool to RT, filtered through Celite filter-aid and washed through with petroleum benzine (3 × 3 mL). The filtrate was reduced *in vacuo* to give **27** (25.0 mg, 83%) as an orange oil which was used without further purification. **^{1}H NMR** (300 MHz, $CDCl_3$): δ 7.74–7.61 (m, 6H, Ar–H), 7.52–7.35 (m, 9H, Ar–H), 7.29–7.10 (m, 2H, Ar–H), 7.06–6.91 (m, 1H, Ar–H), 6.85–6.74 (m, 1H, Ar–H), 3.71–1.13 (br m, 10H, B–H). The OH signal was not observed likely due to proton exchange, and the imine CH signal was not observed likely due to overlap with aromatic protons; **^{11}B{^{1}H} NMR** (96 MHz, $CDCl_3$): δ -3.3 (2B), -8.7 (3B), -10.3 (3B), -14.1 (2B).

9-Iodo-1,2-dicarba-*closo*-dodecaborane(12) (**30**)

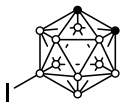

closo-1,2-Carborane (111 mg, 770 μmol) and iodine (97.7 mg, 385 μmol) were dissolved in acetic acid (10 mL) and a mixture of concentrated nitric acid and concentrated sulfuric acid (1:1 *v/v*, 10 mL) was added. The dark purple solution was stirred at 60 °C for 15 min, during which time the solution decolourised. The solution was cooled to 0 °C and the reaction mixture was poured into ice water (20 mL). The solids were collected by filtration, washed thoroughly with water, and dried *in vacuo* to give **30** (192 mg, 92%) as a colourless powder. **^{1}H NMR** (300 MHz, $CDCl_3$): δ 3.87 (s, 1H, C_{cage}–H), 3.66 (s, 1H, C_{cage}–H), 3.59–1.22 (br m, 9H, B–H); **^{11}B{^{1}H} NMR** (96 MHz, $CDCl_3$): δ -0.9 (1B), -7.4 (2B), -12.9 (2B), -13.4 (2B), -14.7 (2B), -16.6 (1B). The characterisation data matches that reported in the literature.[134]

9,12-Diiodo-1,2-dicarba-*closo*-dodecaborane(12) (**34**)

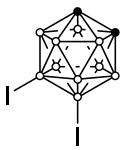

Triflic acid (approx. 30 μL, 0.34 mmol) was added to *closo*-1,2-carborane (108 mg, 746 μmol) and NIS (354 mg, 1.57 mmol) dissolved in HFIP (1 mL) and the dark brown mixture was stirred vigorously at RT for 24 h. The solvent was evaporated and water was added to the reaction residue. The solids were collected by filtration, washed thoroughly with water, and dried *in vacuo* to give **34** (274 mg, 93%) as a colourless powder. **^{1}H NMR** (300 MHz, $CDCl_3$): δ 3.97 (s, 2H, C_{cage}–H), 3.84–1.38 (br m, 8H, B–H); **^{11}B{^{1}H} NMR** (96 MHz, $CDCl_3$): δ -5.7 (2B), -12.9 (4B), -14.3 (4B). The characterisation data matches that reported in the literature.[134]

8,9,10,12-Tetraiodo-1,2-dicarba-*closo*-dodecaborane(12) (**181**)

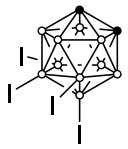

closo-1,2-Carborane (253 mg, 1.76 mmol) and iodine (895 mg, 3.53 mmol) were added to a thick-walled glass vessel and dissolved in acetic acid (30 mL). A mixture of concentrated nitric acid and concentrated sulfuric acid (1:1 *v/v*, 30 mL) was added and the vessel was sealed with a PTFE screw top. The dark purple solution was stirred at 120 °C for 3 h, which soon lightened to a pale-red suspension before eventually turning an orange colour. The solution was cooled to 0 °C, the vessel was opened and the reaction mixture was poured into ice water (60 mL). The solids were collected by filtration, washed thoroughly with water, and dried *in vacuo* to give **181** (1.08 g, 95%) as a colourless powder. **^{1}H NMR** (300 MHz, $CDCl_3$): δ 5.57 (s, 2H, C_{cage}–H), 4.51–1.79 (br m, 6H, B–H); **^{11}B{^{1}H} NMR** (96 MHz, $CDCl_3$): δ -9.3 (2B), -11.8 (4B), -15.5 (2B), -18.7 (2B). The characterisation data matches that reported in the literature.[210]

9-Bromo-1,2-dicarba-*closo*-dodecaborane(12) (**91**)

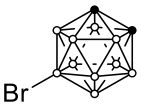

Triflic acid (~5 μL) was added to *closo*-1,2-carborane (84.4 mg, 585 μmol) and NBS (108 mg, 607 μmol) dissolved in HFIP (5 mL) and the mixture was stirred at RT for 1 h. The solvent was recovered from the reaction mixture by distillation at atmospheric pressure and water was added to the reaction residue. The solids were collected by filtration, washed thoroughly with water, and dried *in vacuo* to give **91** (123 mg, 94%) as a colourless, microcrystalline solid. **^{1}H NMR** (500 MHz, $CDCl_3$): δ 3.61 (s, 2H, C_{cage}–H), 3.11–1.47 (br m, 9H, B–H); **^{11}B{^{1}H} NMR** (160 MHz, $CDCl_3$): δ 0.0 (1B), -1.7 (1B), -8.4 (2B), -13.5 (2B), -14.5 (2B), -15.7 (2B). The characterisation data matches that reported in the literature.[134]

9-Iodo-1,7-dicarba-*closo*-dodecaborane(12) (**54**)

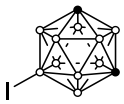

closo-1,7-Carborane (102 mg, 709 μmol) and iodine (90.8 mg, 358 μmol) were dissolved in acetic acid (10 mL) and a mixture of concentrated nitric acid and concentrated sulfuric acid (1:1 *v/v*, 10 mL) was added. The dark purple solution was stirred at 60 °C for 15 min, during which time the solution decolourised. The solution was cooled to 0 °C and the reaction mixture was poured into ice water (20 mL). The solids were collected by filtration, washed thoroughly with water, and dried *in vacuo* to give **54** (181 mg, 94%) as a colourless powder. **^{1}H NMR** (300 MHz, $CDCl_3$): δ 3.76–1.16 (br m, 9H, B–H), 3.04 (s, 2H, C_{cage}–H); **^{11}B{^{1}H} NMR** (96 MHz, $CDCl_3$): δ -5.4 (2B), -8.2 (1B), -11.8 (2B), -13.0 (2B), -16.8 (1B), -18.9 (1B), -23.5 (1B). The characterisation data matches that reported in the literature.[134]

9,10-Diiodo-1,7-dicarba-*closo*-dodecaborane(12) (**43**)

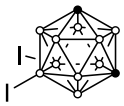

closo-1,7-Carborane (256 mg, 1.77 mmol) and iodine (450 mg, 1.77 mmol) were dissolved in acetic acid (40 mL) and a mixture of concentrated nitric acid and concentrated sulfuric acid (1:1 *v/v*, 30 mL) was added. The dark purple solution was stirred at 100 °C for 15 min, during which time the iodine completely dissolved and the solution lightened to a pale-orange colour. The solution was cooled to 0 °C and the reaction mixture was poured into ice water (70 mL). The solids were collected by filtration, washed thoroughly with water, and dried *in vacuo* to give **43** (670 mg, 96%) as a colourless powder. **^{1}H NMR** (500 MHz, $CDCl_3$): δ 3.82–2.07 (br m, 8H, B–H), 3.15 (s, 2H, C_{cage}–H); **^{11}B{^{1}H} NMR** (160 MHz, $CDCl_3$): δ -4.2 (2B), -11.9 (4B), -18.7 (2B), -20.6 (2B); **^{11}B NMR** (160 MHz, $CDCl_3$): δ -4.2 (d, J = 171 Hz, 2B), -11.9 (d, J = 171 Hz, 4B), -18.7 (d, J = 185 Hz, 2B), -20.6 (s, 2B). The characterisation data matches that reported in the literature.[134]

9-Bromo-1,7-dicarba-*closo*-dodecaborane(12) (**182**)

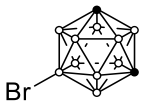

Triflic acid (approx. 50 μL, 0.6 mmol) was added to *closo*-1,7-carborane (509 mg, 3.53 mmol) and NBS (660 mg, 3.71 mmol) dissolved in HFIP (30 mL) and the mixture was stirred at RT for 1 h. The solvent was recovered from the reaction mixture by distillation at atmospheric pressure and water was added to the reaction residue. The precipitate was collected by filtration, washed thoroughly with water, and dried *in vacuo* to give **182** (732 mg, 93%) as a colourless, microcrystalline solid. **^{1}H NMR** (500 MHz, $CDCl_3$): δ 3.35–1.98 (br m, 9H, B–H), 3.00 (s, 1H, C_{cage}H); **^{11}B{^{1}H} NMR** (160 MHz, $CDCl_3$): δ -6.1 (3B), -9.2 (1B), -12.7 (2B), -14.0 (2B), -17.8 (1B), -21.1 (1B). The characterisation data matches that reported in the literature.[134]

8-Bromo-9,12-diiodo-1,2-dicarba-*closo*-dodecaborane(12) (**33**)

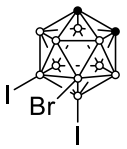

Triflic acid (approx. 30 μL, 0.34 mmol) was added to compound **34** (123 mg, 311 μmol) and NBS (55.6 mg, 312 μmol) dissolved in HFIP (1 mL) and the dark orange/brown mixture was stirred vigorously at RT for 24 h. The solvent was evaporated and water was added to the reaction residue. The aqueous layer was extracted with DCM (3 × 5 mL) and the combined organic extracts were dried over sodium sulfate, filtered and reduced *in vacuo* before being loaded onto Celite filter-aid. The crude product was purified by means of flash chromatography on silica (33% DCM in petroleum benzine) to give recovered **34** (40.6 mg, 33%) and **33** (92.4 mg, 63%) as a colourless, microcrystalline solid. **^{1}H NMR** (500 MHz, $CDCl_3$): δ 4.05 (s, 2H, C_{cage}–H), 3.62–2.06 (br m, 7H, B–H); **^{11}B{^{1}H} NMR** (160 MHz, $CDCl_3$): δ -4.1 (1B), -6.6 (1B), -12.1 (2B), -12.7 (2B), -13.9 (2B), -15.6 (1B), -18.5 (1B); **^{11}B NMR** (160 MHz, $CDCl_3$): δ -4.1 (s, 1B), -6.6 (d, J = 160.2 Hz, 1B), -12.1 (s, 2B), -12.7 (d, J = 192 Hz, 2B), -13.9 (d, J = 187 Hz, 2B), -15.6 (d, J = 182 Hz, 2B), -18.5 (d, J = 185 Hz, 2B); **^{13}C{^{1}H} NMR** (125 MHz, $CDCl_3$): δ 50.5; **LRMS (APCI)**: *m*/*z* 473.98 $[M]^-$ (calcd for $C_2H_9B_{10}BrI_2$ 473.89).

8-Bromo-1,2-dicarba-*closo*-dodecaborane(12) (**32**)

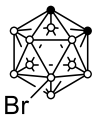

Compound **33** (74.0 mg, 156 μmol), triphenylphosphine (16.4 mg, 62.5 μmol), zinc dust (10.7 mg, 164 μmol), $[NiCl_2(PPh_3)_2]$ (10.3 mg, 15.7 μmol) and caesium carbonate (102.6 mg, 315 μmol) were placed in an oven-dried Schlenk tube and the vessel was evacuated and back-filled with nitrogen three times. Anhydrous THF (2 mL) was added to the vessel and the tube was sealed with a J. Young valve under a counter flow of nitrogen. The pale-green solution quickly changed colour to a deep-red, and the reaction was stirred at RT under irradiation with UV light (365 nm, 20 W LED, 1 cm away) for 48 h. After this time, fresh portions of triphenylphosphine, zinc dust and $[NiCl_2(PPh_3)_2]$ were added to the tube and the reaction was irradiated for a further 48 h. Upon completion, the reaction mixture was diluted with DCM (3 mL), filtered, reduced *in vacuo* and loaded onto Celite filter-aid. The crude product was purified by means of flash chromatography on silica (100% petroleum benzine to 20% DCM in petroleum benzine) to give **32** (32.7 mg, 95%) as a colourless powder. **^{1}H NMR** (500 MHz, $CDCl_3$): δ 3.62 (s, 2H, C_{cage}–H), 3.28–1.43 (br m, 9H, B–H); **^{11}B{^{1}H} NMR** (160 MHz, $CDCl_3$): δ -1.1 (2B, B(9/12)), -5.4 (1B, B8), -10.0 (1B, B10), -13.1 (2B, B(4/7)), -14.3 (2B, B(5/11)), -14.8 (1B, B3), -19.2 (1B, B6); **^{11}B NMR** (160 MHz, $CDCl_3$): δ -1.1 (d, J = 153 Hz, 2B, B(9/12)), -5.4 (s, 1B, B8), -10.0 (d, J = 154 Hz, 1B, B10), -13.1 (d, J = 170 Hz, 1B, B(4/7)), -14.3 (d, J = 174 Hz, 2B, B(5/11)), -14.8 (d, J = 189 Hz, 1B, B3), -19.2 (d, J = 180 Hz, 1B, B6); **^{13}C{^{1}H} NMR** (125 MHz, $CDCl_3$): δ 53.3; **LRMS (APCI)**: *m*/*z* 222.16 $[M - H]^-$ (calcd for $C_2H_{11}B_{10}Br$ 222.10).

5-Bromo-9,10-diiodo-1,7-dicarba-*closo*-dodecaborane(12) (**42**)

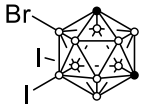

Triflic acid (0.5 mL) was added to a mixture of compound **43** (49.7 mg, 126 μmol), NBS (24.3 mg, 137 μmol) at 0 °C. The deep-red/brown solution was heated at 60 °C for 4 h, during which time it decolourised and solids precipitated. The solution was cooled to 0 °C and the reaction mixture was slowly added into ice water (5 mL). The solids were collected by filtration, washed thoroughly with water, and dried at the pump before being loaded onto Celite filter-aid. The crude product was purified by means of flash chromatography on silica (10% DCM to 20% DCM in petroleum benzine) to give and **42** (40.7 mg, 68%) as a colourless powder. **^{1}H NMR** (500 MHz, $CDCl_3$): δ 3.90–2.14 (br m, 7H, B–H), 3.61 (s, 1H, C_{cage}–H), 3.19 (s, 1H, C_{cage}–H); **^{11}B{^{1}H} NMR** (160 MHz, $CDCl_3$): δ -2.9 (1B), -4.4 (1B), -10.6 (2B), -12.7 (2B), -18.8 (4B); **^{11}B NMR** (160 MHz, $CDCl_3$): δ -2.9 (s, 1B), -4.4 (d, J = 172 Hz, 1B), -10.6 (d, J = 175 Hz, 2B), -12.7 (d, J = 172 Hz, 2B), -18.7 (d, J = 182 Hz, 2B), -19.0 (s, 2B); **^{13}C{^{1}H} NMR** (125 MHz, $CDCl_3$): δ 58.0, 50.4; **LRMS (APCI)**: *m*/*z* 473.90 $[M - H]^-$ (calcd for $C_2H_9B_{10}BrI_2$ 473.89).

5-Bromo-1,7-dicarba-*closo*-dodecaborane(12) (**20**)

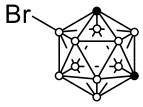

Compound **42** (34.2 mg, 72.0 μmol), triphenylphosphine (11.5 mg, 43.8 μmol), zinc dust (5.8 mg, 89 μmol), $[NiCl_2(PPh_3)_2]$ (7.1 mg, 11 μmol) and caesium carbonate (47.4 mg, 145 μmol) were placed in an oven-dried Schlenk tube and the vessel was evacuated and back-filled with nitrogen three times. Anhydrous THF (2 mL) was added to the vessel and the tube was sealed with a J. Young valve under a counter flow of nitrogen. The pale-green solution quickly changed colour to a deep red, and the reaction was stirred at RT under irradiation with UV light (365 nm, 20 W LED, 1 cm away) for 48 h. After this time, fresh portions of triphenylphosphine, zinc dust and $[NiCl_2(PPh_3)_2]$ were added to the tube and the reaction was irradiated for a further 48 h. Upon completion, the reaction mixture was diluted with DCM (3 mL), filtered, reduced *in vacuo* and loaded onto Celite filter-aid. The crude product was purified by means of flash chromatography on silica (100% petroleum benzine) to give **20** (15.2 mg, 95%) as a colourless powder. **^{1}H NMR** (500 MHz, $CDCl_3$): δ 3.31 (s, 1H, C_{cage}–H), 3.07–1.61 (br m, 9H, B–H), 2.95 (s, 1H, C_{cage}–H); **^{11}B{^{1}H} NMR** (160 MHz, $CDCl_3$): δ -4.8 (1B, B5), -6.8 (1B, B12), -9.9 (2B, B(9/10)), -11.7 (2B, B(4/6)), -13.8 (2B, B(8/11)), -17.0 (2B, B(2/3)); **^{11}B NMR** (160 MHz, $CDCl_3$): δ -4.8 (s, 1B, B5), -6.8 (d, J = 166 Hz, 1B, B12), -9.8 (d, J = 153 Hz, 2B, B(9/10)), -11.7 (d, J = 170 Hz, 2B, B(4/6)), -13.8 (d, J = 167 Hz, 2B, B(8/11)), -17.0 (d, J = 183 Hz, 2B, B(2/3)); **LRMS (APCI)**: *m/z* 222.23 $[M - H]^-$ (calcd for $C_2H_{11}B_{10}Br$ 222.10).

Tetrabutylammonium 7,9-dicarba-*nido*-dodecahydridoundecaborate(1-) (**50**)

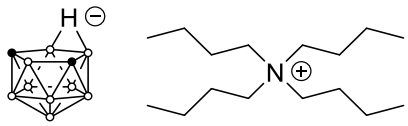

closo-1,7-Carborane (160 mg, 1.11 mmol) was dissolved in a THF solution of tetrabutylammonium fluoride (1 M, 5.0 mL, 5.0 mmol), forming a clear, light-yellow solution. The reaction was stirred at RT for 4 h, at which point TLC showed complete conversion of starting material. DCM (15 mL) was added, and the organic phase was washed with water (3 × 15 mL). The organic layer was dried over sodium sulfate, filtered, diluted with *n*-heptane (5 mL) and reduced *in vacuo*. The resulting waxy solid was suspended in petroleum benzine (5 mL) and the liquids decanted off. The product was dried under vacuum over P_2O_5 to give **50** (410 mg, 98%) as a free-flowing, colourless powder. **^{1}H NMR** (300 MHz, $CDCl_3$): δ 3.19 (m, 8H, TBA-C$\underline{H}_2$), 3.00–-0.50 (br m, 8H, B–$\underline{H}$), 1.63 (m, 8H, TBA-C$\underline{H}_2$), 1.44 (sx, J = 7.3 Hz, 8H, TBA-C$\underline{H}_2$), 1.32 (s, 2H, C_{cage}–$\underline{H}$), 1.01 (t, J = 7.3 Hz, 12H, TBA-C$\underline{H}_3$), -2.15 (br s, 1H, B–$\underline{H}$–B); **^{11}B{^{1}H} NMR** (160 MHz, $CDCl_3$): δ -4.6 (2B), -5.9 (1B), -21.6 (2B), -22.6 (2B), -34.3 (1B), -35.4 (1B). The characterisation data matches that reported in the literature.[211]

Tetrabutylammonium 8-iodo-7,9-dicarba-*nido*-undecahydridoundecaborate(1-) (**49**)

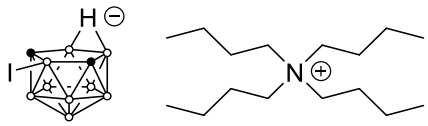

Compound **50** (220 mg, 585 μmol) and anhydrous iron(III) chloride (99.2 mg, 612 μmol) were added to an oven-dried Schlenk tube which was evacuated and backfilled with nitrogen three times. Anhydrous DCM (2.5 mL) was added, creating a clear, yellow-green solution. Iodine (149.7 mg, 591 μmol) was then added, and the dark-purple solution was stirred at 40 °C for 4 h. Over the course of the reaction, the solution lightened and black solids precipitated. The solution was diluted with DCM (5 mL), washed with a 1 M NaOH solution (5 mL) and then with a 1 M HCl solution (5 mL). The organic layer was dried over sodium sulfate, filtered and reduced *in vacuo* before being loaded onto Celite filter-aid. The crude product was purified by means of flash chromatography on silica (100% $CHCl_3$ to 5% MeOH in $CHCl_3$) to give **49** (281 mg, 96%) as a colourless powder. **^{1}H NMR** (500 MHz, acetone-d_6): δ 3.45 (m, 8H, TBA-C$\underline{H}_2$), 2.85–-0.10 (br m, 8H, B–$\underline{H}$), 1.84 (m, 8H, TBA-C$\underline{H}_2$), 1.50 (s, 2H, C_{cage}–$\underline{H}$), 1.45 (sx, J = 7.4 Hz, 8H, TBA-C$\underline{H}_2$), 0.99 (t, J = 7.4 Hz, 12H, TBA-C$\underline{H}_3$), -2.27 (br sep, 1H, B–$\underline{H}$–B); **^{11}B{^{1}H} NMR** (160 MHz, acetone-d_6): δ -4.8 (2B), -15.4 (1B), -19.4 (2B), -22.4 (2B), -33.0 (1B), -36.0 (1B); **^{11}B NMR** (160 MHz, acetone-d_6): δ -4.8 (d, J = 149.8 Hz, 2B), -15.4 (s, 1B), -19.4 (d, J = 149.9 Hz, 2B), -22.4 (dd, $J_{B–H}$ = 133.3, $J_{B–H–B}$ = 55 Hz, 2B), -33.0 (d, J = 142.6 Hz, 1B), -36.0 (d, J = 140.6 Hz, 1B). The characterisation data matches that reported in the literature.[129]

Tetrabutylammonium 5-bromo-8-iodo-7,9-dicarba-*nido*-decahydridoundecaborate(1-) (**51**)

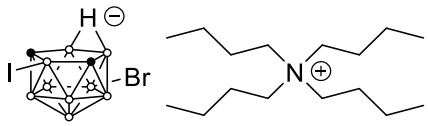

Compound **49** (31.6 mg, 62.8 μmol) and anhydrous iron(III) chloride (12.2 mg, 75.2 μmol) were added to an oven-dried Schlenk tube which was evacuated and backfilled with nitrogen three times. Anhydrous DCM (1 mL) was added, creating a clear, yellow-green solution, which was cooled to -78 °C. A solution of bromine (10.1 mg, 63.2 μmol) in DCM (0.5 mL) was then added dropwise, and the solution was allowed to warm to RT over 30 min. The solution was diluted with DCM (5 mL), washed with a 1 M NaOH solution (5 mL) and then with a 1 M HCl solution (5 mL). The organic layer was dried over sodium sulfate, filtered and reduced *in vacuo* to give a crude mixture of **51** and its isomer(s) (30.2 mg, 83%) as a colourless, gummy solid. Characterisation data follows for the major product, which was identified as the title compound. **^{1}H NMR** (500 MHz, $CDCl_3$): δ 3.01 (m, 8H, TBA-C$\underline{H}_2$), 1.78 (m, 8H, TBA-C$\underline{H}_2$), 1.42 (sx, J = 7.4 Hz, 8H, TBA-C$\underline{H}_2$), 0.99 (t, J = 7.4 Hz, 12H, TBA-C$\underline{H}_3$), -1.40 (br s, 1H, B–$\underline{H}$–B). C_{cage}–$\underline{H}$ not observed, B–$\underline{H}$ signals indistinguishable from baseline; **^{11}B{^{1}H} NMR** (160 MHz, $CDCl_3$): δ -2.9 (2B), -14.9 (1B), -19.0 (2B), -19.8 (2B), -24.1 (1B), -30.5 (1B); **^{11}B NMR** (160 MHz, $CDCl_3$): δ -2.9 (d, J = 153 Hz, 2B), -14.9 (s, 1B), -19.0 (d, J = 147 Hz, 2B), -19.8 (dd, $J_{B–H}$ = 119 Hz, $J_{B–H–B}$ = 54 Hz, 2B), -24.1 (s, 1B), -30.5 (d, J = 144 Hz, 1B).

Tetrabutylammonium 5,8-diiodo-7,9-dicarba-*nido*-decahydridoundecaborate(1-) (**59**)

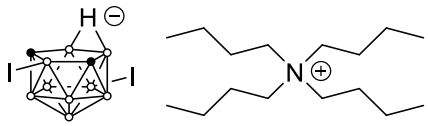

Compound **49** (40.3 mg, 80.0 μmol) and anhydrous iron(III) chloride (16.7 mg, 103 μmol) were added to an oven-dried Schlenk tube which was evacuated and backfilled with nitrogen three times. Anhydrous DCM (1 mL) was added, creating a clear, yellow-green solution, which was cooled to -78 °C. Iodine (20.4 mg, 80.4 μmol) was then added, and the dark purple solution was stirred at 40 °C for 6 h. Over the course of the reaction, the solution lightened and black solids precipitated. The solution was diluted with DCM (5 mL), washed with a 1 M NaOH solution (5 mL) and then with a 1 M HCl solution (5 mL). The organic layer was dried over sodium sulfate, filtered and reduced *in vacuo* before being loaded onto Celite filter-aid. The crude product was purified by means of flash chromatography on silica (50% DCM in petroleum benzine to 100% DCM) to give **59** (45.9 mg, 91%) as an off-white powder. **^{1}H NMR** (500 MHz, $CDCl_3$): δ 3.19 (m, 8H, TBA-C$\underline{H}_2$), 1.83 (s, 2H, C_{cage}–$\underline{H}$), 1.66 (m, 8H, TBA-C$\underline{H}_2$), 1.48 (sx, J = 7.3 Hz, 8H, TBA-C$\underline{H}_2$), 1.05 (t, J = 7.3 Hz, 12H, TBA-C$\underline{H}_3$), -1.30 (br s, 1H, B–$\underline{H}$–B). B–$\underline{H}$ signals indistinguishable from baseline; **^{11}B{^{1}H} NMR** (160 MHz, acetone-d_6): δ -2.8 (2B), -14.4 (1B), -18.3 (2B), -19.2 (2B), -29.7 (1B), -40.2 (1B); **^{11}B NMR** (160 MHz, acetone-d_6): δ -2.8 (d, J = 157 Hz, 2B), -14.4 (s, 1B), -18.3 (d, J = 154 Hz, 2B), -19.2 (dd, $J_{B–H}$ = 134 Hz, $J_{B–H–B}$ = 53 Hz, 2B), -29.7 (d, J = 151 Hz, 1B), -40.2 (s, 1B).

Tetrabutylammonium 1,5-diiodo-7,9-dicarba-*nido*-decahydridoundecaborate(1-) (**57**)

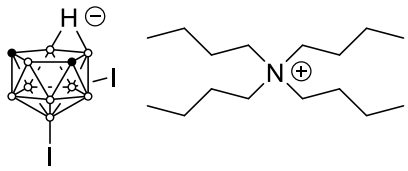

Compound **43** (49.9 mg, 126 μmol) was dissolved in a THF solution of tetrabutylammonium fluoride (1 M, 0.65 mL, 650 μmol), forming a clear, light-yellow solution. The reaction was stirred at RT for 1 h, at which point TLC showed complete conversion of starting material. DCM (10 mL) was added, and the organic phase was washed with water (3 × 10 mL). The organic layer was dried over sodium sulfate, filtered, diluted with *n*-heptane (3 mL) and reduced *in vacuo*. The resulting waxy solid was suspended in petroleum benzine (3 mL) and the liquids decanted off. The product was dried under vacuum over P_2O_5 to give **57** (75.0 mg, 95%) as a free-flowing, colourless powder. **^{1}H NMR** (300 MHz, $CDCl_3$): δ 3.8–0.2 (br m, 7H, B–H), 3.27 (m, 8H, TBA-CH_2), 1.66 (m, 8H, TBA-CH_2), 1.46 (sx, *J* = 7.3 Hz, 8H, TBA-CH_2), 1.02 (t, *J* = 7.3 Hz, 12H, TBA-CH_3), -1.08 (br s, 1H, B–H–B), C_{cage}–H not observed likely due to signal overlap; **^{11}B{^{1}H} NMR** (160 MHz, $CDCl_3$): δ -1.6 (2B), -4.3 (1B), -18.7 (2B), -19.0 (2B), -33.2 (1B), -37.0 (1B); **^{11}B NMR** (160 MHz, $CDCl_3$): δ -1.6 (d, *J* = 159 Hz, 2B), -4.3 (d, *J* = 140 Hz), -18.7 (d, *J* = 144 Hz), -19.0 (dd, *J* value not calculated due to signal overlap, 2B), -33.2 (s, 1B), -37.0 (s, 1B).

Tetrabutylammonium 1,6,8-triiodo-7,9-dicarba-*nido*-nonahydridoundecaborate(1-) (**58**)

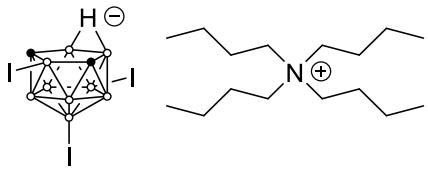

Compound **57** (33.7 mg, 53.7 μmol) and mercury(II) chloride (15.9 mg, 58.6 μmol) were added to an oven-dried Schlenk tube which was evacuated and backfilled with nitrogen three times. Anhydrous DCM (1 mL) was added, creating a clear, yellow-green solution, which was cooled to -78 °C. Iodine (13.7 mg, 54.0 μmol) was then added, the tube was sealed with a J. Young valve and the dark purple solution was stirred at 40 °C for 4 h. Over the course of the reaction, the solution became almost colourless. The solution was filtered through Celite filter-aid, washed through with DCM (3 × 1 mL) and the filtrate was reduced *in vacuo*. The crude product was being loaded onto Celite filter-aid before being purified by means of flash chromatography on silica (50% DCM in petroleum benzine to 100% DCM) to give an inseparable mixture of **58** and its isomer(s) (31.8 mg, 79%) as an off-white powder. Characterisation data follows for the major product, which was identified as the title compound. **^{11}B{^{1}H} NMR** (160 MHz, acetone-d_6): δ 4.9 (1B), -4.8 (2B), -17.3 (2B), -19.0 (2B), -33.4 (1B), -38.6 (1B); **^{11}B NMR** (160 MHz, acetone-d_6): δ 4.9 (s, 1B), -4.8 (d, J = 160 Hz, 2B), -17.3 (d, J = 159 Hz, 2B), -19.0 (dd, $J_{B–H}$ = 129 Hz, $J_{B–H–B}$ = 48 Hz, 2B), -33.4 (s, 1B), -38.6 (s, 1B).

Tetrabutylammonium 8-bromo-7,9-dicarba-*nido*-undecahydridoundecaborate(1-) (**64**)

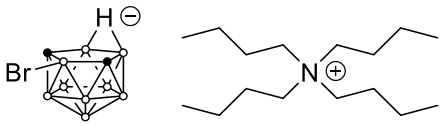

Compound **50** (19.2 mg, 51.1 μmol) was dissolved in acetonitrile (1 mL) in air and the solution was cooled to 0 °C. NBS (9.6 mg, 54 μmol) was added and the clear yellow solution was stirred at RT for 6 h. The now nearly colourless solution was reduced *in vacuo* and loaded onto Celite filter aid. The crude product was purified by means of flash chromatography on silica (50% DCM in petroleum benzine to 100% DCM) to give **64** (22.1 mg, 95%) as a colourless powder. **^{1}H NMR** (500 MHz, acetone-d_6): δ 3.44 (m, 8H, TBA-C$\underline{H}_2$), 2.73–-0.25 (br m, 8H, B–$\underline{H}$), 1.83 (m, 8H, TBA-C$\underline{H}_2$), 1.43 (sx, J = 7.4 Hz, 8H, TBA-C$\underline{H}_2$), 1.39 (s, 2H, C_{cage}–$\underline{H}$), 0.98 (t, J = 7.4 Hz, 12H, TBA-C$\underline{H}_3$), -2.21 (br sep, 1H, B–$\underline{H}$–B); **^{11}B{^{1}H} NMR** (160 MHz, $CDCl_3$): δ -2.6 (1B), -6.8 (2B), -19.8 (2B), -22.4 (2B), -33.1 (1B), -37.1 (1B); **^{11}B NMR** (160 MHz, $CDCl_3$): δ -2.6 (s, 1B), -6.8 (d, J = 150 Hz, 2B), -19.8 (d, J = 149 Hz, 2B), -22.4 (dd, $J_{B–H}$ = 136, $J_{B–H–B}$ = 51 Hz, 2B), -33.1 (d, J = 141 Hz, 1B), -37.1 (d, J = 139 Hz, 1B).

Lithium 8-iodo-7,9-dicarba-*nido*-decahydridoundecaborate(2-) (**52**)

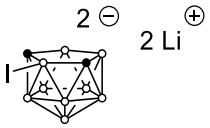

Compound **49** (10.8 mg, 21.5 μmol) was placed in an oven-dried NMR tube and placed under an atmosphere of dry nitrogen. Anhydrous THF (0.4 mL) was added followed *n*-butyllithium (1.6 M in hexanes, 40 μL, 64 μmol). The solution was left to stand for 15 min, during which time solids precipitated and settled to the bottom of the tube. The tube was then sealed and placed in an NMR spectrometer. NMR data was collected unlocked and by shimming using the ^{1}H NMR resonances of THF solvent. The product decomposes rapidly in air and was used *in situ* for further reactions. **^{11}B{^{1}H} NMR** (128 MHz, THF-H_8): δ -17.1 (2B), -20.9 (4B), -24.9 (2B), -43.4 (1B); **^{11}B NMR** (128 MHz, THF-H_8): δ -17.1 (d, J = 143 Hz, 2B), -20.9 (m, 4B), -24.9 (d, J = 119 Hz, 2B), -43.4 (d, J = 134 Hz ,1B).

1-Carboxy-1,2-dicarba-*closo*-dodecaborane(12) (**71**)

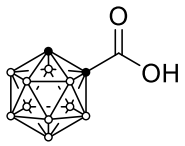

closo-1,2-Carborane (297 mg, 2.06 mmol) was added to an oven-dried, two-neck flask and the flask was evacuated and back-filled with nitrogen three times. The solids were dissolved in anhydrous diethyl ether (10 mL) and the resulting solution was cooled to -78 °C, to which *n*-butyllithium (1.6 M in hexanes, 1.35 mL, 2.16 mmol) was added dropwise. The solution was stirred at the same temperature for 15 min before carbon dioxide gas was bubbled into the reaction mixture. The solution was stirred vigorously -78 °C for 1 h and then for a further 30 min after warming to RT. Upon completion, the solvent was removed *in vacuo* and water (10 mL) was added to the residue. The aqueous layer was extracted with petroleum benzine (2 × 10 mL) and the extracts combined to recover any unreacted *closo*-1,2-carborane. The aqueous layer was acidified (pH 1–2) with 3 M HCl to precipitate the product, which was extracted with ether (3 × 10 mL). The combined organic extracts were dried over sodium sulfate, filtered and reduced *in vacuo* to give **71** (371 mg, 96%) as a colourless powder. **^{1}H NMR** (300 MHz, $CDCl_3$): δ 9.25 (br s, 1H, COO<u>H</u>), 4.04 (s, 1H, C_{cage}–<u>H</u>), 3.42–1.04 (br m, 10H, B–<u>H</u>); **^{11}B{^{1}H} NMR** (96 MHz, $CDCl_3$) δ -2.3 (2B), -8.7 (2B), -11.9 (4B), -13.5 (2B). The characterisation data matches that reported in the literature.[62]

1-Carboxy-1,7-dicarba-*closo*-dodecaborane(12) (**19**)

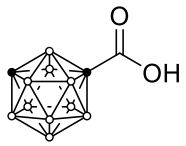

closo-1,7-Carborane (404 mg, 2.06 mmol) was added to an oven-dried, two-neck flask and the flask was evacuated and back-filled with nitrogen three times. The solids were dissolved in anhydrous diethyl ether (15 mL) and the resulting solution was cooled to -78 °C, to which *n*-butyllithium (1.6 M in hexanes, 1.80 mL, 2.88 mmol) was added dropwise. The solution was stirred at the same temperature for 15 min before carbon dioxide gas was bubbled into the reaction mixture. The solution was stirred vigorously -78 °C for 1 h and then for a further 30 min after warming to RT. Upon completion, the solvent was removed *in vacuo* and water (15 mL) was added to the residue. The aqueous layer was extracted with petroleum benzine (2 × 15 mL) and the extracts combined to recover any unreacted *closo*-1,2-carborane. The aqueous layer was acidified (pH 1–2) with 3 M HCl to precipitate the product, which was extracted with ether (3 × 15 mL). The combined organic extracts were dried over sodium sulfate, filtered and reduced *in vacuo* to give **19** (510 mg, 97%) as a colourless powder. **^{1}H NMR** (300 MHz, $CDCl_3$): δ 9.13 (br s, 1H, COO<u>H</u>), 3.98–1.17 (br m, 10H, B–<u>H</u>), 3.03 (s, 1H, C_{cage}–<u>H</u>); **^{11}B{^{1}H} NMR** (96 MHz, $CDCl_3$): δ -4.9 (2B), -6.6 (2B), -10.6 (2B), -11.1 (2B), -13.2 (2B), -15.6 (2B); **^{13}C{^{1}H} NMR** (75 MHz, $CDCl_3$): δ 167.6, 71.3, 55.0. The characterisation data matches that reported in the literature.[212]

1-Formyl-1,2-dicarba-*closo*-dodecaborane(12) (**72**)

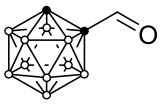

closo-1,2-Carborane (174 mg, 1.21 mmol) was added to an oven-dried, two-neck flask and the flask was evacuated and back-filled with nitrogen three times. The solids were dissolved in anhydrous diethyl ether (5 mL) and the resulting solution was cooled to -78 °C, to which *n*-butyllithium (1.5 M in hexanes, 800 µL, 1.20 mmol) was added dropwise. The solution was stirred at the same temperature for 15 min before methyl formate (0.2 mL, 3 mmol) was added to the reaction mixture in one portion. Stirring was continued for 1 h at -78 °C before the reaction was quenched slowly with 1 M HCl (5 mL) and allowed to warm to RT. The product was extracted with ether (3 × 5 mL) and the combined extracts were dried over sodium sulfate, filtered and reduced *in vacuo*. The crude product was loaded onto Celite filter-aid and purified by means of flash chromatography on silica (100% petroleum benzine to 10% DCM in petroleum benzine) to give **72** (192 mg, 92%) as a waxy, colourless solid. **^{1}H NMR** (300 MHz, $CDCl_3$): δ 9.27 (br s, 1H, CHO), 4.05 (s, 1H, C_{cage}–H), 3.32–1.28 (br m, 10H, B–H); **^{11}B{^{1}H} NMR** (96 MHz, $CDCl_3$): δ -1.7 (2B), -8.7 (2B), -12.2 (2B), -12.6 (2B), -13.6 (2B). The characterisation data matches that reported in the literature.[65]

1-Formyl-1,7-dicarba-*closo*-dodecaborane(12) (**73**)

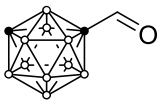

closo-1,7-Carborane (108 mg, 749 μmol) was added to an oven-dried, two-neck flask and the flask was evacuated and back-filled with nitrogen three times. The solids were dissolved in anhydrous diethyl ether (3 mL) and the resultant solution was cooled to -78 °C, to which *n*-butyllithium (1.6 M in hexanes, 490 μL, 784 μmol) was added dropwise. The solution was stirred at the same temperature for 15 min before methyl formate (0.2 mL, 3 mmol) was added to the reaction mixture in one portion. Stirring was continued for 1 h at -78 °C before the reaction was quenched slowly with 1 M HCl (3 mL) and allowed to warm to RT. The product was extracted with ether (3 × 3 mL) and the combined extracts were dried over sodium sulfate, filtered and reduced *in vacuo*. The crude product was loaded onto Celite filter-aid and purified by means of flash chromatography on silica (100% petroleum benzine) to give **73** (115 mg, 89%) as a waxy, colourless solid. **^{1}H NMR** (300 MHz, $CDCl_3$): δ 9.05 (s, 1H, C<u>H</u>O), 3.44–1.06 (br m, 10H, B–<u>H</u>) , 3.08 (s, 1H, C_{cage}<u>H</u>); **^{11}B{^{1}H} NMR** (96 MHz, $CDCl_3$): δ -6.2 (2B), -10.2 (2B), -12.5 (4B), -16.3 (2B). The characterisation data matches that reported in the literature.[65]

1-Hydroxymethyl-1,2-dicarba-*closo*-dodecaborane(12) (**74**)

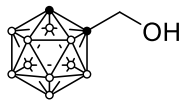

closo-1,2-Carborane (148 mg, 1.03 mmol) and paraformaldehyde (32.8 mg, 1.09 mmol) were dissolved in THF (2 mL) and TBAF (1 M in THF, 3.1 mL, 3.1 mmol) was added in one portion. The mixture was stirred at RT for 30 min, during which time the cloudy solution cleared and became pale yellow. The reaction was quenched with saturated aqueous NH_4Cl (5 mL) and the mixture was extracted with ether (5 mL). The organic layer was washed with brine (5 mL), dried over sodium sulfate, filtered and reduced *in vacuo*. The crude product was loaded onto Celite filter-aid and purified by means of flash chromatography on silica (5% ethyl acetate in petroleum benzine to 30% ethyl acetate in petroleum benzine) to give **74** (150 mg, 84%) as an oily solid which solidified into a colourless solid upon cooling to -196 °C and drying under reduced pressure. **^{1}H NMR** (300 MHz, $CDCl_3$): δ 4.10 (s, 2H, C$\underline{H}_2$), 4.00 (s, 1H, C_{cage}–$\underline{H}$), 3.31–1.11 (br m, 10H, B–$\underline{H}$); **^{11}B{^{1}H} NMR** (96 MHz, $CDCl_3$): δ -3.0 (1B), -5.4 (1B), -9.5 (2B), -11.7 (2B), -13.2 (4B); **LRMS (APCI)**: *m*/*z* 173.22 $[M - H]^-$ (calcd for $C_3H_{14}B_{10}O$ 173.20). The characterisation data matches that reported in the literature.[179]

1- Hydroxymethyl-1,7-dicarba-*closo*-dodecaborane(12) (**75**)

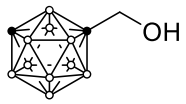

closo-1,7-Carborane (249 mg, 1.72 mmol) was added to an oven-dried, two-neck flask and the flask was evacuated and back-filled with nitrogen three times. The solids were dissolved in anhydrous diethyl ether (3 mL) and the resulting solution was cooled to -78 °C, to which *n*-butyllithium (1.5 M in hexanes, 1.15 mL, 1.73 mmol) was added dropwise. The solution was stirred at the same temperature for 15 min before methyl formate (0.3 mL, 5 mmol) was added to the reaction mixture in one portion. Stirring was continued for 1 h at -78 °C before the reaction was quenched slowly with 1 M HCl (3 mL) and allowed to warm to RT. The formyl-carborane was extracted with ether (3 × 5 mL) and the combined extracts were dried over sodium sulfate, filtered and reduced *in vacuo*. The residue was dissolved in methanol (10 mL), cooled to 0 °C and sodium borohydride (261 mg, 6.90 mmol) was added portion-wise. The heterogeneous mixture was stirred at RT until complete reduction of the aldehyde (monitored by TLC; eluent 10% DCM in petroleum benzine). The methanol was removed *in vacuo* and 1 M HCl (5 mL) was added to the residue. The aqueous layer was extracted with ether (3 × 5 mL) and the combined organic extracts were dried over sodium sulfate, filtered and reduced *in vacuo*. The crude product was loaded onto Celite filter-aid and purified by means of flash chromatography on silica (100% petroleum benzine to 15% ethyl acetate in petroleum benzine) to give **75** (260 mg, 87%) as a colourless powder. **^{1}H NMR** (300 MHz, $CDCl_3$): δ 3.81 (s, 2H, C$\underline{H}_2$), 3.26–1.21 (br m, 10H, B–$\underline{H}$), 2.96 (s, 1H, C_{cage}–$\underline{H}$); **^{11}B{^{1}H} NMR** (96 MHz, $CDCl_3$): δ -4.7 (1B), -9.1 (1B), -10.7 (2B), -11.9 (2B), -13.3 (2B), -15.9 (2B); **LRMS (APCI)**: *m*/*z* 173.19 $[M - H]^-$ (calcd for $C_3H_{14}B_{10}O$ 173.20). The characterisation data matches that reported in the literature.[213]

1-Hydroxy-1,2-dicarba-*closo*-dodecaborane(12) (**76**)

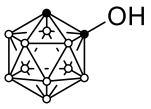

closo-1,2-Carborane (78.3 mg, 543 μmol) was added to an oven-dried, two-neck flask and the flask was evacuated and back-filled with nitrogen three times. The solids were dissolved in anhydrous diethyl ether (2 mL) and the resulting solution was cooled to 0 °C, to which *n*-butyllithium (1.6 M in hexanes, 350 μL, 560 μmol) was added dropwise. The solution was stirred at the same temperature for 15 min before trimethyl borate (80 μL, 720 μmol) was added to the reaction mixture in one portion. The reaction was allowed to warm to 0 °C over 1 h at which point a 1:1 mixture of 30% aqueous H_2O_2 and acetic acid (0.5 mL) was added. The reaction was stirred at RT for 16 h, after which It was quenched by slowly adding saturated $NaHSO_3$ solution (1 mL) and 10% NaOH solution (2 mL). After 1 h, the mixture was diluted with water (2 mL) and the aqueous layer was extracted with ether (3 × 5 mL). The combined organic extracts were dried over sodium sulfate, filtered and reduced *in vacuo*. The crude product was loaded onto Celite filter-aid and purified by means of flash chromatography on silica (10% ethyl acetate to 20% ethyl acetate in petroleum benzine) to give **76** (59.8 mg, 69%) as a colourless powder. **^{1}H NMR** (300 MHz, $CDCl_3$): δ 4.69 (O<u>H</u>), 3.97 (C_{cage}<u>H</u>), 3.19–1.04 (br m, 10H, B–<u>H</u>); **^{11}B{^{1}H} NMR** (96 MHz, $CDCl_3$): δ -3.8 (1B), -12.3 (7B), -14.6 (2B). The characterisation data matches that reported in the literature.[63]

1-Mercapto-1,2-dicarba-*closo*-dodecaborane(12) (**77**)

closo-1,2-Carborane (88.6 mg, 614 μmol) was added to an oven-dried, two-neck flask and the flask was evacuated and back-filled with nitrogen three times. The solids were dissolved in anhydrous THF (2.5 mL) and the resulting solution was cooled to 0 °C, to which *n*-butyllithium (1.6 M in hexanes, 490 μL, 784 μmol) was added dropwise. The solution was stirred at the same temperature for 15 min before elemental sulfur (20.3 mg, 79.1 μmol) was added to the reaction mixture in one portion. The clear, yellow solution was stirred at RT for 2 h, after which time the solvent was removed *in vacuo*. Ether (3 mL) was added to the residue and the organic layer was washed with 1 M HCl (3 mL). The aqueous layer was extracted with ether (2 × 3 mL) and the combined organic extracts were dried over sodium sulfate, filtered and reduced *in vacuo*. The crude product was loaded onto Celite filter-aid and purified by means of flash chromatography on silica (100% petroleum benzine) to give **77** (95.0 mg, 88%) as a waxy, colourless solid. **^{1}H NMR** (300 MHz, $CDCl_3$): δ 3.98 (s, 1H, S<u>H</u>), 3.82 (s, 1H, C_{cage}–<u>H</u>), 3.45–1.27 (br m, 10H, B–<u>H</u>); **^{11}B{^{1}H} NMR** (96 MHz, $CDCl_3$): δ -0.6 (1B), -5.8 (1B), -8.7 (4B), -10.6 (2B), -12.0 (2B); **LRMS (APCI)**: *m*/*z* 175.14 $[M - H]^-$ (calcd for $C_2H_{12}B_{10}S$ 175.16). The characterisation data matches that reported in the literature.[177]

1-Amino-1,2-dicarba-*closo*-dodecaborane(12) (**78**)

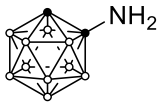

closo-1,2-Carborane (76.4 mg, 530 μmol) was added to an oven-dried, two-neck flask and the flask was evacuated and back-filled with nitrogen three times. The solids were dissolved in anhydrous diethyl ether (5 mL) and the resultant solution was cooled to 0 °C, to which *n*-butyllithium (1.6 M in hexanes, 700 μL, 1.12 mmol) was added dropwise. The mixture was stirred at the same temperature for 15 min before a solution of benzyl azide (143 mg, 1.07 mmol) in diethyl ether (2 mL) was added dropwise. The reaction was stirred at RT for 3 h, during which time the solution darked to a vibrant red/orange colour. Glacial acetic acid (5 mL) was added, causing the colour to disappear and solids to precipitate before a clear, pale-yellow solution formed. The ether was removed *in vacuo* and the remaining acetic acid solution was heated at 90 °C for 2 h. The acetic acid was removed under a stream of nitrogen and the residue was suspended in diethyl ether (5 mL) and filtered. The solids were washed with ether (2 × 5 mL) and the filtrate was reduced *in vacuo*. The crude product was loaded onto Celite filter-aid and purified by means of flash chromatography on silica (10% DCM in petroleum benzine) to give **78** (62.2 mg, 74%) as a colourless powder. **^{1}H NMR** (300 MHz, $CDCl_3$): δ 3.79 (s, 1H, $C_{cage}\underline{H}$), 2.91 (s, 2H, $N\underline{H}_2$), 3.35–1.42 (br m, 10H, B–$\underline{H}$); **^{11}B{^{1}H} NMR** (96 MHz, $CDCl_3$): δ -2.3 (2B), -10.4 (2B), -11.2 (2B), -12.5 (2B), -13.7 (2B). The characterisation data matches that reported in the literature.[64]

General procedure for the synthesis of hydroxy((hetero)aryl)methyl carboranes (General Procedure A)

closo-1,2-Carborane (1 equiv.) and the respective (hetero)aryl aldehyde (1.1 equiv.) were dissolved in THF (0.4 M) and TBAF (1 M in THF, 3 equiv.) was added in one portion. The mixture was stirred at RT for 30 min, during which time the cloudy solution cleared and became pale yellow. The reaction was quenched with saturated aqueous NH_4Cl and the mixture was extracted with diethyl ether. The organic layer was washed with brine, dried over sodium sulfate, filtered and reduced *in vacuo*. The resulting residue was loaded onto Celite filter-aid and purified by means of flash chromatography to give the desired hydroxy((hetero)aryl) carborane.

1-Hydroxy(phenyl)methyl-1,2-dicarba-*closo*-dodecaborane(12) (**79**)

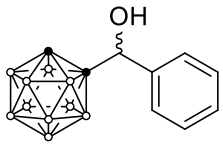

This compound was prepared according to General Procedure A using *closo*-1,2-carborane (38.2 mg, 265 μmol) and benzaldehyde. Purification by means of flash chromatography on silica (5% ethyl acetate to 30% ethyl acetate in petroleum benzine) gave **79** (59.0 mg, 89%) as colourless needles. **^{1}H NMR** (300 MHz, $CDCl_3$): δ 7.42–7.37 (m, 3H, Ar–H), 7.37–7.30 (m, 2H, Ar–H), 5.27 (s, 1H, CH), 3.82 (s, 1H, C_{cage}–H), 3.19–1.08 (br m, 10H, B–H); **^{11}B{^{1}H} NMR** (96 MHz, $CDCl_3$): δ -3.3 (1B), -4.2 (1B), -8.6 (1B), -9.1 (1B), -11.0 (1B), -12.4 (2B), -12.9 (1B), -14.0 (1B), -14.3 (1B). The characterisation data matches that reported in the literature.[61]

1-Hydroxy(pyridin-3-yl)methyl-1,2-dicarba-*closo*-dodecaborane(12) (**81**)

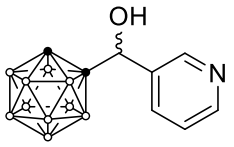

This compound was prepared according to General Procedure A using *closo*-1,2-carborane (42.1 mg, 292 μmol) and 3-pyrdinecarboxaldehyde. Purification by means of flash chromatography on silica (10% ethyl acetate to 40% ethyl acetate in petroleum benzine) gave **81** (46.5 mg, 64%) as a colourless microcrystalline solid. **^{1}H NMR** (300 MHz, acetone-d_6): δ 8.61 (d, J = 2.3 Hz, 1H, Ar–H), 8.57 (dd, J = 4.8, 1.6 Hz, 1H, Ar–H), 7.84 (dt, J = 7.9, 2.0 Hz, 1H, Ar–H), 7.41 (dd, J = 7.9, 4.8 Hz, 1H, Ar–H), 6.30 (d, J = 5.1 Hz, 1H), 5.50 (d, J = 4.9 Hz, 1H), 4.79 (s, 1H, C_{cage}–H), 3.13–1.02 (br m, 10H, B–H); **^{11}B{^{1}H} NMR** (96 MHz, acetone-d_6): δ -3.8 (1B), -4.7 (1B), -9.3 (2B), -11.9 (3B), -13.0 (1B), -13.8 (2B). The characterisation data matches that reported in the literature.[214]

1-Hydroxy(thiophen-2-yl)methyl-1,2-dicarba-*closo*-dodecaborane(12) (**80**)

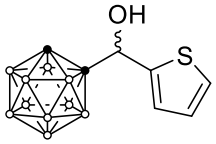

This compound was prepared according to General Procedure A using *closo*-1,2-carborane (39.9 mg, 277 μmol) and 2-thiophenecarboxaldehyde. Purification by means of flash chromatography on silica (20% DCM to 40% DCM in petroleum benzine) gave **80** (29.8 mg, 42%) as a colourless oil. **^{1}H NMR** (300 MHz, $CDCl_3$): δ 7.35 (dd, J = 5.1, 1.3 Hz, 1H, Ar–H), 7.09–6.97 (m, 2H, Ar–H), 5.54 (s, 1H, CH), 3.87 (s, 1H, C_{cage}–H), 3.45–1.05 (br m, 10H, B–H), 3.06 (s, 1H, OH); **^{11}B{^{1}H} NMR** (96 MHz, $CDCl_3$): δ -3.4 (1B), -4.2 (1B), -8.7 (1B), -9.1 (1B), -11.0 (1B), -12.4 (2B), -13.0 (1B), -14.0 (2B); **LRMS (APCI)**: m/z 255.21 $[M - H]^-$ (calcd for $C_7H_{16}B_{10}OS$ 255.19).

N-(Propargyl)phthalimide (**83**)

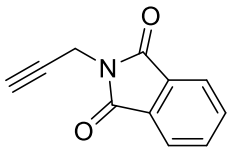

Phthalimide (3.56 g, 24.2 mmol) and potassium carbonate (8.61 g, 62.3 mmol) were suspended in DMF (25 mL) and propargyl chloride (3.5 mL, 49 mmol) was added. The brown heterogeneous solution was heated at 50 ºC for 16 h, becoming clearer and yellow as the reaction progressed. Upon completion, water (125 mL) was added and the mixture was cooled to 0 ºC and filtered. The solids were washed with water (3 × 20 mL), followed by toluene (3 × 5 mL) and finally petroleum benzine (3 × 10 mL). The solids were dried *in vacuo* at 50 ºC to give **83** (3.33 g, 74%) as a colourless powder. **^{1}H NMR** (500 MHz, $CDCl_3$): δ 7.87 (dd, *J* = 5.4, 3.1 Hz, 2H, Ar–H), 7.73 (dd, *J* = 5.5, 3.0 Hz, 3H, Ar–H), 4.45 (d, *J* = 2.5 Hz, 2H, CH_2), 2.22 (t, *J* = 2.5 Hz, 1H, C≡CH); **^{13}C{^{1}H} NMR** (125 MHz, $CDCl_3$): δ 167.1, 134.3, 132.1, 123.7, 77.3, 71.6, 27.1. The characterisation data matches that reported in the literature.[215]

1-Phthalimidomethyl-1,2-dicarba-*closo*-dodecaborane(12) (**84**)

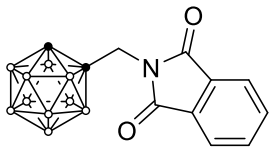

Caution! *nido-Decaborane(14) is a solid with a foul odour that is very toxic by inhalation and can be absorbed through the skin. It should only be handled in a fume-hood and transported in sealed containers. Any glassware/items that come into contact with decaborane must be soaked in methanol for 24 h in order to decompose the borane. Because crude samples can explode upon heating under some conditions, all reactions involving heating of decaborane must be performed behind a blast shield. Concentration of solutions containing decaborane or crude reaction mixtures must always be performed in a fume-hood.*

nido-Decaborane(14) (378 mg, 1.85 mmol) was added to an oven-dried two-neck flask and the flask was evacuated and back-filled with nitrogen three times. The solids were dissolved in anhydrous acetonitrile (2 mL) and the solution was stirred at reflux for 1 h. The reaction was cooled to RT and propargyl phthalimide (704 mg, 3.80 mmol) was added under a counterflow of nitrogen followed by anhydrous toluene (10 mL). The resulting mixture was stirred at reflux for 16 h. Upon completion, the reaction was cooled to 0 °C and ethanol (10 mL) was added. The reaction was stirred at RT for 24 h to destroy any remaining decaborane. The solvents were then removed under a flow of nitrogen and the residue suspended in ethanol (5 mL). The mixture was cooled to 0 °C, filtered and the solids washed with ice-cold ethanol (2 × 5 mL) followed by ice-cold petroleum benzine (5 mL). The solids were collected and dried *in vacuo* to give **84** (354 mg, 63%) as a colourless powder. **^{1}H NMR** (500 MHz, $CDCl_3$): δ 7.91 (dd, *J* = 5.5, 3.1 Hz, 2H, Ar–H), 7.80 (dd, *J* = 5.5, 3.0 Hz, 2H, Ar–H), 4.38 (s, 2H, CH_2), 3.99 (s, 1H, C_{cage}–H), 2.92–1.52 (br m, 10H, B–H); **^{11}B{^{1}H} NMR** (160 MHz, $CDCl_3$): δ -1.0 (1B), -4.8 (1B), -9.7 (2B), -11.3 (2B), -12.6 (4B); **^{13}C{^{1}H} NMR** (125 MHz, $CDCl_3$): δ 167.3, 135.0, 131.3, 124.3, 73.3, 60.1, 42.6; **LRMS (APCI)**: *m*/*z* 304.27 $[M + H]^+$ (calcd for $C_{11}H_{17}B_{10}NO_2$ 304.23). The characterisation data matches that reported in the literature.[216]

1-Aminomethyl-1,2-dicarba-*closo*-dodecaborane(12) hydrochloride (**85**)

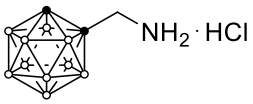

Compound **84** (98.4 mg, 324 μmol) was suspended in a 4:1 mixture of *iso*propanol and water (2 mL) and sodium borohydride (35.9 mg, 949 μmol) was added. The reaction was stirred at RT until complete consumption of the starting material (monitored by TLC; eluent 20% DCM in petroleum benzine). The solvents were removed *in vacuo* and the solids suspended in water (1 mL). The mixture was centrifuged and the supernatant was decanted off. The remaining solids were dissolved in a 4:1:1 mixture of acetic acid, water and concentrated HCl (2 mL) and the mixture was stirred at 80 °C for 2 h. The solvents were removed *in vacuo* and the resultant residue was suspended in chloroform (1 mL). The solids were collected by filtration, washed with a small amount of chloroform (0.5 mL) and dried at the pump to give the hydrochloride salt of **85** (56.9 mg, 84%) as a colourless powder. **^{1}H NMR** (300 MHz, DMSO-d_6): δ 8.79 (3H, NH_3^+), 5.42 (s, 1H, $C_{cage}H$), 3.80 (s, 2H, CH_2), 3.22–0.93 (br m, 10H, B–H); **^{11}B{^{1}H} NMR** (96 MHz, DMSO-d_6): δ -2.6 (1B), -4.8 (1B), -9.6 (2B), -11.9 (4B); **LRMS (APCI)**: *m*/*z* 174.31 $[M - H]^-$ (calcd for $C_3H_{15}B_{10}N$ 174.23). The characterisation data matches that reported in the literature.[181]

General procedure for the Negishi coupling of iodocarboranes (General Procedure B)

Anhydrous cobalt(II) bromide (0.2 equiv.) and zinc powder (7 equiv.) were added to an oven-dried Schlenk tube and the tube was evacuated and back-filled with nitrogen three times. The solids were dissolved in anhydrous acetonitrile (0.4 M) to give a blue mixture, to which allyl chloride (1 equiv.) and TFA (catalytic amount) were added. The resulting dark-orange mixture was stirred at RT for 15 min after which time the appropriate (hetero)aryl halide (1.1 equiv.) was added. The mixture was stirred for a further 1 h before compound **30** (1 equiv.) and $[PdCl_2(PPh_3)_2]$ (0.025 equiv.) were added under a counterflow of nitrogen and the reaction was stirred at RT for 16 h. Upon completion, the mixture was filtered through Celite filter-aid and the filter cake was washed with ethyl acetate. The combined filtrates were reduced *in vacuo*, loaded onto Celite filter-aid and purified by means of flash chromatography to give the desired B-(hetero)aryl carborane.

9-Phenyl-1,2-dicarba-*closo*-dodecaborane(12) (**86**)

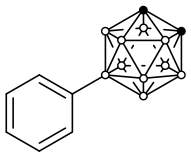

This compound was prepared according to General Procedure B using **30** (204 mg, 754 μmol) and bromobenzene. Purification by means of flash chromatography on silica (10% ethyl acetate in petroleum) gave **86** (161 mg, 97%) as colourless needles. **^{1}H NMR** (500 MHz, $CDCl_3$): δ 7.41–7.36 (m, 2H, Ar–H), 7.25–7.19 (m, 3H, Ar–H), 3.61 (s, 1H, C_{cage}–H), 3.51 (s, 1H, C_{cage}–H), 3.15–1.49 (br m, 9H, B–H); **^{11}B{^{1}H} NMR** (160 MHz, $CDCl_3$): δ 7.8 (1B), -2.1 (1B), -8.6 (2B), -13.7 (2B), -14.2 (2B), -15.3 (2B); **^{11}B NMR** (160 MHz, $CDCl_3$): δ 7.8 (s, 1B), -2.1 (d, J = 150.2 Hz, 1B), -8.6 (d, J = 151.0 Hz, 2B), -13.7 (d, J = 162.2 Hz, 2B), -14.2 (d, J = 162.2 Hz, 2B), -15.3 (d, J = 182.2 Hz, 2B); **LRMS (APCI)**: m/z 221.28 $[M + H]^+$ (calcd for $C_8H_{16}B_{10}$ 221.23). The characterisation data matches that reported in the literature.[185]

9-(Pyridin-3-yl)-1,2-dicarba-*closo*-dodecaborane(12) (**87**)

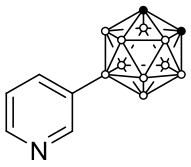

This compound was prepared according to General Procedure B using **30** (125 mg, 462 μmol) and 3-bromopyidine. Purification by means of flash chromatography on silica (10% ethyl acetate in petroleum benzine to 30% ethyl acetate in petroleum benzine) gave **87** (73.4 mg, 72%) as a colourless powder. **^{1}H NMR** (300 MHz, $CDCl_3$): δ 8.58 (s, 1H, Ar–H), 8.50–8.37 (m, 1H, Ar–H), 7.67–7.56 (m, 1H, Ar–H), 7.56–7.42 (m, 1H, Ar–H), 3.55 (s, 1H, C_{cage}–H), 3.47 (s, 1H, C_{cage}–H), 3.13–0.98 (br m, 9H, B–H); **^{11}B{^{1}H} NMR** (160 MHz, $CDCl_3$): δ 3.1 (1B), -2.8 (1B), -8.9 (2B), -13.6 (2B), -14.5 (2B), -15.3 (2B); **^{11}B NMR** (160 MHz, $CDCl_3$): δ 3.1 (s, 1B), -2.8 (d, 1B), -8.9 (d, 2B), -13.6 (d, 2B), -14.5 (d, 2B), -15.3 (d, 2B).

General procedure for the B-N coupling of 9-bromo-*closo*-1,2-carborane
(General Procedure C)

Anhydrous tribasic potassium phosphate (4 equiv.) was added to an oven-dried Schlenk tube and the tube was heated at 150 °C under vacuum for 15 min. The tube was cooled to RT and compound **91** (1 equiv.), the chosen palladium source (0.05–0.10 equiv.) and chosen ligand (0.05–0.20 equiv.) were added as solids. The tube was evacuated and backfilled with nitrogen three times before the *N*-nucleophile was added (injected as a liquid or added under a counterflow of nitrogen if a solid). Anhydrous solvent (0.3 mL) was added followed and the tube was sealed at the J. Young valve and stirred in a preheated oil bath at the required temperature for the specified time. Upon completion, the reaction was cooled to RT and filtered through a short pad of Celite filter-aid. The filter cake was rinsed with ethyl acetate and the combined filtrates were reduced *in vacuo*. An NMR spectrum of the crude product in $CDCl_3$ was taken and crude yields were determined using the $^{11}B\{^1H\}$ NMR spectrum.

Benzyl 1,7-dicarba-*closo*-dodecaborane(12)-1-carboxylate (**101**)

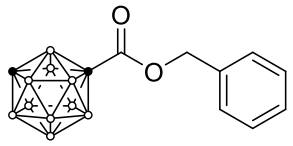

Compound **19** (40.5 mg, 215 μmol) and caesium carbonate (77.1 mg, 237 μmol) were dissolved in acetonitrile (3 mL) and benzyl bromide (32 μL, 0.27 mmol) was added. The resultant mixture was heated at reflux for 16 h, after which time the solvent was removed *in vacuo*. The residue was dissolved in DCM (10 mL), washed with water (2 × 10 mL) and then brine (10 mL). The organic layer was dried over sodium sulfate, filtered and reduced *in vacuo* before being loaded onto Celite filter-aid. The crude product was purified by means of flash chromatography on silica (100% petroleum benzine to 100% DCM) to give **101** (37.6 mg, 63%) as a colourless solid. **^{1}H NMR** (500 MHz, $CDCl_3$): δ 7.41–7.33 (m, 3H, Ar–H), 7.32–7.27 (m, 2H, Ar–H), 5.15 (s, 2H, CH_2), 3.38–1.48 (br m, 10H, B–H), 3.00 (s, 1H, $C_{cage}H$); **^{11}B{^{1}H} NMR** (160 MHz, $CDCl_3$): δ -4.8 (1B), -6.9 (1B), -10.6 (2B), -11.3 (2B), -13.3 (2B), -15.6 (2B); **{^{1}H} NMR** (125 MHz, $CDCl_3$): δ 161.6, 134.5, 128.7, 128.6, 127.7, 72.3, 69.0, 54.7; **LRMS (APCI)**: *m*/*z* 277.20 $[M - H]^-$ (calcd for $C_{10}H_{18}B_{10}O_2$ 277.22).

General procedure for the synthesis of carboranyl esters and amides (General Procedure D)

Compound **19** (1 equiv.) was added to an oven-dried, two-neck flask and the flask was evacuated and back-filled with nitrogen three times. The solids were dissolved in anhydrous DCM (0.1 M) and the solution was cooled to 0 °C before oxalyl chloride (1.1 eq.) and a catalytic amount of DMF were added. Brief effervescence resulted and the solution was allowed to stir at RT for 1 h, after which conversion to the acid chloride was complete. In a separate oven-dried flask, the respective alcohol or amine (3 equiv.) was added and the flask was evacuated and back-filled with nitrogen three times. Anhydrous DCM (0.3 M) was added followed by triethylamine (3 equiv.) and the solution was cooled to 0 °C. The prepared acid chloride solution was then added dropwise and the resulting solution allowed to stir at RT for 16 h. The solution was diluted with DCM, washed with water three times, dried over sodium sulfate and reduced *in vacuo*. The resultant residue was loaded onto Celite filter-aid and purified by means of flash chromatography to give the desired ester or amide.

Phenyl 1,7-dicarba-*closo*-dodecaborane(12)-1-carboxylate (**99**)

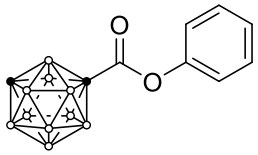

This compound was prepared according to General Procedure D using **19** (55.0 mg, 266 μmol) and sodium phenoxide. Purification by means of flash chromatography on silica (100% petroleum benzine to 100% DCM) gave **99** (33.5 mg, 48%) as a colourless powder. **^{1}H NMR** (300 MHz, $CDCl_3$): δ 7.45–7.34 (m, 2H, Ar–H), 7.32–7.22 (m, 1H, Ar–H), 7.13–7.02 (m, 2H, Ar–H), 3.70–1.01 (br m, 10H, B–H), 3.08 (s, 1H, C_{cage}H); **^{11}B{^{1}H} NMR** (96 MHz, $CDCl_3$): δ -4.7 (2B), -6.6 (2B), -10.6 (2B), -11.1 (2B), -13.1 (2B), -15.5 (2B); **LRMS (APCI)**: *m/z* 265.27 $[M + H]^+$ (calcd for $C_9H_{16}B_{10}O_2$ 265.22). The characterisation data matches that reported in the literature.[217]

4-Nitrophenyl 1,7-dicarba-*closo*-dodecaborane(12)-1-carboxylate (**100**)

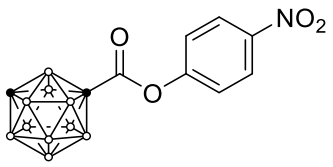

This compound was prepared according to General Procedure D using **19** (50.3 mg, 267 µmol) and 4-nitrophenol. Purification by means of flash chromatography on silica (100% petroleum benzine to 100% DCM) gave **100** (62.2 mg, 75%) as an off-white powder. **^{1}H NMR** (500 MHz, $CDCl_3$): δ 8.21 (d, *J* = 9.2 Hz, 2H, Ar–H), 7.20 (d, *J* = 9.1 Hz, 2H, Ar–H), 3.41–1.36 (br m, 10H, B–H), 3.04 (s, 1H, $C_{cage}H$); **^{11}B{^{1}H} NMR** (160 MHz, $CDCl_3$): δ -4.7 (2B), -6.3 (2B), -10.4 (2B), -11.2 (2B), -13.0 (2B), -15.5 (2B); **^{13}C{^{1}H} NMR** (125 MHz, $CDCl_3$): δ 158.7, 153.6, 145.0, 124.4, 120.9, 70.1, 54.0; **LRMS (APCI)**: *m*/*z* 310.27 $[M + H]^+$ (calcd for $C_9H_{15}B_{10}NO_4$ 310.21).

Butyl 1,7-dicarba-*closo*-dodecaborane(12)-1-carboxylate (**102**)

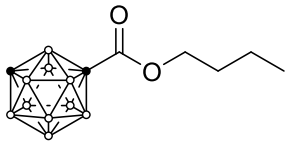

This compound was prepared according to General Procedure D using **19** (56.4 mg, 300 µmol) and 1-butanol. Purification by means of flash chromatography on silica (100% petroleum benzine to 100% DCM) gave **102** (66.7 mg, 91%) as an off-white powder. **^{1}H NMR** (500 MHz, $CDCl_3$): δ 4.12 (t, *J* = 6.5 Hz, 2H, O–CH_2), 3.30–1.04 (br m, 10H, B–H), 2.99 (s, 1H, $C_{cage}H$), 1.61 (p, *J* = 6.8 Hz, 2H, CH_2), 1.36 (q, *J* = 7.5 Hz, 2H, CH_2), 0.93 (t, *J* = 7.4 Hz, 3H, CH_3); **^{11}B{^{1}H} NMR** (160 MHz, $CDCl_3$): δ -4.9 (1B), -7.0 (1B), -10.7 (2B), -11.3 (2B), -13.4 (2B), -15.7 (2B); **^{13}C{^{1}H} NMR** (125 MHz, $CDCl_3$): δ 161.9, 72.7, 67.6, 54.8, 30.4, 19.1, 13.7; **LRMS (APCI)**: *m*/*z* 243.27 $[M - H]^-$ (calcd for $C_7H_{20}B_{10}O_2$ 243.24).

N-(Pyrimidin-2-yl)-1,7-dicarba-*closo*-dodecaborane(12)-1-carboxamide (**103**)

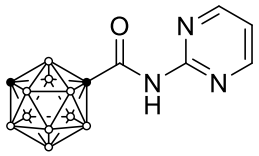

This compound was prepared according to General Procedure D using **19** (100 mg, 531 μmol) and 2-aminopyrimidine. Purification by means of flash chromatography on silica (50% DCM in petroleum benzine to 100% DCM) gave **103** (14.0 mg, 10%) as a colourless, microcrystalline solid. **^{1}H NMR** (500 MHz, $CDCl_3$): δ 8.63 (d, *J* = 4.8 Hz, 1H, Ar–H), 8.22 (s, 1H, NH), 7.09 (t, *J* = 4.8 Hz, 1H, Ar–H), 3.45–1.02 (br m, 10H, B–H), 3.09 (s, 1H, C_{cage}H); **^{11}B{^{1}H} NMR** (160 MHz, $CDCl_3$): δ -5.9 (1B), -7.1 (1B), -10.7 (2B), -11.5 (2B), -12.9 (2B), -15.4 (2B); **^{13}C{^{1}H} NMR** (125 MHz, $CDCl_3$): δ 158.7, 157.4, 156.6, 117.9, 75.9, 55.3; **LRMS (APCI)**: *m*/*z* 266.31 $[M + H]^+$ (calcd for $C_7H_{15}B_{10}N_3O$ 266.23).

N-(2-Aminophenyl)-1,7-dicarba-*closo*-dodecaborane(12)-1-carboxamide (**104**)

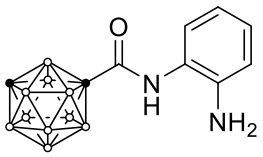

This compound was prepared according to General Procedure D using **19** (100 mg, 531 μmol) and *ortho*-phenylenediamine. Purification by means of flash chromatography on silica (100% petroleum benzine to 100% DCM) gave **104** (92.3 mg, 62%) as an off-white powder. **^{1}H NMR** (500 MHz, $CDCl_3$): δ 7.53 (s, 1H, NH), 7.32 (d, *J* = 7.9 Hz, 1H, Ar–H), 7.06 (t, *J* = 7.7 Hz, 1H, Ar–H), 6.86–6.78 (m, 2H, Ar–H), 3.85–1.33 (br m, 10H, B–H), 3.09 (s, 1H, C_{cage}H); **^{11}B{^{1}H} NMR** (160 MHz, $CDCl_3$): δ -5.8 (1B), -7.4 (1B), -10.7 (2B), -11.4 (2B), -13.0 (2B), -15.5 (2B); **^{13}C{^{1}H} NMR** (125 MHz, $CDCl_3$): δ 158.7, 139.6, 127.7, 124.6, 124.2, 120.5, 118.8, 75.8, 55.2; **LRMS (APCI)**: *m*/*z* 279.33 $[M + H]^+$ (calcd for $C_9H_{18}B_{10}N_2O$ 279.25).

N,*N*'-(1,2-Phenylene)bis(1,7-dicarba-*closo*-dodecaborane(12)-1-carboxamide) (**106**)

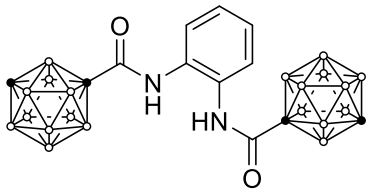

This compound was isolated as a byproduct in the preparation of **104** as an off-white powder (58.9 mg, 25%). **^{1}H NMR** (500 MHz, $CDCl_3$): δ 7.89 (s, 2H, NH), 7.36–7.31 (m, 2H, Ar–H), 7.28–7.23 (m, 2H, Ar–H), 3.46–1.63 (br m, 20H, B–H), 3.10 (s, 2H, C_{cage}H); **^{11}B{^{1}H} NMR** (160 MHz, $CDCl_3$): δ -5.7 (4B), -7.1 (4B), -10.6 (4B), -11.5 (4B), -13.0 (4B), -15.5 (4B); **^{13}C{^{1}H} NMR** (125 MHz, $CDCl_3$): δ 159.8, 129.7, 127.7, 125.9, 75.2, 55.3; **LRMS (APCI)**: *m*/*z* 449.45 $[M + H]^+$ (calcd for $C_{12}H_{28}B_{20}N_2O_2$ 449.42).

N-(2-Hydroxyethyl)-1,7-dicarba-*closo*-dodecaborane(12)-1-carboxamide (**105**)

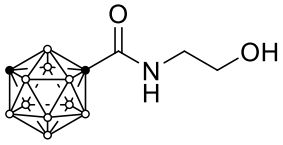

This compound was prepared according to General Procedure D using **19** (100 mg, 531 μmol) and ethanolamine. Purification by means of flash chromatography on silica (100% DCM) gave **105** (86.4 mg, 71%) as a colourless, microcrystalline solid. **^{1}H NMR** (500 MHz, $CDCl_3$): δ 6.28 (s, 1H, NH), 3.70 (t, *J* = 5.1 Hz, 2H, CH_2), 3.41–3.34 (m, 2H, CH_2), 3.27–1.48 (br m, 10H, B–H), 3.03 (s, 1H, C_{cage}H); **^{11}B{^{1}H} NMR** (160 MHz, $CDCl_3$): δ -5.8 (2B), -7.5 (2B), -10.8 (2B), -11.6 (2B), -13.2 (2B), -15.6 (2B); **^{13}C{^{1}H} NMR** (125 MHz, $CDCl_3$): δ 161.1, 75.5, 61.4, 55.1, 43.2; **LRMS (APCI)**: *m*/*z* 232.30 $[M + H]^+$ (calcd for $C_5H_{17}B_{10}NO_2$ 232.23).

N,*N*'-(Propane-1,3-diyl)bis(1,7-dicarba-*closo*-dodecaborane(12)-1-carboxamide) (**108**)

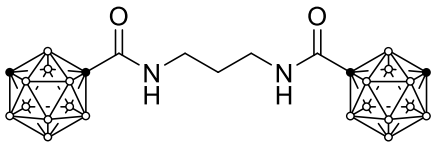

This compound was prepared according to General Procedure D using **19** (100 mg, 531 μmol) and 1,3-diaminopropane. Purification by means of flash chromatography on silica (100% petroleum benzine to 100% DCM) gave **108** as colourless needles (150 mg, 68%). The mono-acylated amine was also produced but could not be isolated in sufficient purity. **^{1}H NMR** (500 MHz, $CDCl_3$): δ 6.41 (br t, 2H, NH), 3.26–1.49 (br m, 20H, B–H), 3.15 (q, *J* = 6.3 Hz, 4H. CH_2), 3.03 (s, 2H, $C_{cage}H$), 1.62–1.54 (m, 2H, CH_2); **^{11}B{^{1}H} NMR** (160 MHz, $CDCl_3$): δ -5.7 (1B), -7.5 (1B), -10.8 (4B), -11.6 (4B), -13.2 (4B), -15.7 (4B); **^{13}C{^{1}H} NMR** (125 MHz, $CDCl_3$): δ 160.3, 74.4, 53.9, 35.8, 28.3; **LRMS (APCI)**: *m*/*z* 415.55 $[M + H]^+$ (calcd for $C_9H_{30}B_{20}N_2O_2$ 415.44).

12-Iodo-1-phthalimidomethyl-1,2-dicarba-*closo*-dodecaborane(12) and
9-iodo-1-phthalimidomethyl-1,2-dicarba-*closo*-dodecaborane(12) (**145a** + **145b**)

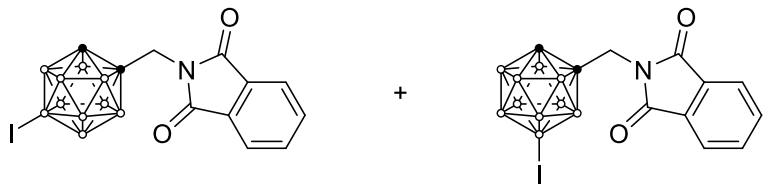

84 (292 mg, 963 μmol) and iodine (123 mg, 485 μmol) were dissolved in acetic acid (30 mL) and a 1:1 mixture of concentrated nitric and concentrated sulfuric acid (3 mL) was added. The dark purple solution was heated at 60 ºC for 3 h or until complete consumption of the starting material (monitored by TLC; eluent 25% ethyl acetate in petroleum benzine). The now colourless solution was added to ice cold water (100 mL) and filtered. The solids were washed well with water and dried thoroughly at the pump to give an inseparable mixture of **145a** and **145b** (390 mg, 94%) as a colourless powder. **^{1}H NMR** (500 MHz, $CDCl_3$): δ 7.95–7.89 (m, 4H, Ar–H (isomers 1 and 2)), 7.85–7.79 (m, 4H, Ar–H (isomers 1 and 2)), 4.39 (s, 2H, CH_2 (isomer 1)), 4.30 (s, 1H, , $C_{cage}H$ (isomer 1)), 4.28 (s, 2H, CH_2 (isomer 2)), 4.10 (s, 1H, , $C_{cage}H$ (isomer 2)), 3.34–1.51 (br m, 9H, B–H, isomers 1 and 2); **^{11}B{^{1}H} NMR** (160 MHz, $CDCl_3$): δ 0.6, -3.3, -8.0, -10.9, -11.7, -12.4, -15.5, -17.5; **^{11}B NMR** (160 MHz, $CDCl_3$): δ 0.6 (d), -3.3 (d), -8.0 (d), -10.9 (d), -11.7 (d), -12.4 (d), -15.5 (s, B–I (isomer 2)), -17.5 (s, B–I (isomer 2)); **^{13}C{^{1}H} NMR** (125 MHz, $CDCl_3$): δ 167.20, 167.16, 135.18 (two overlapping signals), 131.20, 131.19, 124.40, 124.39, 73.8, 70.1, 60.8, 56.2, 42.8, 42.3; **LRMS (APCI)**: *m*/*z* 430.12 $[M + H]^+$ (calcd for $C_{11}H_{16}B_{10}INO_2$ 430.13).

12-Bromo-1-phthalimidomethyl-1,2-dicarba-*closo*-dodecaborane(12) and
9-bromo-1-phthalimidomethyl-1,2-dicarba-*closo*-dodecaborane(12) (**146a** + **146b**)

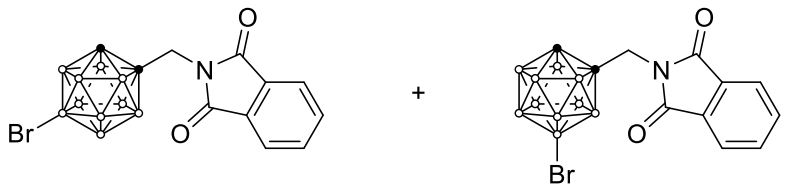

Triflic acid (~150 µL, 1 equiv.) was added to a solution of **84** (443 mg, 146 mmol) and NBS (263 mg, 1.48 mmol) dissolved in HFIP (10 mL) and the reaction mixture was stirred vigorously at RT for 24 h. Upon completion, HFIP was recovered by distillation and water was added to the reaction residue. The aqueous layer was extracted with DCM (2 × 10 mL) and the combined organic extracts were dried over sodium sulfate, filtered and reduced *in vacuo*. The crude product was loaded onto Celite filter-aid and purified by means of flash chromatography on silica (10% to 35% ethyl acetate in petroleum benzine over 15 CVs) to give an inseparable mixture of **146a** and **146b** (418 mg, 75%) as a colourless powder. **^{1}H NMR** (500 MHz, $CDCl_3$): δ 7.95–7.89 (m, 2H, Ar–H (isomers 1 and 2)), 7.85–7.79 (m, 2H, Ar–H (isomers 1 and 2)), 4.39 (s, 2H, CH_2 (isomer 1)), 4.35 (s, 2H, CH_2 (isomer 2)), 4.06 (s, 1H, $C_{cage}H$ (isomer 1)), 4.03 (s, 1H, $C_{cage}H$ (isomer 2)), 3.34–1.51 (br m, 9H, B–H, isomers 1 and 2); **^{11}B{^{1}H} NMR** (160 MHz, $CDCl_3$): δ 1.3, -0.2, -0.7, -4.0, -8.8, -11.4, -12.0, -12.3, -13.5; **^{11}B NMR** (160 MHz, $CDCl_3$): δ 1.3 (s, B–Br (isomer 1)), -0.2 (d), -0.7 (s, B–Br (isomer 2)), -4.0 (d), -8.8 (d), -11.4 (d), -12.0 (d), -12.3 (d), -13.5 (d); **^{13}C{^{1}H} NMR** (125 MHz, $CDCl_3$): δ 167.20, 167.16, 135.2 (two overlapping signals), 131.2 (two overlapping signals), 124.39, 124.37, 72.1, 66.3, 59.1, 52.2, 42.4, 41.9; **LRMS (APCI)**: *m*/*z* 383.14 $[M + H]^+$ (calcd for $C_{11}H_{16}B_{10}BrNO_2$ 383.14).

12-Azido-1-phthalimidomethyl-1,2-dicarba-*closo*-dodecaborane(12) and
9-Azido-1-phthalimidomethyl-1,2-dicarba-*closo*-dodecaborane(12) (**147a** + **147b**)

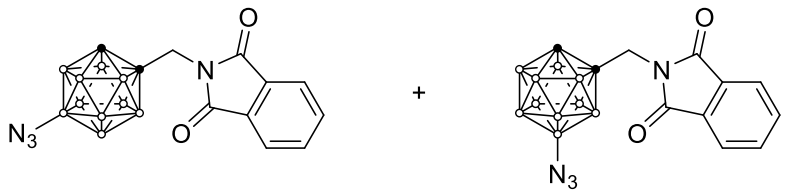

Anhydrous potassium phosphate tribasic (25.7 mg, 121 μmol) was added to an oven-dried Schlenk tube and the tube was heated at 150 °C under vacuum for 15 min. The tube was cooled to RT and compound **146** (19.1 mg, 50.0 μmol), sodium azide (7.8 mg, 0.12 mmol), SPhos (1.7 mg, 4.1 μmol) and SPhos-Pd-G3 (2.6 mg, 3.3 μmol) were added as solids. The tube was evacuated and backfilled with nitrogen three times before anhydrous DME (0.3 mL) was added. The tube was sealed at the J. Young valve and stirred in a preheated oil bath at 80 °C for 3 h. Upon completion, the reaction was cooled to RT and filtered through a short pad of Celite filter-aid. The filter cake was rinsed with ethyl acetate (3 × 0.5 mL) and the combined filtrates were reduced *in vacuo*. The resulting residue was loaded onto Celite filter-aid and purified by means of flash chromatography on silica (10% DCM to 50% DCM in petroleum benzine) to give an inseparable mixture of **147a** and **147b** (13.5 mg, 78%) as a pale-red oil. **^{1}H NMR** (300 MHz, $CDCl_3$): δ 7.97–7.87 (m, 4H, Ar–H), 7.87–7.77 (m, 4H, Ar–H), 4.45 (s, 2H, CH_2), 4.38 (s, 2H, CH_2), 3.98 (s, 1H, C_{cage}–H), 3.86 (s, 1H, C_{cage}–H), 3.42–0.88 (br m, 20H, B–H); **^{11}B{^{1}H} NMR** (96 MHz, $CDCl_3$): δ 9.2 (1B), 6.9 (1B), -2.1 (1B), -6.0 (1B), -10.5 (5B), -13.1 (5B), -14.0 (6B); **LRMS (APCI)**: *m/z* 345.28 $[M + H]^+$ (calcd for $C_{11}H_{16}B_{10}N_4O_2$ 345.24).

12-Hydroxy-1-phthalimidomethyl-1,2-dicarba-*closo*-dodecaborane(12) and
9-hydroxy-1-phthalimidomethyl-1,2-dicarba-*closo*-dodecaborane(12) (**148a** + **148b**)

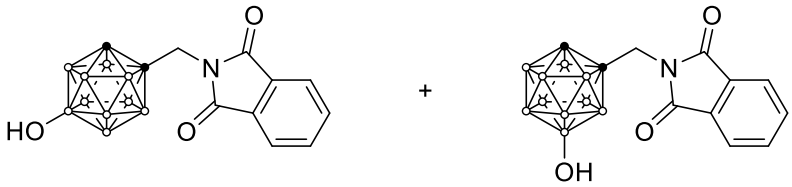

Compound **84** (51.8 mg, 171 μmol) and nitric acid (12 mg, 0.19 mmol) were suspended in triflic acid (0.5 mL) and the mixture was stirred vigorously at RT for 16 h. Upon completion, the reaction was slowly added to ice-cold water (5 mL) before saturated aqueous $NaHCO_3$ solution (5 mL) was added dropwise. The aqueous layer was extracted with ethyl acetate (3 × 5 mL) and the combined organic extracts were dried over sodium sulfate, filtered and reduced *in vacuo*. The crude product was loaded onto Celite filter-aid and purified by means of flash chromatography on silica (10% ethyl acetate to 50% ethyl acetate in petroleum benzine) to give an inseparable mixture of **148a** and **148b** (47.5 mg, 87%) as a colourless powder. A small amount of product nitrated at the phthalimide phenyl ring was identified by NMR. **^{1}H NMR** (500 MHz, acetone-d_6): δ 7.97–7.89 (m, 8H, Ar–H), 4.67 (s, 1H, OH), 4.60 (s, 2H, CH_2), 4.51 (s, 1H, OH), 4.46 (s, 1H, C_{cage}–H), 4.44 (s, 2H, CH_2), 4.31 (s, 1H, C_{cage}–H), 2.90–1.42 (br m, 20H, B–H); **^{11}B{^{1}H} NMR** (160 MHz, acetone-d_6): δ 15.8, 14.3, -3.5, -6.8, -10.6, -12.9, -14.4, -15.1, -15.8, -16.3; **^{11}B NMR** (160 MHz, acetone-d_6): δ 15.8 (s, B–O (isomer 1)), 14.3 (s, B–O (isomer 2)), -3.5 (d), -6.8 (d), -10.6 (d), -12.9 (d), -14.4 (d), -15.1 (d), -15.8 (d), -16.3 (d); **LRMS (APCI)**: *m*/*z* 320.31 $[M + H]^+$ (calcd for $C_{11}H_{17}B_{10}NO_3$ 320.23).

N-Benzoyloxymorpholine (**151**)

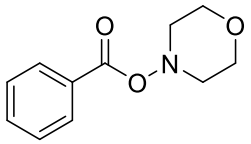

Caution! *Benzoyl peroxide is potentially explosive and can cause fires without external ignition, especially in its pure form. The solid isolated in the first step should be used immediately.*

Benzoyl chloride (0.35 mL, 3.0 mmol) was dissolved in diethyl ether (1 mL) and the resulting solution was cooled to 0 ºC before hydrogen peroxide (30 *wt*% in water, 0.17 mL, 1.7 mmol) was added dropwise. The solution was stirred at this temperature for 10 min before NaOH (0.15 g, 3.8 mmol) in water (1 mL) was added dropwise. The biphasic solution was stirred vigorously for 20 min at RT causing a colourless precipitate to appear. The solids were collected by filtration, washed with water (3 × 1 mL) and diethyl ether (3 × 0.5 mL) and dried at the pump. The crude benzoyl peroxide was used in the next steps immediately without further purification.

Benzoyl peroxide (264 mg, 1.09 mmol) and K_2HPO_4 (286 mg, 1.64 mmol) were added to an oven-dried flask and the flask was evacuated and back-filled with nitrogen three times. Anhydrous DMF (4 mL) was added before morpholine (120 µL, 1.39 mmol) was added to the stirring solution in one portion. The suspension was stirred at RT for 16 h. Deionized water (5 mL) was added and the contents were stirred vigorously for several minutes until all solids dissolved. The aqueous layer was extracted with ethyl acetate (3 × 10 mL) and the combined organic extracts were washed saturated $NaHCO_3$ solution (2 × 10 mL). The organic layer was dried over sodium sulfate, filtered and reduced *in vacuo* before being loaded onto Celite filter-aid. The crude product was purified by means of flash chromatography on silica (25% ethyl acetate to 50% ethyl acetate in petroleum benzine) to give **151** (50.1 mg, 22%) as a colourless powder. **^{1}H NMR** (500 MHz, $CDCl_3$): δ 8.05–7.96 (m, 2H, Ar–H), 7.63–7.51 (m, 1H, Ar–H), 7.50–7.38 (m, 2H, Ar–H), 4.06–3.79 (m, 4H), 3.45 (d, J = 10.1 Hz, 2H), 3.13–2.97 (m, 2H); **^{13}C{^{1}H} NMR** (125 MHz, $CDCl_3$): δ 164.7, 133.3, 129.6, 129.2, 128.6, 66.0, 57.1. The characterisation data matches that reported in the literature.[218]

Benzophenone imine (**152**)

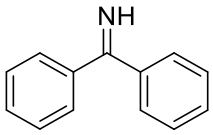

Benzophenone (1.01 g, 5.55 mmol) and bis(trimethylsilyl)amine (2.3 mL, 11 mmol) were added to an oven-dried flask and the flask was evacuated and back-filled with nitrogen three times. TBAF (1.0 M in THF, 560 µL, 560 µmol) was added and the flask was stirred at RT for 16 h. The volatiles were removed *in vacuo* and the crude product was loaded onto Celite filter-aid and purified by means of flash chromatography on silica gel (2% ethyl acetate to 15% ethyl acetate in petroleum benzine + 1% TEA) to give **152** (602 mg, 60%) as an orange oil. **^{1}H NMR** (500 MHz, $CDCl_3$): δ 9.14 (br s, 1H, NH), 7.64–7.54 (m, 4H, Ar–H), 7.54–7.36 (m, 6H, Ar–H); **^{13}C{^{1}H} NMR** (125 MHz, $CDCl_3$): δ 178.6, 139.1, 130.6, 128.6, 128.5. The characterisation data matches that reported in the literature.[219]

General procedure for the direct amination of *closo*-carboranes (General Procedure E)

Carborane (1 equiv.), N-nucleophile (2.5 equiv.), silver(I) acetate (2.5 equiv.) and palladium(II) acetate (10 mol%) were placed in a vial and dissolved in HFIP (0.2 M). The vial was capped and the heterogeneous solution was stirred at 70 ºC for 48 h. After this time, the volatiles were removed, the residue was suspended in ethyl acetate and filtered through a short pad of Celite filter-aid. The filtrate was washed with saturated aqueous $NaHCO_3$ solution and the aqueous layer was extracted with ethyl acetate twice. The combined organic extracts were dried over sodium sulfate, filtered and reduced *in vacuo*. The crude product was loaded onto Celite filter-aid and purified by means of flash chromatography on silica.

12-Benzenesulfonamido-1-phthalimidomethyl-1,2-dicarba-*closo*-dodecaborane(12) and 9-benzenesulfonamido-1-phthalimidomethyl-1,2-dicarba-*closo*-dodecaborane(12) and 8-benzenesulfonamido-1-phthalimidomethyl-1,2-dicarba-*closo*-dodecaborane(12) (**149a** + **149b + 149c**).

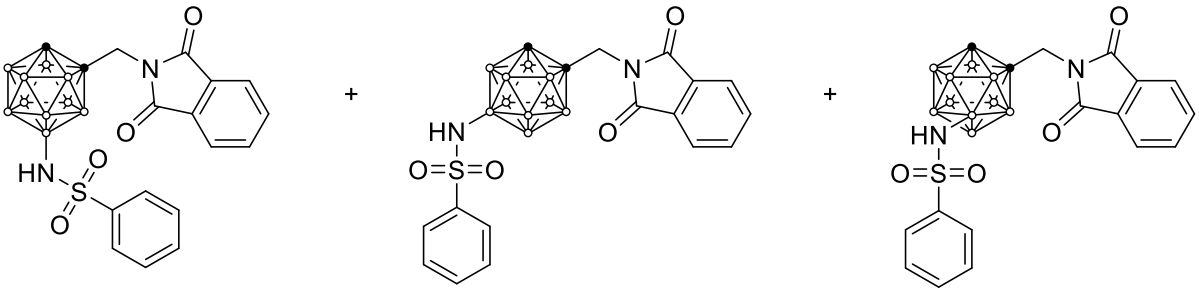

This compound was synthesised according to General Procedure E using compound **84** (50.4 mg, 166 μmol) and benzenesulfonamide. Purification by means of flash chromatography on silica (100% DCM) gave an inseparable mixture of **149a**, **149b** and **149c** (61.2 mg, 80%) as a colourless powder. **^{1}H NMR** (500 MHz, $CDCl_3$): δ 7.94–7.88 (m, 2H, Ar–H (isomers 1,2 and 3)), 7.88–7.76 (m, 4H, Ar–H (isomers 1,2 and 3)), 7.54–7.36 (m, 3H, Ar–H (isomers 1,2 and 3)), 4.67 (s, 1H, NH (isomer 1)), 4.62 (s, 1H, NH (isomer 2)), 4.55 (s, 1H, NH (isomer 3)), 4.38 (s, 2H, CH_2 (isomer 2)), 4.32 (s, 2H, CH_2 (isomer 3)), 4.30 (s, 1H, CH_2 (isomer 1)), 3.92 (s, 1H, $C_{cage}H$ (isomer 1 and 2)), 3.83 (s, 1H, $C_{cage}H$ (isomer 3)), 2.98–1.43 (br m, 9H, B–H, isomers 1,2 and 3); **^{11}B{^{1}H} NMR** (160 MHz, $CDCl_3$): δ 6.8, 4.4, 0.1, -2.0, -5.2, -5.8, -10.3, -12.5, -13.5, -14.4; **^{11}B NMR** (160 MHz, $CDCl_3$): δ 6.8 (s, B–N (isomer 1)), 4.4 (s, B–N (isomer 2)), 0.1 (s, B–N (isomer 3)), -2.0 (d), -5.2 (d), -5.8 (d), -10.3 (d), -12.5 (d), -13.5 (d), -14.4 (d); **^{13}C{^{1}H} NMR** (125 MHz, $CDCl_3$): δ 167.19, 167.15, 167.14, 142.26, 142.19, 142.02, 135.1 (three overlapping signals), 132.2, 132.1 (two overlapping signals), 131.24, 131.20 (two overlapping signals), 128.81, 128.77, 128.73, 127.08, 127.07, 127.0, 124.33, 124.30 (two overlapping signals), 69.9, 64.9, 60.5, 57.0, 56.6, 50.6, 42.49, 42.45, 41.4; **LRMS (APCI)**: *m*/*z* 459.27 $[M + H]^+$ (calcd for $C_{17}H_{22}B_{10}N_2O_4S$ 459.24).

12-Methanesulfonamido-1-phthalimidomethyl-1,2-dicarba-*closo*-dodecaborane(12) and 9-methanesulfonamido 1-phthalimidomethyl-1,2-dicarba-*closo*-dodecaborane(12) and 8-methanesulfonamido-1-phthalimidomethyl-1,2-dicarba-*closo*-dodecaborane(12) (**150a** + **150b + 150c**)

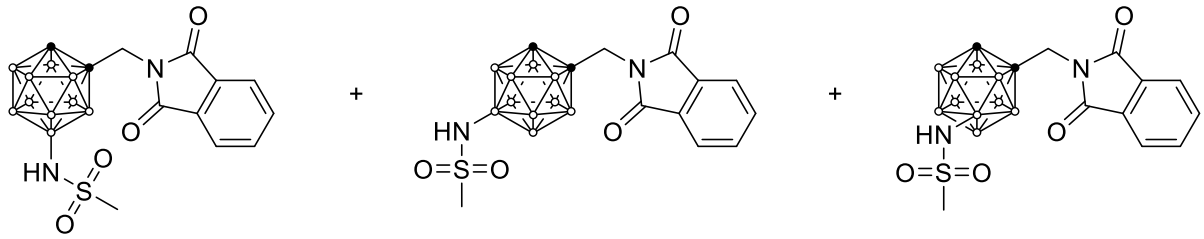

This compound was synthesised according to General Procedure E using **84** (51.4 mg, 169 µmol) and methanesulfonamide. Purification by means of flash chromatography (100% DCM to 20% ethyl acetate in DCM) gave an inseparable mixture of **150a**, **150b** and **150c** (41.1 mg, 61%) as a colourless oil. **^{1}H NMR** (500 MHz, $CDCl_3$): δ 7.93–7.88 (m, 4H, Ar–H (isomers 1,2 and 3)), 7.83–7.78 (m, 4H, Ar–H (isomers 1,2 and 3)), 4.47 (s, 1H, NH (isomer 1)), 4.43 (s, 2H, CH_2 (isomer 2)), 4.42 (s, 1H, NH (isomer 2)), 4.38 (s, 2H, CH_2 (isomer 3)), 4.37 (s, 2H, CH_2 (isomer 1)), 4.32 (s, 1H, NH (isomer 3)), 4.02 (s, 1H, C_{cage}–H (isomer 1 and 2)), 3.91 (s, 1H, C_{cage}–H (isomer 3)), 3.08–1.44 (br m, 9H, B–H, isomers 1,2 and 3), 2.96 (s, 1H, CH_3 (isomer 1)), 2.93 (s, 3H, CH_3 (isomer 2)), 2.90 (s, 3H, CH_3 (isomer 3)); **^{11}B{^{1}H} NMR** (160 MHz, $CDCl_3$): δ 6.9, 4.5, 0.3, -1.9, -5.5, -10.2, -12.3, -13.4, -14.1; **^{11}B NMR** (160 MHz, $CDCl_3$): δ 6.9 (s, B–N (isomer 1)), 4.5 (s, B–N (isomer 2)), 0.3 (s, B–N (isomer 3)), -1.9 (d), -5.5 (d), -10.2 (d), -12.3 (d), -13.4 (d), -14.1 (d); **^{13}C{^{1}H} NMR** (125 MHz, $CDCl_3$): δ 167.23, 167.22, 167.20, 135.13, 135.12, 135.0, 131.3, 131.21, 131.17, 124.35, 124.33 (two overlapping signals), 70.1, 64.8, 60.5, 57.2, 56.6, 50.5, 42.50, 42.26, 41.96, 41.95, 41.9, 41.4; **LRMS (APCI)**: *m*/*z* 397.24 $[M + H]^+$ (calcd for $C_{12}H_{20}B_{10}N_2O_4S$ 397.22).

General procedure for the synthesis of triflate esters of hydroxymethyl carboranes (General Procedure F)

The appropriate hydroxymethyl carborane was added to an oven-dried Schlenk tube and the tube was evacuated and back-filled with nitrogen three times. A solution of pyridine (1 equiv.) in anhydrous DCM (0.3 M) was added and the solution was cooled to 0 ºC. Triflic anhydride (1.1 equiv.) was added dropwise and the reaction was stirred at RT for 2 h. The reaction was diluted with DCM and washed with saturated $NaHCO_3$ solution and water. The organic layer was dried over sodium sulfate, filtered and reduced *in vacuo* before being purified by means of flash chromatography on silica.

1-((((Trifluoromethyl)sulfonyl)oxy)methyl)-1,2-dicarba-*closo*-dodecaborane(12) (**174**)

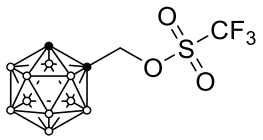

This compound was synthesised according to General Procedure F using **74** (134 mg, 769 μmol). Purification by means of flash chromatography (100% petroleum benzine to 10% DCM in petroleum benzine) gave **174** (211 mg, 90%) as a colourless oil which solidified upon cooling to -20 °C. **^{1}H NMR** (300 MHz, $CDCl_3$): δ 4.79 (s, 2H, C$\underline{H}_2$), 3.79 (s, 1H, $C_{cage}\underline{H}$), 3.44–1.31 (br m, 10H, B–$\underline{H}$); **^{11}B{^{1}H} NMR** (96 MHz, $CDCl_3$): δ -1.6 (1B), -3.4 (1B), -8.7 (2B), -11.6 (2B), -12.7 (4B). The characterisation data matches that reported in the literature.[203]

1-((((Trifluoromethyl)sulfonyl)oxy)methyl)-1,7-dicarba-*closo*-dodecaborane(12) (**157**)

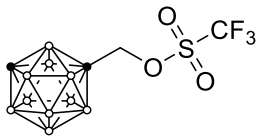

This compound was synthesised according to General Procedure F using **75** (248 mg, 1.42 mmol). Purification by means of flash chromatography (100% petroleum benzine) gave **157** (385 mg, 88%) as a colourless oil which solidified upon cooling to -20 °C. **^{1}H NMR** (500 MHz, $CDCl_3$): δ 4.53 (s, 2H), 3.04 (s, 1H, C_{cage}–H), 3.24–1.51 (br m, 10H, B–H); **^{11}B{^{1}H} NMR** (160 MHz, $CDCl_3$): δ -4.5 (1B), -7.8 (1B), -10.2 (2B), -11.6 (2B), -13.0 (2B), -15.8 (2B); **^{13}C{^{1}H} NMR** (125 MHz, $CDCl_3$): δ 118.6 (q, J = 319.7 Hz), 74.8, 70.0, 55.5. The characterisation data matches that reported in the literature.[202]

9-Bromo-1-((((Trifluoromethyl)sulfonyl)oxy)methyl)-1,7-dicarba-*closo*-dodecaborane(12) (**168**)

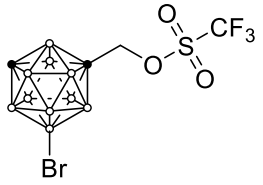

This compound was synthesised according to General Procedure F using **184** (262 mg, 1.04 mmol). Purification by means of flash chromatography (10% DCM in petroleum benzine to 30% DCM in petroleum benzine) gave **168** (211 mg, 90%) as a colourless oil which solidified upon cooling to -20 °C. **^{1}H NMR** (500 MHz, $CDCl_3$): δ 4.55 (s, 2H, CH_2), 3.12 (s, 1H, C_{cage}–H), 3.57–1.70 (br m, 10H, B–H); **^{11}B{^{1}H} NMR** (160 MHz, $CDCl_3$): δ -4.1 (1B), -6.2 (1B), -7.2 (1B), -9.0 (1B), -11.2 (1B), -12.4 (2B), -13.7 (1B), -16.7 (1B), -20.0 (1B); **^{11}B NMR** (160 MHz, $CDCl_3$): δ -4.1 (d, 1B, J = 169 Hz), -6.2 (s, 1B, B10), -7.2 (d, 1B, , J = 171 Hz), -9.0 (d, 1B, , J = 157 Hz), -11.2 (d, 1B, , J = 198 Hz), -12.4 (d, 2B, , J = 198 Hz), -13.7 (d, 1B, J = 194 Hz), -16.7 (d, 1B, , J = 184 Hz), -20.0 (d, 1B, , J = 184 Hz); **^{13}C{^{1}H} NMR** (125 MHz, $CDCl_3$): δ 118.4 (q, J = 320.1 Hz, CF_3), 74.0, 69.4, 54.5; **LRMS (APCI)**: *m*/*z* 386.06 $[M + H]^+$ (calcd for $C_4H_{12}B_{10}BrF_3O_3S$ 386.07).

1-(Pyridin-3-yl(((trifluoromethyl)sulfonyl)oxy)methyl)-1,2-dicarba-*closo*-dodecaborane(12) (**179**)

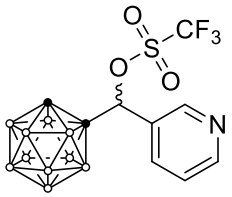

This compound was synthesised according to General Procedure F using **81** (29.0 mg, 115 μmol). The crude product was washed with petroleum benzine to give **179** (38.8 mg, 88%) as an off-white powder which was used without further purification. **^{1}H NMR** (500 MHz, acetone-d_6): δ 9.00 (d, J = 2.1 Hz, 1H, Ar–H), 8.98 (dd, J = 5.5, 1.5 Hz, 1H, Ar–H), 8.56 (dt, J = 8.1, 1.6 Hz, 1H, Ar–H), 8.08 (dd, J = 8.1, 5.5 Hz, 1H, Ar–H), 5.78 (s, 1H, O–CH), 4.89 (s, 1H, C_{cage}–H), 3.11–1.35 (br m, 10H, B–H); **^{11}B{^{1}H} NMR** (160 MHz, acetone-d_6): δ -3.6 (1B), -4.4 (1B), -9.0 (1B), -9.5 (1B), -12.1 (3B), -12.9 (1B), -13.5 (1B), -14.2 (1B); **^{13}C{^{1}H} NMR** (125 MHz, acetone-d_6): δ 145.7, 143.8, 143.1, 140.3, 127.1, 121.8 (q, J = 320.4 Hz, CF_3), 80.0, 71.7, 61.3.

N-Hydroxymethylphthalimide (**183**)

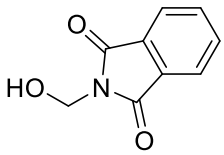

Distilled water (10 mL) was added to phthalimide (4.18 g, 28.4 mmol) and the mixture was stirred at RT for 10 min. An aqueous solution of formaldehyde (~37 *wt*%, 2.7 mL, 36 mmol) was added and the resulting heterogeneous solution was heated at 100 °C for 1.5 h, during which it became clear. The reaction was cooled to 0 °C and the resulting precipitate was collected by filtration, washed with cold water and dried at the pump to give **183** (4.84 g, 96%) as a colourless powder. **^{1}H NMR** (500 MHz, $CDCl_3$): δ 7.89 (dd, J = 5.5, 3.1 Hz, 1H), 7.75 (dd, J = 5.5, 3.1 Hz, 1H), 5.26 (d, J = 7.2 Hz, 1H), 3.41 (t, J = 7.9 Hz, 1H); **^{13}C{^{1}H} NMR** (125 MHz, $CDCl_3$): δ 168.0, 134.6, 132.1, 123.9, 61.7. The characterisation data matches that reported in the literature.[220]

N-Bromomethylphthalimide (**153**)

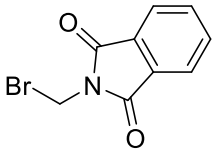

N-hydroxymethylphthalimide (970 mg, 5.48 mmol) was suspended in hydrobromic acid (4 mL, 48% in water) and the heterogeneous solution was cooled to 0 ºC. Concentrated sulfuric acid (1.5 mL) was added dropwise and the solution was heated to 70 ºC for 16 h. The reaction was cooled to 0 °C and the solids were collected by filtration. The solids were washed with ice-cold water (3 × 5 mL), 10% aqueous ammonium hydroxide (2 ° 3 mL) and ice-cold water (3 × 5 mL) again. The solids were dried at the pump and collected to give **153** (922 mg, 70%) as a colourless powder. **^{1}H NMR** (500 MHz, $CDCl_3$): δ 7.92 (dd, *J* = 5.5, 3.1 Hz, 2H), 7.79 (dd, *J* = 5.5, 3.1 Hz, 2H), 5.48 (s, 2H); **^{13}C{^{1}H} NMR** (125 MHz, $CDCl_3$): δ 165.9, 135.0, 132.0, 124.2, 31.3. The characterisation data matches that reported in the literature.[221]

1-Phthalimidomethyl-1,7-dicarba-*closo*-dodecaborane(12) (**154**)

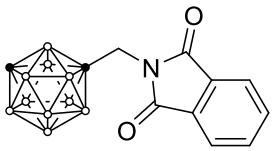

Compound **157** (385 mg, 1.26 mmol) and potassium phthalimide (255 mg, 1.38 mmol) were suspended in anhydrous DMF (1 mL) and the mixture was stirred at 50 °C until the starting material was consumed (monitored by TLC; eluent 10% DCM in petroleum benzine). The reaction was diluted with ether (10 mL) and washed with water (3 × 10 mL). The organic layer was dried over sodium sulfate, filtered and reduced *in vacuo*. The resultant solids were suspended in ice-cold petroleum benzine (2 mL), filtered and washed with ice-cold petroleum benzine (1 mL). The solids were dried at the pump and collected to give **154** (355 mg, 93%) as colourless flakes. **^{1}H NMR** (500 MHz, $CDCl_3$): δ 7.88 (dd, *J* = 5.4, 3.1 Hz, 2H, Ar–H), 7.76 (dd, *J* = 5.5, 3.0 Hz, 2H, Ar–H), 4.11 (s, 2H, CH_2), 2.94 (s, 1H, C_{cage}–H), 2.92–1.52 (br m, 10H, B–H); **^{11}B{^{1}H} NMR** (160 MHz, $CDCl_3$): δ -4.2 (1B), -9.1 (1B), -10.5 (2B), -11.1 (2B), -13.4 (2B), -15.5 (2B); **^{13}C{^{1}H} NMR** (125 MHz, $CDCl_3$): δ 167.2, 134.6, 131.6, 123.9, 74.0, 55.5, 41.6; **LRMS (APCI)**: *m*/*z* 304.28 $[M + H]^+$ (calcd for $C_{11}H_{17}B_{10}NO_2$ 304.23).

9-Bromo-1-phthalimidomethyl-1,7-dicarba-*closo*-dodecaborane(12) (**159**)

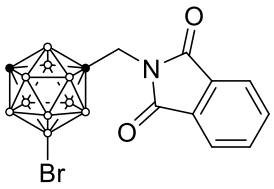

Compound **168** (240 mg, 623 μmol) and potassium phthalimide (127 mg, 685 μmol) were suspended in anhydrous DMF (1 mL) and the mixture was stirred at RT until the starting material was consumed (monitored by TLC; eluent 20% DCM in petroleum benzine). The reaction was diluted with ether (10 mL) and washed with water (3 × 10 mL). The organic layer was dried over sodium sulfate, filtered and reduced *in vacuo*. The resultant solids were loaded onto Celite filter-aid and purified by means of flash chromatography on silica (50% DCM in petroleum benzine) to give **159** (176 mg, 74%) as a colourless, microcrystalline solid. **^{1}H NMR** (500 MHz, $CDCl_3$): δ 7.90 (dd, *J* = 5.5, 3.0 Hz, 2H, Ar–H), 7.78 (dd, *J* = 5.5, 3.0 Hz, 2H, Ar–H), 4.13 (s, 2H, CH_2), 3.51–1.62 (br m, 9H, B–H), 3.01 (s, 1H, C_{cage}–H); **^{11}B{^{1}H} NMR** (160 MHz, $CDCl_3$): δ ^{11}B NMR (160 MHz, $CDCl_3$) δ -3.8 (1B), -6.4 (1B), -8.5 (1B), -9.2 (1B), -10.7 (1B), -11.8 (1B), -12.8 (1B), -14.1 (1B), -16.3 (1B), -19.6 (1B); **^{11}B NMR** (160 MHz, $CDCl_3$): δ -3.8 (d, 1B), -6.4 (s, 1B, B9), -8.5 (d, 1B), -9.2 (d, 1B), -10.7 (d, 1B), -11.8 (d, 1B), -12.8 (d, 1B), -14.1 (d, 1B), -16.3 (d, 1B), -19.6 (d, 1B); **^{13}C{^{1}H} NMR** (125 MHz, $CDCl_3$): δ 167.1, 134.8, 131.5, 124.1, 73.5, 54.7, 41.4; **LRMS (APCI)**: *m/z* 383.18 $[M + H]^+$ (calcd for $C_{11}H_{16}B_{10}BrNO_2$ 383.14).

9-Phenylamino-1-phthalimidomethyl-1,7-dicarba-*closo*-dodecaborane(12) (**160**)

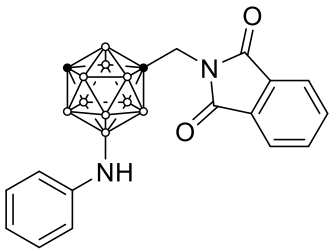

Anhydrous tribasic potassium phosphate (51.4 mg, 242 μmol) was added to an oven-dried Schlenk tube and the tube was heated at 150 °C under vacuum for 15 min. The tube was cooled to RT and compound **159** (20.5 mg, 53.6 μmol), tris(2-methoxyphenyl)phosphine (4.0 mg, 11 μmol) and palladium(II) acetate (1.4 mg, 6.2 μmol) were added as solids. The tube was evacuated and backfilled with nitrogen three times before anhydrous DME (0.5 mL) was added followed by aniline (7.5 μL, 82 μmol). The tube was sealed at the J. Young valve and stirred in a preheated oil bath at 100 °C for 20 h. Upon completion, the reaction was cooled to RT and filtered through a short pad of Celite filter-aid. The filter cake was rinsed with ethyl acetate (3 × 1 mL) and the combined filtrates were reduced *in vacuo*. The resulting residue was loaded onto Celite filter-aid and purified by means of flash chromatography on silica (50% DCM in petroleum benzine to 100% DCM) to give **160** (18.8 mg, 89%) as a colourless oil that discoloured upon standing. **^{1}H NMR** (500 MHz, $CDCl_3$): δ 7.89 (dd, *J* = 5.5, 3.0 Hz, 2H, Ar–H), 7.77 (dd, *J* = 5.5, 3.0 Hz, 2H, Ar–H), 7.15 (t, *J* = 7.6 Hz, 2H, Ar–H), 6.94 (d, *J* = 7.9 Hz, 2H, Ar–H), 6.76 (t, *J* = 7.4 Hz, 1H, Ar–H), 4.11 (s, 2H, CH_2), 3.38–1.46 (br m, 9H, B–H), 2.86 (s, 1H, C_{cage}–H); **^{11}B{^{1}H} NMR** (160 MHz, $CDCl_3$): δ 2.1 (1B), -5.0 (1B), -9.8 (1B), -11.2 (1B), -12.1 (1B), -13.3 (1B), -14.5 (1B), -15.6 (1B), -17.6 (1B), -21.7 (1B); **^{11}B NMR** (160 MHz, $CDCl_3$): δ 2.1 (s, 1B, B9), -5.0 (d, 1B), -9.8 (d, 1B), -11.2 (d, 1B), -12.1 (d, 1B), -13.3 (d, 1B), -14.5 (d, 1B), -15.6 (d, 1B), -17.6 (d, 1B), -21.7 (d, 1B); **^{13}C{^{1}H} NMR** (125 MHz, $CDCl_3$): δ 167.1, 146.5, 134.7, 131.6, 129.2, 124.0, 119.1, 116.6, 69.8, 51.3, 41.6.

9-Methanesulfonamido-1-phthalimidomethyl-1,7-dicarba-*closo*-dodecaborane(12) (**161**)

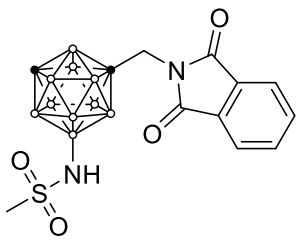

Anhydrous potassium phosphate tribasic (31.3 mg, 147 μmol) was added to an oven-dried Schlenk tube and the tube was heated at 150 °C under vacuum for 15 min. The tube was cooled to RT and compound **159** (23.0 mg, 60.2 μmol), methanesulfonamide (9.4 mg, 99 μmol), SPhos (1.5 mg, 3.7 μmol) and SPhos-Pd-G3 (2.7 mg, 3.5 μmol) were added as solids. The tube was evacuated and backfilled with nitrogen three times before anhydrous DME (0.3 mL) was added. The tube was sealed at the J. Young valve and stirred in a preheated oil bath at 100 °C for 16 h. Upon completion, the reaction was cooled to RT and filtered through a short pad of Celite filter-aid. The filter cake was rinsed with ethyl acetate (3 × 1 mL) and the combined filtrates were reduced *in vacuo*. The resulting residue was loaded onto Celite filter-aid and purified by means of flash chromatography on silica (100% DCM to 10% ethyl acetate in DCM) to give **161** (17.5 mg, 73%) as a colourless oil. **^{1}H NMR** (500 MHz, $CDCl_3$): δ 7.92–7.86 (m, 2H, Ar–H), 7.80–7.75 (m, 2H, Ar–H), 4.48 (br s, 1H, NH), 4.11 (s, 2H, CH_2), 3.37–1.49 (br m, 9H, B–H), 2.99 (s, 3H, CH_3), 2.94 (s, 1H, C_{cage}–H); **^{11}B{^{1}H} NMR** (160 MHz, $CDCl_3$): δ -0.5 (1B), -4.9 (1B), -9.7 (1B), -11.0 (1B), -12.0 (1B), -13.1 (1B), -14.1 (1B), -15.2 (1B), -17.3 (1B), -20.5 (1B); **^{11}B NMR** (160 MHz, $CDCl_3$): δ -0.5 (s, 1B, B9), -4.9 (d, 1B), -9.7 (d, 1B), -11.0 (d, 1B), -12.0 (d, 1B), -13.1 (d, 1B), -14.1 (d, 1B), -15.2 (d, 1B), -17.3 (d, 1B), -20.5 (d, 1B); **^{13}C{^{1}H} NMR** (125 MHz, $CDCl_3$): δ 167.1, 134.8, 131.5, 124.1, 71.2, 52.4, 42.0, 41.4; **LRMS (APCI)**: *m*/*z* 397.25 $[M + H]^+$ (calcd for $C_{12}H_{20}B_{10}N_2O_4S$ 397.22).

9-Hydroxy-1-phthalimidomethyl-1,7-dicarba-*closo*-dodecaborane(12) (**162**)

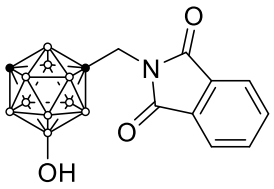

Compound **159** (24.9 mg, 65.1 µmol), SPhos (1.2 mg, 2.9 µmol) and SPhos-Pd-G3 (2.6 mg, 3.3 µmol) were added to an oven-dried Schlenk tube and the tube was evacuated and backfilled with nitrogen three times. Anhydrous dioxane (0.3 mL) was added followed by a deoxygenated aqueous solution of potassium phosphate (1 M, 0.1 mL, 100 µmol). The mixture was stirred vigorously in a preheated oil bath at 80 °C for 1 h. Upon completion, the reaction was cooled to RT and diluted with ethyl acetate (3 mL) and water (3 mL). The organic layer was collected and the aqueous layer was further extracted with ethyl acetate (3 mL). The combined organic extracts were dried over sodium sulfate, filtered and reduced *in vacuo*. The resulting residue was loaded onto Celite filter-aid and purified by means of flash chromatography on silica (10% ethyl acetate to 40% ethyl acetate in petroleum benzine) to give **162** (7.3 mg, 35%) as a colourless powder. **^{1}H NMR** (500 MHz, acetone-d_6): δ 7.96–7.88 (m, 4H, Ar–H), 4.49 (s, 1H, OH), 4.10 (s, 2H, CH_2), 3.39 (s, 1H, C_{cage}–H), 3.13–1.37 (br m, 9H, B–H); **^{11}B{^{1}H} NMR** (160 MHz, acetone-d_6): δ 9.5 (1B), -6.0 (1B), -10.7 (1B), -12.0 (1B), -12.7 (1B), -15.0 (2B), -17.2 (1B), -18.9 (1B), -25.9 (1B); **^{11}B NMR** (160 MHz, acetone-d_6): δ 9.5 (s, 1B, B9), -6.0 (d, 1B), -10.7 (d, 1B), -12.0 (d, 1B), -12.7 (d, 1B), -15.0 (d, 2B), -17.2 (d, 1B), -18.9 (d, 1B), -25.9 (d, 1B); **^{13}C{^{1}H} NMR** (125 MHz, acetone-d_6): δ 167.8, 135.7, 132.5, 124.3, 69.1, 50.8, 42.3; **LRMS (APCI)**: *m*/*z* 320.28 $[M + H]^+$ (calcd for $C_{11}H_{17}B_{10}NO_3$ 320.23).

9-Azido-1-phthalimidomethyl-1,7-dicarba-*closo*-dodecaborane(12) (**163**)

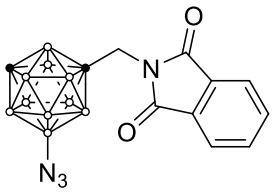

Anhydrous tribasic potassium phosphate (80.0 mg, 377 μmol) was added to an oven-dried Schlenk tube and the tube was heated at 150 °C under vacuum for 15 min. The tube was cooled to RT and compound **159** (145 mg, 380 μmol), sodium azide (52.3 mg, 804 μmol), SPhos (11.2 mg, 27.3 μmol) and SPhos-Pd-G3 (21.3 mg, 27.3 μmol) were added as solids. The tube was evacuated and backfilled with nitrogen three times before anhydrous DME (1 mL) was added. The tube was sealed at the J. Young valve and stirred in a preheated oil bath at 100 °C for 16 h. Upon completion, the reaction was cooled to RT and filtered through a short pad of Celite filter-aid. The filter cake was rinsed with ethyl acetate (3 × 1 mL) and the combined filtrates were reduced *in vacuo*. The resulting residue was loaded onto Celite filter-aid and purified by means of flash chromatography on silica (30% DCM to 50% DCM in petroleum benzine) to give **163** (82.8 mg, 63%) as a pale-red powder. **^{1}H NMR** (500 MHz, $CDCl_3$): δ 7.92–7.87 (m, 2H, Ar–H), 7.81–7.75 (m, 2H, Ar–H), 4.12 (s, 2H, CH_2), 3.37–1.22 (br m, 9H, B–H), 2.91 (s, 1H, C_{cage}–H); **^{11}B{^{1}H} NMR** (160 MHz, $CDCl_3$): δ 1.9 (1B), -5.4 (1B), -10.1 (1B), -11.3 (1B), -12.4 (1B), -13.0 (1B), -14.5 (1B), -15.3 (1B), -17.4 (1B), -21.3 (1B); **^{11}B NMR** (160 MHz, $CDCl_3$): δ 1.9 (s, 1B, B9), -5.4 (d, 1B), -10.1 (d, 1B), -11.3 (d, 1B), -12.4 (d, 1B), -13.0 (d, 1B), -14.5 (d, 1B), -15.3 (d, 1B), -17.4 (d, 1B), -21.3 (d, 1B); **^{13}C{^{1}H} NMR** (125 MHz, $CDCl_3$): δ 167.1, 134.8, 131.5, 124.1, 71.0, 52.1, 41.4; **LRMS (APCI)**: *m*/*z* 345.24 $[M + H]^+$ (calcd for $C_{11}H_{16}B_{10}N_4O_2$ 345.24).

9-Bromo-1-(((diphenylmethylene)amino)methyl)-1,7-dicarba-*closo*-dodecaborane(12) (**169**)

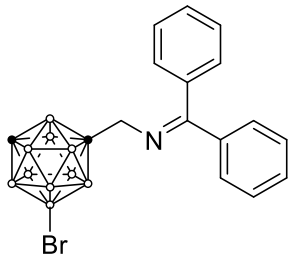

Compound **168** (67.3 mg, 175 μmol), benzophenone imine (35.9 mg, 198 μmol) and anhydrous sodium acetate (53.5 mg, 652 μmol) were suspended in anhydrous acetonitrile (1 mL) and the mixture was stirred at reflux for 16 h. The solvent was removed *in vacuo* and ethyl acetate (5 mL) was added to the residue. The organic layer was washed with water (3 × 5 mL), dried over sodium sulfate, filtered and reduced *in vacuo*. The resultant solids were loaded onto Celite filter-aid and purified by means of flash chromatography on silica (25% toluene in petroleum benzine to 50% toluene in petroleum benzine) to give **169** (176 mg, 47%) as a colourless oil. **^{1}H NMR** (500 MHz, $CDCl_3$): δ 7.84–7.78 (m, 4H, Ar–H), 7.63–7.55 (m, 2H, Ar–H), 7.52–7.45 (m, 4H, Ar–H), 4.30 (s, 2H, CH_2), 3.43–1.64 (br m, 9H, B–H), 3.02 (s, 1H, C_{cage}–H); **^{11}B{^{1}H} NMR** (160 MHz, $CDCl_3$): δ -3.9 (1B), -6.5 (1B), -8.1 (1B), -9.3 (1B), -11.0 (1B), -12.4 (1B), -12.7 (1B), -14.1 (1B), -16.6 (1B), -19.8 (1B); **^{11}B NMR** (160 MHz, $CDCl_3$): δ -3.9 (d, 1B), -6.5 (s, 1B, B9), -8.1 (d, 1B), -9.3 (d, 1B), -11.0 (d, 1B), -12.4 (d, 1B), -12.7 (d, 1B), -14.1 (d, 1B), -16.6 (d, 1B), -19.8 (d, 1B); **^{13}C{^{1}H} NMR** (125 MHz, $CDCl_3$): δ 169.5, 137.8, 132.6, 130.2, 128.4, 72.5, 64.0, 54.3; **LRMS (APCI)**: *m*/*z* 417.17 $[M + H]^+$ (calcd for $C_{16}H_{22}B_{10}BrN$ 417.20).

N-(2-Bromoethyl)phthalimide (**170**)

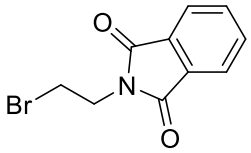

N-(2-hydroxyethyl)phthalimide (676 mg, 3.54 mmol) was added to an oven-dried flask and the flask was evacuated and back-filled with nitrogen three times. PBr_3 (1.0 mL, 11 mmol) was added and the mixture was heated at reflux for 30 min. The reaction was cooled, poured onto ice water and the solids were collected by filtration. The crude product was loaded onto Celite filter-aid and purified by means of flash chromatography on silica (5% ethyl acetate to 20% ethyl acetate in petroleum benzine) to give **170** (148 mg, 17%) as a colourless powder. **^{1}H NMR** (500 MHz, $CDCl_3$): δ 7.88 (dd, *J* = 5.5, 3.1 Hz, 2H, Ar–H), 7.75 (dd, *J* = 5.5, 3.0 Hz, 2H, Ar–H), 4.11 (t, *J* = 6.7 Hz, 2H, CH_2), 3.62 (t, *J* = 6.8 Hz, 2H, CH_2). The characterisation data matches that reported in the literature.[222]

1-Phthalimidoethyl-1,2-dicarba-*closo*-dodecaborane(12) (**172**)

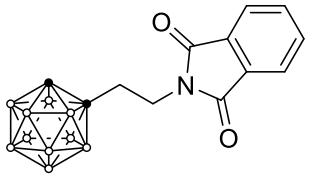

Compound *closo*-1,2-carborane (73.7 mg, 511 μmol) was added to an oven-dried, two-neck flask and the flask was evacuated and back-filled with nitrogen three times. The solids were dissolved in anhydrous DME (2 mL) and the resulting solution was cooled to -78 °C, to which *n*-butyllithium (1.5 M in hexanes, 340 μL, 510 μmol) was added dropwise. The mixture was stirred at the same temperature for 15 min before a solution of *N*-(2-bromoethyl)phthalimide (131 mg, 514 μmol) in anhydrous DME (2 mL) was added dropwise. The reaction was stirred at RT for 16 h, before the mixture was reduced *in vacuo*. Water (3 mL) was added to the residue and the aqueous layer was extracted with diethyl ether (2 × 3 mL). The combined organic extracts were dried over sodium sulfate, filtered and reduced *in vacuo*. The crude product was loaded onto Celite filter-aid and purified by means of flash chromatography on silica (30% DCM to 70% DCM in petroleum benzine) to give **172** (54.9 mg, 34%) as colourless prisms. **^{1}H NMR** (300 MHz, $CDCl_3$): δ 7.84 (dd, *J* = 5.4, 3.1 Hz, 2H, Ar–H), 7.74 (dd, *J* = 5.5, 3.1 Hz, 2H, Ar–H), 3.80 (t, *J* = 8.4 Hz, 2H, CH_2), 3.75 (s, 1H, C_{cage}–H), 3.33–1.12 (br m, 10H, B–H), 2.58 (t, *J* = 8.4 Hz, 2H, CH_2); **^{11}B{^{1}H} NMR** (96 MHz, $CDCl_3$): δ -2.1 (1B), -5.2 (1B), -9.0 (2B), -11.7 (2B), -12.2 (1B), -12.7 (2B). The characterisation data matches that reported in the literature.[204]

1-Phthalimidopropyl-1,2-dicarba-*closo*-dodecaborane(12) (**173**)

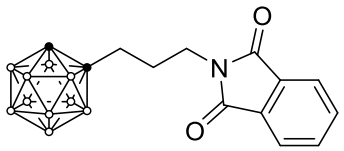

Compound *closo*-1,2-carborane (58.1 mg, 192 μmol) was added to an oven-dried, two-neck flask and the flask was evacuated and back-filled with nitrogen three times. The solids were dissolved in anhydrous DME (2 mL) and the resultant solution was cooled to -78 °C, to which *n*-butyllithium (1.5 M in hexanes, 270 μL, 405 μmol) was added dropwise. The mixture was stirred at the same temperature for 15 min before a solution of *N*-(2-bromopropyl)phthalimide (110 mg, 410 μmol) in anhydrous DME (2 mL) was added dropwise. The reaction was stirred at RT for 16 h, before the mixture was reduced *in vacuo*. Water (3 mL) was added to the residue and the aqueous layer was extracted with diethyl ether (2 × 3 mL). The combined organic extracts were dried over sodium sulfate, filtered and reduced *in vacuo*. The crude product was loaded onto Celite filter-aid and purified by means of flash chromatography on silica (30% DCM to 70% DCM in petroleum benzine) to give **173** (82.5 mg, 62%) as a colourless powder. **^{1}H NMR** (300 MHz, $CDCl_3$): δ 7.86 (dd, *J* = 5.4, 3.1 Hz, 2H, Ar–H), 7.74 (dd, *J* = 5.5, 3.1 Hz, 2H, Ar–H), 3.66 (t, *J* = 6.9 Hz, 2H, N–CH_2), 3.60 (s, 1H, C_{cage}–H), 3.23–1.12 (br m, 10H, B–H), 2.28 (t, *J* = 8.1 Hz, 2H, C_{cage}–CH_2), 1.93–1.81 (m, 2H, C–CH_2–C); **^{11}B{^{1}H} NMR** (96 MHz, $CDCl_3$): δ -2.2 (1B), -5.6 (1B), -9.2 (2B), -11.6 (2B), -12.1 (1B), -13.0 (2B). The characterisation data matches that reported in the literature.[181]

1-((2-Aminophenyl)amino)methyl-1,2-dicarba-*closo*-dodecaborane(12) (**175**)

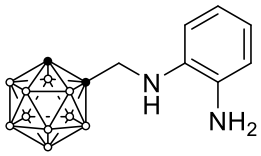

Compound **174** (32.0 mg, 104 μmol), *ortho*-phenylenediamine (40.1 mg, 371 μmol) and sodium acetate (20.4 mg, 318 μmol) were suspended in anhydrous acetonitrile (1 mL) and the reaction was stirred at RT for 16 h. The solvent was removed *in vacuo*, ethyl acetate (5 mL) was added and the organic layer was washed with water (3 × 5 mL). The organic layer was dried over sodium sulfate, filtered and reduced *in vacuo*. The crude product was loaded onto Celite filter-aid and purified by means of flash chromatography on silica (10% ethyl acetate to 50% ethyl acetate in petroleum benzine) to give **175** (6.7 mg, 24%) as an off-white powder. **^{1}H NMR** (300 MHz, $CDCl_3$): δ 6.87–6.78 (m, 1H, Ar–H), 6.79–6.74 (m, 2H, Ar–H), 6.66–6.60 (m, 1H, Ar–H), 3.87 (s, 2H, CH_2), 3.81 (s, 1H, C_{cage}–H), 3.35–1.01 (br m, 10H, B–H); **^{11}B{^{1}H} NMR** (96 MHz, $CDCl_3$): δ -2.3 (1B), -5.2 (1B), -9.2 (2B), -11.5 (2B), -13.0 (4B).

1-((Phthalimido)oxy)methyl-1,2-dicarba-*closo*-dodecaborane(12) (**176**)

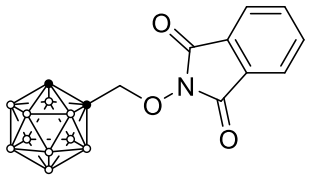

Compound **174** (22.1 mg, 72.2 μmol), *N*-hydroxyphthalimide (16.1 mg, 98.7 μmol) and K_2CO_3 (15.8 mg, 114 μmol) were suspended in anhydrous DMF (1 mL) and the reaction was stirred at RT for 16 h. The reaction was diluted with ether (5 mL) and washed with brine (5 mL) and water (2 × 5 mL). The organic layer was dried over sodium sulfate, filtered and reduced *in vacuo*. The crude product was loaded onto Celite filter-aid and purified by means of flash chromatography on silica (10% DCM to 50% DCM in petroleum benzine) to give **176** (2.6 mg, 11%) as a colourless oil. **^{1}H NMR** (300 MHz, $CDCl_3$): δ 7.91–7.83 (m, 2H, Ar–H), 7.83–7.75 (m, 2H, Ar–H), 4.62 (s, 2H, CH_2), 4.57 (s, 1H, C_{cage}–H), 3.33–0.84 (br m, 10H, B–H); **^{11}B{^{1}H} NMR** (96 MHz, $CDCl_3$): δ -2.5 (1B), -3.9 (1B), -8.9 (2B), -11.7 (2B), -12.8 (4B).

1-(1*H*-Benzo[*d*]imidazol-2-yl)-1,2-dicarba-*closo*-dodecaborane(12) (**178**)

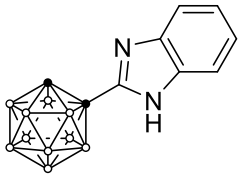

Compound **72** (32.5 mg, 189 μmol) and *ortho*-phenylenediamine (21.6 mg, 200 μmol) were dissolved in anhydrous toluene (1 mL) and anhydrous iron(III) trichloride (5.9 mg, 36 μmol) was added. The reaction was stirred vigorously in an open flask at reflux for 24 h. Upon completion, the reaction was allowed to cool to RT and reduced *in vacuo*. The crude product was loaded onto Celite filter-aid and purified by means of flash chromatography on silica (1% ethyl acetate to 15% ethyl acetate in petroleum benzine) to give **178** (34.6 mg, 70%) as a colourless powder. **^{1}H NMR** (300 MHz, $CDCl_3$): δ 9.31 (s, 1H, NH), 7.74–7.65 (m, 1H, Ar–H), 7.50–7.41 (m, 1H, Ar–H), 7.42–7.27 (m, 2H, Ar–H), 4.73 (s, 1H, C_{cage}–H), 3.41–1.05; **^{11}B{^{1}H} NMR** (96 MHz, acetone-d_6): δ -3.5 (2B), -9.2 (2B), -10.5 (2B), -11.9 (2B); **LRMS (APCI)**: *m*/*z* 260.28 $[M + H]^+$ (calcd for $C_9H_{16}B_{10}N_2$ 261.24). The characterisation data matches that reported in the literature.[205]

1-Amino(pyridin-3-yl)methyl-1,2-dicarba-*closo*-dodecaborane(12) (**180**)

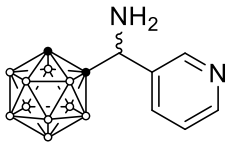

Compound **179** (35.0 mg, 91.3 umol) was dissolved in DMF (0.5 mL) and a solution of ammonia in methanol (6.5 M, 60 uL, 0.39 mmol) was added. The dark-yellow solution was stirred at RT for 16 h before saturated $NaHCO_3$ (3 mL) was added. The aqueous layer was extracted with ethyl acetate (5 mL) and the organic layer was washed with brine (2 × 3 mL). The organic layer was dried over sodium sulfate, filtered and reduced *in vacuo*. The crude product was loaded onto Celite filter-aid and purified by means of flash chromatography on silica (10% ethyl acetate to 50% ethyl acetate in petroleum benzine) to give **180** (17.4 mg, 76%) as an off-white powder. **^{1}H NMR** (300 MHz, $CDCl_3$): δ 8.61 (d, *J* = 2.3 Hz, 1H, Ar–H), 8.57 (dd, *J* = 4.8, 1.6 Hz, 1H, Ar–H), 7.84 (dt, *J* = 8.0, 2.1 Hz, 1H, Ar–H), 7.41 (dd, *J* = 7.9, 4.8 Hz, 1H, Ar–H), 6.44 (br s, 1H, NH_2), 5.51 (s, 1H, NH_2–CH), 4.80 (s, 1H, C_{cage}–H); 3.27–1.05 (br m, 10H, B–H); **^{11}B{^{1}H} NMR** (96 MHz, $CDCl_3$): δ -3.9 (1B), -4.8 (1B), -9.6 (2B), -11.9 (3B), -13.0 (1B), -13.8 (2B).

9-Bromo-1-hydroxymethyl-1,7-dicarba-*closo*-dodecaborane(12) (**184**)

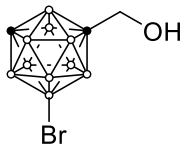

Compound **182** (340 mg, 1.52 mmol) was added to an oven-dried, two-neck flask and the flask was evacuated and back-filled with nitrogen three times. The solids were dissolved in anhydrous diethyl ether (3 mL) and the resulting solution was cooled to -78 °C, to which *n*-butyllithium (1.6 M in hexanes, 1.0 mL, 1.6 mmol) was added dropwise. The solution was stirred at the same temperature for 15 min before methyl formate (0.3 mL, 5 mmol) was added to the reaction mixture in one portion. Stirring was continued for 1 h at -78 °C before the reaction was quenched slowly with 1 M HCl (3 mL) and allowed to warm to RT. The formyl-carborane was extracted with ether (3 × 5 mL) and the combined extracts were dried over sodium sulfate, filtered and reduced *in vacuo*. The residue was dissolved in methanol (5 mL), cooled to 0 °C and sodium borohydride (284 mg, 7.51 mmol) was added portion-wise. The heterogeneous mixture was stirred at RT until complete reduction of the aldehyde (monitored by TLC; eluent 25% DCM in petroleum benzine). The methanol was removed *in vacuo* and 1 M HCl (5 mL) was added to the residue. The aqueous layer was extracted with ether (3 × 5 mL) and the combined organic extracts were dried over sodium sulfate, filtered and reduced *in vacuo*. The crude product was loaded onto Celite filter-aid and purified by means of flash chromatography on silica (10% ethyl acetate to 30% ethyl acetate in petroleum benzine) to give **184** (266 mg, 69%) as a colourless powder. **^{1}H NMR** (500 MHz, $CDCl_3$): δ 3.84 (s, 2H, C$\underline{H}_2$), 3.47–1.63 (br m, 9H, B–$\underline{H}$), 3.02 (s, 1H, C_{cage}–$\underline{H}$); **^{11}B{^{1}H} NMR** (160 MHz, $CDCl_3$): δ -4.2 (1B), -6.6 (1B), -8.5 (1B), -9.5 (1B), -11.3 (1B), -12.7 (2B), -14.1 (1B), -16.8 (1B), -20.0 (1B); **^{11}B NMR** (160 MHz, $CDCl_3$): δ -4.2 (d, J = 167.0 Hz, 1B), -6.6 (s, 1B), -8.5 (d, J = 171.1 Hz, 1B), -9.5 (d, J = 153.2 Hz, 1B), -11.3 (d, J = 175.5 Hz, 1B), -12.7 (d, J = 183.6 Hz, 2B), -14.1 (d, J = 175.5 Hz, 1B), -16.8 (d, J = 183.5 Hz, 1B), -20.0 (d, J = 182.1 Hz, 1B); **^{13}C{^{1}H} NMR** (125 MHz, $CDCl_3$): δ 65.1, 54.2, $\underline{C}_{cage}$–CH_2 not observed; **LRMS (APCI)**: *m*/*z* 254.16 $[M + H]^{+zz}$ (calcd for $C_3H_{13}B_{10}BrO$ 254.12).

In vitro MPO inhibition assays

Taurine chloramine assay

This assay was adapted from a procedure described in the literature.[192] The reactions were performed at 24 °C in clear flat-bottomed 96-well plates at a final reaction volume of 210 µL. The assay buffer was a 20 mM phosphate buffer at pH 7.4 containing NaCl (140 mM) and taurine (5 mM) supplemented with DMSO (5% *v/v*) and Polysorbate 20 (0.01% *v/v*). Stock solutions of fragments were prepared in DMSO immediately before use. MPO (10 nM) was incubated with the buffer containing the fragment at RT for 5 min. Reactions were initiated by adding H_2O_2 (50 µM) to each well and thoroughly mixing the contents. After 6 min, the reaction was terminated by adding catalase (20 µg/mL final concentration). The final reaction solution was then thoroughly mixed with a developing solution (50 µL) containing TMB (2 mM), sodium iodide (100 µM) and DMF (10% *v/v*) dissolved in 400 mM acetate buffer at pH 5.4. After 5 min, the absorbance of this solution at 650 nm was recorded. Percent (%) inhibition was determined by comparing the absorbance with an uninhibited reaction.

Multi-substrate assay

This assay was adapted from a procedure described in the literature.[165] The reactions were performed at 24 °C in clear flat-bottomed 96-well plates at a final reaction volume of 200 µL. The assay buffer was a 20 mM phosphate buffer at pH 7.4 containing NaCl (140 mM), NaSCN (50 µM), tyrosine (50 µM), urate (200 µM) and bovine serum albumin (1 mg/ml) supplemented with DMSO (5% *v/v*) and Polysorbate 20 (0.01% *v/v*). Stock solutions of fragments were prepared in DMSO immediately before use. MPO (7.5 nM) was incubated with the buffer containing the fragment at RT for 5 min and TNB (50 µM) was added. Reactions were initiated by adding H_2O_2 (50 µM) to each well and thoroughly mixing the contents. The loss of TNB absorbance at 412 nm was monitored at 15 s intervals for 10 min. The rate of reaction was calculated by fitting a line to the linear portion of the graph. Each reaction was run in parallel with an identical reaction without MPO to determine protein-independent bleaching, which was subtracted from the final rate. Percent (%) inhibition was determined by comparing the rate of the reaction with an uninhibited reaction.

7

References

(1) Bohacek, R. S.; McMartin, C.; Guida, W. C. The Art and Practice of Structure-Based Drug Design: A Molecular Modeling Perspective. *Med. Res. Rev.* **1996**, *16* (1), 3–50. https://doi.org/10.1002/(SICI)1098-1128(199601)16:1<3::AID-MED1>3.0.CO;2-6.

(2) Raju, T. N. The Nobel Chronicles. *Lancet* **2000**, *355* (9208), 1022. https://doi.org/10.1016/s0140-6736(05)74775-9.

(3) Taylor, R. D.; Maccoss, M.; Lawson, A. D. G. Rings in Drugs. *J. Med. Chem.* **2014**, *57* (14), 5845–5859. https://doi.org/10.1021/jm4017625.

(4) O' Connor, C. J.; Beckmann, H. S. G.; Spring, D. R. Diversity-Oriented Synthesis: Producing Chemical Tools for Dissecting Biology. *Chem. Soc. Rev.* **2012**, *41* (12), 4444–4456. https://doi.org/10.1039/c2cs35023h.

(5) Wills, T. J.; Lipkus, A. H. Structural Approach to Assessing the Innovativeness of New Drugs Finds Accelerating Rate of Innovation. *ACS Med. Chem. Lett.* **2020**, *11* (11), 2114–2119. https://doi.org/10.1021/acsmedchemlett.0c00319.

(6) Brown, P. H.; Bellaloui, N.; Wimmer, M. A.; Bassil, E. S.; Ruiz, J.; Hu, H.; Pfeffer, H.; Dannel, F.; Römheld, V. Boron in Plant Biology. *Plant. Biol.* **2002**, *4* (2), 205–223. https://doi.org/10.1055/s-2002-25740.

(7) Nielsen, F. H. Update on Human Health Effects of Boron. *J. Trace Elem. Med. Biol.* **2014**, *28* (4), 383–387. https://doi.org/10.1016/j.jtemb.2014.06.023.

(8) Leśnikowski, Z. J. Recent Developments with Boron as a Platform for Novel Drug Design. *Expert Opin. Drug Discov.* **2016**, *11* (6), 569–578. https://doi.org/10.1080/17460441.2016.1174687.

(9) Baker, S. J.; Ding, C. Z.; Akama, T.; Zhang, Y. K.; Hernandez, V.; Xia, Y. Therapeutic Potential of Boron-Containing Compounds. *Future Med. Chem.* **2009**, *1* (7), 1275–1288. https://doi.org/10.4155/fmc.09.71.

(10) Groll, M.; Berkers, C. R.; Ploegh, H. L.; Ovaa, H. Crystal Structure of the Boronic Acid-Based Proteasome Inhibitor Bortezomib in Complex with the Yeast 20S Proteasome. *Structure* **2006**, *14* (3), 451–456. https://doi.org/10.1016/j.str.2005.11.019.

(11) Adams, J.; Behnke, M.; Chen, S.; Cruickshank, A. A.; Dick, L. R.; Grenier, L.; Klunder, J. M.; Ma, Y. T.; Plamondon, L.; Stein, R. L. Potent and Selective Inhibitors of the Proteasome: Dipeptidyl Boronic Acids. *Bioorg. Med. Chem. Lett.* **1998**, *8* (4), 333–338. https://doi.org/10.1016/S0960-894X(98)00029-8.

(12) Azab, A. K.; Muz, B.; Ghazarian, R.; Ou, M.; Luderer, M.; Kusdono, H. Spotlight on Ixazomib: Potential in the Treatment of Multiple Myeloma. *Drug Des. Devel. Ther.* **2016**, *10*, 217. https://doi.org/10.2147/DDDT.S93602.

(13) Dowlut, M.; Hall, D. G. An Improved Class of Sugar-Binding Boronic Acids, Soluble and Capable of Complexing Glycosides in Neutral Water. *J. Am. Chem. Soc.* **2006**, *128* (13), 4226–4227. https://doi.org/10.1021/ja057798c.

(14) Liu, C. T.; Tomsho, J. W.; Benkovic, S. J. The Unique Chemistry of Benzoxaboroles: Current and Emerging Applications in Biotechnology and Therapeutic Treatments. *Bioorg. Med. Chem.* **2014**, *22* (16), 4462–4473. https://doi.org/10.1016/j.bmc.2014.04.065.

(15) Rock, F. L.; Mao, W.; Yaremchuk, A.; Tukalo, M.; Crépin, T.; Zhou, H.; Zhang, Y.-K.; Hernandez, V.; Akama, T.; Baker, S. J.; Plattner, J. J.; Shapiro, L.; Martinis, S. A.; Benkovic, S. J.; Cusack, S.; Alley, M. R. K. An Antifungal Agent Inhibits an Aminoacyl-TRNA Synthetase by Trapping TRNA in the Editing Site. *Science* **2007**, *316* (5832), 1759–1761. https://doi.org/10.1126/science.1142189.

(16) Akama, T.; Baker, S. J.; Zhang, Y. K.; Hernandez, V.; Zhou, H.; Sanders, V.; Freund, Y.; Kimura, R.; Maples, K. R.; Plattner, J. J. Discovery and Structure-Activity Study of a Novel Benzoxaborole Anti-Inflammatory Agent (AN2728) for the Potential Topical Treatment of Psoriasis and Atopic Dermatitis. *Bioorg. Med. Chem. Lett.* **2009**, *19* (8), 2129–2132. https://doi.org/10.1016/j.bmcl.2009.03.007.

(17) Novelli, A.; Del Giacomo, P.; Rossolini, G. M.; Tumbarello, M. Meropenem/Vaborbactam: A next Generation β-Lactam β-Lactamase Inhibitor Combination. *Expert Rev. Anti-Infect. Ther.* **2020**, *18* (7), 643–655. https://doi.org/10.1080/14787210.2020.1756775.

(18) Hecker, S. J.; Reddy, K. R.; Totrov, M.; Hirst, G. C.; Lomovskaya, O.; Griffith, D. C.; King, P.; Tsivkovski, R.; Sun, D.; Sabet, M.; Tarazi, Z.; Clifton, M. C.; Atkins, K.; Raymond, A.; Potts, K. T.; Abendroth, J.; Boyer, S. H.; Loutit, J. S.; Morgan, E. E.; Durso, S.; Dudley, M. N. Discovery of a Cyclic Boronic Acid β-Lactamase Inhibitor (RPX7009) with Utility vs Class A Serine Carbapenemases. *J. Med. Chem.* **2015**, *58* (9), 3682–3692. https://doi.org/10.1021/acs.jmedchem.5b00127.

(19) Lanier, M.; Cole, D. C.; Istratiy, Y.; Klein, M. G.; Schwartz, P. A.; Tjhen, R.; Jennings, A.; Hixon, M. S. Repurposing Suzuki Coupling Reagents as a Directed Fragment Library Targeting Serine Hydrolases and Related Enzymes. *J. Med. Chem.* **2017**, *60* (12), 5209–5215. https://doi.org/10.1021/acs.jmedchem.6b01224.

(20) Zheng, F.; Yui, T. H.; Zhang, J.; Xie, Z. Synthesis and X-Ray Characterization of 15- and 16-Vertex *closo*-Carboranes. *Nat. Commun.* **2020**, *11* (1), 1–5. https://doi.org/10.1038/s41467-020-19661-5.

(21) Fisher, S. P.; Tomich, A. W.; Lovera, S. O.; Kleinsasser, J. F.; Guo, J.; Asay, M. J.; Nelson, H. M.; Lavallo, V. Nonclassical Applications of *closo*-Carborane Anions: From Main Group Chemistry and Catalysis to Energy Storage. *Chem. Rev.* **2019**, *119* (14), 8262–8290. https://doi.org/10.1021/acs.chemrev.8b00551.

(22) Marfavi, A.; Kavianpour, P.; Rendina, L. M. Carboranes in Drug Discovery, Chemical Biology and Molecular Imaging. *Nat. Rev. Chem.* **2022**, *6* (7), 486–504. https://doi.org/10.1038/s41570-022-00400-x.

(23) Meng, Y.; Lin, X.; Huang, J.; Zhang, L. Recent Advances in Carborane-based Crystalline Porous Materials. *Molecules* **2024**, *29* (16), 3916. https://doi.org/10.3390/molecules29163916.

(24) Zhang, X.; Rendina, L. M.; Müllner, M. Carborane-Containing Polymers: Synthesis, Properties, and Applications. *ACS Polym. Au* **2024**, *4* (1), 7–33. https://doi.org/10.1021/acspolymersau.3c00030.

(25) Grimes, R. N. Icosahedral Carboranes. In *Carboranes*; Elsevier, 2016; pp 283–502. https://doi.org/10.1016/b978-0-12-801894-1.00009-3.

(26) Grafstein, D.; Dvorak, J. Neocarboranes, a New Family of Stable Organoboranes Isomeric with the Carboranes. *Inorg. Chem.* **1963**, *2* (6), 1128–1133. https://doi.org/10.1021/ic50010a011.

(27) Papetti, S.; Heying, T. L. *p*-Carborane [1,12-Dicarbaclovododecaborane(12)]. *J. Am. Chem. Soc.* **1964**, *86* (11), 2295. https://doi.org/10.1021/ja01065a045.

(28) Laubbngayer, A. W.; Rysz, W. R. The Dipole Moments of the Isomers of Dicarbadecaborane, $B_{10}H_{10}C_2H_2$. *Inorg. Chem.* **1965**, *4* (10), 1513–1514. https://doi.org/10.1021/ic50032a043.

(29) Busby, D. C.; Hawthorne, M. F. The Crown Ether Promoted Base Degradation of *p*-Carborane. *Inorg. Chem.* **1982**, *21* (11), 4101–4103. https://doi.org/10.1021/ic00141a046.

(30) Soloway, A. H.; Tjarks, W.; Barnum, B. A.; Rong, F. G.; Barth, R. F.; Codogni, I. M.; Wilson, J. G. The Chemistry of Neutron Capture Therapy. *Chem. Rev.* **1998**, *98* (4), 1515–1562. https://doi.org/10.1021/cr941195u.

(31) Hatanaka, H.; Nakagawa, Y. Clinical Results of Long-Surviving Brain Tumor Patients Who Underwent Boron Neutron Capture Therapy. *Int. J. Radiat. Oncol. Biol. Phys.* **1994**, *28* (5), 1061–1066. https://doi.org/10.1016/0360-3016(94)90479-0.

(32) Calvaresi, M.; Zerbetto, F. In Silico Carborane Docking to Proteins and Potential Drug Targets. *J. Chem. Inf. Model.* **2011**, *51* (8), 1882–1896. https://doi.org/10.1021/ci200216z.

(33) Fanfrlík, J.; Lepšík, M.; Horinek, D.; Havlas, Z.; Hobza, P. Interaction of Carboranes with Biomolecules: Formation of Dihydrogen Bonds. *ChemPhysChem* **2006**, *7* (5), 1100–1105. https://doi.org/10.1002/cphc.200500648.

(34) Stockmann, P.; Gozzi, M.; Kuhnert, R.; Sárosi, M. B.; Hey-Hawkins, E. New Keys for Old Locks: Carborane-Containing Drugs as Platforms for Mechanism-Based Therapies. *Chem. Soc. Rev.* **2019**, *48* (13), 3497–3512. https://doi.org/10.1039/c9cs00197b.

(35) Hewitt, S. C.; Korach, K. S. Estrogen Receptors: Structure, Mechanisms and Function. *Rev Endocr. Metab. Disord.* **2002**, *3* (3), 193–200. https://doi.org/10.1023/A:1020068224909.

(36) Rizza, P.; Barone, I.; Zito, D.; Giordano, F.; Lanzino, M.; De Amicis, F.; Mauro, L.; Sisci, D.; Catalano, S.; Wright, K. D.; Gustafsson, Jan-Ake; Andò, S. Estrogen Receptor Beta as a Novel Target of Androgen Receptor Action in Breast Cancer Cell Lines. *Breast Cancer Res.* **2014**, *16* (1), R21. https://doi.org/10.1186/bcr3619.

(37) Berthois, Y.; Katzenellenbogen, J. A.; Katzenellenbogen, B. S. Phenol Red in Tissue Culture Media Is a Weak Estrogen: Implications Concerning the Study of Estrogen-Responsive Cells in Culture. *Proc. Natl. Acad. Sci. U. S. A.* **1986**, *83* (8), 2496–2500. https://doi.org/10.1073/pnas.83.8.2496.

(38) Dickson, R. B.; Lippman, M. E. Growth Factors in Breast Cancer. *Endocr. Rev.* **1995**, *16* (5), 559–589. https://doi.org/10.1210/edrv-16-5-559.

(39) Pike, A. C. W.; Brzozowski, A. M.; Hubbard, R. E.; Bonn, T.; Thorsell, A. G.; Engström, O.; Ljunggren, J.; Gustafsson, J. Å.; Carlquist, M. Structure of the Ligand-Binding Domain of Oestrogen Receptor Beta in the Presence of a Partial Agonist and a Full Antagonist. *EMBO J.* **1999**, *18* (17), 4608–4618. https://doi.org/10.1093/emboj/18.17.4608.

(40) Endo, Y.; Iijima, T.; Yamakoshi, Y.; Yamaguchi, M.; Fukasawa, H.; Shudo, K. Potent Estrogenic Agonists Bearing Dicarba-*closo*-dodecaborane as a Hydrophobic Pharmacophore. *J. Med. Chem.* **1999**, *42* (9), 1501–1504. https://doi.org/10.1021/jm9900725.

(41) Endo, Y.; Iijima, T.; Yamakoshi, Y.; Fukasawa, H.; Miyaura, C.; Inada, M.; Kubo, A.; Itai, A. Potent Estrogen Agonists Based on Carborane as a Hydrophobic Skeletal Structure: A New Medicinal Application of Boron Clusters. *Chem. Biol.* **2001**, *8* (4), 341–355. https://doi.org/10.1016/S1074-5521(01)00016-3.

(42) Ohta, K.; Ogawa, T.; Kaise, A.; Endo, Y. Enhanced Estrogen Receptor Beta (ERβ) Selectivity of Fluorinated Carborane-Containing ER Modulators. *Bioorg. Med. Chem. Lett.* **2013**, *23* (24), 6555–6558. https://doi.org/10.1016/j.bmcl.2013.10.067.

(43) Ohta, K.; Ogawa, T.; Kaise, A.; Oda, A.; Endo, Y. Aliphatic Substitution of *o*-Carboranyl Phenols Enhances Estrogen Receptor Beta Selectivity. *Chem. Pharm. Bull.* **2014**, *62* (4), 386–391. https://doi.org/10.1248/cpb.c13-00796.

(44) Ohta, K.; Ogawa, T.; Oda, A.; Kaise, A.; Endo, Y. Design and Synthesis of Carborane-Containing Estrogen Receptor-Beta (ERβ)-Selective Ligands. *Bioorg. Med. Chem. Lett.* **2015**, *25* (19), 4174–4178. https://doi.org/10.1016/j.bmcl.2015.08.007.

(45) Sedlák, D.; Wilson, T. A.; Tjarks, W.; Radomska, H. S.; Wang, H.; Kolla, J. N.; Leśnikowski, Z. J.; Špičáková, A.; Ali, T.; Ishita, K.; Rakotondraibe, L. H.; Vibhute, S.; Wang, D.; Anzenbacher, P.; Bennett, C.; Bartunek, P.; Coss, C. C. Structure-Activity Relationship of *para*-Carborane Selective Estrogen Receptor β Agonists. *J. Med. Chem.* **2021**, *64* (13), 9330–9353. https://doi.org/10.1021/acs.jmedchem.1c00555.

(46) Supuran, C. T. Carbonic Anhydrases: Novel Therapeutic Applications for Inhibitors and Activators. *Nat. Rev. Drug. Discov.* **2008**, *7* (2), 168–181. https://doi.org/10.1038/nrd2467.

(47) Brynda, J.; Mader, P.; Šícha, V.; Fábry, M.; Poncová, K.; Bakardiev, M.; Grüner, B.; Cígler, P.; Řezáčová, P. Carborane-Based Carbonic Anhydrase Inhibitors. *Angew. Chem., Int. Ed.* **2013**, *52* (51), 13760–13763. https://doi.org/10.1002/anie.201307583.

(48) Pecina, A.; Lepšik, M.; Rezac, J.; Brynda, J.; Mader, P.; Řezáčová, P.; Hobza, P.; Fanfrlík, J. QM/MM Calculations Reveal the Different Nature of the Interaction of Two Carborane-Based Sulfamide Inhibitors of Human Carbonic Anhydrase II. *J. Phys. Chem. B* **2013**, *117* (50), 16096–16104. https://doi.org/10.1021/jp410216m.

(49) Dvořanová, J.; Kugler, M.; Holub, J.; Šícha, V.; Das, V.; Nekvinda, J.; El Anwar, S.; Havránek, M.; Pospíšilová, K.; Fábry, M.; Král, V.; Medvedíková, M.; Matějková, S.; Lišková, B.; Gurská, S.; Džubák, P.; Brynda, J.; Hajdúch, M.; Grüner, B.; Řezáčová, P. Sulfonamido Carboranes as Highly Selective Inhibitors of Cancer-Specific Carbonic Anhydrase IX. *Eur. J. Med. Chem.* **2020**, *200*, 112460. https://doi.org/10.1016/j.ejmech.2020.112460.

(50) Scholz, M.; Blobaum, A. L.; Marnett, L. J.; Hey-Hawkins, E. *ortho*-Carbaborane Derivatives of Indomethacin as Cyclooxygenase (COX)-2 Selective Inhibitors. *Bioorg. Med. Chem.* **2012**, *20* (15), 4830–4837. https://doi.org/10.1016/j.bmc.2012.05.063.

(51) Neumann, W.; Xu, S.; Sárosi, M. B.; Scholz, M. S.; Crews, B. C.; Ghebreselasie, K.; Banerjee, S.; Marnett, L. J.; Hey-Hawkins, E. *nido*-Dicarbaborate Induces Potent and Selective Inhibition of Cyclooxygenase-2. *ChemMedChem* **2016**, *11* (2), 175–178. https://doi.org/10.1002/cmdc.201500199.

(52) Hann, M. M.; Leach, A. R.; Harper, G. Molecular Complexity and Its Impact on the Probability of Finding Leads for Drug Discovery. *J. Chem. Inf. Comput. Sci.* **2001**, *41* (3), 856–864. https://doi.org/10.1021/ci000403i.

(53) Teague, S. J.; Davis, A. M.; Leeson, P. D.; Oprea, T. The Design of Leadlike Combinatorial Libraries. *Angew. Chem., Int. Ed.* **1999**, *38* (24), 3743–3748. https://doi.org/10.1002/(SICI)1521-3773(19991216)38:24<3743::AID-ANIE3743>3.0.CO;2-U.

(54) Hopkins, A. L.; Groom, C. R.; Alex, A. Ligand Efficiency: A Useful Metric for Lead Selection. *Drug Discov. Today* **2004**, *9* (10), 430–431. https://doi.org/10.1016/S1359-6446(04)03069-7.

(55) Carr, R. A. E.; Congreve, M.; Murray, C. W.; Rees, D. C. Fragment-Based Lead Discovery: Leads by Design. *Drug Discov. Today* **2005**, *10* (14), 987–992. https://doi.org/10.1016/S1359-6446(05)03511-7.

(56) Erlanson, D. A.; Fesik, S. W.; Hubbard, R. E.; Jahnke, W.; Jhoti, H. Twenty Years on: The Impact of Fragments on Drug Discovery. *Nat. Rev. Drug. Discov.* **2016**, *15* (9), 605–619. https://doi.org/10.1038/nrd.2016.109.

(57) Lanman, B. A.; Allen, J. R.; Allen, J. G.; Amegadzie, A. K.; Ashton, K. S.; Booker, S. K.; Chen, J. J.; Chen, N.; Frohn, M. J.; Goodman, G.; Kopecky, D. J.; Liu, L.; Lopez,

P.; Low, J. D.; Ma, V.; Minatti, A. E.; Nguyen, T. T.; Nishimura, N.; Pickrell, A. J.; Reed, A. B.; Shin, Y.; Siegmund, A. C.; Tamayo, N. A.; Tegley, C. M.; Walton, M. C.; Wang, H. L.; Wurz, R. P.; Xue, M.; Yang, K. C.; Achanta, P.; Bartberger, M. D.; Canon, J.; Hollis, L. S.; McCarter, J. D.; Mohr, C.; Rex, K.; Saiki, A. Y.; San Miguel, T.; Volak, L. P.; Wang, K. H.; Whittington, D. A.; Zech, S. G.; Lipford, J. R.; Cee, V. J. Discovery of a Covalent Inhibitor of KRASG12C (AMG 510) for the Treatment of Solid Tumors. *J. Med. Chem.* **2020**, *63* (1), 52–65. https://doi.org/10.1021/acs.jmedchem.9b01180.

(58) Bon, M.; Bilsland, A.; Bower, J.; McAulay, K. Fragment-Based Drug Discovery—the Importance of High-Quality Molecule Libraries. *Mol. Oncol.* **2022**, *16* (21), 3761–3777. https://doi.org/10.1002/1878-0261.13277.

(59) Murray, C. W.; Newell, D. R.; Angibaud, P. A Successful Collaboration between Academia, Biotech and Pharma Led to Discovery of Erdafitinib, a Selective FGFR Inhibitor Recently Approved by the FDA. *MedChemComm* **2019**, *10* (9), 1509–1511. https://doi.org/10.1039/c9md90044f.

(60) Shatenshtein, A. I.; Zakharkin, L. I.; Petrov, E. S.; Yakovleva, E. A.; Yakushin, F. S.; Vukmirovich, Z.; Isaeva, G. G.; Kalinin, V. N. The Equilibrium and Kinetic Acidities of Isomeric Carborane Methines. *J. Organomet. Chem.* **1970**, *23* (2), 313–322. https://doi.org/10.1016/S0022-328X(00)92944-9.

(61) Nakamura, H.; Aoyagi, K.; Yamamoto, Y. Tetrabutylammonium Fluoride Promoted Novel Reactions of *o*-Carborane: Inter- and Intramolecular Additions to Aldehydes and Ketones and Annulation via Enals and Enones. *J. Am. Chem. Soc.* **1998**, *120* (6), 1167–1171. https://doi.org/10.1021/ja973832e.

(62) Kasar, R. A.; Knudsen, G. M.; Kahl, S. B. Synthesis of 3-Amino-1-carboxy-*o*-carborane and an Improved, General Method for the Synthesis of All Three C-Amino-C-Carboxycarboranes. *Inorg. Chem.* **1999**, *38* (12), 2936–2940. https://doi.org/10.1021/ic990037o.

(63) Ohta, K.; Goto, T.; Yamazaki, H.; Pichierri, F.; Endo, Y. Facile and Efficient Synthesis of C-Hydroxycarboranes and C,C′-Dihydroxycarboranes. *Inorg. Chem.* **2007**, *46* (10), 3966–3970. https://doi.org/10.1021/ic062025q.

(64) Nie, Y.; Wang, Y.; Miao, J.; Li, Y.; Zhang, Z. Synthesis and Characterization of Carboranyl Schiff Base Compounds from 1-Amino-*o*-carborane. *J. Organomet. Chem.* **2015**, *798*, 182–188. https://doi.org/10.1016/j.jorganchem.2015.05.046.

(65) Dozzo, P.; Kasar, R. A.; Kahl, S. B. Simple, High-Yield Methods for the Synthesis of Aldehydes Directly from *o*-, *m*-, and *p*-Carborane and Their Further Conversions. *Inorg. Chem.* **2005**, *44* (22), 8053–8057. https://doi.org/10.1021/ic0506660.

(66) Zakharkin, L. I.; Grebennikov, A. V.; Kazantsev, A. V. Alkylation of Carborane Grignard Reagents. *Bull. Acad. Sci. USSR, Div. Chem. Sci. (Engl. Transl.)* **1967**, *16* (9), 1991–1993. https://doi.org/10.1007/BF00909599.

(67) Popescu, A. R.; Musteti, A. D.; Ferrer-Ugalde, A.; Viñas, C.; Núñez, R.; Teixidor, F. Influential Role of Ethereal Solvent on Organolithium Compounds: The Case of

Carboranyllithium. *Chem. – Eur. J.* **2012**, *18* (11), 3174–3184. https://doi.org/10.1002/chem.201102626.

(68) Gomez, F. A.; Johnson, S. E.; Hawthorne, M. F. A Versatile Protecting Group for l,2-Dicarba-*closo*-dodecaborane(12) and the Structure of a Silylcarborane Derivative. *J. Am. Chem. Soc.* **1991**, *113* (15), 5915–5917. https://doi.org/10.1021/ja00015a086.

(69) Gomez, F. A.; Hawthorne, M. F. A Simple Route to C-Monosubstituted Carborane Derivatives. *J. Org. Chem.* **1992**, *57* (5), 1384–1390. https://doi.org/10.1021/jo00031a016.

(70) Qiu, Z.; Xie, Z. Functionalization of *o*-Carboranes via Carboryne Intermediates. *Chem. Soc. Rev.* **2022**, *51* (8), 3164. https://doi.org/10.1039/d2cs00024e.

(71) Maurer, J. L.; Berchier, F.; Serino, A. J.; Knobler, C. B.; Hawthorne, M. F. Glycosylcarborane Derivatives and the Determination of the Absolute Configuration of a Diastereomeric Triol from X-Ray Diffraction. *J. Org. Chem.* **1990**, *55* (3), 838–843. https://doi.org/10.1021/jo00290a012.

(72) Beall, H.; Lipscomb, W. N. Molecular and Crystal Structure of *m*-$B_{10}Br_2H_8C_2H_2$. *Inorg. Chem.* **1967**, *6* (5), 874–879. https://doi.org/10.1021/ic50051a005.

(73) Plešek, J.; Plzák, Z.; Stuchlík, J.; Heřmánek, S. Synthesis of B-Alkyl Derivatives of *o*-Carborane by Alkylation under Electrophilic Conditions; Scope and Limitation. *Collect. Czech. Chem. Commun.* **1981**, *46* (8), 1748–1763. https://doi.org/10.1135/cccc19811748.

(74) Zakharkin, L. I.; Ol'shevskaya, V. A. Synthesis of 9-Benzyl- *o*- and 9-Benzyl- *m*-Carboranes Containing Functional Substituents in the Benzene Ring by Electrophilic Alkylation of *o*- and *m*-Carboranes by the Corresponding R-Benzyl Halides. *Russ. Chem. Bull.* **1995**, *44* (6), 1099–1101. https://doi.org/10.1007/BF00707061.

(75) Wang, Y.; Gao, Y.; Guo, W.; Zhao, Q.; Ma, Y. N.; Chen, X. Highly Selective Electrophilic B(9)-Amination of *o*-Carborane Driven by HOTf and HFIP. *Org. Chem. Front.* **2022**, *9* (18), 4975–4980. https://doi.org/10.1039/d2qo00732k.

(76) Cao, K.; Huang, Y.; Yang, J.; Wu, J. Palladium Catalyzed Selective Mono-Arylation of *o*-Carboranes via B-H Activation. *Chem. Commun.* **2015**, *51* (33), 7257–7260. https://doi.org/10.1039/c5cc01331c.

(77) Xu, T. T.; Cao, K.; Wu, J.; Zhang, C. Y.; Yang, J. Palladium-Catalyzed Selective Mono-/Tetraacetoxylation of *o*-Carboranes with Acetic Acid via Cross Dehydrogenative Coupling of Cage B-H/O-H Bonds. *Inorg. Chem.* **2018**, *57* (5), 2925–2932. https://doi.org/10.1021/acs.inorgchem.8b00038.

(78) Ma, Y. N.; Gao, Y.; Ma, Y.; Wang, Y.; Ren, H.; Chen, X. Palladium-Catalyzed Regioselective B(9)-Amination of *o*-Carboranes and *m*-Carboranes in HFIP with Broad Nitrogen Sources. *J. Am. Chem. Soc.* **2022**, *144* (18), 8371–8378. https://doi.org/10.1021/jacs.2c03031.

(79) Xu, T. T.; Cao, K.; Zhang, C. Y.; Wu, J.; Ding, L. F.; Yang, J. Old Key Opens the Lock in Carborane: The in Situ NHC-Palladium Catalytic System for Selective Arylation of

B(3,6)-H Bonds of *o*-Carboranes via B-H Activation. *Org. Lett.* **2019**, *21* (22), 9276–9279. https://doi.org/10.1021/acs.orglett.9b03790.

(80) Au, Y. K.; Zhang, J.; Quan, Y.; Xie, Z. Ir-Catalyzed Selective B(3)-H Amination of *o*-Carboranes with NH_3. *J. Am. Chem. Soc.* **2021**, *143* (11), 4148–4153. https://doi.org/10.1021/jacs.1c00593.

(81) Cheng, R.; Qiu, Z.; Xie, Z. Iridium-Catalyzed Regioselective B(3)-Alkenylation/B(3,6)-Dialkenylation of *o*-Carboranes by Direct B-H Activation. *Chemistry* **2020**, *26* (32), 7212–7218. https://doi.org/10.1002/chem.202000549.

(82) Cheng, R.; Qiu, Z.; Xie, Z. Iridium-Catalysed Regioselective Borylation of Carboranes via Direct B-H Activation. *Nat. Commun.* **2017**, *8* (1), 1–7. https://doi.org/10.1038/ncomms14827.

(83) Hawthorne, M. F.; Wegner, P. A. The Reconstruction of the 1,2-Dicarbaclovododecaborane(12) Structure by Boron-Atom Insertion with (3)-1,2-Dicarbollide Ions. *J. Am. Chem. Soc.* **1968**, *90* (4), 896–901. https://doi.org/10.1021/ja01006a009.

(84) Roscoe, J. S.; Kongpricha, S.; Papetti, S. Icosahedral Carboranes. XIV. Preparation of Boron-Substituted Carboranes by Boron-Insertion Reaction. *Inorg. Chem.* **1970**, *9* (6), 1561–1563. https://doi.org/10.1021/ic50088a052.

(85) Chen, W.; Rockwell, J. J.; Knobler, C. B.; Harwell, D. E.; Hawthorne, M. F. Synthesis and Characterization of *ortho*-3- and *meta*-2-Substituted Carboranes through a Boron-Insertion Reaction, Including the Structure of the Product of a Double-Insertion Reaction. *Polyhedron* **1999**, *18* (12), 1725–1734. https://doi.org/10.1016/S0277-5387(99)00038-8.

(86) Safronov, A. V.; Shlyakhtina, N. I.; Hawthorne, M. F. New Approach to the Synthesis of 3-Alkyl-1,2-dicarba-*closo*-dodecaboranes: Reaction of Alkyldichloroboranes with Thallium Dicarbollide. *Organometallics* **2012**, *31* (7), 2764–2769. https://doi.org/10.1021/om201060e.

(87) Ramachandran, B. M.; Knobler, C. B.; Hawthorne, M. F. Synthesis and Structural Characterization of Symmetrical *closo*-4,7-I_2-1,2-$C_2B_{10}H_{10}$ and [$(CH_3)_3NH$][*nido*-2,4-I_2-7,8-$C_2B_9H_{10}$]. *Inorg. Chem.* **2006**, *45* (1), 336–340. https://doi.org/10.1021/ic051395w.

(88) Safronov, A. V.; Sevryugina, Y. V.; Jalisatgi, S. S.; Kennedy, R. D.; Barnes, C. L.; Hawthorne, M. F. Unfairly Forgotten Member of the Iodocarborane Family: Synthesis and Structural Characterization of 8-Iodo-1,2-dicarba-*closo*-dodecaborane, Its Precursors, and Derivatives. *Inorg. Chem.* **2012**, *51* (4), 2629–2637. https://doi.org/10.1021/ic2025846.

(89) Zhang, J.; Xie, Z. Directing Group Assisted Transition Metal Catalyzed Selective BH Functionalization of *o*-Carboranes. *Synthesis* **2024**, *56*. https://doi.org/10.1055/a-2343-0780.

(90) Quan, Y.; Xie, Z. Iridium Catalyzed Regioselective Cage Boron Alkenylation of *o*-Carboranes via Direct Cage B-H Activation. *J. Am. Chem. Soc.* **2014**, *136* (44), 15513–15516. https://doi.org/10.1021/ja509557j.

(91) Lyu, H.; Quan, Y.; Xie, Z. Palladium-Catalyzed Direct Dialkenylation of Cage B-H Bonds in *o*-Carboranes through Cross-Coupling Reactions. *Angew. Chem., Int. Ed.* **2015**, *54* (36), 10623–10626. https://doi.org/10.1002/anie.201504481.

(92) Quan, Y.; Xie, Z. Palladium-Catalyzed Regioselective Diarylation of *o*-Carboranes By Direct Cage B−H Activation. *Angew. Chem., Int. Ed.* **2016**, *55* (4), 1295–1298. https://doi.org/10.1002/anie.201507697.

(93) Quan, Y.; Tang, C.; Xie, Z. Palladium Catalyzed Regioselective B-C(Sp) Coupling: Via Direct Cage B-H Activation: Synthesis of B(4)-Alkynylated o-Carboranes. *Chem. Sci.* **2016**, *7* (9), 5838–5845. https://doi.org/10.1039/c6sc00901h.

(94) Lyu, H.; Quan, Y.; Xie, Z. Transition Metal Catalyzed Direct Amination of the Cage B(4)-H Bond in *o*-Carboranes: Synthesis of Tertiary, Secondary, and Primary *o*-Carboranyl Amines. *J. Am. Chem. Soc.* **2016**, *138* (39), 12727–12730. https://doi.org/10.1021/jacs.6b07086.

(95) Lyu, H.; Quan, Y.; Xie, Z. Rhodium-Catalyzed Regioselective Hydroxylation of Cage B−H Bonds of *o*-Carboranes with O_2 or Air. *Angew. Chem., Int. Ed.* **2016**, *55* (39), 11840–11844. https://doi.org/10.1002/anie.201605880.

(96) Quan, Y.; Lyu, H.; Xie, Z. Dehydrogenative Cross-Coupling of *o*-Carborane with Thiophenes via Ir-Catalyzed Regioselective Cage B-H and C(Sp_2)-H Activation. *Chem. Commun.* **2017**, *53* (35), 4818–4821. https://doi.org/10.1039/c7cc01485f.

(97) Lyu, H.; Quan, Y.; Xie, Z. Transition Metal Catalyzed, Regioselective B(4)-Halogenation and B(4,5)-Diiodination of Cage B−H Bonds in *o*-Carboranes. *Chem. – Eur. J.* **2017**, *23* (59), 14866–14871. https://doi.org/10.1002/chem.201703006.

(98) Au, Y. K.; Lyu, H.; Quan, Y.; Xie, Z. Catalytic Cascade Dehydrogenative Cross-Coupling of BH/CH and BH/NH: One-Pot Process to Carborano-Isoquinolinone. *J. Am. Chem. Soc.* **2019**, *141* (32), 12855–12862. https://doi.org/10.1021/jacs.9b06204.

(99) Chen, Y.; Quan, Y.; Xie, Z. Ir-Catalyzed Selective Dehydrogenative Cross-Coupling of Aryls with: *o*-Carboranes via a Mixed Directing-Group Strategy. *Chem. Commun.* **2020**, *56* (51), 7001–7004. https://doi.org/10.1039/d0cc02531c.

(100) Cheng, B.; Chen, Y.; Xie, Z. Iridium-Catalyzed Annulation of *o*-Carboranyl Carboxylic Acids with Alkynes: Synthesis of Carborano-Isocoumarins. *J. Org. Chem.* **2021**, *86* (17), 12412–12418. https://doi.org/10.1021/acs.joc.1c01395.

(101) Cheng, B.; Chen, Y.; Zhou, P.; Xie, Z. Rhodium-Catalyzed Sequential B(3)-, B(4)-, and B(5)-Trifunctionalization of: *o*-Carboranes with Three Different Substituents. *Chem. Commun.* **2022**, *58* (5), 629–632. https://doi.org/10.1039/d1cc05936j.

(102) Lyu, H.; Xie, Z. Transition Metal Catalyzed Selective B(3)-H or B(4)-H Amination of *o*-Carboranes via Dehydrogenative BH/NH Cross-Coupling. *Chem. Commun.* **2022**, *58* (60), 8392–8395. https://doi.org/10.1039/d2cc02852b.

(103) Zhang, L. B.; Xie, Z. Iridium-Catalyzed Selective B(4)-H Amination of *o*-Carboranes with Anthranils. *Org. Lett.* **2022**, *24* (39), 7077–7081. https://doi.org/10.1021/acs.orglett.2c02590.

(104) Zhang, L. B.; Xie, Z. Iridium-Catalyzed Selective B(4)-H Acylmethylation of *o*-Carboranes with Sulfoxonium Ylides. *Org. Lett.* **2022**, *24* (6), 1318–1322. https://doi.org/10.1021/acs.orglett.1c04335.

(105) Lyu, H.; Zhang, J.; Yang, J.; Quan, Y.; Xie, Z. Catalytic Regioselective Cage B(8)-H Arylation of *o*-Carboranes via "Cage-Walking" Strategy. *J. Am. Chem. Soc.* **2019**, *141* (10), 4219–4224. https://doi.org/10.1021/jacs.9b00302.

(106) Kaesz, H. D.; Bau, R.; Beall, H. A.; Lipscomb, W. N. Rearrangements in the Icosahedral Carboranes. *J. Am. Chem. Soc.* **1967**, *89* (16), 4218–4220. https://doi.org/10.1021/ja00992a045.

(107) Hart, H. V.; Lipscomb, W. N. Rearrangements of Icosahedral Monohalo-*m*-Carboranes. *J. Am. Chem. Soc.* **1969**, *91* (3), 771–772. https://doi.org/10.1021/ja01031a058.

(108) Zakharkin, L. I.; Kalinin, V. N.; Rys, E. G. Synthesis of 2- and 4-Amino-1,7-dicarba-*closo*-dodecaboranes from 3-Amino-1,2-dicarba-*closo*-dodecaborane. *Synth. React. Inorg. Met.-Org. Chem.* **1975**, *5* (4), 257–266. https://doi.org/10.1080/00945717508057316.

(109) Akharkin, L. I.; Kalinin, V. N.; Kobel'kova, N. I. On The Specificities of Thermal, Isomerization of 3-Substituted 1,2-Dicarbaclosodecaboranes(12) Into B-Substituted 1,7-Dicarbaclosododecaboranes(12). *Synth. React. Inorg. Met.-Org. Chem.* **1976**, *6* (2), 91–103. https://doi.org/10.1080/00945717608057346.

(110) Dziedzic, R. M.; Martin, J. L.; Axtell, J. C.; Saleh, L. M. A.; Ong, T. C.; Yang, Y. F.; Messina, M. S.; Rheingold, A. L.; Houk, K. N.; Spokoyny, A. M. Cage-Walking: Vertex Differentiation by Palladium-Catalyzed Isomerization of B(9)-Bromo-*meta*-Carborane. *J. Am. Chem. Soc.* **2017**, *139* (23), 7729–7732. https://doi.org/10.1021/jacs.7b04080.

(111) Dziedzic, R. M.; Axtell, J. C.; Rheingold, A. L.; Spokoyny, A. M. Off-Cycle Processes in Pd-Catalyzed Cross-Coupling of Carboranes. *Org. Process Res. Dev.* **2019**, *23* (8), 1638–1645. https://doi.org/10.1021/acs.oprd.9b00257.

(112) Mei, T. S.; Giri, R.; Maugel, N.; Yu, J. Q. Pd^{II}-Catalyzed Monoselective *ortho* Halogenation of C-H Bonds Assisted by Counter Cations: A Complementary Method to Directed *ortho* Lithiation. *Angew. Chem., Int. Ed.* **2008**, *47* (28), 5215–5219. https://doi.org/10.1002/anie.200705613.

(113) Weis, E.; Johansson, M. J.; Martín-Matute, B. Ir^{III}-Catalyzed Selective *ortho*-Monoiodination of Benzoic Acids with Unbiased C−H Bonds. *Chem. – Eur. J.* **2020**, *26* (45), 10185–10190. https://doi.org/10.1002/chem.202002204.

(114) Cao, K.; Zhang, C. Y.; Xu, T. T.; Wu, J.; Ding, L. F.; Jiang, L.; Yang, J. Palladium Catalyzed/Counter Ion Tuned Selective Methylation of *o*-Carboranes. *J. Organomet. Chem.* **2019**, *902*, 120956. https://doi.org/10.1016/j.jorganchem.2019.120956.

(115) Quan, Y.; Xie, Z. Palladium-Catalyzed Regioselective Intramolecular Coupling of *o*-Carborane with Aromatics via Direct Cage B-H Activation. *J. Am. Chem. Soc.* **2015**, *137* (10), 3502–3505. https://doi.org/10.1021/jacs.5b01169.

(116) Zhang, X.; Zheng, H.; Li, J.; Xu, F.; Zhao, J.; Yan, H. Selective Catalytic B-H Arylation of *o*-Carboranyl Aldehydes by a Transient Directing Strategy. *J. Am. Chem. Soc.* **2017**, *139* (41), 14511–14517. https://doi.org/10.1021/jacs.7b07160.

(117) Marshall, W. J.; Young, R. J.; Grushin, V. V. Mechanistic Features of Boron-Iodine Bond Activation of B-Iodocarboranes. *Organometallics* **2001**, *20* (3), 523–533. https://doi.org/10.1021/om0008575.

(118) Viñas, C.; Barberà, G.; Teixidor, F. The BI Activation in *o*-Carborane Clusters: Their Fate towards BH. Easy Synthesis of $[7,10\text{-}C_2B_{10}H_{13}]^-$. *J. Organomet. Chem.* **2002**, *642* (1–2), 16–19. https://doi.org/10.1016/S0022-328X(01)01108-1.

(119) Saleh, L. M. A.; Dziedzic, R. M.; Khan, S. I.; Spokoyny, A. M. Forging Unsupported Metal–Boryl Bonds with Icosahedral Carboranes. *Chem. – Eur. J.* **2016**, *22* (25), 8466–8470. https://doi.org/10.1002/chem.201601292.

(120) Gazvoda, M.; Dhanjee, H. H.; Rodriguez, J.; Brown, J. S.; Farquhar, C. E.; Truex, N. L.; Loas, A.; Buchwald, S. L.; Pentelute, B. L. Palladium-Mediated Incorporation of Carboranes into Small Molecules, Peptides, and Proteins. *J. Am. Chem. Soc.* **2022**, *144* (17), 7852–7860. https://doi.org/10.1021/jacs.2c01932.

(121) Lane, R. A. Studies of the Synthesis and Derivative Chemistry of Icosahedral Carboranes, Durham University, 1982. http://etheses.dur.ac.uk/7680/ (accessed 2025-01-04).

(122) Li, S.; Xie, Z. Visible-Light-Promoted Nickel-Catalyzed Cross-Coupling of Iodocarboranes with (Hetero)Arenes via Boron-Centered Carboranyl Radicals. *J. Am. Chem. Soc.* **2022**, *144* (18), 7960–7965. https://doi.org/10.1021/jacs.2c02329.

(123) Li, S.; Zhang, J.; Xie, Z. Visible-Light-Induced Palladium-Catalyzed Cross-Coupling of Iodocarboranes with (Hetero)Arenes. *Org. Lett.* **2022**, *24* (41), 7497–7501. https://doi.org/10.1021/acs.orglett.2c02648.

(124) Li, S.; Liu, Y.; Xie, Z. Visible-Light-Promoted Palladium-Catalyzed Cross-Coupling of Iodocarboranes with Disulfides and Phenylselenyl Chloride. *Chin. J. Chem.* **2024**, *42* (2), 129–134. https://doi.org/10.1002/cjoc.202300481.

(125) Speight, J. G. *Lange's Handbook of Chemistry*, 16th ed.; McGraw-Hill Education: New York, 2005.

(126) Dziedzic, R. M.; Saleh, L. M. A.; Axtell, J. C.; Martin, J. L.; Stevens, S. L.; Royappa, A. T.; Rheingold, A. L.; Spokoyny, A. M. B-N, B-O, and B-CN Bond Formation via Palladium-Catalyzed Cross-Coupling of B-Bromo-Carboranes. *J. Am. Chem. Soc.* **2016**, *138* (29), 9081–9084. https://doi.org/10.1021/jacs.6b05505.

(127) Mu, X.; Hopp, M.; Dziedzic, R. M.; Waddington, M. A.; Rheingold, A. L.; Sletten, E. M.; Axtell, J. C.; Spokoyny, A. M. Expanding the Scope of Palladium-Catalyzed B-N

Cross-Coupling Chemistry in Carboranes. *Organometallics* **2020**, *39* (23), 4380–4386. https://doi.org/10.1021/acs.organomet.0c00576.

(128) Zhu, M.; Wang, P.; Wu, Z.; Zhong, Y.; Su, L.; Xin, Y.; Spokoyny, A. M.; Zou, C.; Mu, X. A Pd-Catalyzed Route to Carborane-Fused Boron Heterocycles. *Chem. Sci.* **2024**, *15* (27), 10392–10401. https://doi.org/10.1039/d4sc02214a.

(129) Safronov, A. V.; Kabytaev, K. Z.; Jalisatgi, S. S.; Hawthorne, M. F. Novel Iodinated Carboranes: Synthesis of the 8-Iodo-7,9-dicarba-*nido*-undecaborate Anion and 2-Iodo-1,7-dicarba-*closo*-dodecaborane. *Dalton Trans.* **2014**, *43* (33), 12467–12469. https://doi.org/10.1039/c4dt00764f.

(130) Li, J.; Logan, C. F.; Jones, M. Simple Syntheses and Alkylation Reactions of 3-Iodo-*o*-carborane and 9,12-Diiodo-*o*-carborane. *Inorg. Chem.* **1991**, *30* (25), 4866–4868. https://doi.org/10.1021/ic00025a037.

(131) Robertson, S.; Ellis, D.; McGrath, T. D.; Rosair, G. M.; Welch, A. J. Synthesis and Characterisation of Labelled Diphenylcarboranes. *Polyhedron* **2003**, *22* (10), 1293–1301. https://doi.org/10.1016/S0277-5387(03)00103-7.

(132) Batsanov, A. S.; Fox, M. A.; Howard, J. A. K.; Hughes, A. K.; Johnson, A. L.; Martindale, S. J. 9,12-Diiodo-1,2-dicarba-*closo*-dodecaborane(12). *Acta Crystallogr. C* **2003**, *59* (2), o74–o76. https://doi.org/10.1107/S0108270102023582.

(133) Guo, W.; Guo, C.; Ma, Y. N.; Chen, X. Practical Synthesis of B(9)-Halogenated Carboranes with *N*-Haloamides in Hexafluoroisopropanol. *Inorg. Chem.* **2022**, *61* (13), 5326–5334. https://doi.org/10.1021/acs.inorgchem.2c00074.

(134) Lu, W.; Wu, Y.; Ma, Y. N.; Chen, F.; Chen, X. A Method for Highly Selective Halogenation of *o*-Carboranes and *m*-Carboranes. *Inorg. Chem.* **2023**, *62* (2), 885–892. https://doi.org/10.1021/acs.inorgchem.2c03694.

(135) Pichaandi, K. R.; Safronov, A. V.; Sevryugina, Y. V.; Everett, T. A.; Jalisatgi, S. S.; Hawthorne, M. F. Rodlike Polymers Containing Nickel and Cobalt Metal Bis(Dicarbollide) Anions: Synthesis and Characterization. *Organometallics* **2017**, *36* (19), 3823–3829. https://doi.org/10.1021/acs.organomet.7b00578.

(136) Sayler, A. A.; Beall, H. The Crystal and Molecular Structure of Tribromo-*m*-carborane. *Can. J. Chem.* **1976**, *54* (11), 1771–1776. https://doi.org/10.1139/v76-252.

(137) Zakharkin, L. I.; Kalinin, V. N.; Podvisotskaya, L. S. Preparation of B-Hydroxybarenes by the Action of Nitric Acid on Barenes. *Bull. Acad. Sci. USSR, Div. Chem. Sci. (Engl. Transl.)* **1965**, *14* (9), 1684. https://doi.org/10.1007/BF01083835.

(138) Rudakov, D. A.; Genaev, A. M.; Gatilov, Y. V.; Dikusar, E. A.; Zvereva, T. D.; Zubreichuk, Z. P.; Potkin, V. I. Synthesis and Structure of 9-Hydroxy-1,2-dicarba-*closo*-dodecaborane(11). *Russ. Chem. Bull.* **2020**, *69* (2), 320–324. https://doi.org/10.1007/s11172-020-2763-1.

(139) Ma, Y. N.; Ren, H.; Wu, Y.; Li, N.; Chen, F.; Chen, X. B(9)-OH-*o*-Carboranes: Synthesis, Mechanism, and Property Exploration. *J. Am. Chem. Soc.* **2023**, *145* (13), 7331–7342. https://doi.org/10.1021/jacs.2c13570.

(140) Rajesh, K.; Somasundaram, M.; Saiganesh, R.; Balasubramanian, K. K. Bromination of Deactivated Aromatics: A Simple and Efficient Method. *J. Org. Chem.* **2007**, *72* (15), 5867–5869. https://doi.org/10.1021/jo070477u.

(141) Pak, R. H.; Kane, R. R.; Knobler, C. B.; Hawthorne, M. F. Synthesis and Structural Characterization of [Me_3NH][*nido*-9,11-I_2-7,8-$C_2B_9H_{10}$] and [Me_3NH][*nido*-9-I-7,8-$C_2B_9H_{11}$]. *Inorg. Chem.* **1994**, *33* (23), 5355–5357. https://doi.org/10.1021/ic00101a031.

(142) Santos, E. C.; Pinkerton, A. B.; Kinkead, S. A.; Hurlburt, P. K.; Jasper, S. A.; Sellers, C. W.; Huffman, J. C.; Todd, L. J. Syntheses of *nido*-9,11-X_2-7,8-$C_2B_9H_{10}^-$ Anions (X=Cl, Br or I) and the Synthesis and Structural Characterization of $N(C_2H_5)_4$[*commo*-3,3'-Co(4,7-Br_2-3,1,2-$CoC_2B_9H_9)_2$]. *Polyhedron* **2000**, *19* (15), 1777–1781. https://doi.org/10.1016/S0277-5387(00)00461-7.

(143) Fox, M. A.; Gill, W. R.; Herbertson, P. L.; MacBride, J. A. H.; Wade, K.; Colquhoun, H. M. Deboronation of C-Substituted *ortho*- and *meta-closo*-Carboranes Using "Wet" Fluoride Ion Solutions. *Polyhedron* **1996**, *15* (4), 565–571. https://doi.org/10.1016/0277-5387(95)00297-6.

(144) Brattsev, V. A. Skeletal Rearrangements Following Electrophilic Alkylation of 7,8- and 7,9-Dicarbollide Anions (a Review). In *Contemporary Boron Chemistry*; The Royal Society of Chemistry, 2007; pp 205–211. https://doi.org/10.1039/9781847550644-00205.

(145) Fox, M. A.; Hughes, A. K.; Johnson, A. L.; Paterson, M. A. J. Do the Discrete Dianions $C_2B_9H_{11}^{2-}$ Exist? Characterisation of Alkali Metal Salts of the 11-Vertex *nido* Dicarboranes, $C_2B_9H_{11}^{2-}$, in Solution. *J. Chem. Soc., Dalton Trans.* **2002**, No. 9, 2009–2019. https://doi.org/10.1039/b109804g.

(146) Fox, M. A.; Hughes, A. K.; Malget, J. M. Cage-Closing Reactions of the *nido*-Carborane Anion 7,9-$C_2B_9H_{12}^-$ and Derivatives; Formation of Neutral 11-Vertex Carboranes by Acidification. *J. Chem. Soc., Dalton Trans.* **2002**, No. 18, 3505–3517. https://doi.org/10.1039/b203920f.

(147) Young, D. C.; Howe, D. V.; Hawthorne, M. F. Ligand Derivatives of (3)-1,2-Dicarbadodecahydroundecaborate(-1). *J. Am. Chem. Soc.* **1969**, *91* (4), 859–862. https://doi.org/10.1021/ja01032a011.

(148) Kang, H. C.; Lee, S. S.; Knobler, C. B.; Hawthorne, M. F. Syntheses of Charge-Compensated Dicarbollide Ligand Precursors and Their Use in the Preparation of Novel Metallacarboranes. *Inorg. Chem.* **1991**, *30* (9), 2024–2031. https://doi.org/10.1021/ic00009a015.

(149) Carraro, T. J. C.; Dasgupta, S.; Ku, J.; Thomas, S. R.; Rendina, L. M. Boron-Based Functionalities Enhance the Potency of 2,5-Dimethylfuran-Based IDO1 Inhibitors. *ChemBioChem* **2025**.

(150) Carraro, T. J. C.; Rendina, L. M. Unpublished results.

(151) Klebanoff, S. J. Myeloperoxidase: Friend and Foe. *J. Leukoc. Biol.* **2005**, *77* (5), 598–625. https://doi.org/10.1189/jlb.1204697.

(152) Aratani, Y. Myeloperoxidase: Its Role for Host Defense, Inflammation, and Neutrophil Function. *Arch. Biochem. Biophys.* **2018**, *640*, 47–52. https://doi.org/10.1016/j.abb.2018.01.004.

(153) Davies, M. J. Myeloperoxidase: Mechanisms, Reactions and Inhibition as a Therapeutic Strategy in Inflammatory Diseases. *Pharmacol. Ther.* **2021**, *218*, 107685. https://doi.org/10.1016/j.pharmthera.2020.107685.

(154) Weber, C.; Noels, H. Atherosclerosis: Current Pathogenesis and Therapeutic Options. *Nat. Med.* **2011**, *17* (11), 1410–1422. https://doi.org/10.1038/nm.2538.

(155) Green, P. S.; Mendez, A. J.; Jacob, J. S.; Crowley, J. R.; Growdon, W.; Hyman, B. T.; Heinecke, J. W. Neuronal Expression of Myeloperoxidase Is Increased in Alzheimer's Disease. *J. Neurochem.* **2004**, *90* (3), 724–733. https://doi.org/10.1111/j.1471-4159.2004.02527.x.

(156) Odobasic, D.; Yang, Y.; Muljadi, R. C. M.; O'Sullivan, K. M.; Kao, W.; Smith, M.; Morand, E. F.; Holdsworth, S. R. Endogenous Myeloperoxidase Is a Mediator of Joint Inflammation and Damage in Experimental Arthritis. *Arthritis Rheumatol.* **2014**, *66* (4), 907–917. https://doi.org/10.1002/art.38299.

(157) Valadez-Cosmes, P.; Raftopoulou, S.; Mihalic, Z. N.; Marsche, G.; Kargl, J. Myeloperoxidase: Growing Importance in Cancer Pathogenesis and Potential Drug Target. *Pharmacol. Ther.* **2022**, *236*, 108052. https://doi.org/10.1016/j.pharmthera.2021.108052.

(158) Nicholls, S. J.; Hazen, S. L. Myeloperoxidase and Cardiovascular Disease. *Arterioscler. Thromb. Vasc. Biol.* **2005**, *25* (6), 1102–1111. https://doi.org/10.1161/01.ATV.0000163262.83456.6d.

(159) Nussbaum, C.; Klinke, A.; Adam, M.; Baldus, S.; Sperandio, M. Myeloperoxidase: A Leukocyte-Derived Protagonist of Inflammation and Cardiovascular Disease. *Antioxid. Redox Signal* **2013**, *18* (6), 692–713. https://doi.org/10.1089/ars.2012.4783.

(160) Ramachandra, C. J. A.; Ja, K. P. M. M.; Chua, J.; Cong, S.; Shim, W.; Hausenloy, D. J. Myeloperoxidase as a Multifaceted Target for Cardiovascular Protection. *Antioxid. Redox Signal* **2020**, *32* (15), 1135–1149. https://doi.org/10.1089/ars.2019.7971.

(161) Furtmüller, P. G.; Zederbauer, M.; Jantschko, W.; Helm, J.; Bogner, M.; Jakopitsch, C.; Obinger, C. Active Site Structure and Catalytic Mechanisms of Human Peroxidases. *Arch. Biochem. Biophys.* **2006**, *445* (2), 199–213. https://doi.org/10.1016/j.abb.2005.09.017.

(162) Van Dalen, C. J.; Whitehouse, M. W.; Winterbourn, C. C.; Kettle, A. J. Thiocyanate and Chloride as Competing Substrates for Myeloperoxidase. *Biochem. J.* **1997**, *327* (2), 487–492. https://doi.org/10.1042/bj3270487.

(163) Davies, M. J. Myeloperoxidaseederived Oxidation: Mechanisms of Biological Damage and Its Prevention Overview of the Action of Myeloperoxidase and Other Heme Peroxidases. *J. Clin. Biochem. Nutr.* **2011**, *48* (1), 8–19. https://doi.org/10.3164/jcbn.111006FR.

(164) Marquez, L. A.; Dunford, H. B. Kinetics of Oxidation of Tyrosine and Dityrosine by Myeloperoxidase Compounds I and II. *J. Biol. Chem.* **1995**, *270* (51), 30434–30440. https://doi.org/10.1074/jbc.270.51.30434.

(165) Forbes, L. V.; Kettle, A. J. A Multi-Substrate Assay for Finding Physiologically Effective Inhibitors of Myeloperoxidase. *Anal. Biochem.* **2018**, *544*, 13–21. https://doi.org/10.1016/j.ab.2017.12.022.

(166) Kettle, A. J.; Winterbourn, C. C. Mechanism of Inhibition of Myeloperoxidase by Anti-Inflammatory Drugs. *Biochem. Pharmacol.* **1991**, *41* (10), 1485–1492. https://doi.org/10.1016/0006-2952(91)90565-M.

(167) Tide, A. K.; Sjögren, T.; Svensson, M.; Bernlind, A.; Senthilmohan, R.; Auchère, F.; Norman, H.; Markgren, P. O.; Gustavsson, S.; Schmidt, S.; Lundquist, S.; Forbes, L. V.; Magon, N. J.; Paton, L. N.; Jameson, G. N. L.; Eriksson, H.; Kettle, A. J. 2-Thioxanthines Are Mechanism-Based Inactivators of Myeloperoxidase That Block Oxidative Stress during Inflammation. *J. Biol. Chem.* **2011**, *286* (43), 37578–37589. https://doi.org/10.1074/jbc.M111.266981.

(168) Geoghegan, K. F.; Varghese, A. H.; Feng, X.; Bessire, A. J.; Conboy, J. J.; Ruggeri, R. B.; Ahn, K.; Spath, S. N.; Filippov, S. V.; Conrad, S. J.; Carpino, P. A.; Guimarães, C. R. W.; Vajdos, F. F. Deconstruction of Activity-Dependent Covalent Modification of Heme in Human Neutrophil Myeloperoxidase by Multistage Mass Spectrometry (MS 4). *Biochemistry* **2012**, *51* (10), 2065–2077. https://doi.org/10.1021/bi201872j.

(169) Moscovitz, J. E.; Lin, Z.; Johnson, N.; Tu, M.; Goosen, T. C.; Weng, Y.; Kalgutkar, A. S. Induction of Human Cytochrome P450 3A4 by the Irreversible Myeloperoxidase Inactivator PF-06282999 Is Mediated by the Pregnane X Receptor. *Xenobiotica* **2018**, *48* (7), 647–655. https://doi.org/10.1080/00498254.2017.1353163.

(170) *Biohaven Provides Update From Pivotal Phase 2/3 Trial with Verdiperstat in Amyotrophic Lateral Sclerosis (Healy ALS Platform Trial)*. https://www.prnewswire.com/news-releases/biohaven-provides-update-from-pivotal-phase-23-trial-with-verdiperstat-in-amyotrophic-lateral-sclerosis-healy-als-platform-trial-301636535.html (accessed 2025-02-02).

(171) *Study to Evaluate the Efficacy and Safety of AZD4831 in Participants With Heart Failure With Left Ventricular Ejection Fraction > 40% (ENDEAVOR)*. https://clinicaltrials.gov/study/NCT04986202 (accessed 2025-02-02).

(172) *An Efficacy and Safety Study of Mitiperstat (AZD4831) (MPO Inhibitor) vs Placebo in the Treatment of Moderate to Severe COPD. (CRESCENDO)*. https://clinicaltrials.gov/study/NCT05492877 (accessed 2025-02-02).

(173) *A Study in Participants With Non-cirrhotic NASH With Fibrosis (COSMOS)*. https://clinicaltrials.gov/study/NCT05638737 (accessed 2025-02-02).

(174) Forbes, L. V.; Sjögren, T.; Auchère, F.; Jenkins, D. W.; Thong, B.; Laughton, D.; Hemsley, P.; Pairaudeau, G.; Turner, R.; Eriksson, H.; Unitt, J. F.; Kettle, A. J. Potent Reversible Inhibition of Myeloperoxidase by Aromatic Hydroxamates. *J. Biol. Chem.* **2013**, *288* (51), 36636–36647. https://doi.org/10.1074/jbc.M113.507756.

(175) Hu, C. H.; Neissel Valente, M. W.; Halpern, O. S.; Jusuf, S.; Khan, J. A.; Locke, G. A.; Duke, G. J.; Liu, X.; Duclos, F. J.; Wexler, R. R.; Kick, E. K.; Smallheer, J. M. Small Molecule and Macrocyclic Pyrazole Derived Inhibitors of Myeloperoxidase (MPO). *Bioorg. Med. Chem. Lett.* **2021**, *42*, 128010. https://doi.org/10.1016/j.bmcl.2021.128010.

(176) Kahl, S. B.; Kasar, R. A. Simple, High-Yield Synthesis of Polyhedral Carborane Amino Acids. *J. Am. Chem. Soc.* **1996**, *118* (5), 1223–1224. https://doi.org/10.1021/ja9534260.

(177) Baše, T.; Macháček, J.; Hájková, Z.; Langecker, J.; Kennedy, J. D.; Carr, M. J. Thermal Isomerizations of Monothiolated Carboranes (HS)$C_2B_{10}H_{11}$ and the Solid-State Investigation of 9-(HS)-1,2-$C_2B_{10}H_{11}$ and 9-(HS)-1,7-$C_2B_{10}H_{11}$. *J. Organomet. Chem.* **2015**, *798*, 132–140. https://doi.org/10.1016/j.jorganchem.2015.06.020.

(178) Peng, B.; Nie, Y.; Miao, J.; Zhang, Z.; Xu, M.; Sun, G. Synthesis, Structures and Photophysical Properties of (*o*-Carboranyl)-(pyridyl)methanols. *J. Mol. Struct.* **2012**, *1007*, 214–219. https://doi.org/10.1016/j.molstruc.2011.10.050.

(179) Toppino, A.; Genady, A. R.; El-Zaria, M. E.; Reeve, J.; Mostofian, F.; Kent, J.; Valliant, J. F. High Yielding Preparation of Dicarba-Closo-Dodecaboranes Using a Silver(I) Mediated Dehydrogenative Alkyne-Insertion Reaction. *Inorg. Chem.* **2013**, *52* (15), 8743–8749. https://doi.org/10.1021/ic400928v.

(180) Batsanov, A. S.; Goeta, A. E.; Howard, J. A. K.; Hughes, A. K.; Malget, J. M. The Synthesis of *closo*- and *nido*-(Aminoalkyl)Dicarbaboranes: A Re-Examination of Contradictory Literature Reports, Crystal Structure of [7-{$H_3N(CH_2)_3$}-7,8-$C_2B_9H_{11}$]·NH_2NH_2. *J. Chem. Soc., Dalton Trans.* **2001**, No. 12, 1820–1826. https://doi.org/10.1039/b102009i.

(181) Wilson, J. G.; Anisuzzaman, A. K. M.; Soloway, A. H.; Alam, F. Development of Carborane Synthons: Synthesis and Chemistry of (Aminoalkyl)carboranes. *Inorg. Chem.* **1992**, *31* (10), 1955–1958. https://doi.org/10.1021/ic00036a043.

(182) Zakharkin, L. I.; Balagurova, E. V.; Lebedev, V. N. Suzuki Cross Coupling in the Carborane Series. *Russ. J. Gen. Chem.* **1998**, *68* (6), 922–924.

(183) Eriksson, L.; Beletskaya, I. P.; Bregadze, V. I.; Sivaev, I. B.; Sjöberg, S. Palladium-Catalyzed Cross-Coupling Reactions of Arylboronic Acids and 2-I-*p*-carborane. *J. Organomet. Chem.* **2002**, *657* (1–2), 267–272. https://doi.org/10.1016/S0022-328X(02)01431-6.

(184) Aizawa, K.; Ohta, K.; Endo, Y. Synthesis of 3-Aryl-1,2-dicarba-*closo*-dodecaboranes by Suzuki-Miyaura Coupling Reaction. *Heterocycles* **2010**, *80* (1), 369–377. https://doi.org/10.3987/COM-09-S(S)32.

(185) Anufriev, S. A.; Shmal'ko, A. V.; Suponitsky, K. Yu.; Sivaev, I. B. One-Pot Synthesis of B-Aryl Carboranes with Sensitive Functional Groups Using Sequential Cobalt- and Palladium-Catalyzed Reactions. *Catalysts* **2020**, *10* (11), 1348. https://doi.org/10.3390/catal10111348.

(186) Beletskaya, I. P.; Bregadze, V. I.; Ivushkin, V. A.; Petrovskii, P. V.; Sivaev, I. B.; Sjöberg, S.; Zhigareva, G. G. New B-Substituted Derivatives of *m*-Carborane, *p*-Carborane, and Cobalt Bis(1,2-Dicarbollide) Anion. *J. Organomet. Chem.* **2004**, *689* (18), 2920–2929. https://doi.org/10.1016/j.jorganchem.2004.05.047.

(187) Zakharkin, L. I.; Kovredov, A. I.; Ol'shevskaya, V. A.; Shaugumbekova, Z. S. Synthesis of B-Organo-Substituted 1,2-, 1,7-, and 1,12-Dicarbaclosododecarboranes(12). *J. Organomet. Chem.* **1982**, *226* (3), 217–222. https://doi.org/10.1016/S0022-328X(00)83405-1.

(188) Zakharkin, L. I.; Ol'shevskaya, V. A.; Zhigareva, G. G. Synthesis of B-Organyl-o- and -m-Carboranes by the Cross Coupling of B-Iodo-*o*- and -*m*-Carboranes with Organozinc Compounds, Catalyzed by Palladium Complexes. *Russ. J. Gen. Chem.* **1998**, *68* (6), 925–927.

(189) Zakharkin, L. I.; Ol'shevskaya, V. A.; Anikina, E. V. Electrophilic Alkylation of *o*- and *m*-Carboranes by 4-Chlorobutyric Acid and 5-Chlorovaleric Acid in the Presence of $AlCl_3$. *Bull. Acad. Sci. USSR, Div. Chem. Sci. (Engl. Transl.)* **1987**, *36* (4), 795–797. https://doi.org/10.1007/BF00962323.

(190) Sevryugina, Y.; Julius, R. L.; Hawthorne, M. F. Novel Approach to Aminocarboranes by Mild Amidation of Selected Iodo-carboranes. *Inorg. Chem.* **2010**, *49* (22), 10627–10634. https://doi.org/10.1021/ic101620h.

(191) Wang, T.; Zhang, Z.; Meanwell, N. A. Benzoylation of Dianions: Preparation of Monobenzoylated Derivatives of Symmetrical Secondary Diamines. *J. Org.Chem.* **1999**, *64* (20), 7661–7662. https://doi.org/10.1021/jo9908501.

(192) Dypbukt, J. M.; Bishop, C.; Brooks, W. M.; Thong, B.; Eriksson, H.; Kettle, A. J. A Sensitive and Selective Assay for Chloramine Production by Myeloperoxidase. *Free Radic. Biol. Med.* **2005**, *39* (11), 1468–1477. https://doi.org/10.1016/j.freeradbiomed.2005.07.008.

(193) Meotti, F. C.; Jameson, G. N. L.; Turner, R.; Harwood, D. T.; Stockwell, S.; Rees, M. D.; Shane R Thomas; Kettle, A. J. Urate as a Physiological Substrate for Myeloperoxidase: Implications for Hyperuricemia and Inflammation. *J. Biol. Chem.* **2011**, *286* (15), 12901–12911. https://doi.org/10.1074/jbc.M110.172460.

(194) Simic, M. G.; Jovanovic, S. V. Antioxidation Mechanisms of Uric Acid. *J. Am. Chem. Soc.* **1989**, *111* (15), 5778–5782. https://doi.org/10.1021/ja00197a042.

(195) Pérez-Rosés, R.; Risco, E.; Vila, R.; Peñalver, P.; Cañigueral, S. Antioxidant Activity of Tween-20 and Tween-80 Evaluated through Different in-Vitro Tests. *J. Pharm. Pharmacol.* **2015**, *67* (5), 666–672. https://doi.org/10.1111/jphp.12369.

(196) Wurtz, N. R.; Viet, A.; Shaw, S. A.; Dilger, A.; Valente, M. N.; Khan, J. A.; Jusuf, S.; Narayanan, R.; Fernando, G.; Lo, F.; Liu, X.; Locke, G. A.; Kopcho, L.; Abell, L. M.; Sleph, P.; Basso, M.; Zhao, L.; Wexler, R. R.; Duclos, F.; Kick, E. K. Potent Triazolopyridine Myeloperoxidase Inhibitors. *ACS Med. Chem. Lett.* **2018**, *9* (12), 1175–1180. https://doi.org/10.1021/acsmedchemlett.8b00308.

(197) Jankowiak, A.; Kaszyński, P. Practical Synthesis of 1,12-Difunctionalized *o*-Carborane for the Investigation of Polar Liquid Crystals. *Inorg. Chem.* **2014**, *53* (16), 8762–8769. https://doi.org/10.1021/ic5014494.

(198) Zheng, Z.; Jiang, W.; Zinn, A. A.; Knobler, C. B.; Hawthorne, M. F. Facile Electrophilic Iodination of Icosahedral Carboranes. Synthesis of Carborane Derivatives with Boron-Carbon Bonds via the Palladium-Catalyzed Reaction of Diiodocarboranes with Grignard Reagents. *Inorg. Chem.* **1995**, *34* (8), 2095–2100. https://doi.org/10.1021/ic00112a023.

(199) Tanaka, T.; Nishiura, Y.; Araki, R.; Saido, T.; Abe, R.; Aoki, S. 11B NMR Probes of Copper(II): Finding and Implications of the Cu^{2+}-Promoted Decomposition of *ortho*-Carborane Derivatives. *Eur. J. Inorg. Chem.* **2016**, *2016* (12), 1819–1834. https://doi.org/10.1002/ejic.201600117.

(200) Izmaylov, B. A.; Vasnev, V. A.; Markova, G. D. On the Reactions of Haloidmagnesiummethyl-*m*-carboranes with Organoalkoxysilanes and Chlorosilanes. *Inorg. Chim. Acta* **2018**, *471*, 475–480. https://doi.org/10.1016/j.ica.2017.11.056.

(201) Busby, D. C.; Hawthorne, M. F. The Crown Ether Promoted Base Degradation of *p*-Carborane. *Inorg. Chem.* **1982**, *21* (11), 4101–4103. https://doi.org/10.1021/ic00141a046.

(202) Kellert, M.; Friedrichs, J. S. J.; Ullrich, N. A.; Feinhals, A.; Tepper, J.; Lönnecke, P.; Hey-Hawkins, E. Modular Synthetic Approach to Carboranyl-Biomolecules Conjugates. *Molecules* **2021**, *26* (7), 2057. https://doi.org/10.3390/molecules26072057.

(203) Kalinin, V. N.; Rys, E. G.; Tyutyunov, A. A.; Starikova, Z. A.; Korlyukov, A. A.; Ol'shevskaya, V. A.; Sung, D. D.; Ponomaryov, A. B.; Petrovskii, P. V.; Hey-Hawkins, E. The First Carborane Triflates: Synthesis and Reactivity of 1-TrifluoromethanesulfonyImethyl- And 1,2-Bis(Trifluoromethanesulfonylmethyl)-*o*-Carborane. *Dalton Trans.* **2005**, No. 5, 903–908. https://doi.org/10.1039/b417199c.

(204) Wu, Y.; Carroll, P. J.; Kang, S. O.; Quintana, W. Synthesis, Characterization, and Reactivity of Isocyanato Dicarbaboranes Obtained from *o*-Carborane. *Inorg. Chem.* **1997**, *36* (21), 4753–4761. https://doi.org/10.1021/ic970360w.

(205) Wu, J.; Cao, K.; Zhang, C. Y.; Wen, X. Y.; Li, B.; Yang, J. Iron(III)-Catalyzed Aerobic Oxidation for the Synthesis of 1-Benzoxazolyl-*o*-carboranes. *J. Organomet. Chem.* **2021**, *945*, 121881. https://doi.org/10.1016/j.jorganchem.2021.121881.

(206) Tang, C.; Zhang, J.; Xie, Z. Direct Nucleophilic Substitution Reaction of Cage B−H Bonds by Grignard Reagents: A Route to Regioselective B4-Alkylation of o-Carboranes. *Angew. Chem., Int. Ed.* **2017**, *56* (30), 8642–8646. https://doi.org/10.1002/anie.201702347.

(207) Quan, Y.; Tang, C.; Xie, Z. Nucleophilic Substitution: A Facile Strategy for Selective B-H Functionalization of Carboranes. *Dalton Trans.* **2019**, *48* (22), 7494–7498. https://doi.org/10.1039/c9dt01140d.

(208) Zhang, J.; Xie, Z. N-Ligand-Enabled Aromatic Nucleophilic Amination of 1,2-Diaryl-*o*-Carboranes with $(R_2N)_2Mg$ for Selective Synthesis of 4-R_2N-*o*-carboranes and 2-R_2N-*m*-carboranes. *Angew. Chem., Int. Ed.* **2022**, *61* (32), e202202675. https://doi.org/10.1002/anie.202202675.

(209) Bruno, N. C.; Tudge, M. T.; Buchwald, S. L. Design and Preparation of New Palladium Precatalysts for C-C and C-N Cross-Coupling Reactions. *Chem. Sci.* **2013**, *4* (3), 916–920. https://doi.org/10.1039/c2sc20903a.

(210) Vaca, A.; Teixidor, F.; Kivekäs, R.; Sillanpää, R.; Viñas, C. A Solvent-Free Regioselective Iodination Route of *ortho*-Carboranes. *Dalton Trans.* **2006**, No. 41, 4884–4885. https://doi.org/10.1039/b612465h.

(211) Fox, M. A.; Wade, K. Deboronation of 9-Substituted-*ortho*- and -*meta*-Carboranes. *J. Organomet. Chem.* **1999**, *573* (1–2), 279–291. https://doi.org/10.1016/S0022-328X(98)00881-X.

(212) Gona, K. B.; Thota, J. L. V. N. P.; Baz, Z.; Gómez-Vallejo, V.; Llop, J. Synthesis and ^{11}C-Radiolabelling of 2-Carboranyl Benzothiazoles. *Molecules* **2015**, *20* (5), 7495–7508. https://doi.org/10.3390/molecules20057495.

(213) Sadrerafi, K.; Zargham, E. O.; Lee, M. W. Improved Synthesis of MC4-PPEA and the Biological Evaluation of Its Hydroxymethyl Derivative. *Bioorg. Med. Chem. Lett.* **2016**, *26* (2), 618–621. https://doi.org/10.1016/j.bmcl.2015.11.068.

(214) Ching, H. Y. V.; Clifford, S.; Bhadbhade, M.; Clarke, R. J.; Rendina, L. M. Synthesis and Supramolecular Studies of Chiral Boronated Platinum(II) Complexes: Insights into the Molecular Recognition of Carboranes by β-Cyclodextrin. *Chem. – Eur. J.* **2012**, *18* (45), 14413–14425. https://doi.org/10.1002/chem.201201746.

(215) Sedikides, A. T.; Lennox, A. J. J. Silver-Catalyzed (Z)-β-Fluoro-Vinyl Iodonium Salts from Alkynes: Efficient and Selective Syntheses of Z-Monofluoroalkenes. *J. Am. Chem. Soc.* **2024**, *146* (23), 15672–15680. https://doi.org/10.1021/jacs.4c03826.

(216) Neumann, W.; Frank, R.; Hey-Hawkins, E. One-Pot Synthesis of an Indole-Substituted 7,8-Dicarba-*nido*-dodecahydroundecaborate(-1). *Dalton Trans.* **2015**, *44* (4), 1748–1753. https://doi.org/10.1039/c4dt03218g.

(217) Tribovane, D. C.; Scholz, M. S. Non-Natural Lipids: Synthesis and Characterization of Esters from *meta*-Carborane-1-carboxylic Acid. *Chem. Phys. Lipids* **2018**, *210*, 149–154. https://doi.org/10.1016/j.chemphyslip.2017.08.008.

(218) Ali, K.; Cho, E. J. Nickel-Catalyzed Double Deoxygenative C-N Coupling of Acyloxyamines. *Org. Lett.* **2024**, *26* (24), 5192–5195. https://doi.org/10.1021/acs.orglett.4c01758.

(219) Kondo, Y.; Morisaki, K.; Hirazawa, Y.; Morimoto, H.; Ohshima, T. A Convenient Preparation Method for Benzophenone Imine Catalyzed by Tetrabutylammonium Fluoride. *Org. Process Res. Dev.* **2019**, *23* (8), 1718–1724. https://doi.org/10.1021/acs.oprd.9b00226.

(220) Dian, L.; Wang, S.; Zhang-Negrerie, D.; Du, Y.; Zhao, K. Organocatalytic Amination of Alkyl Ethers via N-Bu_4NI/t-BuOOH-Mediated Intermolecular Oxidative C(Sp_3)—N Bond Formation: Novel Synthesis of Hemiaminal Ethers. *Chem. Commun.* **2014**, *50* (79), 11738–11741. https://doi.org/10.1039/c4cc05758a.

(221) Yu, C. P.; Tang, Y.; Cha, L.; Milikisiyants, S.; Smirnova, T. I.; Smirnov, A. I.; Guo, Y.; Chang, W. C. Elucidating the Reaction Pathway of Decarboxylation-Assisted Olefination Catalyzed by a Mononuclear Non-Heme Iron Enzyme. *J. Am. Chem. Soc.* **2018**, *140* (45), 15190–15193. https://doi.org/10.1021/jacs.8b10077.

(222) Kong, X.; He, Z.; Zhang, Y.; Mu, L.; Liang, C.; Chen, B.; Jing, X.; Cammidge, A. N. A Mesogenic Triphenylene-Perylene-Triphenylene Triad. *Org. Lett.* **2011**, *13* (4), 764–767. https://doi.org/10.1021/ol103018v.